

AC/DC BOOK OF KNOWLEDGE

Practical tips for the User

By Steve Roberts M.Sc. B.Sc.

Technical Director, RECOM

RECOM

AC/DC Book of Knowledge

Practical Tips for the User

By Steve Roberts, M.Sc. B.Sc.
Technical Director, RECOM

First Edition

©2018 All rights RECOM Engineering GmbH & Co.KG, Austria (hereafter RECOM)

The contents of this book or excerpts thereof may not be reproduced, duplicated or distributed in any form without the written permission of RECOM.

The disclosure of the information contained in this book is correct to the best of the knowledge of the author, but no responsibility can be accepted for any mistakes, omissions or typographical errors. The diagrams indicate typical applications and are not necessarily complete.

Preface from RECOM Management

When we introduced our first DC/DC converter nearly 30 years ago, there were little published technical material available and hardly any international standards to follow. There was a pressing need to communicate practical application information to our customers, which prompted us to add some simple Application Notes as an appendix to our first published product catalogue. The content of these guidelines grew over the years as we gained more and more expertise. Although they are still of a rudimentary nature, they are well received by our customer base and today they have become an 70-page Application Note package available on our Website for download

The advance of semiconductor technology and the shift towards highly integrated digital electronics has diminished the knowledge base of analogue techniques in many design labs, universities and technical colleges over the years. We often see a lack of practical know-how in analogue circuit design, particularly with regard to applied techniques, test and measurement and the understanding of filtering and noise suppression. Therefore, as experts in this arena, we saw the need for a much more comprehensive technical handbook that could be used as reference by hardware designers and students alike.

Eventually at the start of 2014, Steve Roberts, our Technical Director, started to invest his free time to start documenting the extensive application knowledge on the design, test and application of DC/DC converters available within the RECOM group. Despite all of the pressures of his demanding job, he managed to complete this onerous task in time for Electronica 2014. Two years later, in the time for Electronica 2016 the third edition of the RECOM DC/DC Book of Knowledge was enlarged to include an additional chapter on magnetics.

In keeping with this biennial tradition, electronica 2018 sees the release of the RECOM AC/DC Book of Knowledge. We released our first AC/DC converter back in 2006, so we have also accumulated a considerable body of knowledge on AC/DC power conversion that has allowed us to offer products from 1W up to 1kW and beyond with industrial, medical and household certifications.

Steve has presented us with a new handbook that we are sure will greatly benefit the engineering community and all those who are interested in AC/DC power conversion and its applications. The handbook will initially be available as a printed hard-copy version and as PDF soft-copy available for free download from the RECOM website.

**Board of Directors,
RECOM Group**

Gmunden, 2018

Preface from the Author

This AC/DC Book of Knowledge is a companion book to the DC/DC Book of Knowledge. They are designed to be read together, so I have deliberately avoided repeating information except where it is necessary for clarity. Some chapters are equally applicable to DC/DC as to AC/DC applications, so I have taken the opportunity to cover topics that were not in the DC/DC book, but perhaps should have been.



The success of the DC/DC Book of Knowledge has been partly due to the lack of other text books or sources of information specifically for DC/DC applications. This is not the case for AC/DC applications, where there are a multitude of books, application notes and technical papers that are available. Therefore, I have decided to just cover the aspects that interest me in particular (it is my book, after all). Some AC/DC topics have had whole text books written about them which I dismiss in just a few sentences, other topics are less well covered and deserving of far more detail than I have space for in this book. I have had to tread a fine line between giving useful information for the majority of readers and being overly wordy about topics that I find fascinating, but might not interest everyone.

This book is all my own work but I am acutely conscious that the breadth of knowledge required to do proper justice to this topic is wider than a single person can ever hope to achieve. Therefore, I have relied heavily on my colleagues and the published knowledge of many others as well as my own experience. My thanks go to everyone who has had the courage to poke their head above the parapet and publish their ideas, concepts, designs or experimental results and risk the barrage of criticism from the mass of other experts in this field. Bearing this in mind, feel free to contact me if you find any errors, omissions or inaccuracies in this book and I will get them corrected.

Steve Roberts

Gmunden, 2018

Technical Director

s.roberts@recom-power.com

RECOM

Table of Contents

CHAPTER 1	11
A Historical Introduction	11
CHAPTER 2	19
Linear AC/DC Power Supplies	19
CHAPTER 3	24
Apparent, Reactive and Active Power	24
CHAPTER 4	28
AC Theory	28
4.1 AC Theory - basics	28
CHAPTER 5	34
Passive Components	34
5.1 Capacitors	34
5.1.1 Class X and Y capacitors	34
5.1.2 Electrolytic Capacitors	36
5.1.2.1 Design considerations of electrolytic capacitors.	37
5.1.2.2 Electrolytic lifetime calculation	39
5.1.2.3 Deriving ripple current from E-cap temperature rise	40
5.2 Common Mode Chokes	42
5.2.1 EMC Common Mode Filter worked example	43
CHAPTER 6	46
Active Components	46
6.1 Silicon MOSFET	46
6.2 SiC MOSFET	49
6.3 IGBT	50
6.4 GaN HEMT	51
6.4.1 GAN Transistor gate driver considerations	53
6.5. Power Transistor Layout Considerations	56
6.5 Unplanned turn-on due to the effect of the Miller capacitance	57
6.6 Unplanned turn-on due to the effect of the parasitic inductances (L_{gate} and $L_{emitter}$)	58

CHAPTER 7 63

Power Factor Correction 63

7.1 Passive PFC..... 63
 7.1.1 Valley Fill PFC..... 65
7.2 Active PFC 66
 7.2.1 DCM power factor correction 66
 7.2.2 CCM power factor correction. 67
 7.2.3 CrCM power factor correction. 68
 7.2.4 Mixed-Mode PFC 69
 7.2.5 Interleaved PFC 70
 7.2.6 Bridgeless (totem pole) PFC 71

CHAPTER 8 75

AC/DC Converter Topologies..... 75

8.1 Single Ended Flyback..... 75
 8.1.1 Single Ended Flyback Snubber Networks..... 79
 8.1.3 Ringing Snubbers..... 81
 8.1.2 Active Clamp and Regenerative Snubbers 84
 8.1.2.1 High Side Active Clamp 84
 8.2.1.2 Low Side Active Clamp 85
 8.2.1.3 Regenerative Clamp 87
8.3 Quasi-Resonant Flyback Converter 87
8.4 Half-Bridge Resonant Mode Converter 88
8.5 Full-Bridge Resonant Mode Converters 90
 8.5.1 Phase-Shifted Resonant Full Bridge 90
 8.5.2 Resonant Full Bridge..... 91
8.6 Single-Ended Forward Converter..... 94
 8.6.1 Interleaved Single-Ended Forward..... 98
 8.6.2 Current-fed Single-Ended Forward 102
8.7 Two-Transistor Topologies..... 104
 8.7.1 Two-transistor Forward Converter 104
 8.7.2 Push-Pull Forward Converter 106
 8.7.3 Current-Fed Push-Pull Forward Converter 107
8.8 Using paralleled transformers to increase the power. 110
8.9 Poly-Phase supplies..... 113
 8.9.1 Three phase PFC..... 114

CHAPTER 9 117

Transformerless AC Power supplies 117

9.1 Capacitively-coupled AC/DC 117
9.2 Non-Isolated Buck Regulator 119

9.3 High Voltage Linear Regulators	120
9.4 Off-Line Regulator IC	121
CHAPTER 10	124
Wireless power	124
10.1. Resonant wireless power transfer	126
10.2. Inductive wireless power transfer	126
10.3 PCB Inductive power transfer.....	128
CHAPTER 11	133
Feedback.....	133
11.1 Measuring Loop Stability	134
11.2 Type 1 Feedback Loop Compensation Calculation	138
11.3 Type 2 Feedback Loop Compensation	139
11.5 Optocoupler Feedback Loop Compensation.....	142
11.6 Secondary side feedback compensation.....	145
11.7 Magnetic feedback	146
11.7.1 Output side powered PWM feedback transformer.	146
11.7.2 Direct magnetic feedback.....	147
11.7.3 Primary side driven magnetic feedback.	148
11.8 Capacitively coupled feedback.....	150
11.9 Primary side regulation.....	152
CHAPTER 12	155
Low Standby Power Consumption Techniques	155
12.1 Passive Losses	156
12.1.1 HV start up disconnect	156
12.1.2 Half-wave HV start up	158
12.1.3 Bleeder Resistor Losses	158
12.2 Feedback Losses	159
12.2 Active losses	161
12.2.1 Clamp Losses	161
12.2.2 Variable switching frequency	162
12.2.3 Variable valley switching	163
12.2.4 Pulse skipping	163
12.2.5 Synchronous rectification	164
12.2.6 Output Load detection (Zero-Power).....	166
12.3 Measuring standby power consumption.....	168

CHAPTER 13:	169
Measuring AC	169
13.1 AC voltage measurements	169
13.1.1 High frequency AC voltage measurements.....	173
13.2 AC Current Measurement Techniques.....	174
13.2.1 Precision Shunt Resistor	174
13.2.2 Shunt + Current Mirror	176
13.2.3 Shunt + isolation amplifier	177
13.3 Current transformer.....	178
13.3.1 Compensated CT (AC Zero-flux)	180
13.4 Rogowski Coil.....	180
13.5 Hall Effect Current Sensor.....	181
13.6 Flux Gate current sensor.....	183
13.7 GMR current sensor	184
REFERENCES AND FURTHER READING	186
SOME RECOMMENDED APPLICATION NOTES	186
ABOUT RECOM	187

Chapter 1

A Historical Introduction

Depending where you are travelling in the world, the mains voltage available from the wall plate will be 50Hz or 60Hz AC (Alternating Current) with a nominal voltage of around 120VAC or 230VAC. Unless you are plugging in a hair dryer, kettle or a lamp, you will probably need an adaptor to convert the high voltage AC supply down to a low voltage DC (Direct Current) to be useful, for example to charge your phone or power your laptop. Considering that all electronic equipment runs natively on DC power, you might think why is the mains power always AC? And while we are on the subject, who chose 50/60Hz or 120V/230Vac as the “correct” numbers for the mains supply anyway?

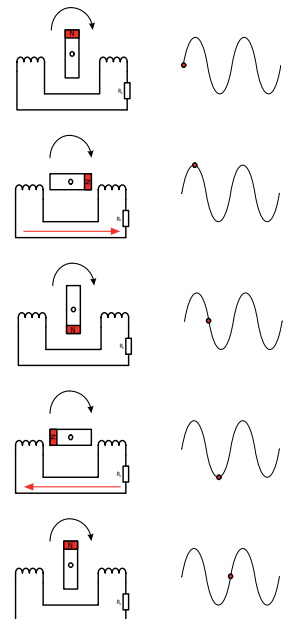
Back in the nineteenth century, when public power distribution networks were first being developed, the choice was much wider. Both AC and DC mains supplies were offered, with the standard AC frequency ranging from as low as 16⅔Hz up to as high as 133Hz. Electronic appliances had not yet been invented, so the most common use of electricity was for lighting or heating; both of which worked equally well with either AC or DC supplies, so the AC frequency was not so important. The most common AC frequency was 42Hz and in America, Edison patented DC power distribution and heavily promoted it as being safer and more reliable than AC¹. To a certain extent, this was true, as early electrical generators were less than reliable and the banks of batteries both stabilized the output voltage and bridged any short duration generator faults with the DC supply. This was not the case with AC generators which needed very good speed regulators to maintain the correct output voltage with changes in demand and had no back-up supply possibility in the event of a generator fault.

AC eventually won over DC distributed networks for three main reasons: the simplicity of the first AC generators which led to a rapid improvement in reliability, the ease in which the voltage could be changed up or down using transformers and the advantages of multiple pole alternators to reduce the rotation speed of more powerful generators.

The simple electrical generators used at the time converted mechanical energy into electrical energy by rotating a magnet within coils of wire (figure 1.1).

Note that there are no moving electrical contacts.

Fig. 1.1: Principle of operation of an alternator



¹ Edison famously ran newspaper adverts explaining that the newly invented electric chair used AC to kill the condemned men, callously implying that his DC system was safer.

The arrangement shown in figure 1.1 is more commonly called an alternator because the current flows alternately in one direction and then in the other as the magnet spins. If a non-alternating output is desired, then a mechanical switch called a commutator is needed to reverse the connections every half cycle:

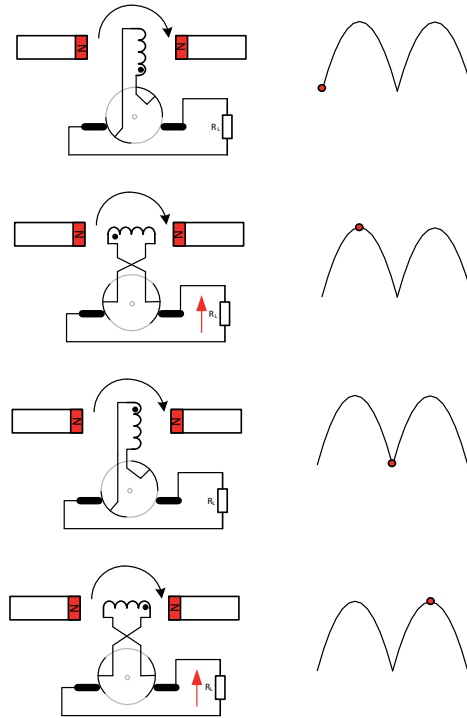


Fig. 1.2: Commutator Action

In this arrangement, the coil of wire rotates within a fixed magnetic field instead of rotating a magnet within the coils of wire, but the generating effect is the same. The commutator switching action is typically performed by a split slip ring on the shaft of the generator which reverses the connections every half turn:

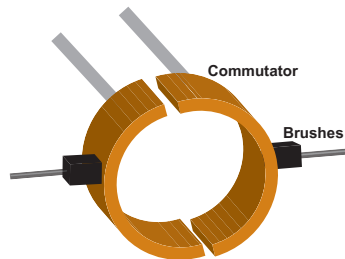


Fig. 1.3: Split slip ring commutator

As the power distribution network developed and the demand increased, the current flowing through the commutator brushes increased and made the DC system more unreliable than the simple AC generators used at the time which needed no slip rings.

The second reason for the demise of the DC power transmission scheme was the increasing losses as more and more houses were connected to the system. The power losses in a cable with resistance R are equal to the square of the current I , flowing through it (i^2R loss), so if the voltage can be doubled to halve the current (Power = VI), then the same power cable can carry the current four times further. This principle applies to both DC and AC power transmission, but it was much easier to use transformers to step up the AC supply voltage for long-distance transmission and to step it back down again at the far end again using transformers. Edison tried to compete with his DC system by using generator sets (a DC motor connected to a dynamo to step up or down the supply voltage) but although a low voltage DC motor for the step-up part was easy to make, a high-voltage DC motor for the corresponding step-down part was not so reliable and the system broke down often. In the end, even Edison abandoned the DC distribution concept and also changed to alternating current power distribution.

Although most mains power sockets are single phase, electrical AC power stations generate three phases at 120° from each other. The advantage of this is that $3 \times 120^\circ = 360^\circ$. In other words, the phases cancel out when connected to a common point.

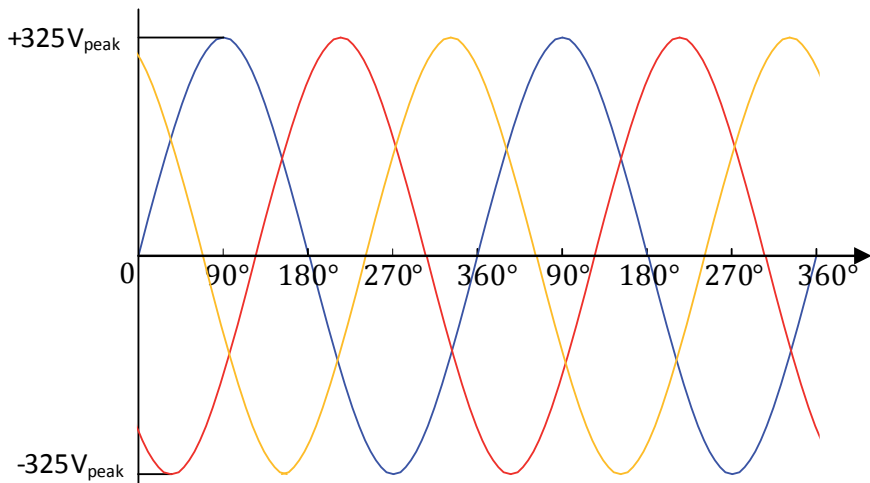


Fig. 1.4: Three Phase waveform. The sum of all three phases added together is always zero.

This means that unlike DC power distribution where the current flows equally in the positive and negative cables which therefore both need to be equally massive, an AC power distribution grid can be made with three heavy duty phase cables and a light gauge neutral wire which is only needed to carry any imbalance current if the loads on the three phases are not exactly equal. If you look at an electricity pylon, you can see the thick power cables suspended from the cross beams with a single, thinner cable running across the tops of the pylons. This is the

neutral return wire. The earth (or ground) connection is for safety only. It carries no current in normal conditions. If a current flows from any phase to earth then it is due to a fault and a protective device (fuse or residual current trip) should cut off the power.

The following simplified diagram illustrates this arrangement when applied to whole streets in a town.

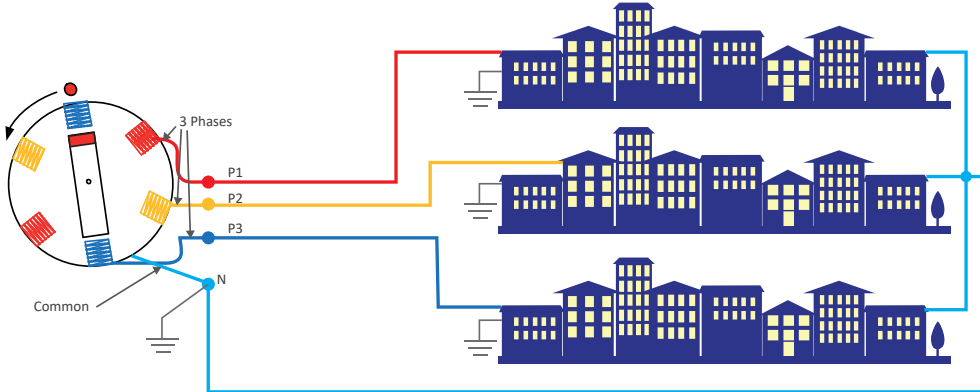


Fig. 1.5: Diagrammatic representation of a three phase power distribution system. The neutral wire will carry no current if the load on each phase is balanced.

Why three phases and not two? Well, two phase power distribution is still used in some parts of the USA (2x120VAC at 180° so that 240VAC equipment for heavier loads such as ovens and washing machines could be used on a 120V system), but the big advantage of an asymmetrical number of phases is for use with AC motors. It does not matter where the rotor sits, a three phase motor will always start up in the same direction and as the load is equally balanced on all three phases, a neutral wire is not required (L1, L2, L3 and Earth). An AC motor with a symmetrical number of phases could either not start if the rotor was exactly in line with the poles or, worse, start up in the wrong direction.

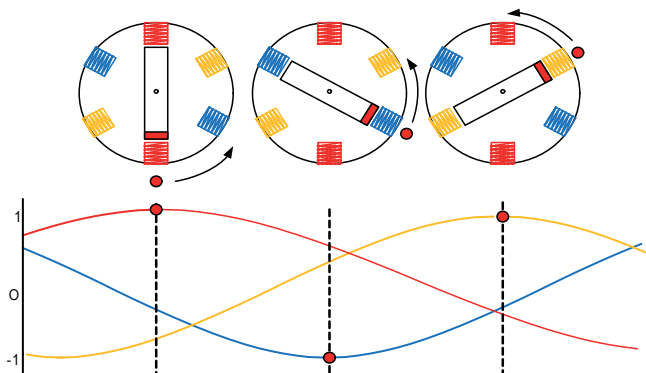


Fig. 1.6: Principle of operation of a three phase motor. As each phase peaks, the rotor is pulled around to line up with that set of windings. The rotor then follows the rotating magnetic field.

But the final nail in the coffin for DC distribution was the popularity of electrical lighting. As more and more houses, public buildings and streets switched from gas lighting to electric lamps, the demand for electrical power increased rapidly. The lower cabling cost of three phase transmission compared to DC became the deciding factor when raising the investment needed to electrify whole towns.

More powerful and larger generators were manufactured to meet this demand. These generators were very heavy and the slower a very massive generator rotor can rotate, the less stress on the bearings and framework. This is why there were originally so many different AC frequencies used; a smaller generator spinning at 2500 RPM created a 42Hz output, while a larger one spinning at 1000 RPM created a 16 $\frac{2}{3}$ Hz output (note that “a nice whole number” of revolutions per minute (RPM) was more often used, an indication that mechanical engineers built the alternators, not electrical engineers). However, while an incandescent filament may not flicker much at 42Hz, at 16 $\frac{2}{3}$ Hz it was disturbingly visible. The AC flicker was even more pronounced with arc lighting which became increasingly used in theatres, open spaces and for street lighting.

The solution for high frequency AC output with slower rotation speeds was to use multiple pole alternators: instead of two windings, four windings could be used wired alternately in series. Then instead of one AC cycle per rotation, two cycles would be generated. For the same output AC frequency, the rotor speed could be halved, significantly reducing the stress on the generator.

In the meantime, the mechanical problems with slip rings had been solved and multiple windings could be wound on the rotor with multiple magnetic poles built into the stator. This meant that the optimum rotation speed could be chosen for the physical size of the generator and almost any output frequency could be generated by selecting the appropriate number of rotor windings and stator poles. The original Niagara Falls power station in the USA used 12 pole, low speed (250 RPM) generators to output 25Hz AC, but this was later doubled up to 50Hz by simply rearranging the windings while keeping the original low RPM which was optimally matched to the water turbines.

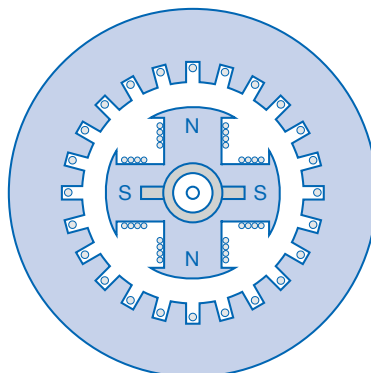


Fig. 1.7: Example of a Multiple Pole Alternator.

By this time (mid 1850's), AEG was the leading electrical equipment manufacturer in Europe. 50Hz was supposedly chosen as the standard AC frequency in Europe because it was an even number of 100 peaks per second, which appealed to the Teutonic mind. In America, Westinghouse chose 60Hz, supposedly because 50Hz flicker was still just about visible with arc lighting and therefore Nicola Tesla (who licenced his AC generation patents to Westinghouse) had recommended a higher mains frequency, but equally probably to protect their home market from foreign competition. Either way, commercial interests decided that 50Hz in some regions and 60Hz in other regions should eventually become standard.

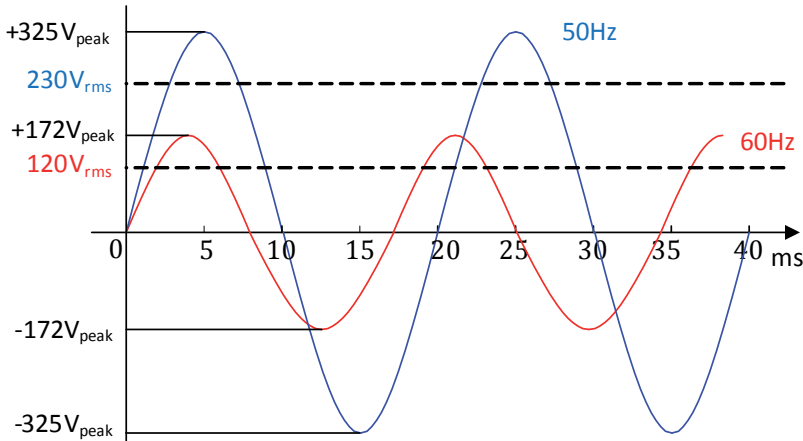


Fig. 1.8: Waveforms of 230VAC/50Hz and 120VAC/60Hz single phase supplies.

The effective voltage (dotted line) is the square root of the mean of the squares of the AC voltage (RMS), in other words, the DC voltage that would have the same heating effect as the AC voltage.

So protectionism could explain why the AC mains is 50Hz in some countries and 60Hz in others, but why the different supply voltages of 120VAC or 230VAC? Originally, 110-120VAC was a pretty much universal standard (also in pre-war Europe) because the influential Edison used 110V for his DC distribution system. The competition therefore also chose similar voltages so that any heating or lighting equipment designed to run on Edison's system could also be used with their own power supply network. As the number of domestic appliances per household increased, the I²R losses of the 120VAC supply became more and more significant, but the wealth of post-war US citizens meant that so many refrigerators, air conditioners and televisions with 120VAC input were already in use that an increase in mains supply voltage in the USA was impractical. Europe, on the other hand, was recovering from the war with no such legacy problems and realizing that the demand for electrical power would only increase in the future chose to double the 110/120VAC voltage (220VAC in continental Europe, 240VAC in UK) to halve the current and quarter the losses. Eventually, in 1994, the EU decided to harmonize throughout Europe on 230VAC which was within the operating range of both 220VAC and 240VAC equipment. In practice, however, the allowable voltage tolerance

limits were wide enough so that UK could stay at 240V and the rest of Europe remain at 220V and both say that they delivered a nominally 230VAC supply. A typical European solution to the problem! In the meantime, the power stations have all been adjusted to deliver 230VAC on average, although my colleague in the UK still measures 240V on his supply as he is very close to a substation.

There are still several countries that for various reasons have “non-standard” mains voltages. Many ex-Commonwealth countries still use the original British 240VAC supply voltage. Japan has opted for 100VAC supplies for safety reasons, but because the south island was supplied with generators from Westinghouse and the north island from AEG, they have either 60Hz or 50Hz supply frequencies depending where you are in Japan. Four frequency converter substations have now been built to balance out the load between the islands by transferring 50Hz and 60Hz power back-and-forth. In the USA, many large buildings use 115/277VAC split supplies. The higher voltage is primarily used for lighting to increase the overall building efficiency, as lighting can account for 40% of the total power consumption of a large office block.

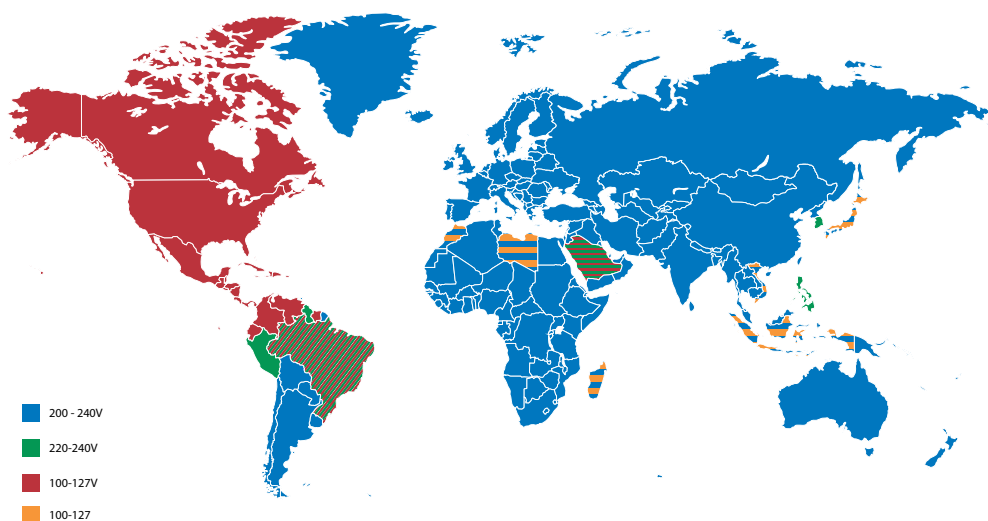


Fig. 1.9: Map of world mains voltages and frequencies

What all this means for a modern AC/DC power supply designer is that an universal input single phase power supply will need to accommodate an AC input voltage range (including $\pm 10\%$ tolerance) of 90 – 264VAC for world-wide use (covering 100/120/230/240VAC nominal) or 90-305VAC to also accommodate 277VAC supplies sometimes used in the USA.

Nominal Supply (RMS)	Phase-to-Neutral		Phase-to-Phase		
	RMS (10% tolerance)	Peak Voltage	RMS (Nominal)	RMS (10% tolerance)	Peak Voltage
100VAC	90-110V	141V	173V	156-190V	245V
120VAC	108-132V	170V	208V	187-229V	360V
230VAC	207-253V	325V	400V	360-440V	693V
240VAC	216-264V	340V	415V	373-457V	588V
277VAC	249-305	392V	480V	432-528V	831V

Table 1.1: Mains voltage ranges.

Footnote: Modern Power Distribution

Today, technologies exist that allow the conversion of AC to DC in either direction with very high power and efficiencies. Although AC mains voltages will remain standard for the near future, there are several advantages in going back to DC power distribution. One reason is our increasing dependence on electrical power. In order to guarantee supply, power distribution is not just from one generator to the consumer, but from many sources connected together to form a power grid. It is more efficient and cheaper to transmit power over long distances (>500km) using high voltage DC as there are no impedance losses and the generators do not need to be all synchronized to the same frequency or even the same voltage. For example, a 2000MW high voltage DC power link connects England and France to allow the two countries to exchange power according to domestic demand.

In the home, a DC power distribution network that links photovoltaic solar cells on the roof with a fixed battery or the battery in an electric car allows a reliable, high efficiency, low running-cost electrical supply which can be mains independent (off-grid). There are many advantages in connecting together groups of homes to share energy sources (Photovoltaic, house battery or external mains grid supply) to make a very efficient localized power supply grid.

See <http://www.isea.rwth-aachen.de> for one such concept.

Chapter 2

Linear AC/DC Power Supplies

Figure 2.1 shows an unregulated AC/DC power supply that was common practice when I started my career.

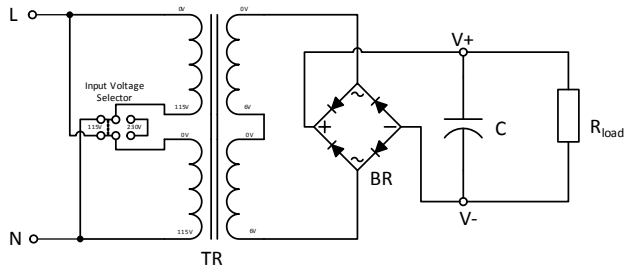


Fig. 2.1: Simple linear AC/DC power supply

The transformer has two primary windings of 115V which can be connected in parallel or series with the input voltage selector switch. The two 6V secondary windings are wired in series to give a nominal 12VAC output which is then rectified by the bridge rectifier BR and DC smoothed by the output capacitor, C, to give a typical output voltage of about 14VDC. The bridge rectifier uses four diodes, but there are other options for the secondary rectification using the same transformer and fewer diodes:

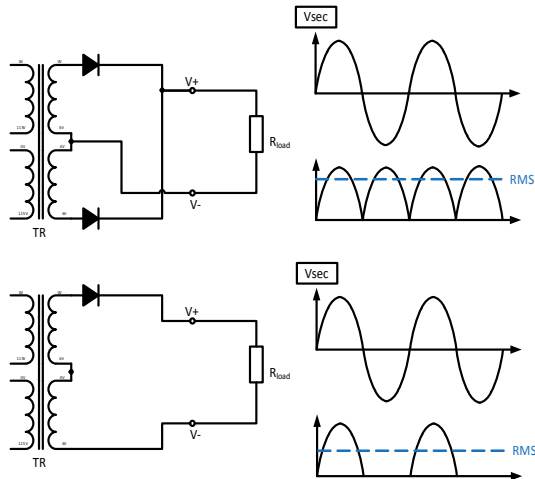


Fig. 2.2: Alternative output rectifier options: top: centre-tap, bottom: half-wave

If V_s is the nominal voltage for each secondary winding, then Table 2.1 can be used to work out the equivalent DC output voltage (V_f is the forward voltage drop through a power diode $\approx 0.7V$):

Rectification Method	No. of Diodes	Output Freq.	V_{peak}	$V_{DC, av}$
Bridge Rectifier	4	$2f_{in}$	$2\sqrt{2V_s} - 2V_f$	$2V_{peak}/\pi$
Centre-Tap	2	$2f_{in}$	$\sqrt{2V_s} - V_f$	$2V_{peak}/\pi$
Half-wave	1	f_{in}	$\sqrt{2V_s} - V_f$	V_{peak}/π

Table 2.1: Comparison of rectified DC outputs for different rectification methods

For the simple example shown in Figure 2.2 with 50Hz mains and 2x 6VACrms secondaries, Table 2.1 becomes:

Rectification Method	No. of Diodes	Output Freq.	V_{peak}	$V_{DC, av}$
Bridge Rectifier	4	100Hz	15.6V	10V
Centre-Tap	2	100Hz	7.8V	5V
Half-wave	1	50Hz	7.8V	2.5V

Table 2.2: results of the calculations in Table 2.1 with 2x 6V secondary windings

However, this average DC output value is calculated without the smoothing capacitor and without a load. The larger the capacitor, the closer the measured DC output will be to the peak voltage. On the other hand, the higher the load, the lower the measured DC output voltage will be. To determine the effective output voltage, we need to know the load and output capacitance in order to calculate the output ripple.

Returning to the original, full wave bridge rectified design, we can add the output waveform shown below:

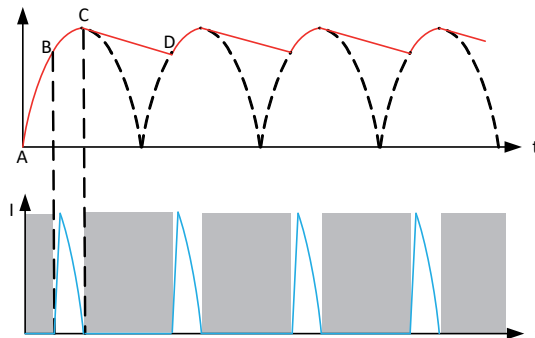


Fig. 2.3: Output capacitor voltage and current waveforms

At the start of each half cycle, the output voltage rises from zero up to the peak voltage C . Above point B (the residual voltage stored on the output capacitor), it starts to supply the load current and charge the output capacitor. The current (shown in blue) rises sharply. As the secondary voltage drops below its peak, the output capacitor holds the output voltage higher than the AC voltage and the diode bridge become reverse biased and ceases to conduct. The AC current falls to zero. The greyed-out part of the waveform from point C until point D shows where only the capacitor supplies the load current. The input current is thus highly discontinuous with a very high harmonic distortion.

The line C-D is shown as a straight line on the diagram, although it is in fact an exponential decay curve with the relationship:

$$\text{Eq. 2.1: } V = V_{peak} e^{\frac{-t}{R_{load}C}}$$

However, for practical circuits with large output capacitors, this expression can be approximated by:

$$\text{Eq. 2.2: } V = V_{peak} \left(\frac{-t}{R_{load}C} \right)$$

With a peak-to-peak ripple voltage of:

$$\text{Eq. 2.3: } V_{ripple_{p-p}} = \left(\frac{V_{peak}}{4f_{in}R_{load}C} \right)$$

And an average DC output voltage of:

$$\text{Eq. 2.4: } V_{DC_{av}} = V_{peak} \left(1 - \frac{1}{4f_{in}R_{load}C} \right)$$

So, for a 50Hz mains supply with a 1k load and a 100 μ F capacitor, we could expect to see a measured DC output voltage of:

$$V_{DC_{av}} = V_{peak} \left(1 - \frac{1}{4f_{in}R_{load}C} \right) = 15.6 \left(1 - \frac{1}{4 \times 50 \times 1000 \times 100 \times 10^{-6}} \right) = 14.8V$$

With a peak-to-peak ripple of approximately:

$$V_{ripple_{p-p}} = \left(\frac{V_{peak}}{4f_{in}R_{load}C} \right) = \left(\frac{15.6}{4 \times 50 \times 1000 \times 100 \times 10^{-6}} \right) = 0.8V$$

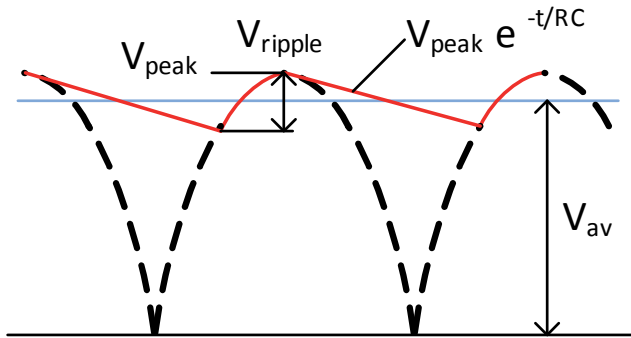


Fig. 2.4: Voltage on output capacitor, C, with load R.

As the output voltage changes with load and has a high ripple, it is common practice to use a linear regulator to regulate the output and to provide output short circuit protection. For this example, a 12V regulator would be most suitable as the minimum supply voltage would be about 14V, giving 2V headroom for the linear regulator.

Linear power supplies are still used where their advantages outweigh their disadvantages:

1. As the power supply has only passive components, it is a low noise solution. A well designed linear regulated power supply can have a very smooth output with an output noise level below $5\mu V_{RMS}$. Linear power supplies are still used in high end audio systems and RF amplifiers.
2. The same design can be used for very high input voltages by simply selecting different primary side voltage taps (e.g. 208V/380V/480VAC) or very low input voltages (e.g. 12VAC input) by using a different transformer. It is still a technical challenge to make a switching power supply that will work well with a 12VAC input
3. there are very few components to go wrong, so a well-specified linear power supply can have a working lifetime of more than 20 years.
4. they are generally low cost. However, due to the very high production volume of switching power supplies, the difference between a linear and switching solution is often very small.

The main reasons why linear AC/DC power supplies have been mainly supplanted by switching converters are the following:

1. A 50/60Hz transformer is much bulkier and heavier than a transformer designed for switching power supplies. For example, a 10VA mains frequency transformer has a volume of typically $65cm^3$, whereas a 10W switching transformer can be built into a $2cm^3$ core – a saving of more than x30 in size and weight.

2. linear power supplies are inefficient. Power is transferred only at the peaks of the mains cycle – the remaining part of the cycle is not used. On the secondary side, the rectification diodes dissipate a significant amount of power due to the high capacitor charging peak currents. If linear regulators are used to stabilize the output, then the efficiency drops even lower. Overall efficiencies of below 50% are not unusual. In comparison, switching power supplies with efficiencies exceeding 90% are common.
3. Linear power supplies have poor regulation. The output voltage is load dependent and also directly proportional to the input voltage. The hold-up time is short, so the output voltage will be adversely affected by mains brown-outs and any dropped cycles. The transient load response time is also very poor as the power supply must wait until the next AC peak to transfer any extra energy required to cope with a sudden load increase.
4. The no load power consumption is too high to meet modern energy efficiency regulations. In addition, the fact that power is transferred only at the cycle peaks means that the power factor is also too low for many applications (a linear power supply has a power factor of typically 0.5 – 0.7)
5. the cost of switching power supplies is now so low that a low power linear power supply may actually be more expensive than the more complex switching converter alternative.

Chapter 3

Apparent, Reactive and Active Power

Transformer power is measured in VA, not in Watts. This is because the simple Watts = Volts x Amps equivalence cannot be used if the voltage and current are not aligned and are out of phase. For AC circuits, the reactance of any capacitive or inductive load elements shifts the phase of the current to the voltage. For mainly capacitive loads, the current waveform lags the voltage and for mainly inductive loads, the current leads the voltage. A simple way to remember which way the phase difference goes is the word CIVIL:

CIVIL

For capacitance, C, current I leads voltage V.

For Inductance, L, current I lags voltage V.

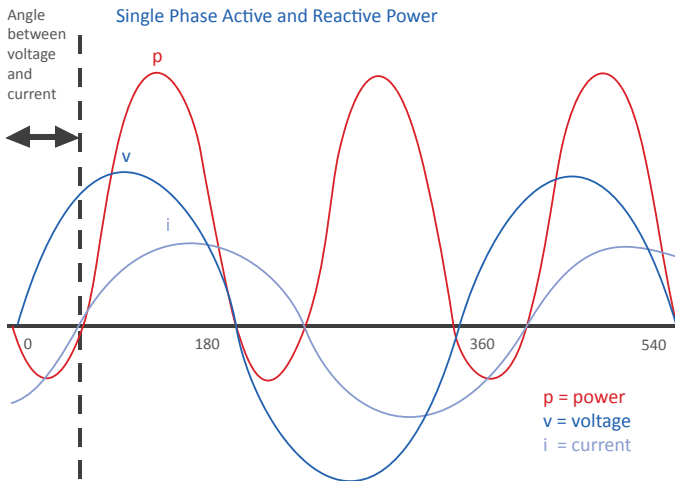


Fig. 3.1: AC voltage, current and apparent power for a mainly inductive load. The current lags the voltage and the reactive power can go negative (the load is supplying power back into the source)

If the AC current is out of alignment with the AC input voltage, then the shift can be described as a phase angle. A phase angle of 0° means that the current and voltage are perfectly aligned (in other words, the load is purely resistive). A phase angle of 90° means that the load is purely reactive (either $+90^\circ$ = purely inductive or -90° = purely capacitive). As the resistive load is zero, a purely reactive load consumes no power; for two quarters of the cycle the sum of the current and voltage are positive but for the other two quarters of the cycle the sum is negative and the two balance out.

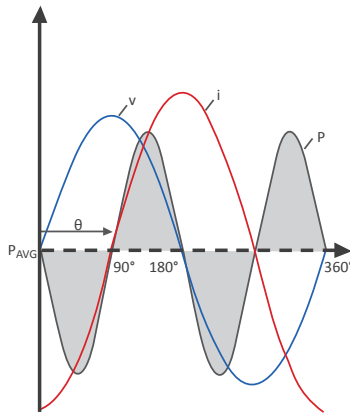


Fig. 3.2: Waveforms and apparent power for a purely inductive load

In practice purely reactive loads do not exist as there are always some resistive losses in the wiring. In a power supply circuit, there will be a mix of both reactive and resistive losses leading to a power factor (the ratio of active power to reactive power) somewhere between 1 and 0 (a power factor of 1 corresponds to a phase angle of zero and a power factor of 0 corresponds to a phase angle of 90°):

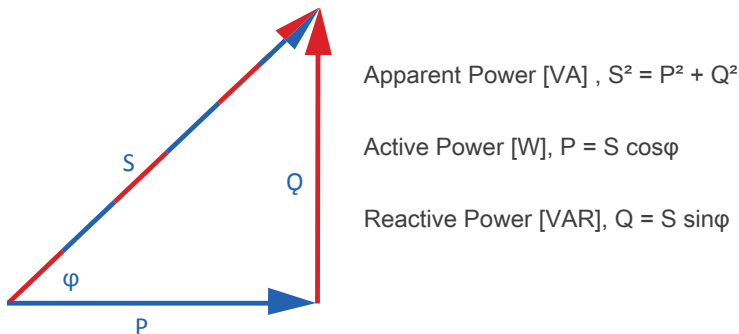


Fig. 3.3: Apparent power vector diagram.

By convention, capacitive loads generate reactive power and inductive loads consume reactive power. This is very useful, as a capacitor can be used to bring the power factor closer to 1 for a mainly inductive load such as a motor or an inductor can be used to bring the power factor closer to 1 for a mainly capacitive load. Adding such reactive components to adjust the power factor is called passive power factor correction.

But why bother correcting the power factor? The purely reactive element of the load consumes no power overall as energy absorbed in one part of the cycle is returned in another part so most electricity meters only measure the active power consumed and ignore the reactive power. The main problem is that the electricity company has to supply enough power to cope with the peak power demand which is the combination of active and reactive powers. Even if some of this energy is returned in other parts of the cycle, the distribution system has to cope

with the worst case instantaneous power consumption. Also the reactive power circulating current and therefore the cable losses in a system with “poor” power factor will be higher than one with a “good” power factor (closer to 1). By encouraging customers to power factor correct their energy consumption (by either charging more for poor power factor loads or by lobbying governments to force customers to add power factor correction), the power companies can save money.

It is a common mistake to think that, for example, an LED driver with power factor correction is somehow “greener” and consumes less power. The additional power factor correction circuitry actually reduces overall efficiency by adding additional power stages to the design.

A more serious issue is the problem of electromagnetic interference if the power supply is not properly power factor corrected. Take the example shown above of a linear power supply. The input current is in phase with the input voltage, but severely distorted. Using the relationship shown in figure 3.3 might give the impression that the power factor = 1 as $\text{Cos } \phi = 1$.

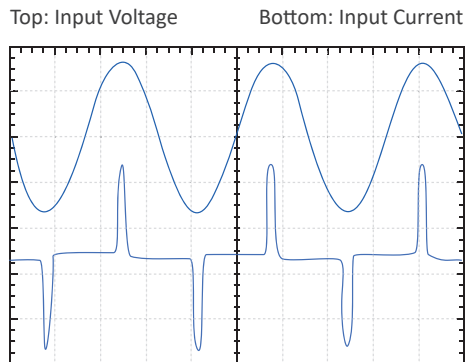


Fig. 3.4: Linear power supply input current vs voltage

However, looking at the harmonics generated by the distorted input current reveals a different story:

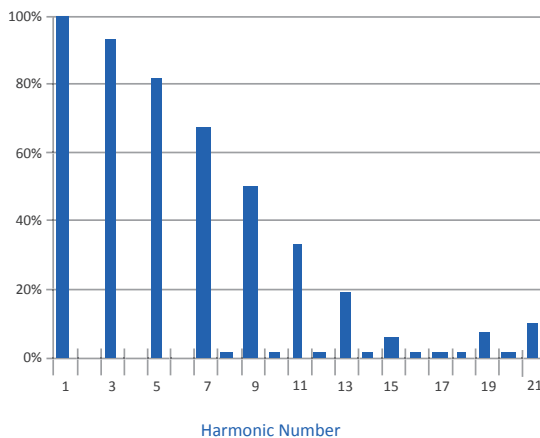


Fig. 3.5: Harmonics generated by the input current shown in Fig 3.4.

The fundamental harmonic (number 1) is the input frequency (50Hz or 60Hz). This represents the real power supplied to the converter. The remaining odd harmonics 3, 5, 7, 9, etc. represent the apparent power. As the current waveform is almost perfectly symmetrical, the even harmonics hardly show. As can be seen from this diagram, there is a considerable amount of energy present in the higher harmonics and therefore the power factor is not 1 but in fact closer to 0.6, even though the current is in phase with the voltage. The problem lies in that the input is a pure sine wave but the current is a much distorted waveform. This distortion factor can be added to the basic $\cos \phi$ relationship to give the true real power /apparent power relationship:

Eq. 3.1: $P_{total} = V_{in,rms} I_{in,rms} \cos \phi \cos \theta$, where $\cos \theta$ is the distortion factor

In comparison, a near-perfect power factor correction circuit where the current is not only in phase with the input, but also a sine wave gives an ideal harmonic graph with almost of the input power in the fundamental harmonic only:

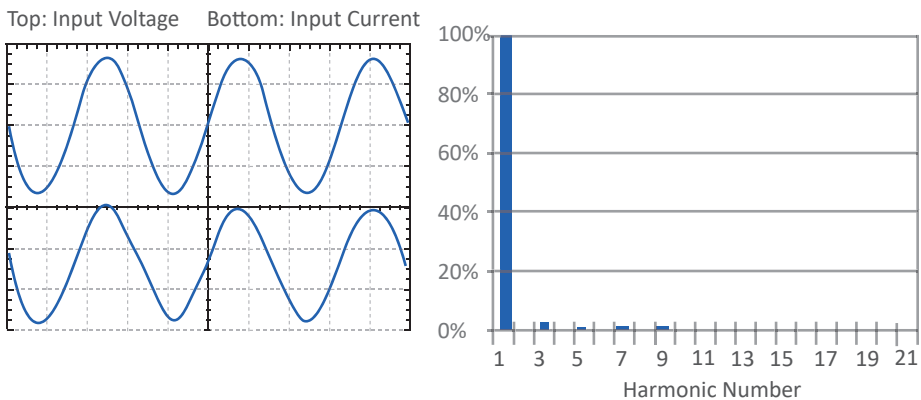


Fig. 3.6: Near-ideal power factor and its harmonics

The sum of the unwanted harmonics (2nd harmonic and higher) is called the total harmonic distortion (THD) and its relationship to power factor, PF, is given by:

Eq. 3.2: $THD(\%) = 100 \sqrt{\sum_{p=2}^{\infty} \frac{I_p^2}{I_1^2}}$ $PF = \cos \theta = \sqrt{\frac{1}{1+THD^2}}$

Chapter 4

AC Theory

Note: This next section is optional. You can skip straight to the next chapter or you can read further. While you are deciding, following the advice of Steven Sandler who claims that all successful books must contain a dragon, preferably a medieval dragon; please find a picture of a dragon:



Fig. 4.1: Dragon (source: MS Clipart)

4.1 AC Theory - basics

In the previous section, the concept of apparent power was introduced as being a vector composed of the elements of reactive power and active power. A vector is a two dimensional quantity composed of two single dimensional quantities called scalars at right angles to each other (P and Q in Fig. 3.3) .

- A vector can be denoted by an arrow above it (e .g. \vec{S}) or more simply by bold type, e.g. **S**.
- The length of a vector (its magnitude or modulus) is the square root of the squares of the two scalars that define it and is shown by bars on either side **|S|**.

So in figure 3.3: $|S| = \sqrt{P^2 + Q^2}$

Just as apparent power is a vector, so are impedances. The reactance of an inductor consists of two elements, its DCR resistance, R, which does not change with frequency and its impedance, which is directly proportional to frequency, as both are measured in Ohms, and they can be represented on the same vector diagram.

If the frequency is zero (DC), then $X_L = 2\pi fL$ is also zero which makes $|\mathbf{Z}|=R$, where R is the DCR of the inductor. As the frequency is increased, the scalar X_L (the AC impedance) increases and the resulting AC reactance is the vector, \mathbf{Z} , with modulus $|\mathbf{Z}|$. At infinite frequency, the AC impedance is infinite and the resistance scalar R becomes zero.

The angle between the scalars, ϕ , represents the angular frequency $2\pi f$.

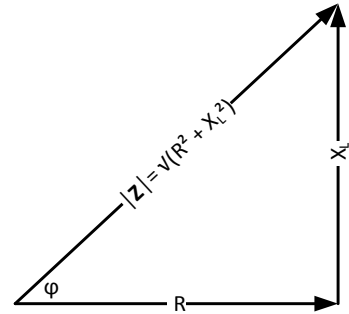


Fig. 4.2: Inductor impedance vector diagram.

The same concept applies to capacitive reactances:

If the frequency is infinite, then $X_C = -1/2\pi fC$ is zero which makes $|\mathbf{Z}|=R$. The resistance R is just the ESR resistance. As the frequency is decreased, the scalar X_C (the AC impedance) increases and the resulting AC reactance is the vector, \mathbf{Z} , with modulus $|\mathbf{Z}|$. At zero frequency (DC), the impedance is infinite and the resistance scalar R is zero. The angle between the scalars, ϕ , represents the angular frequency $2\pi f$.

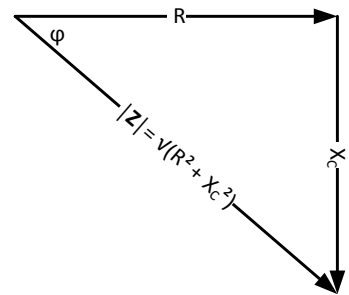


Fig. 4.3: Capacitor impedance vector diagram.

Note: The reason why ϕ is conventionally shown as positive with an inductor and negative with a capacitor is because voltage leads current in an inductor, but lags it in a capacitor.

A phasor is a particular type of vector. If an impedance vector is multiplied by a current, it is transformed to a voltage (this is commonly known as Ohm's Law, $|\mathbf{V}| = I|\mathbf{Z}|$), but it does not change direction. The phase information is retained. Such constant phase vectors are called phasors.

The advantage of phasors is that we can add reactances in series (the current is therefore the same for all elements and can be represented by a reference phasor \hat{I} , which is equal to the magnitude of the current and work out the resulting voltage phasor \hat{V} .)

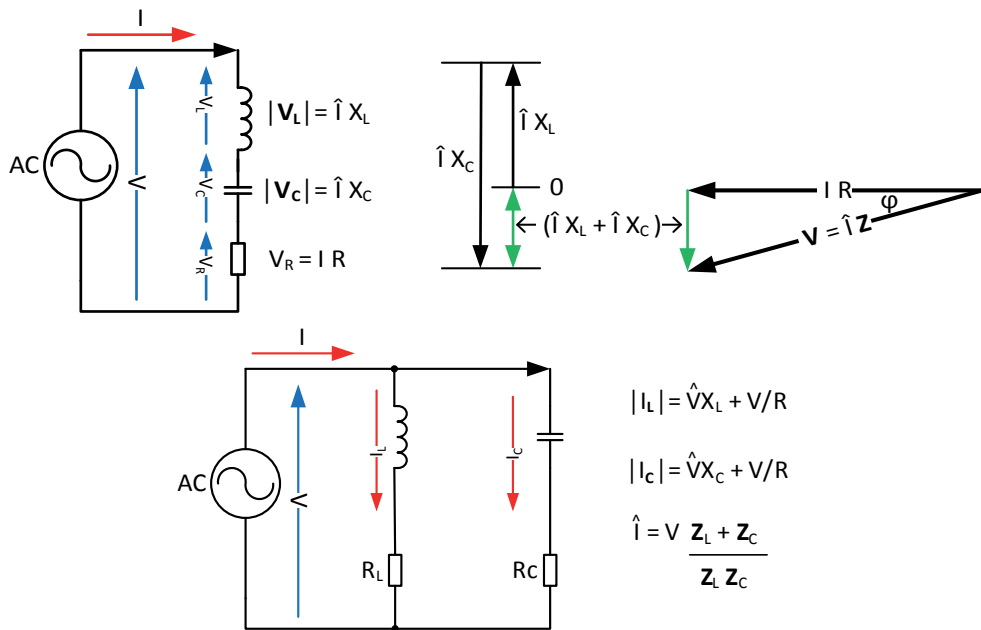


Fig. 4.4: Adding AC reactances in series and parallel

The same applies to adding reactances in parallel (then the voltage phasor is therefore the same for all elements) and work out the resulting current phasor. The same relationship for adding resistors in parallel applies to adding reactances in parallel:

$$\text{Eq. 4.1: } R_{\text{parallel}} = \frac{R_1 R_2}{(R_1 + R_2)} \quad \text{is like} \quad X_{\text{parallel}} = \frac{X_1 X_2}{(X_1 + X_2)}$$

This is all well and good, but we can't solve every impedance problem by drawing vector of phasor diagrams. We need some more mathematics.

The Z phasor consists of resistive and reactive elements, R and X , so if we get Eq. 4.2 for the magnitude of Z for a parallel circuit:

$$\text{Eq. 4.2: } \frac{1}{|Z|} = \left(\frac{1}{R}\right)^2 + \left(\frac{1}{X}\right)^2 = \left(\frac{1}{R} + \frac{1}{X}\right)^2 - 2 \left(\frac{1}{R} + \frac{1}{X}\right)$$

This expression has the form of a quadratic binomial ($ax^2 + bx + c = 0$), which if you remember from your school maths lessons has the general solution of $\frac{-b \pm \sqrt{b^2 - 4ac}}{2a}$

The problem is if the term $4ac$ turns out to be larger than b^2 , then we have the square root of a negative number. We can't simply ignore this. This is applied mathematics based on real components, so such results exist in real life.

Leonard Euler (*1707 - †1783) gave the term “i” for the quantity $\sqrt{-1}$, but as “i” can be confused with the symbol for current, in electronics we use “j” instead.

Any relationship including $\sqrt{-1}$ is a complex number with a real part and an imaginary part. The word “imaginary” somehow implies that the term does not really exist, which is not true. It is maybe more helpful to think of a number line of real numbers from $-\infty$ to $+\infty$ with imaginary numbers placed at 90° also going from $-\infty$ to $+\infty$ in the imaginary plane:

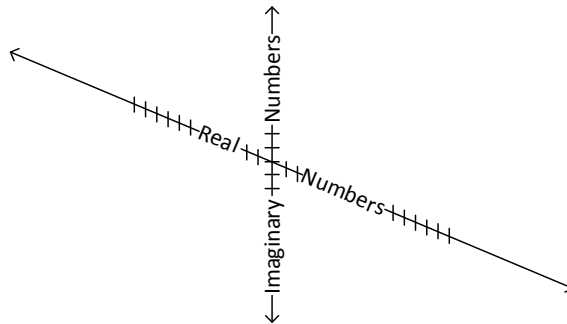


Fig. 4.5: number line representation of a complex number

If we now spin the imaginary number line around the real number axis, we get this image:

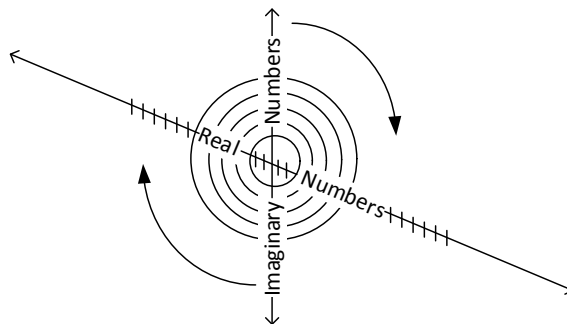


Fig. 4.6: Fig 4.5 with the J axis rotated

Does this look familiar? Maybe like the typical image of the field surrounding a straight wire? And Lo and behold! Maxwell’s electromagnetic field equation can be written in the form of:

$$\text{Eq. 4.3: } \mathbf{F} = \sqrt{\epsilon_0} \mathbf{E} \pm j\sqrt{\mu_0} \mathbf{H}$$

Where \mathbf{F} is the combined EM field created by the combination of the \mathbf{E} electric and \mathbf{H} magnetic fields. In the case of magnetics, the fact that the imaginary part has both a positive and a negative solution is not relevant; we can choose just the positive or the negative part as they are symmetrical.

In other situations, the \pm terms are not equivalent: when Equation 4.3 is applied to light transmission, for example, then the positive and negative terms are more commonly called right and left circularly polarized light.

In general, we can simplify the description of the rectangular form reactance vector diagram into a much neater complex number representation: $\mathbf{Z} = \cos\phi |\mathbf{Z}| + \sin\phi |\mathbf{Z}|j \rightarrow R + jX$

The beauty of this notation is that it allows us to extend the familiar Ohm's Law relationships from DC to AC situations (from resistances to reactances) and to use traditional solutions such as Thevenin's Theorem to analyse component networks.

Ohm's Law (DC)	$V = IR$	$R = V/I$	$I = V/R$
Ohm's Law (AC)	$V = I(R + jX)$	$(R + jX) = V/I$	$I = V/(R + jX) = V(R + jX)/(R^2 + X^2)$

Adding reactances together becomes simpler because the results are always in the form of $\mathbf{Z} = R + jX$, for example, the reactance of an inductor, capacitor and resistor placed in series becomes:

Eq. 4.4: $\mathbf{Z}_{L+C+R} = R_{L+C+R} + j(X_L + X_C)$

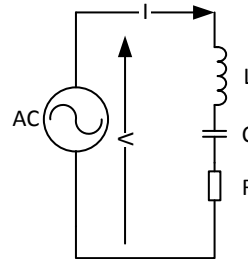


Fig. 4.7: LCR network

To also show how useful this notation is, let us take the network shown above which is a resonant tank and work out its response. As the network is in series, the current flowing through all three components must be the same.

At resonance, the L and C reactances cancel out, so the peak current, I_0 , flowing through the network is simply $|V|/R$ (assuming that R is much larger than the capacitor ESR and the inductor DCR). At other frequencies, the current I that flows through the network is:

Eq. 4.5:
$$\frac{I}{I_0} = \frac{|V|/|Z|}{|V|/R} = \frac{R}{|Z|} = \frac{R}{\sqrt{R^2 + (2\pi fL - 1/2\pi fC)^2}}$$

The magnification factor, Q , determines how quickly the current decreases away from the peak at the resonant frequency. It is defined as X_0/R where X_0 is the reactance of the network at resonance, $\sqrt{L/C}$

If the results of Equation 4.5 are plotted with different Q values, we get the following typical curves:

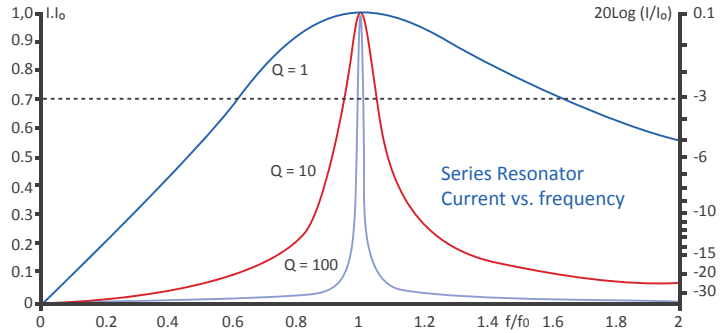


Fig. 4.8: Example of a series resonant current plot with different Q values.

Thus we can calculate in advance the response of our resonant tank circuit without actually having to build it and determine the optimum Q factor experimentally.

Chapter 5

Passive Components

5.1 Capacitors

Capacitors play an important part in AC power supplies because the input voltage drops to zero twice during every AC mains cycle. An energy storage element is usually needed to keep the power supply running (although there are AC powered LED drivers that allow the output to fail at every zero crossing as a 100Hz or 120Hz LED flicker is not perceptible to most people). An inductor can be used to effectively store current in the form of its magnetic field, but capacitors are needed to store DC voltage in the form of the electric field between its electrodes.

In addition, AC filter capacitors are needed between the line inputs and between line and ground for EMC and surge protection. As such, they are classed as safety critical components.

5.1.1 Class X and Y capacitors

AC filter capacitors are typically ceramic disc or metallized film. Both of these constructions are symmetric and work equally well with either voltage polarity. A ceramic disc capacitor consists of two metal electrodes separated by a ceramic dielectric substrate. This gives a very stable capacitance value over a wide operating temperature range, but limited capacitance in the range of Pico farads to tens of Nano farads. Multiple layers can be used to increase the insulation, so withstand voltages in the range of 1kV up to 15kV are available, as are SMD versions.

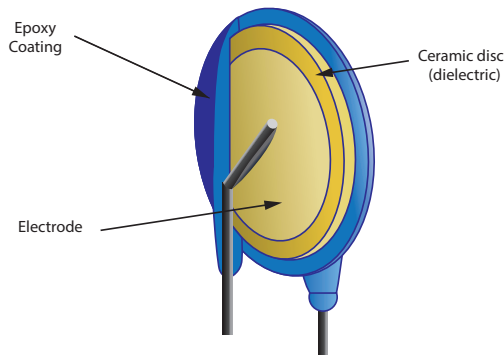


Fig. 5.1: Ceramic disc capacitor

Metalized film capacitors use many layers plastic film insulators which are coated on one or both sides with a metal film to make the electrodes. There are many different plastic films that can be used but PTFE, polypropylene and polyester are the most common. As many layers can be interleaved, high capacitance values are possible (Nano farads to tens of microfarads),

but they can become very bulky with both high rated voltage and high capacitance values. Film capacitors also have inherently low ESR and ESL values which makes them also suitable for snubber and filtering applications. Film capacitors are almost exclusively available as through-hole mounting only.

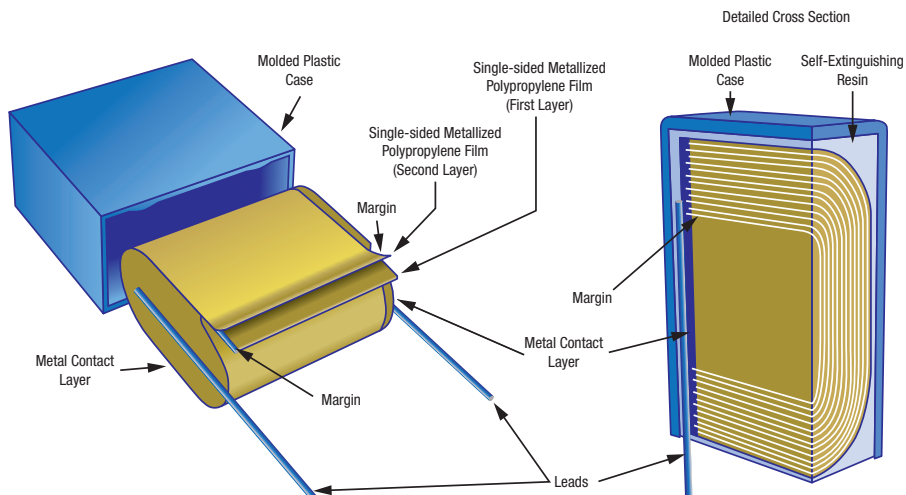


Fig. 5.2: Film capacitor construction (source: Kemet)

A class X capacitor is designed to go across a mains input (from line to neutral or from phase to phase). It is assumed that there is some form of current limiting in the supply, such as a fuse or over-current trip, so if the capacitor fails short circuit the protection device will open. Therefore, X class capacitors are designed to fail short circuit because as long as the capacitor does not catch fire or ignite any other adjacent components, it will then fail safe.

A class Y capacitor is designed to go from line to ground (class 1 power supplies), line to a zero potential (class II power supplies) or across the isolation barrier from primary to the secondary side. A short circuit would lead to hazardous voltages appearing on the zero potential or secondary side connections, so they are designed to fail open circuit. For many applications, a double fault must not cause an unacceptable hazard, so for medical and household applications, two Y-class capacitors in series are specified across the isolation barrier or from line to ground/zero potential.

You might wonder how you can design the failure mode of a capacitor? The answer is in the internal construction. If an arc-over occurs due to an over-voltage event or a mechanical failure such as a pinhole in the insulation, X-class capacitors tend to fuse together, shorting the electrodes, while a Y-class capacitor has thinner conductors that will locally evaporate away and break the conduction path. They are thus said to be self-healing. A Y-class capacitor can be used in place of an X-class capacitor, but not the other way around. However, there are so-called safety capacitors that are rated for both X-class and Y-class applications. The marking will indicate the appropriate voltage ratings for each type of application class.

Both X-class and Y-class capacitors are classified according to their peak or rated operating voltage and over-voltage withstand ability as defined by IEC 60384-14:

Class	Peak Voltage	Over-voltage withstand ability
X1	$\leq 4\text{kVDC}$	$4\text{kV per } C \leq 1\mu\text{F}$ or $4/\sqrt{C} \text{ kV per } C > 1\mu\text{F}$
X2	$\leq 2.5\text{kVDC}$	$2.5\text{kV per } C \leq 1\mu\text{F}$ or $2.5/\sqrt{C} \text{ kV per } C > 1\mu\text{F}$
X3	$\leq 1.2\text{kVDC}$	None

Class	Rated Voltage	Over-voltage withstand ability
Y1	$\leq 500\text{VAC}$	8kV
Y2	$\leq 300\text{VAC}$	5kV
Y3	$\leq 250\text{VAC}$	None
Y4	$\leq 150\text{VAC}$	2,5kV

Table 5.1: X-Class and Y-class capacitor ratings

Another use of film capacitors is in tuned filter and resonance circuits, phase shifters and power factor correction circuits. The inherently low parasitic inductance and low ESR makes the frequency response very stable and the capacitance value tolerances remain linear over a wide range of operating temperatures, simplifying the design parameters.

5.1.2 Electrolytic Capacitors

As mentioned previously, the other main function of capacitors is to store energy. Electrolytic capacitors are almost exclusively used as the bulk storage capacitors in AC/DC converters due to their high volumetric efficiency, high voltage and temperature rating and low cost. The downside is that electrolytics are polarized (DC only), so they can only be used after the rectification stage and that they can explosively fail if the electrolyte overheats and starts to evaporate.

The internal construction is similar to the foil capacitor, except with a liquid or solid (polymer) dielectric, so that they have much in common with a battery cell construction. For example, Supercapacitors are low voltage capacitors with very high capacitance (several Farads) which are a cross-over between a rechargeable battery and a capacitor. The most common electrolytic capacitor is the aluminium type that uses aluminium oxide (Al_2O_3) as the liquid electrolyte

between foil electrodes which have an etched surface to increase their effective surface area. This allows a high capacitance volume CV product with low ESR (equivalent series resistance), both important factors for bulk storage capacitors.

5.1.2.1 Design considerations of electrolytic capacitors.

Q: When is a low-ESR 100 μ F electrolytic not a low-ESR 100 μ F capacitor? Answer: when it is operated with a high frequency DC ripple. As the frequency increases beyond around 1 kHz, the effective capacitance decays. If the capacitor is used to smooth rectified mains frequency, then the datasheet capacitance value can be reliably used. However, if the capacitor is used in the PFC circuit operating at a higher switching frequency (typically 100 kHz), then a 450VDC 100 μ F capacitor will act like a 60 μ F capacitor.

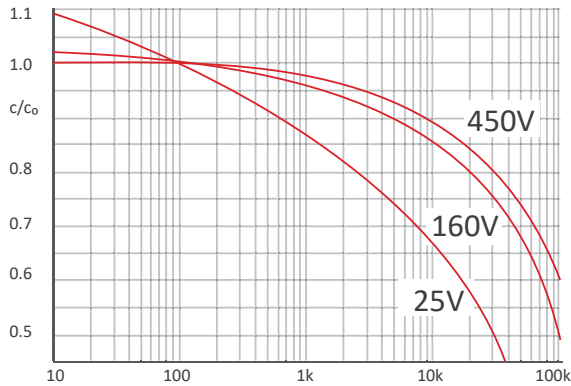


Fig. 5.3: Electrolytic capacitance vs frequency.

Question: When is a low-ESR 100 μ F electrolytic not a low-ESR 100 μ F capacitor?

Answer: when the ambient temperature is not 25°C. At low temperatures, the liquid electrolytic becomes viscous and less conductive, so the ESR increases and the capacitance decreases. At high ambient temperatures, the capacitor expands, effectively increasing the separation between the electrodes, so the capacitance increases. A 100 μ F capacitor at 25°C will be a 62 μ F capacitor at -40°C and an 110 μ F capacitor at 105°C.

(Note: polymer electrolytics do not exhibit this effect)

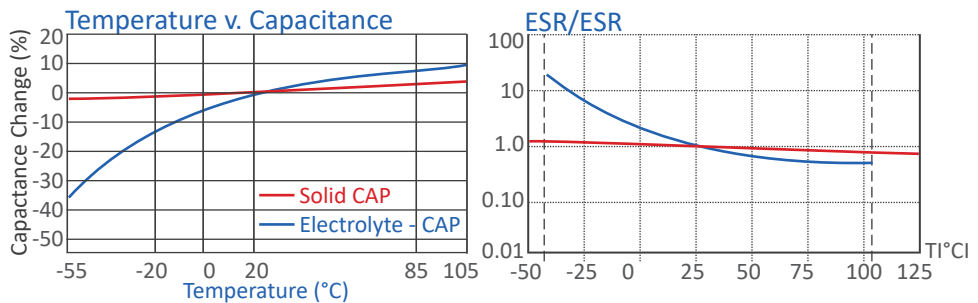


Fig. 5.4: Electrolytic capacitance vs temperature and ESR vs temperature

The equivalent series resistance, ESR, has three main components: the ohmic resistance of the connections ($\approx 10\text{m}\Omega$) plus the frequency dependent resistance of the dielectric oxide layer, called the dissipation factor, Dox , plus the temperature dependence of the electrolyte, $\text{Re}[T]$ which is typically:

$$\text{Eq. 5.1: } R_e [T] = R_e [25^\circ\text{C}] 2^{-\left[\frac{T-25}{40}\right]^{0.6}}$$

The combination of the first two factors (ohmic resistance and frequency dependence) gives the blue line in the diagram above that will also change with temperature according to the third factor (dissipation factor). The equivalent series inductance, ESL will also vary, but this effect is minor and can usually be ignored.

Question: When is a low-ESR $100\mu\text{F}$ electrolytic not a low-ESR $100\mu\text{F}$ capacitor?

Answer: When the capacitor is old. As an electrolytic capacitor ages, the liquid electrolyte dries out and the ESR and equivalent series inductance, ESL, increases while the capacitance decreases. The definition of the end of useful life is when the ESR, ESL or capacitance fall outside of their respective limits. This does not mean that the capacitor will immediately fail, but the higher dissipation will gradually increase the internal temperature until failure is inevitable...

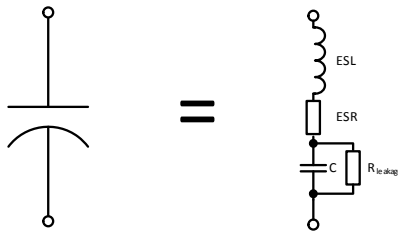


Fig. 5.5: Electrolytic capacitor equivalent circuit

The tan-delta figure is thus an important indicator of capacitor reliability:

$$\text{Eq. 5.2: } \tan \delta = \frac{ESR}{ESZ} = 2\pi f C ESR, \text{ where } C \text{ is the ideal capacitance (} R_{\text{leakage}} \text{ ignored)}$$

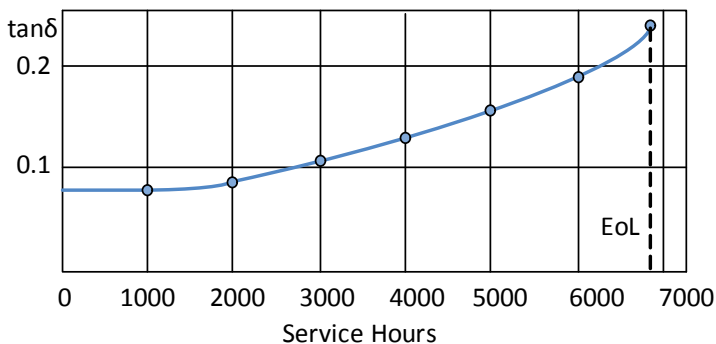


Fig. 5.6: Typical Electrolytic tanδ vs service hours

From figure 5.6 it can be seen that after around 6800 operating hours, a typical 100µF capacitor operated at its limits will have become a 75µF capacitor and the ESR/ESZ ratio ($\tan \delta$) will have increased by a factor of 3.5.

Bearing in mind these aging effects with electrolytic capacitors, it is vital to ensure reliability-by-design by derating the operating conditions to give an increased lifetime. Despite the graphs shown above, it is easily possible to have a 20 year lifetime of an electrolytic capacitor when it is not overstressed.

5.1.2.2 Electrolytic lifetime calculation

The electrolytic capacitor manufacturer's datasheet will specify a lifetime under maximum stress conditions (maximum voltage and temperature); therefore any reduction in the operating stress will increase the lifetime according to various multiplication factors:

Eq. 5.3:
$$L = L_0 K_T K_R K_V$$

Where:

L is the service lifetime in hours

L_0 is the datasheet lifetime at maximum ripple and full temperature limit and voltage stress.

K_T is the temperature factor, $2^{\frac{T_0 - T_A}{10}}$, where T_0 is the temperature limit and T_A is the temperature in the application.

For example, if the T_0 temperature is 105°C and the T_A temperature is 70°C, then the K_T lifetime multiplier is x11.3.

K_R is the ripple current factor, $K_i 1 - \left(\frac{I_A}{I_R}\right)^2 \frac{\Delta T_0}{10}$, where I_A is the ripple current in the application, I_R is the maximum ripple limit, ΔT_0 is the internal temperature rise and K_i is an empirical safety factor in the range of 2 to 4.

For example, if the ripple is kept to half of the maximum ripple limit, the internal temperature rise kept below 5°C and the safety factor is chosen to be 2, then the K_R lifetime multiplication factor is x1.3

K_V is the voltage factor, $\left(\frac{V_A}{V_R}\right)^{-n}$, where V_A is the operating voltage, V_R is the maximum rated voltage and n is an exponent that is either:

$n = 2.5$ (V_A to V_R ratio more than 50%)

$n = 5$ (V_A to V_R ratio more than 80%).

For example, if the operating voltage is 0.9 of the rated voltage, then $n = 5$ and the K_V lifetime multiplication factor is x 1.7.

Thus the calculated service lifetime, $L = 7000 \times 32 \times 1.3 \times 0.6 = 174,000$ hours or nearly 20 years when all of the lifetime multipliers are taken into account.

To simplify such electrolytic capacitor lifetime calculations, RECOM offers an on-line calculator tool on its website (www.recom-power.com)

It is useful to play around with the data in the lifetime calculator to see how small changes in the operating conditions can affect the lifetime:

For the example given above:

$$L = L_0 K_T K_R K_V = 7000 \times 11.3 \times 1.3 \times 1.7 = 20 \text{ years.}$$

However:

Changing the maximum voltage from 90% rated to 80% rated increases the lifetime to nearly 36 years. Changing the maximum ambient temperature from 70°C to 85°C reduces the lifetime from 20 years down to only 7 years. Changing the ripple current from 50% rated to 60% rated reduces the lifetime by only 6% (from 174 khrs down to 167.5 khours), but changing it to 100% rated current loses nearly 4 years off the lifetime.

Component selection is often a compromise between performance and cost, so by careful design, the optimal price/specification benefit can be realized.

5.1.2.3 Deriving ripple current from E-cap temperature rise

It is also often very difficult to find out the capacitor ripple current. Adding even a 10mOhm shunt resistor to measure the current can seriously affect the measured result if the ESR of the capacitors is also around 10mOhm. An alternate method is to derive the ripple current based on the temperature rise and volumetric thermal conductivity of the capacitor.

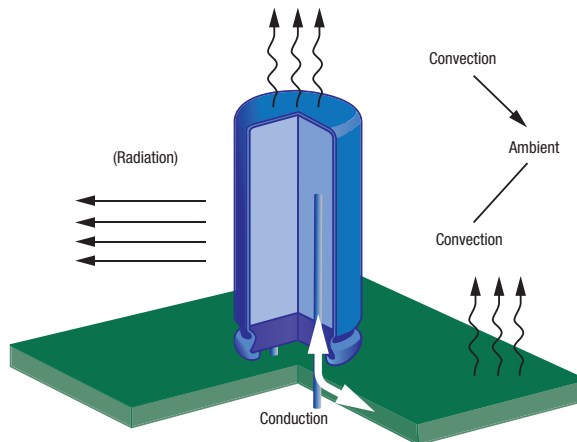


Fig. 5.7: Heat extraction paths from a cylindrical PCB-mounted capacitor

Heat generated inside a capacitor can be dissipated to the surroundings by radiation, convection or conduction. Black body radiation contributes only a small amount to the overall thermal performance of the capacitor at sea level air pressure and can be ignored in most practical cases. Free air convection cooling is dependent on the surface area and ambient temperature difference. Conduction cooling is via the pins into the PCB which then acts a large flat area heatsink to transfer the heat to the surroundings via convection. Due to the construction of a typical electrolytic capacitor, the thermal path between the foil electrode layers and the connection pins is less than ideal and conduction cooling from the core through the pins can also be largely ignored.

This leaves convection cooling as the primary mechanism for heat dissipation.

Step 1. Calculate the free surface area. A cylinder has a side surface area of $2\pi rh$, where r is the radius and h is the height of the cylinder. The top of the cylinder has an area of πr^2 . Together they give the exposed surface area as:

$$\text{Eq. 5.4: } SA_{cap} = \frac{\pi\left(\frac{D}{2}\right)^2 + \pi Dh}{100}$$

Where SA_{cap} is the surface area of a capacitor in cm^2 with diameter D in mm and height h in mm.

Step 2. Calculate the internal power dissipation

The ripple current dissipates energy in the equivalent series resistance, ESR, of the capacitor. This value can be found from the E-cap datasheets. The dissipated energy will cause a temperature rise in the core of the capacitor.

$$\text{Eq. 5.5: } P_{diss} (mW) = 1000 F_e K_{SB} SA_{cap} T_{rise}^4$$

Where P_{diss} is the power dissipated in the E-cap core, F_e is the emissions factor (typically 0.95 for free air convection), K_{SB} is the Stefan Boltzmann's Constant ($5.56 \times 10^{-8} \text{ Wm}^2\text{K}^4$) and T_{rise} is the temperature difference between ambient and the top centre point of the capacitor. The ripple current that causes this temperature rise is:

$$\text{Eq. 5.6: } I_{ripple} (A) = \sqrt{\frac{P_{diss}}{1000 ESR}}$$

Practical Tip: In the introduction to this section, it was stated that heat transfer from the capacitor through the pins into the PCB can largely be ignored. This is valid for heat transfer from the capacitor core out into the PCB copper tracks as the thermal impedance is higher from the core through the pins to the PCB than directly from the core to the capacitor case. However, if there is an external source of heat, for example a power diode placed close to a capacitor, then the low thermal impedance copper PCB tracks can transfer sufficient heat back into the capacitor via the pins to significantly add to the thermal load inside the capacitor and reduce its lifetime. Another "unexpected" source of internal heat generation can be varying external magnetic fields. Both electrolytic and foil capacitors are often placed very close to inductors,

chokes and transformers. Any stray AC magnetic fields can generate eddy currents in the metallized foil conductors which will increase the core temperature and reduce lifetime.

5.2 Common Mode Chokes

Inductors are specified with a maximum continuous RMS current, I_{RMS} , and a maximum peak current, I_{SAT} . The I_{RMS} current is usually defined as that causing a 40°C rise in the core temperature. Two losses contribute to the temperature rise: the copper loss in the windings = $DCR \times I_{RMS}^2$ and the magnetic core loss which is frequency and duty cycle dependent. In a common mode choke (CMC) input filter configuration, the flux from the two windings cancel out, making the I_{SAT} figure largely irrelevant.

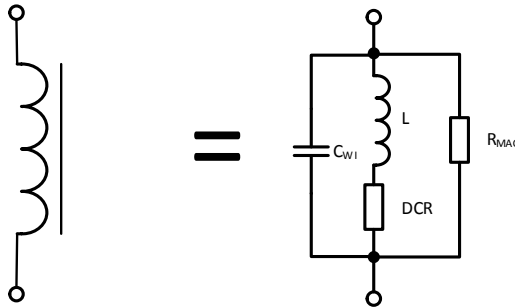


Fig. 5.8: Inductor equivalent circuit. DCR is the ohmic resistance of the winding, RMAG is the magnetic core loss (represented as a resistance) and CWI is the winding capacitance.

The rated operating voltage is also important if the inductor is used as a common mode choke on the input side as the two windings carry the full mains input voltage across them. The rated voltage must be sufficient over the entire operating temperature range. It is often necessary to insulate the conductive ferrite core and put a separator between the two windings to guarantee the creepage and clearances so that there is no flash-over.

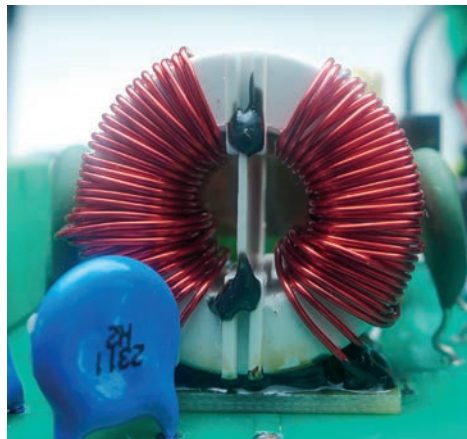


Fig. 5.9: Toroidal common mode choke with insulation and separator

The impedance of a CMC increases with increasing frequency until it reaches a peak at the self-resonant frequency (SRF), then it declines due to the effect of the interwinding capacitance. The SRF should be chosen to be close to the frequency of the maximum noise interference (usually the switching frequency or a multiple thereof) to give the largest attenuation.

$$\text{Eq. 5.7: } SRF = \frac{1}{2\pi\sqrt{L C_{WI}}}$$

Where SRF is the self-resonant frequency (assuming DCR is low and R_{MAG} is high)

5.2.1 EMC Common Mode Filter worked example

Power supply specification: 100W, 115 – 230V supply, 45 kHz switching frequency, 85% efficient flyback design.

Step 1. Determine the probable noise level

The circuit switches at 45 kHz with a 50% duty cycle at full load. This will generate a fundamental noise peak at 45 kHz with harmonics at higher frequency intervals of $n f_0$, where $n = 1,3,5,\dots$ decreasing in intensity with $-20\text{dB}\mu\text{V}/\text{decade}$. Frequencies below 150 kHz are ignored by the industrial EMC standards, so we need only concern ourselves from the fifth harmonic at $5f_0$ or 225 kHz and above. If we assume a 1V drop across the diode bridge, then the fundamental frequency will have an amplitude:

$$\text{Eq. 5.8: } A_0 = 20 \log \frac{1}{1\mu\text{V}} = 120 \text{ dB}\mu\text{V}$$

And the 5th harmonic will have an amplitude of

$$\text{Eq. 5.9: } A_n = 20 \log \frac{4}{n \pi 1\mu\text{V}} = 108 \text{ dB}\mu\text{V} \text{ (for } n = 5)$$

Step 2. Determine the filter attenuation

The required attenuation is equal to the noise amplitude (first odd harmonic above 150 kHz) minus the EN55011 EMI QP limit (65 dB μ V) plus a 3dB safety margin. For our example, the attenuation, A, at the fifth harmonic needs to be $108 - 65 + 3 = 46 \text{ dB}\mu\text{V}$.

Step 3. Find the filter corner frequency

The filter should attenuate the noise from the fifth harmonic at 225 kHz with a $+40\text{dB}/\text{decade}$ attenuation. This gives a corner frequency of:

$$f_c = f_{n=4} 10^{\frac{-A}{40}} = 225\text{kHz} 10^{\frac{-46}{40}} = 16\text{kHz}$$

Step 4: Determine the maximum AC current

The maximum input current occurs at full load with the minimum input voltage (115VAC $-10\% \approx 103\text{VAC}$). The input current will then be $(100/0.85)/103 = 1.14\text{A}$

Step 5: select a suitable common mode choke and the X and Y capacitors to make up the filter as shown below:

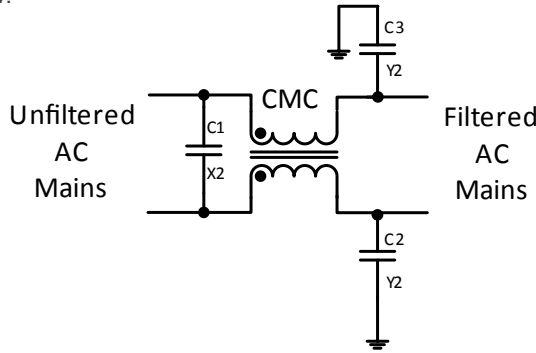


Fig. 5.10: Basic AC input filter

As the application is a universal mains filter, the choke needs to be rated for 250VAC operation. From step 4, we need a current rating of 1.14A or higher. From step 3, it should have a peak attenuation close to 225 kHz.

We could choose a 5mH choke rated at 250VAC, 2A @ Tamb + 40°C for example. The high common mode inductance will give an attenuation curve that peaks at around 0.2MHz, which is ideal. The stray inductance is typically 1%, i.e. 47µH

The X-capacitor reacts with the stray inductance to make a differential mode filter:

$$C_x = \frac{1}{8\pi^2 L_{\text{stray}} f_c^2} = \frac{1}{8\pi^2 47\mu\text{H} 16\text{kHz}^2} = 1\mu\text{F}$$

The Y-capacitors react with the common mode inductance to make a common mode filter:

$$C_y = \frac{1}{8\pi^2 L_{\text{cm}} f_c^2} = \frac{1}{8\pi^2 5\text{mH} 16\text{kHz}^2} = 10\text{nF}$$

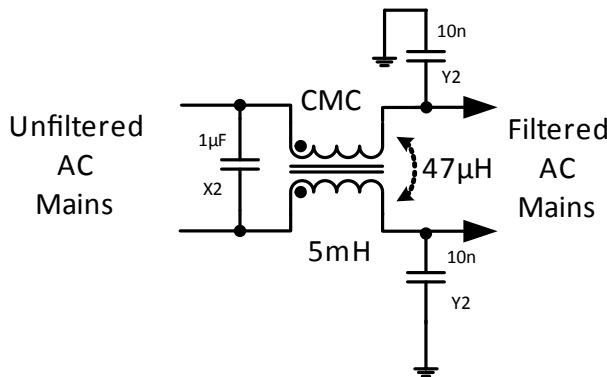


Fig. 5.11: Initial Design of the EMC Filter

It must be stressed that the above calculation is not sufficient to guarantee an EMC test pass. It is just a first step to allow a test set-up to be made.

Practical Tip: It is often quite difficult to find a common mode choke with enough stray leakage inductance to keep the size of the X-capacitor reasonable. It is often worth using either using a differential mode choke in series with the common mode choke or using a hybrid choke which incorporates elements of both DM and CM types in one body.

Chapter 6

Active Components

6.1 Silicon MOSFET

The metal oxide silicon field effect transistor (MOSFET) is the workhorse of the majority of AC/DC circuits. The basic construction is simple with a gate insulated from the body by a thin metal oxide layer. The source and drain regions are heavily doped (n+ and p+) so that there is a semiconductor barrier to the flow of charge. When a gate-source voltage higher than the threshold voltage is applied, this barrier is overcome and current flows freely:

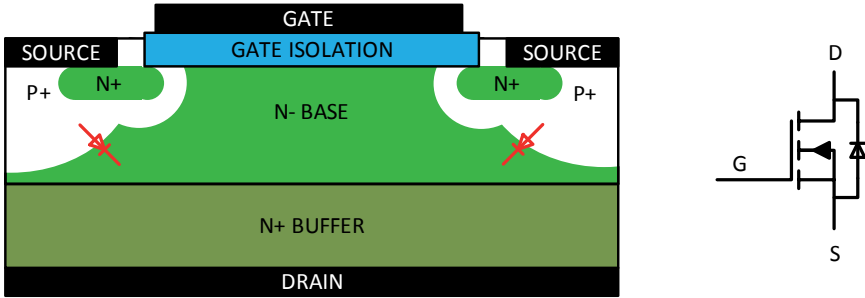


Fig. 6.1: Basic construction of a planar epitaxial n-MOSFET

Integral to the MOSFET's construction is a body diode formed from the PN junction between the P+ and N- interface (shown in red in the figure). This means that a MOSFET can only be used to switch unipolar voltages. However, in some applications, the body diode is useful as a freewheeling diode to conduct negative voltages across a MOSFET that is switched off.

The equivalent model shows the various parasitic elements that affect the switching performance:

- L_{gate} , L_{drain} and L_{source} are the lead impedances
- R_{gate} is the gate resistance
- R_{DSon} is the drain source resistance when fully enhanced
- C_{miller} is the gate-drain capacitance
- C_{GS} is the gate-source capacitance
- C_{oS} is the drain-source capacitance equal to $(C_{DS} + C_{miller})$
- C_{oss} is the overall output small signal capacitance

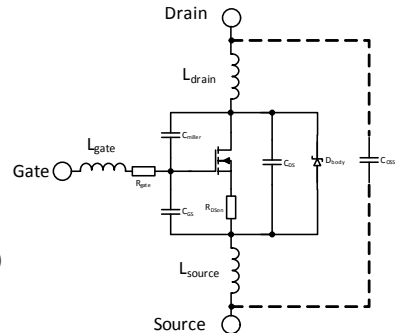


Fig. 6.2: MOSFET equivalent switching model

The turn-on characteristic of a MOSFET can be divided into 4 stages:

- Stage 1. The gate turn-on voltage is applied. C_{gs} is charged up via L_{gate} and R_{gate} . The transistor is still off.
- Stage 2. The gate threshold voltage, V_{th} , is reached. I_D starts to linearly increase proportional to V_{gate}
- Stage 3. The Miller plateau is reached. The I_D is at maximum and V_{DS} is starting to decrease. The gate voltage remains constant as any excess gate current is diverted to charge up the miller capacitance.
- Stage 4. V_{DS} has almost reached its minimum ($V_{DS,min} = I_D R_{DSon}$) and the gate voltage can now rise further, fully enhancing the transistor and reducing the R_{DSon} to its minimum value.

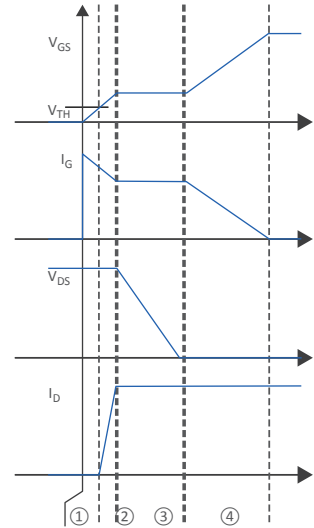


Fig. 6.3: MOSFET Turn-on Characteristic

The turn-off characteristic is essentially the same process in reverse:

- Stage 1. The gate turn-off voltage is applied. C_{gs} and C_{gd} are discharged via R_{gate} . The transistor is still on.
- Stage 2. C_{miller} is now fully discharged and the negative gate current can now start to deplete the charge on C_{GS} , turning off the transistor. V_{DS} starts to linearly increase while V_{gs} remains constant.
- Stage 3. V_{DS} is now at the supply voltage and I_D starts to decrease. The gate voltage can decrease further as C_{DS} is now fully discharged.
- Stage 4. The transistor is fully off as V_{gate} is now below V_{TH} . The remaining time is just to fully discharge any parasitic gate capacitances.

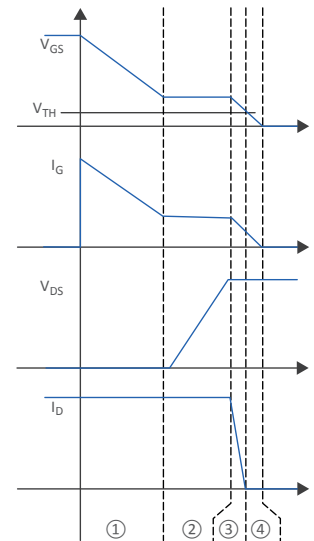


Fig. 6.4: MOSFET turn off characteristic

Practical Tip: As can be seen from the turn on and turn off characteristics, there are periods when the voltage across the transistor and the current through the resistor are in transition. One dangerous area is turn off, stage 2. The output voltage is ramping up and this dv/dt will feed back through the miller capacitance and attempt to pull up the gate voltage. If the effective gate drive impedance is too high, the transistor can switch itself back on again!

A similar effect can occur during switch on, stage 2. The drain current is ramping up which can cause the drain voltage to rise up due to inductances in the drain to ground path (ground bounce). This will reduce the effective V_{GS} voltage and could turn the transistor back off again.

See the final section in this chapter (Use of Kelvin contacts) for considerations to reduce or eliminate these effects.

During these stage 2 and stage 3 transition periods, the transistor is behaving as a variable resistor and dissipating a lot of power. When the transistor is fully off, only leakage currents flow and when the transistor is fully on the main loss is through the R_{DSON} resistance, which is typically in the region of mOhms and also very low. However, during repetitive on-off transitions, the power dissipation will be much higher than in the fully on condition.

A simplified gate drive and switching loss calculation is shown below:

$$\text{Eq. 6.1: } P_{gate,on} = \frac{1}{2} f_{sw} Q_{gate} V_{gate} \frac{R_{DS,on}}{R_{DS,on} + R_{gate,on}}$$

$$P_{gate,off} = \frac{1}{2} f_{sw} Q_{gate} V_{gate} \frac{R_{DS,off}}{R_{DS,off} + R_{gate,off}}$$

Where Q_{gate} is the total charge needed to charge the gate capacitances.

The power dissipation in the transistor is dependent on the transition times:

$$\text{Eq. 6.2: } P_{sw} = \frac{V_{Supply} I_L}{2} \cdot \frac{t_{stage 2} + t_{stage 3}}{T}$$

Where I_L is the load current and $t_{stage 2} / t_{stage 3}$ is the time spent in stages 2 and 3 of the total switching time, T , respectively.

With a high current gate drive, these stage 2 and stage 3 times can be reduced, so it is important to use a low impedance gate voltage source. To reduce the switching losses further, the gate voltage can be increased to charge and discharge the gate capacitances more quickly. In particular, if the gate voltage switches to a negative value, the switch-off time can be reduced significantly compared to just switching from above V_{TH} down to zero volts. There is a limit to the gate voltage defined by the breakdown voltage between gate and source, B_{VDSS} . In order to reduce the gate capacitance to a minimum, the metal oxide insulation layer is made very thin, at the cost that the breakdown voltage is then very low ($V_{GS,max}$ is typically $\pm 15-20$ volts).

Another way to reduce switching losses is to reduce the switching frequency, f_{sw} , but this can increase losses in other parts of the circuit or reduce the response time to unacceptable levels. The only other factor remaining is the gate charge, Q_{gate} . A typical low voltage MosFET will have a total gate charge of around 5-10nC, but this value also increases with increased V_{DS} capability. A 700V MosFET will have a total gate charge of around 10-25nC, simply due to the thicker epitaxial layers needed for the higher breakdown voltage strength.

6.2 SiC MOSFET

Silicon Carbide or SiC MOSFETs are increasingly finding new applications in power electronics. Full-bridge and half-bridge circuits for high-voltage applications (several hundred volts) were previously reserved for only the IGBT domain (see next section) because Silicon MOSFETs, especially Super Junction MOSFETs are not suitable for these applications due to the extremely poor parasitic body diode performance; when silicon MOSFETs experience an unwanted turn-on effect, the body diode quickly goes into thermal destruction. Often, even a single false switching operation on the conductive body diode either exceeds the maximum di/dt of the body diode and thus destroys the FET, or the switching operation incites the gate to oscillate, so that the maximum gate source voltage is exceeded and transistor is also destroyed.

SiC FETs use a different substrate with a 10x higher dielectric breakdown strength than Silicon, so the layers can be made thinner to reduce the gate charge and R_{DSon} values. In addition, SiC has a three times better thermal conductivity, so the power handling capacity can be increased in the same sized package.

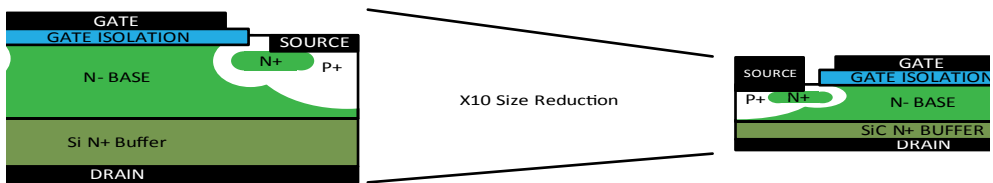


Fig. 6.5: Diagrammatic comparison between Si-MOSFET and SiC-MOSFET construction.

Due to the higher dielectric strength, the SiC substrate can be made up to 10x thinner than the Si Substrate, reducing the body resistance by a factor of up to 1:1000. The thinner layers also reduce the internal capacitances. So, for the same switching frequency, a SiC MOSFET will have around a third to a quarter of the switching losses of an equivalent Si MOSFET. Put another way, a SiC MOSFET can be operated four times faster for the same power dissipation.

SiC FETs also have a far more robust body diode than Si MOSFETs. The maximum switching di/dt of the body diode of super junction MOSFETs is around $60A\mu s^{-1}$ for the latest generation of fast switching MOSFETs up to $900A\mu s^{-1}$ for SJ MOSFETs with ultra-fast body diodes, but these values pale in comparison with SiC MOSFETs with up to $6000A\mu s^{-1}$. The main disadvantage of SiC-MOSFETs is that they are often more expensive than Si-MOSFETs, but this difference will reduce over time (the price difference between a SiC-MOSFET and a superjunction Si-MOSFET is already comparable)

6.3 IGBT

Insulated gate bipolar transistors combine the insulated gate characteristics of MOSFETs with the high current capability of bipolar transistors. It is in effect a voltage controlled transistor:

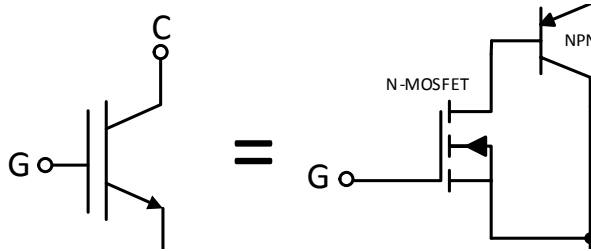


Fig. 6.6: Equivalent model of an insulated gate bipolar transistor (n-channel IGBT)

One of the main differences to a MOSFET is that an IGBT has no body diode, so it will not conduct reverse currents. If an anti-parallel free-wheeling diode is required, then it needs to be added externally.

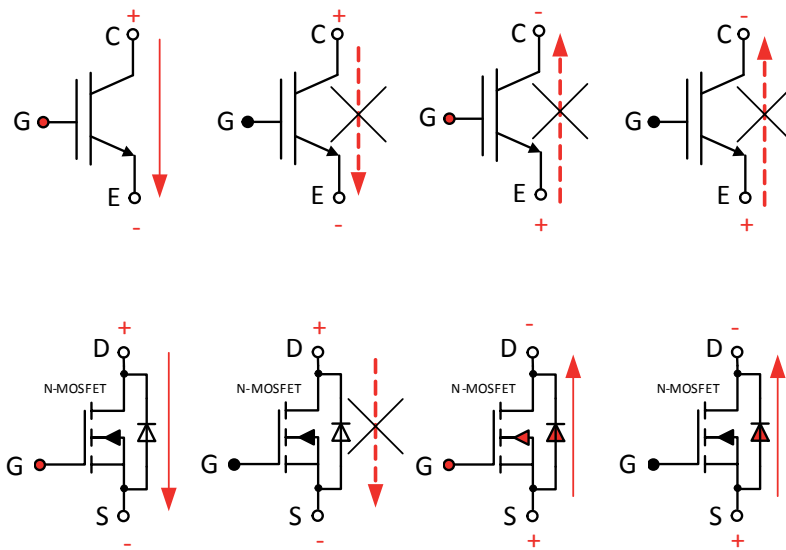


Fig. 6.7: comparison of IGBT and MOSFET blocking capabilities.

Although IGBTs switch on quickly, they switch off more slowly. This is due to an effect called the recombination tail. Once the gate voltage has been turned off, any remaining charge in the transistor body region must be dissipated by recombination of the holes with electrons as there is no terminal to remove them. This process is relatively slow and delays the switch off characteristic:

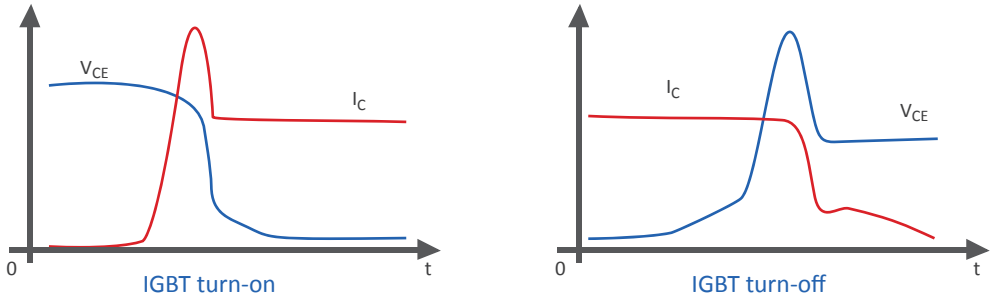


Fig. 6.8: Comparison of the switch-on and switch-off characteristics of an IGBT. The recombination tail in the turn off characteristic slows down the switching speed and increases the power dissipation.

Despite this disadvantage, IGBTs are widely used in power switching for high current / high voltage applications such as motor inverters, power rectifiers and photovoltaic power.

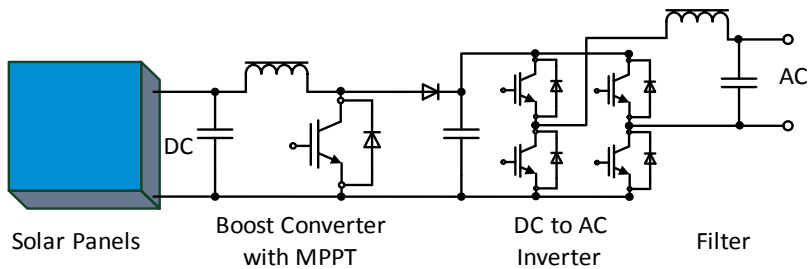


Fig. 6.9: Photovoltaic application using IGBTs for the Maximum Power Point Tracking and for the DC/AC inverter stages.

6.4 GaN HEMT

Gallium Nitride (GaN) semiconductors are High Electron Mobility Transistor (HEMT) devices, a class of transistors with almost perfect switching characteristics. HEMT means that electrons travel within the internal crystal structure as a two dimensional electron gas with very high mobility, thus creating a device with very high conductivity and low $R_{DS(ON)}$. The use of GaN chemistry increases the breakdown voltage which means that the layers within the transistor can be made very thin and close together. This both accelerates the switching speed and reduces the gate capacitance.

The enhancement mode type (E-HEMT) has a depletion zone under the gate which blocks the flow of electrons and requires a positive gate voltage with respect to the source pin to turn on. As the depletion zone under the gate is so thin, very little injected charge is needed to turn the transistor on and off, so switching speeds in the MHz region are possible without incurring high switching losses.

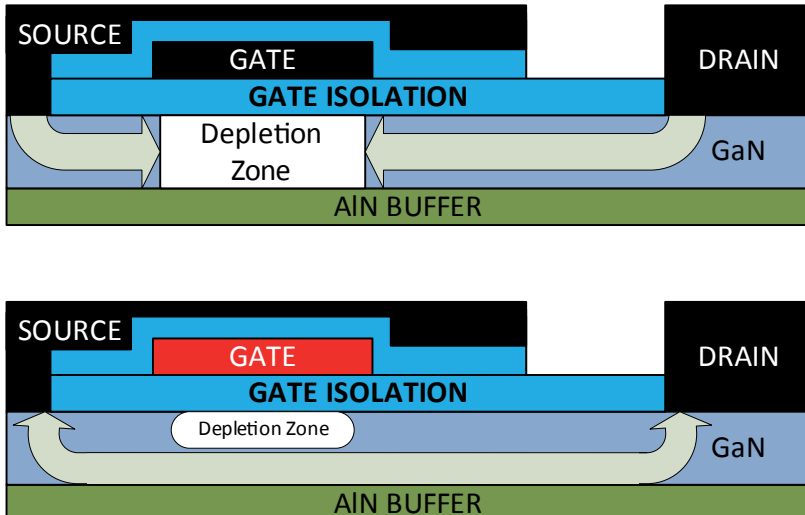


Fig. 6.10: Enhancement Mode GaN Transistor in the OFF (top) and ON (bottom) conditions.

The extreme thinness of the gate isolation layer means that high gate-source voltages will cause an internal flashover, even though the material itself has a high breakdown voltage rating. A GaN E-HEMT has a typical full enhancement voltage of 7V but will be damaged if the VGS exceeds $\pm 10V$, much lower than the gate voltages that are typically used in IGBT or SiC gate drivers. Due to the extremely fast rise and fall times of the low-capacitance gate channel, any excessive inductance in the external gate drive could cause spikes or voltage ringing and exceed these voltage limits. Therefore a 6V gate drive voltage is a good compromise between high efficiency and staying within a safe operating area.

IGBT or SiC gate drive circuits also typically turn off with a negative gate drive voltage. This speeds up the charge extraction from the gate capacitance and therefore the switch-off time. GaN Transistors have such low gate capacitance that a negative gate drive is not necessary. A gate voltage of 0V will completely and reliably turn off the HEMT in nanoseconds.

Only if the layout has excessive inductance would a negative gate drive offer protection against unintentional turn-on caused by ringing. However, as HEMT do not have a body diode like a MOSFETs and are symmetrically conductive devices, a negative gate voltage will increase reverse conduction losses. A single ended 6V gate drive voltage is sufficient, although for very high frequency switching applications, a bipolar +6V/-1V is sometimes suggested to account for layout parasitics.

Figure 6.11 shows typical gate driver voltages that are commonly used to drive the switching transistors. The 1st Generation SiC MOSFETS use +20/-5V supplies, but 2nd Generation devices will use +15/-3V supply voltages:

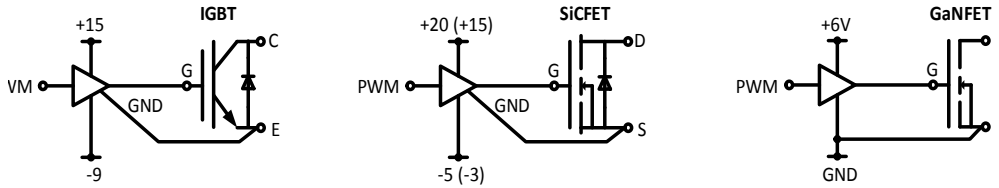


Fig. 6.11: Typical Gate Driver supply voltages for IGBT, SiC and GaN drivers

6.4.1 GAN Transistor gate driver considerations

1. The majority of ultrafast gate drivers ICs have an under-voltage lock-out (UVLO) function that disables the output if the supply voltage is too low. Those meant for IGBT/SiC applications will often have a relatively high UVLO level as they are designed to operate from supply voltages up to 24V. A gate driver that is compatible with the much lower gate voltages used in GaN must be selected.
2. The current needed to charge and discharge the gate capacitance is dependent on the gate capacitance and the rate of change of the gate voltage. Although the GaN gate capacitance is very low, the high dv/dt means that a gate driver with a current drive capability of at least $\pm 0.5A$ (or better 1A sink) is required. This peak current will be supplied from a ceramic capacitor mounted as close to the driver pins as possible, so the average supply current will be much lower (in the tens of milliamps range). The gate driver sink drive should be low-impedance ($< 2\ \Omega$) to reduce the chance of cross-conduction (see next comment).
3. The maximum and minimum pulse widths should be limited to avoid false triggering and interaction with the overlap protection circuit. At 5 MHz operating frequency, this minimum pulse width limits the duty cycle to 90%. At higher frequencies, this limitation becomes more significant and the duty cycle may need to be controlled so that it does not exceed 80%.
4. An ultrafast gate drive design is susceptible to undesired turn-on (cross-conduction) due to parasitic gate driver inductances interacting with the high Miller capacitance discharge current thus creating a ringing oscillation that could send the gate voltage momentarily high again. The slew rates can be limited by a dv/dt limiting resistor to reduce the possibility of this effect.

A turn-on gate resistor in the range of 10-20 Ohms will typically give an 80-40kV/ μ s slew rate. The turn-off resistance should be smaller to reduce the turn-off losses. A Schottky diode with a resistor in parallel with the gate resistor can be used to independently control the turn-on and turn-off slew rates:

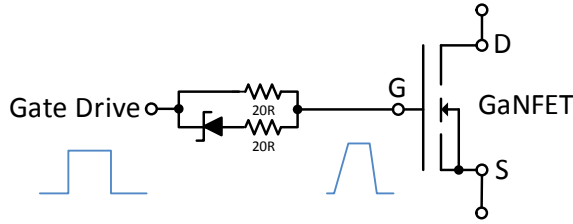


Fig. 6.12: slope control using gate resistors

- High side gate drivers are often implemented with a bootstrap power supply circuit (figure 6.13) Although this means that the same isolated power supply can be used for both high-side and low-side drivers, it has some inherent weaknesses.

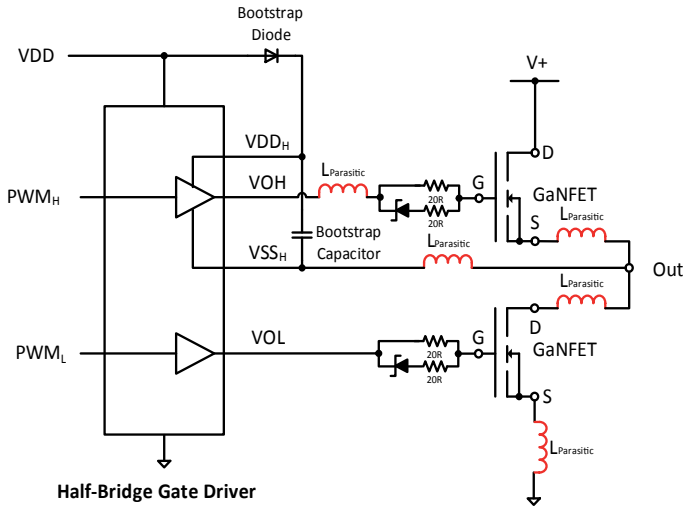


Fig. 6.13: typical high-side bootstrap supply circuit showing unwanted parasitic inductances. For a nominal 6V V_{DD_H} , the bootstrap voltage can vary between 5.5V and 8.5V depending on operating conditions (see text below).

The bootstrap diode must have an ultrafast recovery characteristic. If it cannot switch as quickly as the GaN output then a reverse current will flow back into the VDD supply. Not only will these current spikes affect the lifetime of the diode but the resulting high frequency interference on the supply rail will cause havoc with the EMC compliance. The gate driver bootstrap supply voltage is dependent on the difference between the VDD supply and the capacitively-coupled output (switching node) voltage. This means that the voltage across the bootstrap capacitor can vary by more than $\pm 20\%$ during operation.

There will be a volt drop across the bootstrap diode of around 0.7V meaning a 6.7V VDD would be needed to have a V_{DD_H} voltage of 6V. The switching node voltage may not go completely to the ground voltage during forward conduction, meaning that the effective gate driver

supply voltage may be as low as 5.5V. If the gate driver supply voltage is too low, the GaN HEMT will not be fully enhanced and the conduction losses will be higher.

However it is not advisable to increase the VDD supply voltage because during reverse conduction conditions, the switching node voltage can swing to as much as -2.5V below ground, meaning an effective bootstrap voltage is $+6.7V - 0.7V + 2.5V = 8.5V$. This is getting perilously close to the absolute maximum gate voltage of 10V. In addition, the interaction with the load current and parasitic inductances can cause negative-going spikes to be generated at the switching node by high di/dt transitions. There could be operating conditions where the bootstrap voltage will exceed 10V when the di/dt undershoot spikes are also taken into account.

A more reliable solution is to use a separate galvanically isolated supply for the high-side gate driver. This will ensure a stable gate voltage swing irrespective of the operating conditions.

6. Gate driver inductances can be minimized by good design, but it is more difficult to control the parasitic inductances of the power ground as the layout choices for high current paths are more restricted. Although a low-side switching circuit has common power ground and gate driver ground, any parasitic layout inductances will create ground bounce under high di/dt conditions. For operational safety, it is therefore advisable also to galvanically isolate the low-side drivers as well as the high-side drivers. If the gate drivers are isolated, then the influence of the layout power ground inductances can be eliminated by connecting the gate driver ground directly to the transistor source connection (or to the Kelvin connection if this is supported in the transistor package).
7. The PWM isolator and galvanically isolated DC/DC converter should have low isolation capacitance. The high dv/dt slew rates and switching frequencies possible with GaN devices will stress the isolation barrier, even if the absolute voltage swings are well within the voltage ratings of the components. For high dv/dt applications, the isolation capacitance should be $<4\text{pF}$ for the PWM isolator and $<10\text{pF}$ for the high side DC/DC converter. If a DC/DC converter is also used on the low side to eliminate ground bounce, then the isolation capacitance is not so critical, however an isolation capacitance of $<100\text{pF}$ is desirable.

Practical Tip: Isolated GaN Power Switch.

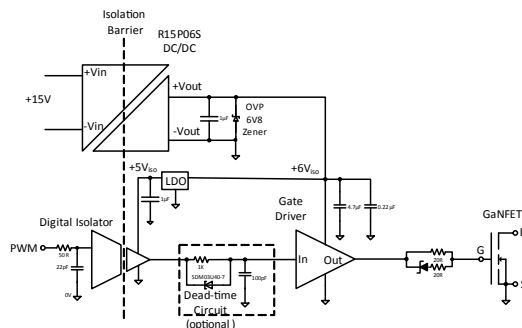


Fig. 6.14: Example of an isolated high side or low side GaN power switch

This floating design uses an isolated DC/DC converter and digital isolator to create a gate driver circuit for a GaN HEMT that could be used as a boost converter, buck converter or buck/boost converter switching application on either the high side or low side. The single-channel digital isolator output stage is powered from a low power LDO regulator connected to the 6V gate driver supply. The UCC27322 high speed driver can deliver up to $\pm 9A$ peak current and the Schmitt-trigger input switches cleanly from the 5V output of the digital isolator. A dead-time delay can be implemented with a simple RC filter.

The lateral construction of GaN transistors also creates the possibility to integrate the gate driver inside the transistor package. This reduces the parasitic gate inductances and allows higher switching frequencies or higher slew rates without the risk of false triggering. Nevertheless, an isolated gate driver power supply and drive signal isolator are still required.

6.5. Power Transistor Layout Considerations

Irrespective of the power transistor type used (see table below), a careful PCB layout is required when switching high voltages and high currents.

Transistor Type	MosFET	SiC	IGBT	GaN
Max. Voltage	Up to 1000V	More than 5000V	More than 5000V	Up to 1000V
Max. Current	Up to 200A	Up to 1000A	Up to 1200A	Up to 50A
Gate Drive	Voltage $V_g = 3-10V$	Voltage $V_g = -3/+15$	Voltage $V_g = -9/+15$	Voltage $V_g = -1/+6$
Switching speed	fast	Very fast	slow	Very, very fast
Cost	Low	Medium	Low	High

Table 6.1. Comparison of power transistor characteristics

The following discussion is based on IGBT switching transistors, but the basic principles are the same for Si-MosFETS, SiC-MosFETS and GaN-MOSFETS.

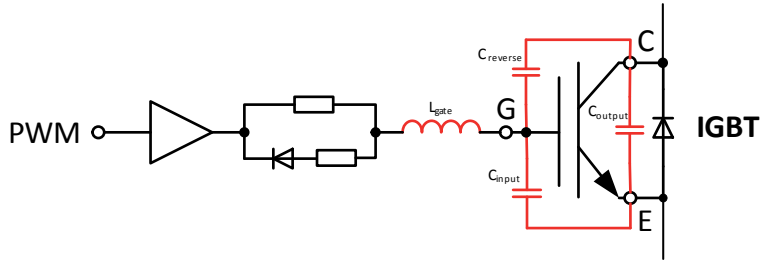


Fig. 6.15: IGBT gate driver with parasitic components and an anti-parallel diode.

The driver circuit must be designed to prevent unwanted turn-on in all operating conditions. Otherwise, this can lead to shoot-through short circuits, which can manifest itself in increased losses, increased component stress, shorter service life, worse EMC and in extreme cases, to the destruction of the transistor.

Essentially we have 2 kinds of unwanted switch-on timing:

- An unwanted turn-on due to the effect of the CGE capacitance ($C_{reverse}$).
- An unwanted turn-on due to the effect of the parasitic inductances (L_{gate} and $L_{emitter}$)

6.5 Unplanned turn-on due to the effect of the Miller capacitance

As the Collector Emitter voltage rises, either when the low-side IGBT is turned off or in a bridge circuit, the high-side IGBT is turned on and current flows through the anti-parallel diode, the Miller capacitance, $C_{reverse}$, must be charged up. The Miller capacitance charging current can be calculated as follows:

$$\text{Eq. 6.3: } I_{C_{reverse}} = C_{reverse} \frac{dV_{CE}}{dt}$$

The Miller capacitance is given in most transistor datasheets, but this is, however, just a rough value. The value of $C_{reverse}$ is strongly voltage dependent and also varies with temperature and current. Most data sheets only define the Miller capacitance under certain ideal conditions, so measuring the value under real operating conditions is strongly recommended.

The following graph shows the effect of VCE on the reverse capacitance:

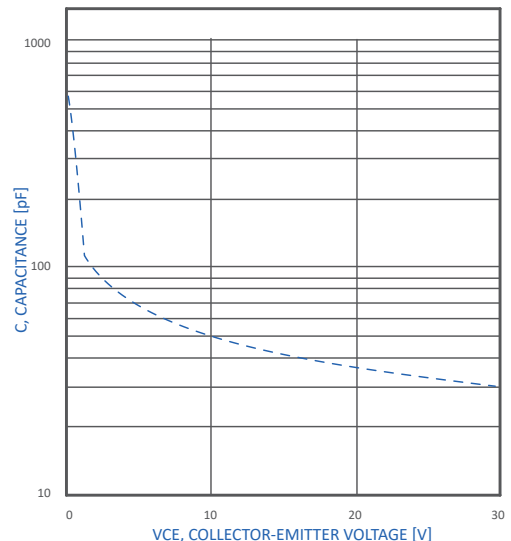


Fig. 6.16: Variation of $C_{reverse}$ with V_{CE} in an IGBT

The additional capacitive load of $C_{reverse}$ will not be a problem for most driver circuits; it only becomes an issue when the Gate-Emitter capacitance C_{input} becomes sufficiently charged by the remaining current flowing from $C_{reverse}$ that the gate voltage can rise so that transistor turns on again.

The charging current of C_{input} can be defined from the following relationship:

$$\text{Eq. 6.4 } I_{C_{input}} = I_{C_{reverse}} - I_{driver}$$

Where I_{driver} is dependent on the gate driver internal impedance, the DC gate resistance and the AC impedance of L_{gate} .

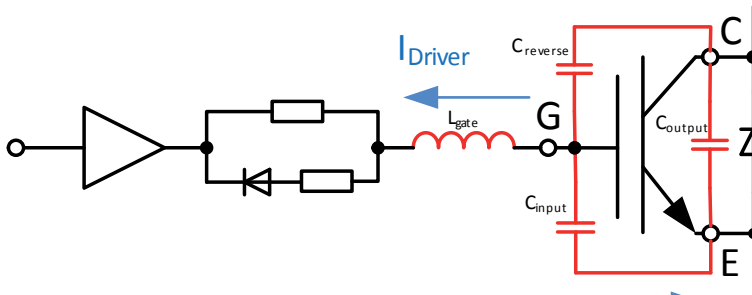


Fig. 6.17: Residual input capacitance charging current

So what measures can be taken to avoid undesired turn-on due to the reverse capacitance current?

- h. Limit the dV/dt . By slowing the rate of change of the V_{CE} voltage, the $C_{reverse}$ current is reduced. However, this means higher switching losses.
- i. Reduce the parasitic inductance L_{gate} . By suitable choice of layout and package, the $C_{reverse}$ current can be diverted away from charging up the gate-emitter capacitance, C_{input} . However, this restricts the design freedom of the PCB layouter.
- j. Use a negative gate emitter voltage. If the driver output goes negative, the gate is held hard off and the safety distance between the gate turn-on threshold voltage and actual gate voltage is increased. Thus an unwanted turn-on is impossible even under worst case dv/dt conditions.
- k. Use GaN HEMTs which have a negligible reverse capacitance.

6.6 Unplanned turn-on due to the effect of the parasitic inductances (L_{gate} and $L_{emitter}$).

In the ON state, current flows through the transistor and also through the emitter-side inductance of the load current. If the current is now turned abruptly off, a negative voltage is generated by emitter-side load inductance voltage according to the following relationship:

Practical Tip: How do you check whether your gate driver design is safely under the gate emitter threshold voltage during operational switching operations?

It is not as simple as just attaching an oscilloscope probe and monitoring the gate voltage as direct access to the gate and emitter is difficult in practice and the readings will be affected by the capacitance loading of the probe itself. Thus, the measured values do not necessarily reflect reality. (Wer Mist misst, misst Mist: Who wrongly measures, measures wrongly).

Rather, you need to measure the inductances $L_{emitter}$, L_{gate} and in some cases even L_{Layout} and do the necessary calculations.

One way to find out if there are momentary unwanted turn-on effects in a bridge design is to measure the current in each branch of the bridge. Again, one must be careful that you do not change the switching behaviour of IGBTs by measuring the current. Thus, there must be no additional resistances or inductances in the gate-emitter path. One method which has been proven to be reasonably accurate is to use a current shunt in the high side collector connection and an isolated oscilloscope as shown below:

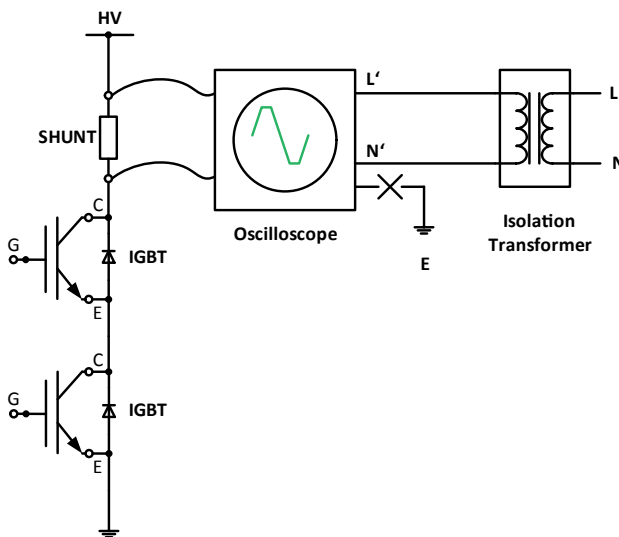


Fig. 6.19: Measurement setup to check bridge current flow.

Even if this measurement does not reveal any unwanted current peaks, you still cannot assume that the design is safe under all operating conditions. To be sure, you would have to select transistors having the minimum threshold voltages given in the datasheet and test at the maximum permissible temperature and maximum di/dt and dv/dt levels. So what can be done to minimize the unwanted effects of parasitic inductances?

- Reduce di/dt . Slower current decay rates result in lower voltages induced in the parasitic inductances and thus lower voltages between gate and emitter. However, this increases the switching losses.

- b. Reduce the layout inductance. The lower the layout inductance (track or cable lengths), the smaller the parasitic voltage generated.
- c. Use negative gate emitter voltages. By using a negative gate-emitter voltage instead of GND, the safety distance of the gate-emitter voltage to the gate emitter threshold voltage is increased.
- d. Galvanically separate the gate drive from the power ground. Through the use of isolated gate drivers for each transistor, the influences of the emitter inductances can be eliminated as the driver supply ground point is connected directly to the respective transistor emitters. Now that the $L_{emitter}$ parasitics are not part of the driver current loop, their effect is eliminated.

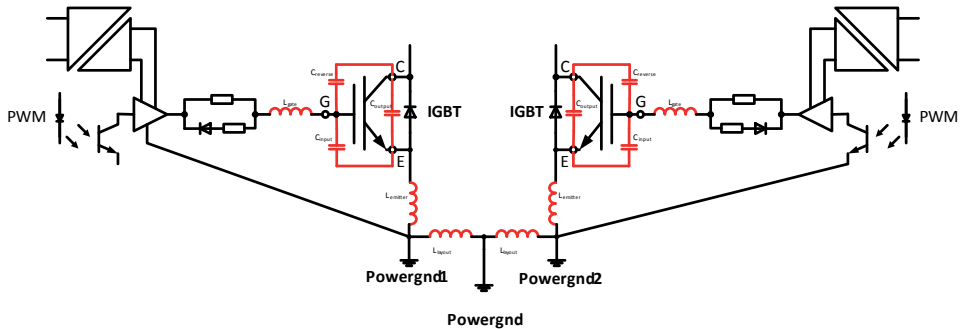


Fig. 6.20: isolated low side gate drivers.

- e. Use Kelvin contacts.

Several transistor manufacturers now offer packages in which a separate kelvin connection is provided for the emitter. Although this also has its own small parasitic inductance due to the connection path, the main load current does not flow through it, so no induced voltage is generated by any load current variations. This solution eliminates the effects of both the $L_{emitter}$ and L_{layout} parasitic inductances.

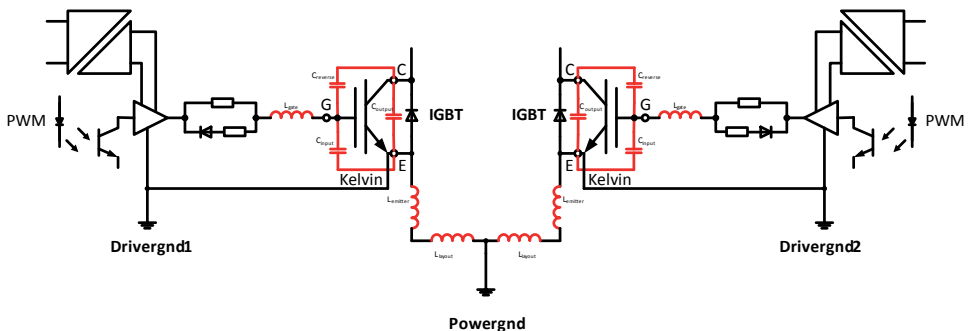


Fig. 6.21: isolated low side gate driver with Kelvin contacts

In summary: there are many ways to prevent undesired turn-on of a power transistor, but there are, however, just as many dangers that it happens! The safest way to prevent unwanted turn-on switching is to use an isolated dual supply for the gate driver with a negative turn-off voltage and to keep the parasitic inductances as low as possible. Ideally, a transistor package with Kelvin connections should be used to eliminate the effect of layout inductances.

Recom has developed an evaluation board (R-REF01-HB) to allow circuit designers to experiment and compare the different IGBT, SiC and GaN switching technologies using the same layout and driver IC. Only the DC/DC converters (included) need to be selected to match the transistors being used. The layout can be used for both three pin and four pin transistors with Kelvin contact.

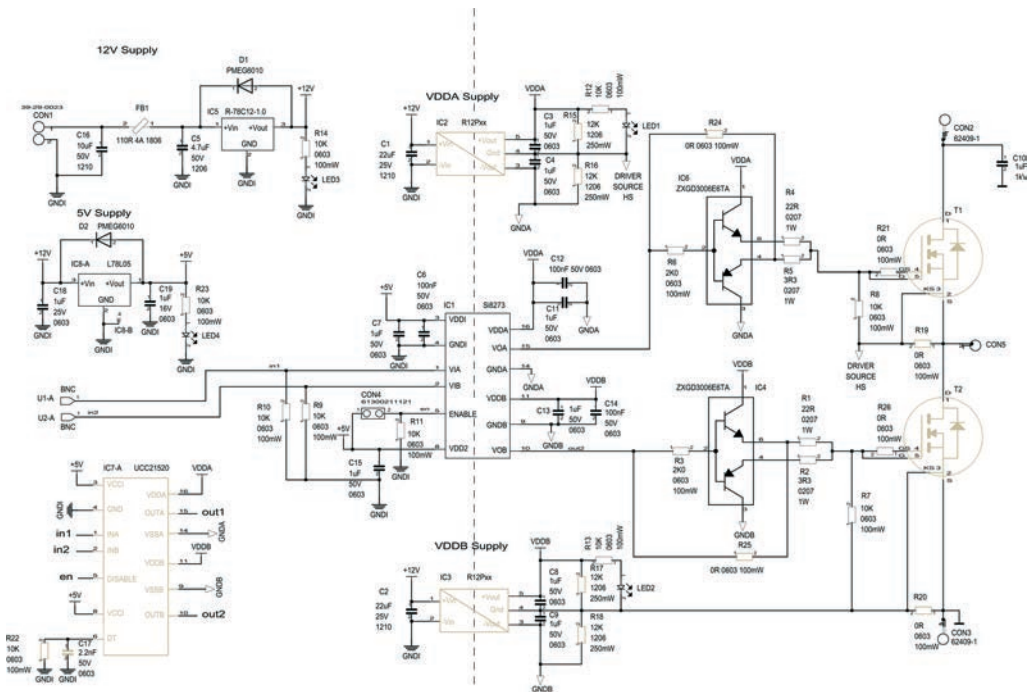


Fig 6.22: R-Ref01-HB Schematic

Chapter 7

Power Factor Correction

Power factor correction (PFC) is required for AC/DC power supplies with more than 75W output power (25W in the case of LED drivers) in order to comply with IEC/EN 61000-3-2. PFC circuits also allow higher output powers without exceeding the maximum input current limit of the mains supply:

Eq. 7.1. $P_{out} = \eta PF V_{in,rms} I_{in,rms\ limit}$ where PF = power factor and η = efficiency.

For an 85% efficient AC/DC converter operating from a fixed 230VAC supply fitted with a 10A over-current protection:

PF = 0.70 allows a maximum output power of $0.70 \times 0.85 \times 230V \times 10A \approx 1370W$

PF = 0.95 allows a maximum output power of $0.95 \times 0.85 \times 230V \times 10A \approx 1860W$

7.1 Passive PFC

Returning to our simple linear power supply design in Chapter 2, the reactive power is mainly capacitive although the load across the mains supply is the transformer, a primarily inductive component. This is because the transformer “reflects” the secondary load phase shift to the primary side. Thus the reactive power seen by the mains supply is mainly capacitive and the current leads the voltage. It would be possible to shift the current waveform to partially correct the power factor by adding a series inductor - but it is not possible to fill in all of the greyed-out areas in the waveform shown in figure 2.3 with current, so the power factor cannot be made perfectly equal to 1.

In practice, a passive power factor correction (PFC) solution can improve an uncorrected power factor from around 0.4 to around 0.7 by using PFC chokes (typically an iron-cored transformer with only a single winding) but such inductors are often nearly as large and as heavy as the isolation transformer itself:

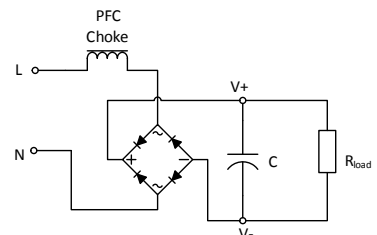
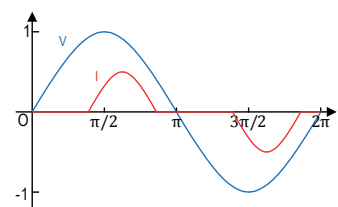


Fig. 7.1: Passive power factor correction. The PFC choke partially cancels out the phase shift caused by the output capacitor C. The resulting voltage/current graph shows how the input current has been “delayed” by the PFC choke to give a better overall PF value.



One of the main problems with the simple passive PFC correction circuit shown above is that the PFC choke can only operate over a limited input voltage range and still adequately correct the power factor. A solution often used in very low cost passive PFC circuits is to add a voltage selector switch between 115VAC and 230VAC operation (fig 7.2). The switch is either open (230V) and the PFC choke is connected in series with the full wave rectifier or closed (115V) making the circuit then the same as a half wave voltage doubler so that the output voltage stays the same (only the left half of the PFC choke and the left half of the full bridge are active).

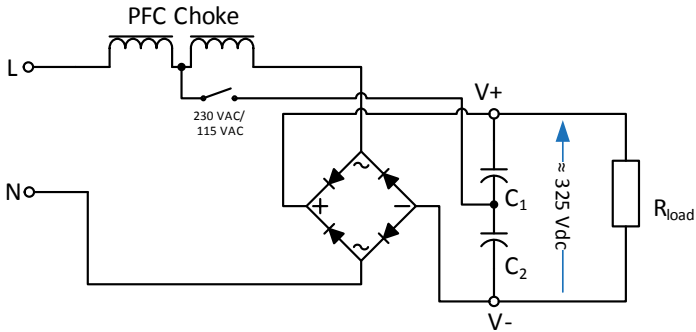


Fig. 7.2: Passive PFC with input voltage range switch.

The voltage doubler capacitors can be calculated from the relationship:

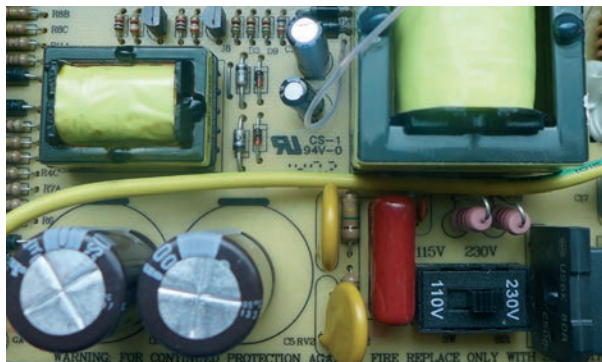
$$\text{Eq. 7.2.} \quad C_1 = C_2 = \frac{2I_{in}t_{holdup}}{V_{ripple}}$$

For a 100W power supply with 80% efficiency at 115VAC/60Hz input:
 $I_{in} = 100W/325VDC = 0.3A/0.8 = 0.375A$, $t_{holdup} = 1/120Hz = 0.008$

So, assuming an acceptable ripple Voltage of $V_{ripple} = 30V$

$$C_1 = C_2 = \frac{2I_{in}t_{holdup}}{V_{ripple}} = \frac{2 \times 0.375 \times 0.008}{30} = 200\mu F$$

Fig. 7.3: An example of a passive PFC design with mains selector switch. The PFC choke can be seen above the two voltage doubler capacitors. The advantage of this circuit as that the electrolytic capacitors need only be rated for 200V operation, even with a 230VAC input.



7.1.1 Valley Fill PFC

Although the switched range passive PFC is very effective for high power (100W to 250W) power factor correction, with PFC values of >0.95 at 230VAC and >0.98 at 115VAC possible, it is not so effective at lower power levels. However, it is also possible to get >0.9 power factor at low power levels using only passive components.

The technique required is called “valley-fill” and relies on using steering diodes to charge up two output capacitors to half of the peak voltage. This means that they will start to draw input current much earlier in each mains half-cycle (at half the peak input voltage instead of nearly at peak input voltage) and continue to draw current until much later in the half-cycle (again until the voltage falls to half of the peak voltage). The disadvantage of this arrangement is a very high output ripple of 50% of the DC output voltage.

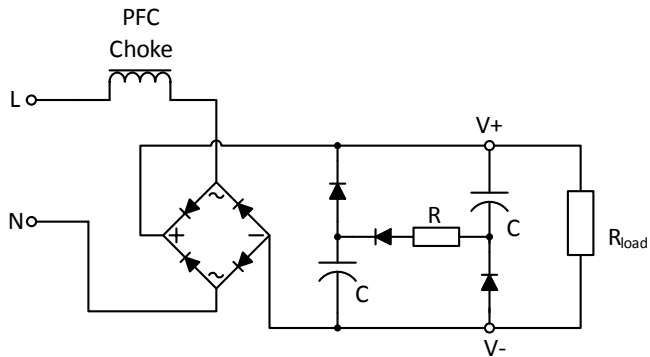


Fig. 7.4: Valley-fill passive PFC circuit

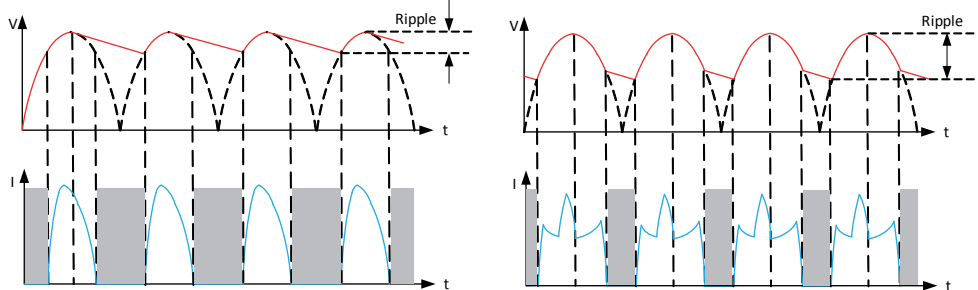


Fig. 7.5: Resulting waveforms for passive PF corrected (left) with a power factor of 0.7 and the valley-fill circuits (right) with a power factor of 0.9. Note that the greyed-out areas where no input current flows are shorter in the valley-fill design leading to an improved PF.

Valley-fill circuits are most commonly used in triac-dimmable LED drivers. Firstly, the valley-fill circuit also works well with a phase cut mains input consisting of short sections of the mains sinusoidal waveform and secondly, a high output ripple is not so important (the human eye is

not very good at noticing LED flicker at frequencies of around 100Hz). Finally, it is a low cost solution which is important for the cheaper end of the lighting market. However, for industrial-grade power factor corrected supplies, the high output ripple is often unacceptable. To get a good power factor with low output ripple, active PFC is required.

7.2 Active PFC

Active power factor correction uses a variable mark-space PWM control to manipulate the input current to force it to align with the input voltage. To do this, it is necessary to increase the voltage on the capacitor to ensure that at any point during the half-cycle, it can still be charged. Therefore all active PFC circuits are effectively DC boost converters. The boost voltage must be equal to or higher than the highest rectified input peak voltage, so typically 400V-425V is selected. Any higher and there will be unnecessary voltage stress on the boost capacitor and switching elements, any lower and the PFC circuit cannot ensure that the charging current can be controlled throughout the half-cycle.

There are four main topologies used for active power factor correction; discontinuous, continuous, critical-conduction and mixed-mode.

7.2.1 DCM power factor correction

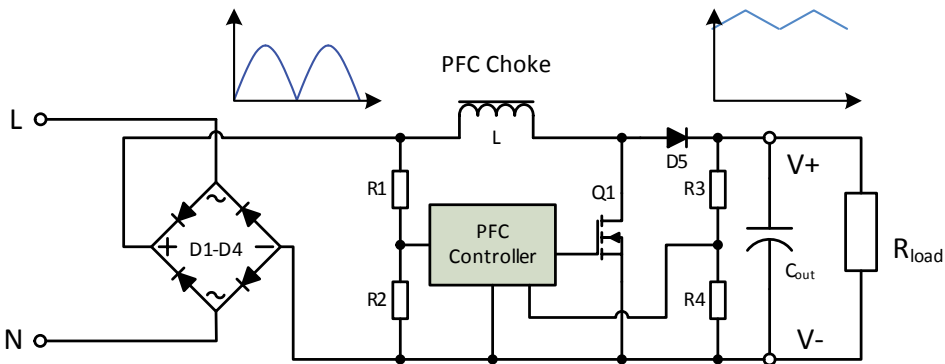


Fig. 7.6 Active PFC circuit

The PFC controller alters the duty cycle during the rectified input half-sine wave so that the mark/space ratio is smallest at the peak of the input voltage and highest at the start and end of the cycle. The PWM frequency remains constant. The rectified input voltage is divided down by $R1/R2$ and used to synchronize the PFC controller. The output voltage is divided down by $R3/R4$ for the feedback loop that stabilizes the output voltage. The storage capacitor C_{out} is charged up to a much higher voltage than the peak input voltage through the action of the boost converter formed by L , $Q1$ and $D5$, but the charging current is a series of short pulses throughout the input half-cycle, longer at low input voltage and shorter at higher input voltage. The average current through the choke therefore follows the input waveform voltage so the power factor is very close to 1.

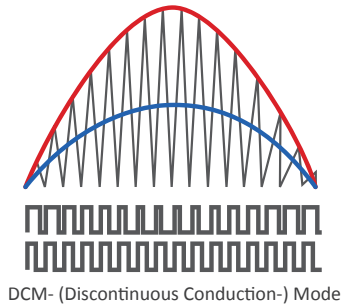


Fig. 7.7: Discontinuous conduction mode (DCM).

The inductor current is shown in black, the input voltage in red and the average input current in blue. The inductor current falls to zero at the end of each PWM pulse.

The main advantages of DCM power factor correction is that the inductor is fully magnetized and de-magnetized during each PWM cycle, so the inductor current falls to zero at the end of each pulse. The switching transistor then switches on at zero voltage/zero current, so it is very efficient and almost lossless. Also the recovery speed of the boost rectification diode is not critical.

The disadvantage of this method is the high EMI generated from the high peak currents of the chopped input waveform. A discontinuous PFC circuit needs a very good input EMC input filter to meet the regulatory conducted interference limits. The PFC choke must also be capable of handling the high peak currents, so the choke is large and heavy.

7.2.2 CCM power factor correction.

A solution to the EMC problems of DCM power factor correction is to use a continuous conduction power factor correction controller. This is the same circuit as above, but the inductance is increased so that the current in the choke varies only slightly above and below the ideal sinusoidal waveform. Typically, the CCM current ripple is chosen to be around 20%-40% of the average inductor current. Again the PWM frequency is constant:

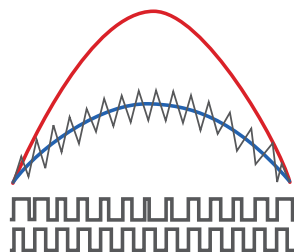


Fig. 7.8: Continuous conduction mode (CCM)

The inductor current is shown in black, the input voltage in red and the average input current in blue. The inductor current does not fall to zero at the end of each PWM pulse.

The PWM controller is more complex as it must track the input voltage and adjust the input current more precisely, but the EMI generated is much lower as the input current is continuous and not pulsating.

The major disadvantages are the significantly higher switching losses in the transistor and higher recovery losses in both the diode and the transistor. For a CCM design, the boost rectification diode must be ultra-fast (very low Q_{rr}) . The choke needs to have a much larger inductance than for a DCM design, although the peak current is lower.

7.2.3 CrCM power factor correction.

Both the DCM and CCM power factor correction circuits use a fixed PWM frequency. However, if the frequency is also made variable and synchronized to the input half-cycle, then the inductor current can be adjusted so that it only just touches zero at the end of each PWM pulse, whatever the input voltage is during the half-cycle (this is called boundary conduction mode (BCM) or critical conduction mode (CrCM)).

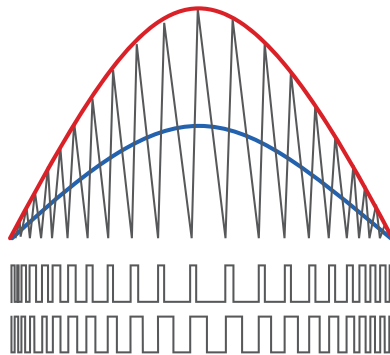


Fig. 7.9: Boundary or Critical Conduction mode (CrCM)

The inductor current is shown in black, the input voltage in red and the average input current in blue. The inductor current falls to zero at the end of each PWM pulse and the PWM frequency varies.

With CrCM control, the switching losses in the transistor and the recovery losses in the diode are as low as in the DCM circuit plus the inductor can be made smaller than in the CCM circuit because the peak currents are lower.

The disadvantage is the variable frequency PWM requires EMC filters that are effective over a wider range of frequencies.

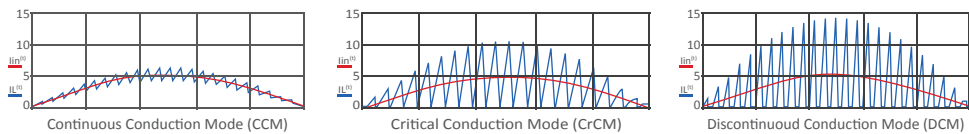


Fig. 7.10: Comparison between the inductor current waveforms in CCM, CrCM and DCM PFC circuits.

All three solutions have the same average inductor current, but the peak-to-peak inductor current in the CrCM is a compromise between the very high levels of the DCM inductor and the very low levels of the CCM circuit.

7.2.4 Mixed-Mode PFC

There are many PFC controllers on the market that are capable of switching between different modes of operation according to the operating conditions of the converter. A chosen value of choke that works well with a CCM controller at low input voltage (90 – 125VAC) may transition to DCM due to the lower input current at higher input voltages (180-265VAC), thus harming the power factor correction figure. To avoid having to make a compromise, the controller can be made variable frequency/variable PWM to keep the circuit in CCM/CrCM throughout the input voltage range. There are also powder core chokes called “swinging chokes” that change their inductance according to the current through them. At low currents, the inductance increases, thus keeping the PFC in CCM/CrCM whatever the operating conditions.

Practical Tip: PFC stages are susceptible to damage from input surge voltages. The bridge rectifier will rectify both positive and negative-going surges into a high positive voltage into the PFC choke. The resulting high current can rapidly saturate the core so that the choke no longer behaves like an inductor, but lets all of the surge voltage through. The PFC diode now has to cope with the high charging current (sometimes hundreds of amps) into the PFC capacitor and can quickly fail. The solution is to add a high current diode in parallel with the PFC choke and diode. Under normal operating conditions, the PFC voltage will be higher than the input voltage and the bypass diode will be reverse biased. Under surge conditions, the input exceeds the PFC voltage and it will conduct, relieving the stress on both the PFC diode and PFC choke as well as reducing the voltage across the bridge rectifier.

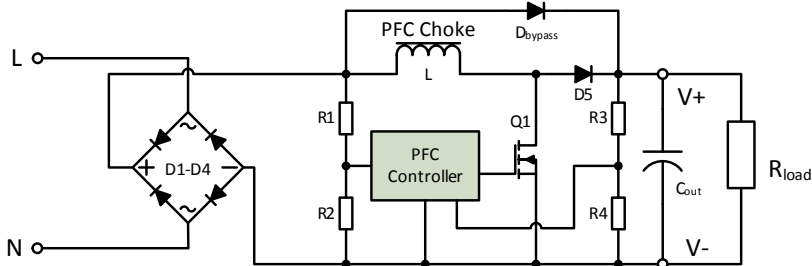


Fig. 7.11: Active PFC with surge bypass diode

7.2.5 Interleaved PFC

As has been mentioned several times in this chapter, the EMC considerations are an important factor in choosing the appropriate conduction mode for the PFC controller. If the EMI is too high to be effectively filtered out then an alternative topology is to use two interleaved PFC circuits so that the ripple current in each stage is halved and added in anti-phase.

Interleaving also has the advantage of sharing the output current across two inductors and two diodes, thus allowing either higher output currents or improved operating temperatures.

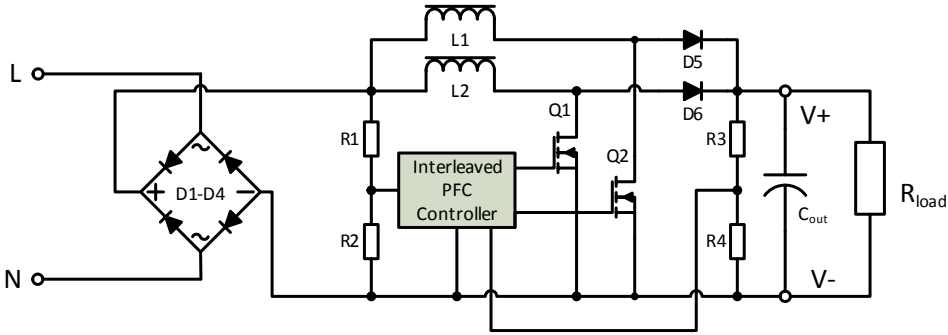
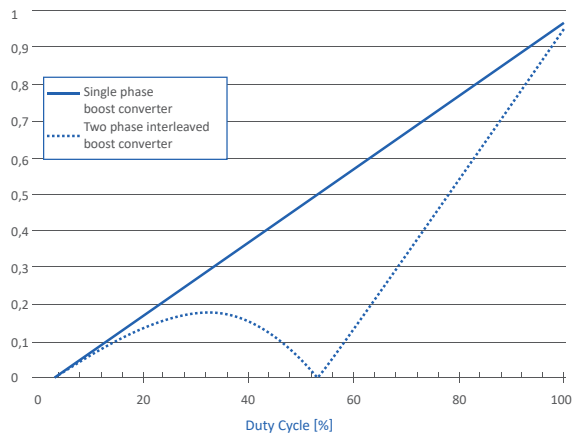


Fig. 7.12: Interleaved PFC circuit

An interleaved PFC is mainly used for high power AC/DC converters where the high input current would make the EMC input filter very bulky and more expensive than the extra circuitry of using two CrCM PFC boost converters. The PWM outputs operate 180° out of phase, so although the current in either of the inductors falls to zero at the end of each pulse, the current flowing into the PFC capacitor is continuous (current flows alternately through D1 and D2).

The output voltage ripple is significantly lower than is possible with a single stage PFC and with a 50% duty cycle, the interleaved topology has zero input current ripple as the two PFC stages cancel out. Besides the increased cost, the biggest disadvantage is that all of the components used must be very carefully matched to maintain the same performance over all operation conditions.

Fig. 7.13: Comparison of the duty cycle vs input ripple current for single phase and interleaved phase PFC boost circuits.



7.2.6 Bridgeless (totem pole) PFC

The bridgeless or totem-pole PFC topology is becoming more popular because of its very high efficiency. The bridge rectifier diodes are replaced by two high voltage transistors that alternately switch at the mains frequency to rectify the input. The diode forward voltage drops are therefore eliminated and the internal body diodes of the transistors aid the current flow and increase the efficiency.

It is usual to use different transistor types for the slower 50Hz switching and the high frequency PFC switching.

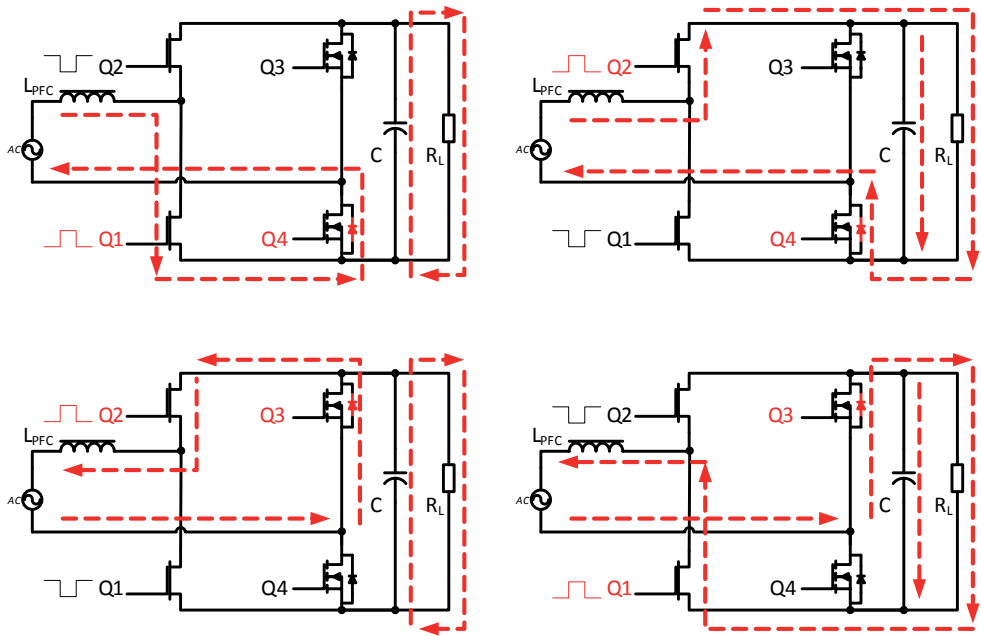


Fig. 7.14: Bridgeless Totem-Pole PFC topology and switching current paths

The single switching FET in the previous PFC designs is replaced by two FETs Q1 and Q2. During a positive mains half-cycle, Q4 is switched on, Q3 is off, Q1 is operated with a PWM signal to boost the output voltage and Q2 is operated with the inverted PWM signal to act as a rectifier. During a negative mains half-cycle, Q3 is switched on, Q4 is off, Q2 is operated with a PWM signal to boost the output voltage and Q1 is operated with the inverted PWM signal to act as a rectifier.

As Q3 and Q4 are switched at a low frequency (50/60Hz), they do not need to switch quickly and can be regular MOSFETs. Diodes are placed in parallel to help increase the efficiency by sharing the peak current, but the power switching is done with the MOSFETs. The forward voltage losses of the conventional bridge rectifier are thus eliminated, so the rectification losses can be very low (<1%).

The transistors Q1 and Q2 cannot be MOSFETs because the reverse recovery losses would be too high. The switching delay would cause shoot-through and large current spikes during AC zero-crossing. One solution is to use JFET transistor in a cascode configuration with a MOSFET:

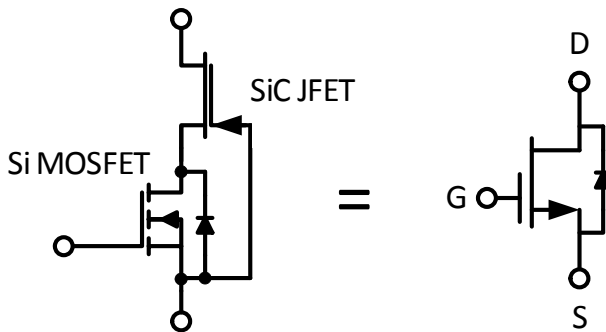


Fig. 7.15: SiC/JFET Cascode

The JFET is normally on and has a gate input that is effectively grounded. When the MOSFET is off, the MOSFET V_{DS} rises until the JFET V_{GS} is sufficiently negative to switch the JFET off. The supply voltage then appears almost entirely across the JFET. When the MOSFET is switched on, the V_{DS} drops to close to zero and the JFET turns on. The advantage of this arrangement is that the JFET gate and the MOSFET V_{DS} and V_{GS} are all close to zero, so the reverse recovery, C_{oss} and Miller capacitance losses are also close to zero. The switching speed is vastly improved.

More recently, high electron mobility transistors (HEMT) such as GaN FETS are being used to replace the cascode as they are ideal for such totem-pole topologies (very fast switching slew rates, no body diode, and low gate capacitance). Overall PFC stage efficiencies in excess of 99% are possible with GaN FET totem pole designs.

The following bridgeless totem pole PFC circuit uses two half bridge power stages to replace the bridge rectifier and the PFC switcher normally required by AC powered applications. The synchronous rectifier consists of two silicon MOSFETs alternately switched with a 50% duty cycle at 50/60Hz in time with the AC mains input. This creates a rectified output without the need for an input bridge rectifier. The PFC half-bridge circuit runs with a higher frequency and variable duty cycle PWM signal to perform the power factor correction function using low loss GaN transistors. With the low component count, the gate driver components can be placed closer together and parasitic inductances and stray capacitances minimized. Two RP-1506S converters and a dual channel digital isolator are used to create the fully isolated high speed half-bridge GaN gate driver circuit for the PFC with a BOM count of only 20 parts.

The 50/60Hz AC synchronous rectification half-bridge runs at a much lower frequency, so lower-cost MOSFETs can be used without sacrificing overall efficiency or performance. The isolated +15V high-side MOSFET gate drive power is supplied by a RP-1515S converter. All

three DC/DC converters used offer 5.2kVDC isolation and <10pF isolation capacitance. The low-side MOSFET gate driver can be supplied directly from the 15V on-board power supply (no isolation is needed).

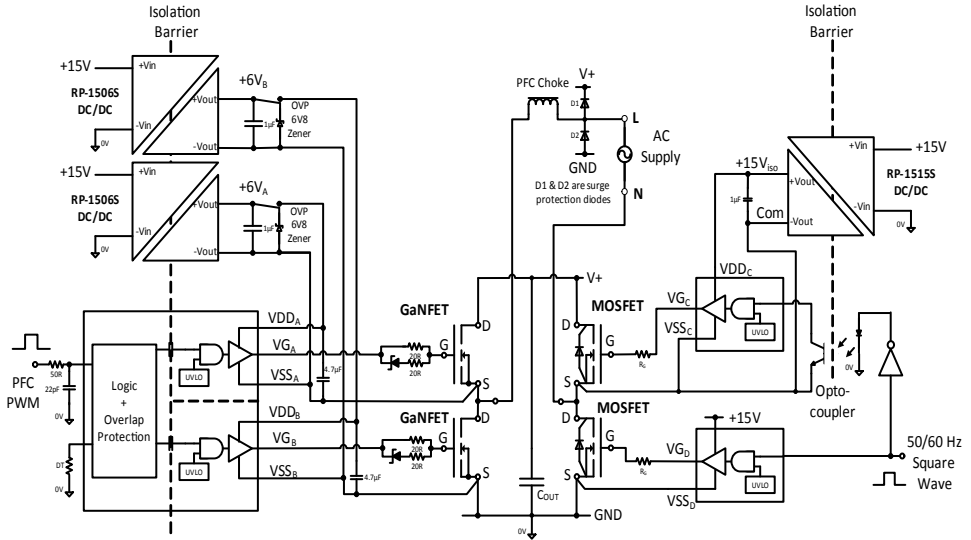


Fig. 7.16: Simplified Circuit of a bridgeless combination GaN/MOSFET PFC

The disadvantages of the bridgeless PFC is the extra complexity (four isolated FET drivers are required), the accuracy of the timing needed (especially during mains zero-crossing, where it is important to introduce enough dead time to avoid shoot through, but not too much as this will harm efficiency) and the difficulty of synchronising the circuit to a noisy mains supply. In addition, the controller IC needs to have a current transformer or Hall Effect sensor to be able to monitor the bidirectional inductor current accurately enough to maintain a high efficiency over the entire load and supply voltage range.

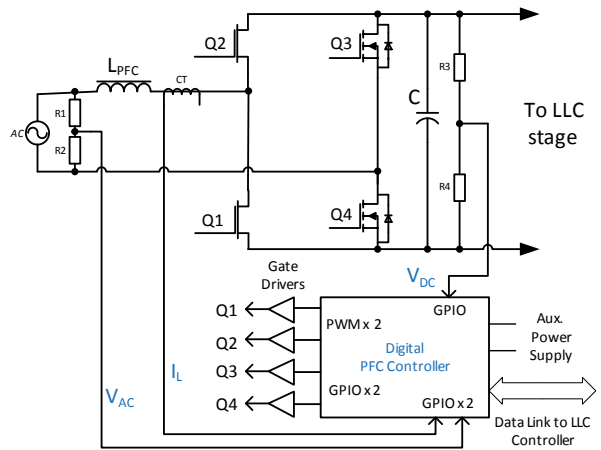


Fig. 7.17: Block Diagram of a Bridgeless PFC controller (with digital control and compensation).

This digital controller uses three control loops: a voltage control outer loop (using the V_{dc} input), a sine wave reference loop (synchronized to the V_{ac} input) and a current control inner loop (using the I_L input) to maintain accurate regulation with a high power factor. Such control complexity means that only digital controllers are really suitable for this topology.

In addition, a data link to the digital LLC controller allows interactive operation to change the response characteristics according to load conditions.

Chapter 8

AC/DC Converter Topologies

(This section is largely based on the DC/DC book of knowledge discussion of the different topologies, but as DC/DC and AC/DC share several conversion topologies², it is reproduced here for the sake of completeness)

In the family of isolated AC / DC converters there is a wide variety of topologies available, but only some of them are applicable to the discussion of modern AC / DC converters.

This section will limit its consideration to flyback (single and doubled ended versions), forward (active clamp, single and double ended versions), push-pull, bridge converter (half-bridge and full bridge) and resonant (ZVS, LLC) topologies. In these types of isolated converters, the transfer of energy from input to the output is performed via an isolating transformer. Line voltage and output load regulation is performed by a PWM controller. Ideal components are again assumed.

8.1 Single Ended Flyback

The flyback converter converts an input voltage into a regulated output voltage by storing energy in the transformer core gap during the ON time and transferring it to the secondary during the OFF time. Technically the transformer consists of two coupled inductors as the energy transfer is not by true transformer action.

Figure 8.1 shows the simplified circuit:

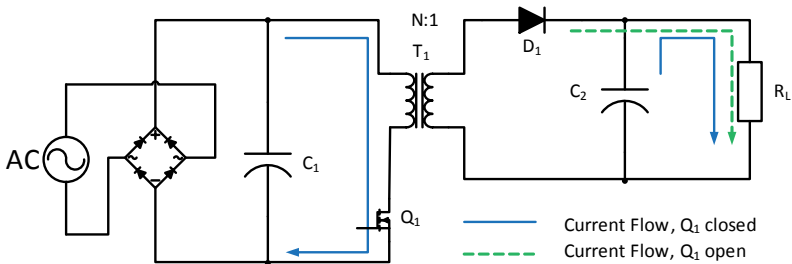


Fig. 8.1: Isolated Flyback Converter Simplified Schematic.

For a power supply without PFC, the rectified mains input voltage will be between 126VDC and 320VDC, but the output voltage is typically between 3.3V and 24V. This is a big voltage difference! If a PFC front end is used, the rectified input voltage will be even higher and the difference even greater.

² Note: DC cannot be converted directly via a transformer, so all DC/DC converters are essentially DC-to-AC//AC-to-DC couplers. On the other hand, AC switch power supplies run at a higher frequency than the mains input, so they rectify the AC input to DC and are AC-to-DC-to-AC//AC-to-DC couplers. It is not surprising that they have many elements in common.

The big advantage of a flyback transformer design is that the turns ratio decides the fundamental input/output voltage ratio (Eq. 8.1). The variable mark-space PWM controller on the input power stage can then easily compensate for any variation in input voltage or output load. Duty cycles higher than 0.5 are possible with the flyback topology, but in general should be avoided to reduce the average current in the output diode.

Eq. 8.1:
$$V_{out} = V_{in} \frac{1}{N} \frac{\delta}{1-\delta}, \text{ valid for } V_{in} < \text{or } > V_{out}$$

So for a universal input AC/DC with a minimum input range of 90VAC (no PFC, so 126VDC when rectified) and an output voltage of 24VDC, the transformer turns ratio would be chosen to be 5:1.

At this input voltage, the PWM would have 50% duty cycle. At the highest input voltage of 264VAC (370VDC when rectified), the PWM would have a 25% duty cycle. The relevant relationships are as follows:

Eq. 8.2:
$$\text{Duty Cycle} = \frac{V_{OR}}{V_{OR} + V_{IN}}$$

Where the reflected output voltage, V_{OR} , equals $(V_{out} + V_{Drop} \cdot D1)$ multiplied by the turns ratio, N .

Given the above values, $V_{OR} = (24V + 1V) \times 5 = 125V$.

For the same power supply with a PFC front end, the DC boost voltage would be chosen to be around 385VDC, so the transformer turns ratio would be 16:1 and the PWM would have an ideal 50% duty cycle over the whole input voltage range.

Another advantage of the flyback topology is that multiple outputs (with different polarities if required) can be easily implemented by adding multiple secondary windings. In particular, a low voltage secondary winding wound on the primary side of the transformer can be used to power the primary controller IC. (See section 12). The component count is also very low, so this topology is good for low cost designs.

With output voltage or current monitoring and an isolated feedback path (typically via an optocoupler) a very stable regulated output can be generated. But flyback converters can also be primary side regulated by monitoring the primary winding waveform and using the knee-point to detect when the secondary current has reached zero. This eliminates the optocoupler and reduces the component count still further.

The disadvantage is that the transformer core needs careful selection, The air-gapped core should not saturate even though there is an average DC current flowing through the transformer and efficiency can be lost if it has a large magnetic hysteresis. Also eddy current losses in the windings can be a problem due to the high peak currents. These two effects limit the practical operational frequency range of this topology.

Finally the large inductive spike on the primary winding when S1 is turned off places a lot of strain on the switch. In addition, there is a resonant oscillation caused by the interaction between the leakage inductance of the transformer, the primary winding capacitance and the body-diode capacitance of the switching FET. As all of these values are very small, the resonant frequency is very high – typically in the region of tens of MHz. This not only causes serious EMC problems but can induce very high currents to flow:

Eq. 8.3: Peak Voltage Stress=Vin+Reflected Secondary voltage+Resonance Voltage

$$V_{pk} = V_{in,DC} + \frac{V_{out} + V_F}{N} + I_{pri} \sqrt{\frac{L_{lk}}{C_{pri} + C_{oss}}}$$

Where V_F is the forward voltage drop across the secondary diode, N is the turns ratio, I_{pri} is the primary current, L_{lk} is the total leakage inductance, C_{pri} is the primary winding capacitance and C_{oss} is the FET drain-source capacitance.

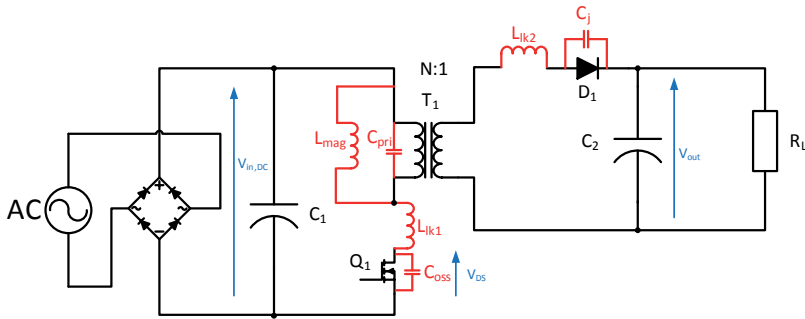


Fig. 8.2: Single ended Flyback showing parasitic elements (in red)

Switching losses arise on both switch-on (the current through the FET starts to rise before the voltage across the FET falls to zero) and on switch-off (the voltage across the FET starts to rise before the current through the FET falls to zero) according to the following relationships:

Eq. 8.3: $P_{diss,switch-on} = f \left(\frac{1}{2} C_{eq} V_{DS}^2 \right)$

Eq. 8.4: $P_{diss,switch-off} = f \int_{t1}^{t2} V_{DS}(t) \cdot \frac{I_D(t)}{N} \cdot dt$

Where C_{eq} is $C_{oss} + C_{pri}$, V_{DS} is the voltage across the FET, f is the switching frequency, N is the turns ratio and $t2-t1$ is the switching time.

From these relationships, we can see:

1. the FET switching losses increase linearly with switching frequency. Reducing the switching frequency will reduce the losses.

2. The switch-on losses are proportional to the C_{eq} capacitance. The C_{oss} component is mainly due to the junction capacitance of the internal body diode, so it cannot be reduced, but the parasitic capacitances in the transformer and layout usually exceed C_{oss} anyway. The transformer can be wound for low leakage capacitance at the expense of higher leakage inductance (see point 4).
3. The switch-on losses are proportional to the square of V_{DS} , so soft-switching techniques such as ZVS (Zero Voltage Switching) will substantially reduce the switch-on losses.
4. The switch-off losses are dependent on the rate of change of V_{DS} (dV_{DS}/dt), which in turn is affected by the primary leakage inductance of the transformer, L_{lk1} . The transformer can be wound for low leakage inductance at the expense of higher leakage capacitance (see point 2).
5. The switch-off losses are also dependent on the reflected output diode recovery current rate (dI_D/dt), which in turn is dependent on the primary-secondary leakage inductance of the transformer, L_{lk2} and the turns ratio, N . A fast recovery diode on the output side will reduce the switch-off losses on the primary side.

The effect of these parasitic elements means that the switching voltage and current waveforms will not be clean:

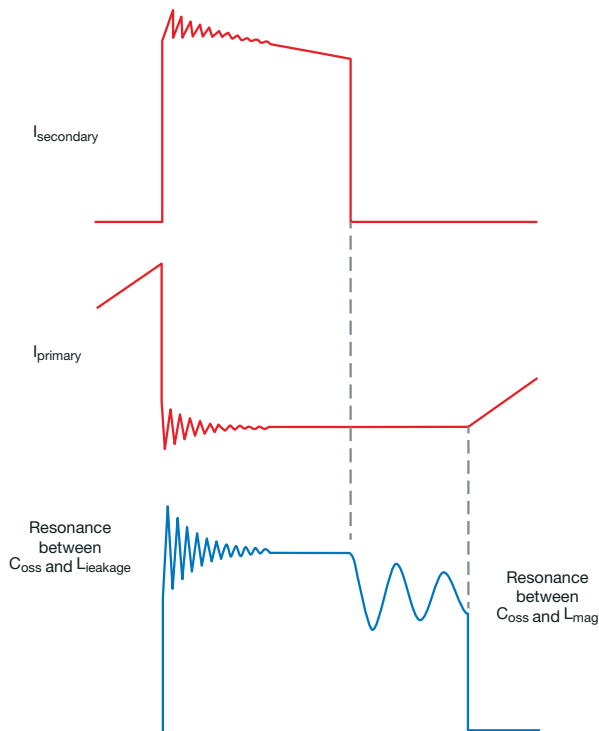


Fig. 8.3: Voltage and current resonances as a result of the parasitic elements shown in Fig 8.2.

8.1.1 Single Ended Flyback Snubber Networks

To absorb this damaging high frequency parasitic oscillation, a snubber is often required. The most common arrangement on the high side is a RCD (Resistor-Capacitor-Diode) snubber:

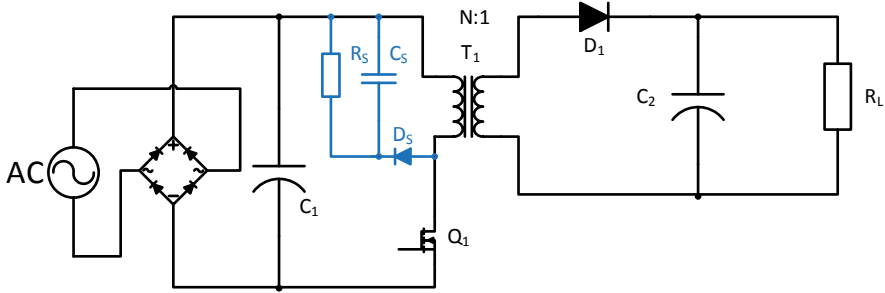


Fig. 8.4 Single-ended flyback with RCD snubber circuit (shown in blue).

The capacitor and resistor absorb the energy of the resonance ringing and cause it to decay more rapidly. The recovery diode is typically a standard power diode (not a fast diode) as a relatively slow reverse recovery time (T_{rr}) also helps to dampen out the ringing. The negative current that flows during this recovery time allows the snubber capacitor to dampen the ringing more effectively by absorbing current on the positive cycle and delivering current on the negative cycle despite the diode rectification.

The power dissipated in the snubber network is highest at minimum V_{in} and full load:

$$\text{Eq. 8.5: } P_{diss,snubber} = \frac{1}{2} f L_k I_{peak}^2 \frac{V_{Cs}}{V_{Cs} - n(V_{out} + V_D)}$$

Where f is the switching frequency and V_{Cs} is the voltage across the snubber capacitor C_s .

Practical Tip: V_{Cs} can be adjusted by changing the value of the snubber capacitor. If the capacitor is too small, the voltage will be high and the snubber ineffective. If the capacitor is too large, then V_{Cs} will be small, but the power dissipation will be high. For optimum results, C_s should be chosen to be have a V_{Cs} equal of twice the sum of $n(V_{out} + V_D)$.

The optimum value of the snubber capacitance is also dependent on the snubber resistor, R_s , as they both operate together to absorb the ringing energy.

$$\text{Eq. 8.6: } C_s [\mu F] = \frac{V_{Cs}}{\Delta V_{Cs} f R_s}$$

Where ΔV_{Cs} is the ripple voltage across the snubber capacitor (typically chosen to be 5%-10% of V_{Cs}). R_s can be found from the relationship:

$$\text{Eq. 8.7: } R_s = \frac{V_{Cs}^2}{\frac{1}{2} f L_k I_{peak}^2 \frac{V_{Cs}}{V_{Cs} - n(V_{out} + V_D)}}$$

If needed, a resistor in series with the diode can be added to damp the resonant peak between the primary leakage inductance and the snubber capacitor. This is called a R2CD snubber network.

For low standby current applications, the RCD snubber can be replaced by a TVS diode in series with an ultra-fast recovery diode and a damping resistor. It is a more expensive solution, but avoids the RCD snubber dissipation, which is constant irrespective of load. Unlike the RCD snubber, a TVS snubber needs an ultra-fast diode for high efficiency.

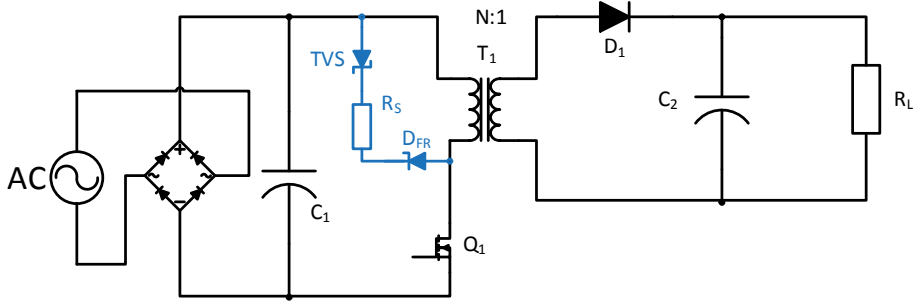


Fig. 8.5: Single-ended flyback with TVS snubber network (shown in blue).

Practical Tip: When using quasi-resonant primary side regulation, care must be taken not to over-damp the resonances with snubber networks, because the regulation circuit needs to track the first or second valley of the L_m/C_{oss} DCM resonance.

A practical example

Consider a 10W AC/DC power supply with the following specifications:

- $V_{in} = 100\text{-}240\text{VAC}$ nominal (no PFC).
- $V_{out} = 5\text{V @ } 2\text{A}$, $V_D = 0.5\text{V}$
- Operating frequency = 50kHz
- Turns ratio = 12
- $L_k = 750\text{nH}$ (by measurement)
- Peak $I_{pri} = 400\text{mA}$ (by measurement)
- 450V rated FET with $C_{oss} = 20\text{pF}$
- Primary winding capacitance = 10pF (by measurement)

For reliability, the peak voltage stress on the FET should be below 80% of its rated voltage. At maximum V_{in} , the peak voltage stress (from equation 8.2) is:

$$\text{Peak Voltage Stress, } V_{pk} = V_{in,max,rectified} + \frac{V_{out} + V_D}{n} + I_{pri} \sqrt{\frac{L_k}{C_{pri} + C_{oss}}}$$

$$V_{pk} = 373 + \frac{5.5}{12} + 0.4 \sqrt{\frac{750\text{nH}}{10\text{pF} + 20\text{pF}}} \approx 437\text{V}$$

Although 437V is within the rating of the FET, it is much higher than 80% of V_{DSS} , so the reliability will be poor as the transistor is close to its voltage stress limit. Adding an RCD snubber will significantly improve the lifetime of the FET.

First we choose V_{CS} to be twice $n(V_{out} + V_D) = 2 \times 12(5V + 0.5V) = 132V$.

Next we define the snubber resistor, R_s , from Equation 8.7:

$$R_s = \frac{V_{Cs}^2}{\frac{1}{2} f L_k I_{peak}^2 \frac{V_{Cs}}{V_{Cs} - n(V_{out} + V_D)}} = \frac{132V^2}{\frac{1}{2} 50kHz 100\mu H 0.4^2 \frac{132V}{132V - 66V}} = 21.78k \text{ Ohm} \approx 22k \text{ Ohm}$$

The power dissipation in the snubber resistor will be $V^2/R = 132V^2/22k \text{ Ohm} = 0.8W$.

Choose a resistor with at least double this power rating or place two 1W resistors in parallel.

With 10% ripple, the snubber capacitor, C_s , will be from Equation 8.6:

$$C_s (\mu F) = \frac{V_{Cs}}{\Delta V_{Cs} f R_s} = \frac{132}{13.2 50kHz 22kOhm} = 9.1nF \approx 10nF$$

Finally, the diode should be chosen to manage the peak voltage stress (choose at least double the rated voltage) and be able to cope with the diode power dissipation.

Suitable components for the snubber network would be a 22k/2W resistor in parallel with a 10nF/200V capacitor and a 1N4004 diode.

8.1.3 Ringing Snubbers.

Besides reducing the voltage stress on the main switching transistor, snubbers can also be used to damp ringing in the primary FET or secondary rectifier diode.

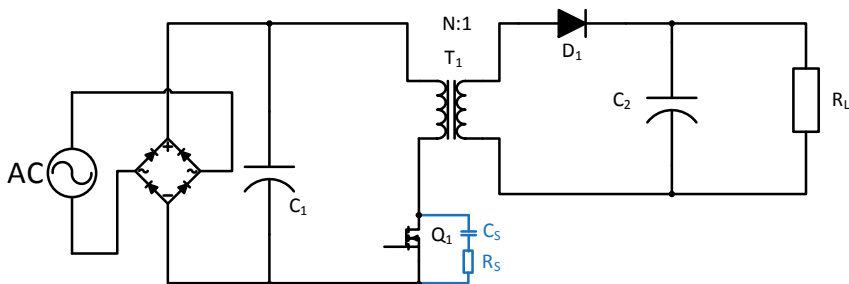


Fig. 8.6: Single-ended flyback with primary snubber (low side snubber).

The low side snubber provides damping for the LC resonance of the switching FET caused by the interaction of the primary leakage inductance and the MOSFET junction capacitance when the FET is turned off.

Practical Tip: If a current sense resistor is used, the snubber must be placed across the transistor only and not from the drain connection to ground, otherwise the sense resistor will be affected by the snubber discharge current. One way to calculate the required snubber components is to measure the transformer primary inductance with the outputs short circuited using an inductance meter (or a frequency response analyser if you have one) and use an oscilloscope to measure the ringing frequency f_r (hold the probe close to, but not touching the drain pin – the probe will pick up the signal without dampening it with the probe's own capacitance ;-)

The snubber resistor is then:

$$\text{Eq. 8.8: } R_s = 2\pi f_r L_{pri}$$

And the snubber capacitor:

$$\text{Eq. 8.9: } C_s = \frac{1}{2\pi f_r R_s}$$

The power dissipation in the snubber resistor needs also to be checked:

$$\text{Eq. 8.10: } P_{diss,R_s} = f C_s V_{DS}^2$$

Where f is the switching frequency (not the ringing frequency) and V_{DS} is the peak FET voltage.

Practical Tip: another way to determine the ringing snubber component values is by experiment:

1. find out f_r using the method above.
2. add capacitance (MLCC's are best) across the FET until the frequency halves. The stray capacitance is then equal 1/3 of the additional capacitance e.g. if adding 62pF halves the frequency, then $C_{oss} \approx 20\text{pF}$.
3. calculate the stray leakage inductance using the equation Eq. 8.11:

$$\text{Eq. 8.11: } L = \frac{1}{(2\pi f_r)^2 C_{oss}}$$

4. The snubber resistor is then the same as the characteristic impedance, Z :

$$\text{Eq. 8.12: } R_s = Z = \sqrt{\frac{L}{C_{oss}}}$$

5. The snubber capacitor can be chosen to be four to five times C_{oss} (the leakage capacitance varies a lot in practice, so by choosing a larger capacitor, we can be sure that the ringing is properly damped - including production tolerances)

Ringing also occurs on the secondary output diode when it becomes reverse biased, so it can be useful to also put a snubber across it:

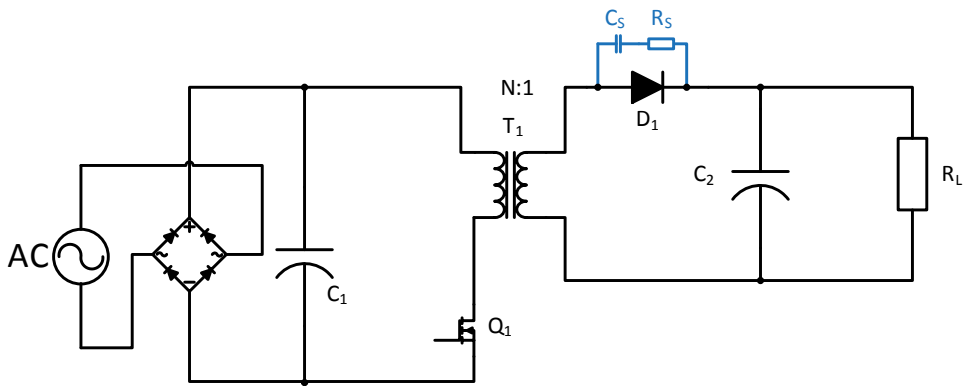


Fig. 8.7: Single-ended flyback with output diode snubber (shown in blue).

The peak ringing voltage across the secondary side diode if a snubber was not fitted would be:

$$\text{Eq. 8.13: Diode Peak Voltage Stress, } V_{pk,diode} = V_{in,max,rectified} n + I_{sec} \sqrt{\frac{L_{k2}}{C_j}}$$

Where L_{k2} is the secondary leakage inductance and C_j is the junction capacitance of the diode.

For a typical power diode, the junction capacitance will be around 5pF. For a typical 12:1 turns ratio transformer, the secondary leakage inductance would be around 8nH (very approximate). This would give a ringing voltage across the secondary diode of:

$$\text{Ringing Voltage} = 2 \sqrt{8nH/5pF} = 80V$$

The output capacitor will absorb most of the ringing voltage if it has a low ESR and the PCB track inductance is not too high, but the diode must be able to survive this peak reverse voltage.

Adding the secondary side snubber not only dissipates the energy safely and protects the diode, but reduces the EMI generated by the secondary ringing which can be in the order of 10s of MHz. On the other hand, as the ringing frequency is much higher than the switching frequency, it is relatively easy to filter out without incurring a high power dissipation loss.

Typical values for secondary snubber components are 4x the junction capacitance for the capacitor and a resistor value equal to the $\sqrt{\frac{L_{k2}}{C_j}}$ term.

In our example, suitable component values for the secondary side diode snubber would be a 20pF capacitor in series with a 40 ohm resistor.

8.1.2 Active Clamp and Regenerative Snubbers

RC snubbers are dissipative circuits: the energy stored in the leakage inductance is diverted by the capacitor and dissipated in the snubber resistor. This consumes between 2%-5% of the total power so the resistor and diodes must be adequately dimensioned to cope with their internal temperature rise.

A more efficient solution is to use active clamping and store the excess energy in a capacitor so that it can be returned to the next cycle. There are two ways to do this; a low-side p-Channel clamp in series with the main switch or a high-side n-Channel Clamp to replace the clamping diode.

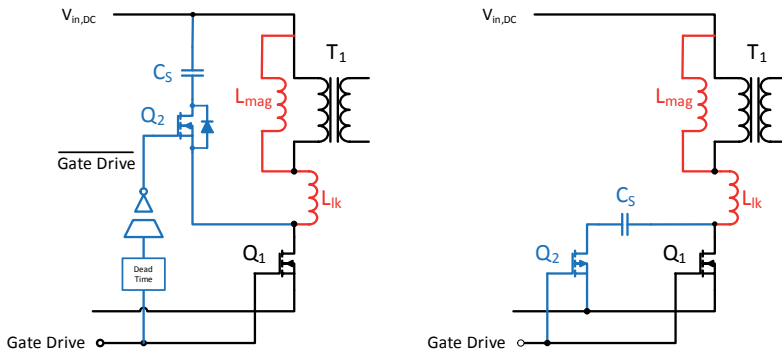


Fig. 8.8: Single-ended flyback active clamp configurations: high side and low side configurations.

8.1.2.1 High Side Active Clamp

The high side solution shown in Fig 8.8 requires an isolated gate driver but uses a lower cost n-channel MOSFET. Q2 is driven in antiphase to the main power transistor Q1 but with a dead time between cycles to avoid shoot-through.

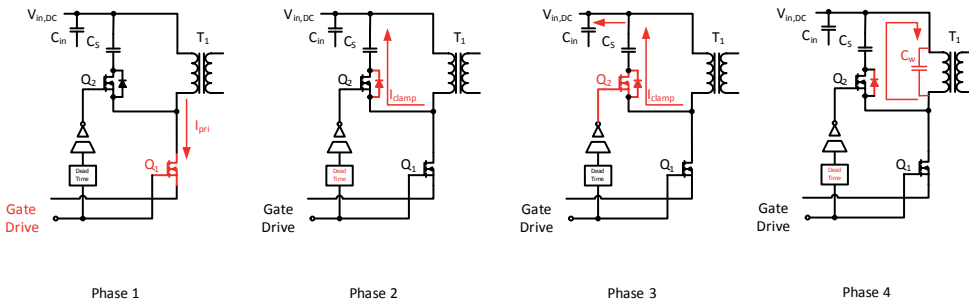


Fig. 8.9: Single-ended flyback low side active clamp current flow

Phase 1. Q1 on. Q2 off. Energy is stored in the magnetising and leakage inductances.

Phase 2. Q1 off. Q2 off (dead time). The clamp capacitor starts to absorb the voltage overshoot via the Q2 body diode.

Phase 3. Q1 off. Q2 on. The clamp capacitor charging current is taken over by the FET, reducing the resistance and shorting out the over-voltage spike into the clamp capacitor. Once the leakage inductance energy has been absorbed, the current in the clamp capacitor reverses and the energy is returned to the Vin capacitor.

Phase 4. Q1 off. Q2 off (dead time). Any remaining energy in the circuit pre-charges the winding capacitance ready for the next cycle.

For higher power applications, an external diode can be placed in parallel with Q2 to reduce the current flowing through the body diode before the transistor is fully enhanced..

The voltage across the high side clamp capacitor is proportional to the duty cycle and Vin:

$$\text{Eq. 8.14} \quad V_{C,clamp} = V_{in} \frac{D}{1-D}$$

Practical tip: Equation 8.14 shows that at the lowest Vin, where the duty cycle will be largest, that the factor (D/D-1) will approach 1. The voltage across the clamp capacitor will be equal to Vin,min. At the maximum input voltage, the duty cycle will be low and the factor (D/D-1) will be much less than 1. Therefore the clamp capacitor does not need to be a high voltage type.

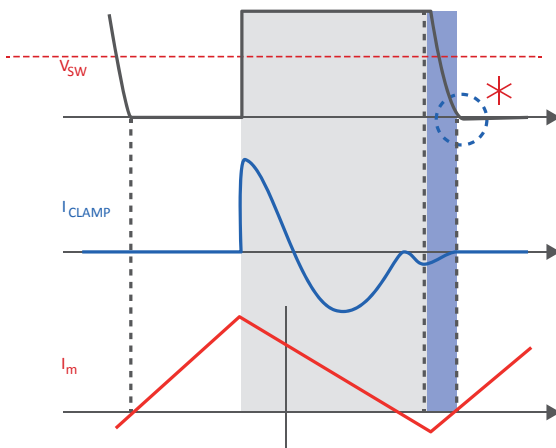


Fig. 8.10: Single-ended flyback high Side clamp current.

8.2.1.2 Low Side Active Clamp

The p-Channel solution shown in Fig 8.11 is easier to drive but needs a more expensive FET. Q2 is driven in phase with the main power transistor. As the active clamp is p-channel and the main switch is n-channel, Q2 is always off when Q1 is on and vice-versa. A dead-time circuit is not needed as there is no danger of shoot-through, but the different threshold voltages of n-channel and p-channel FETs means that there is a transition period when both transistors are off.

This solution has the advantage that both Q1 and Q2 operate in near ZVS.

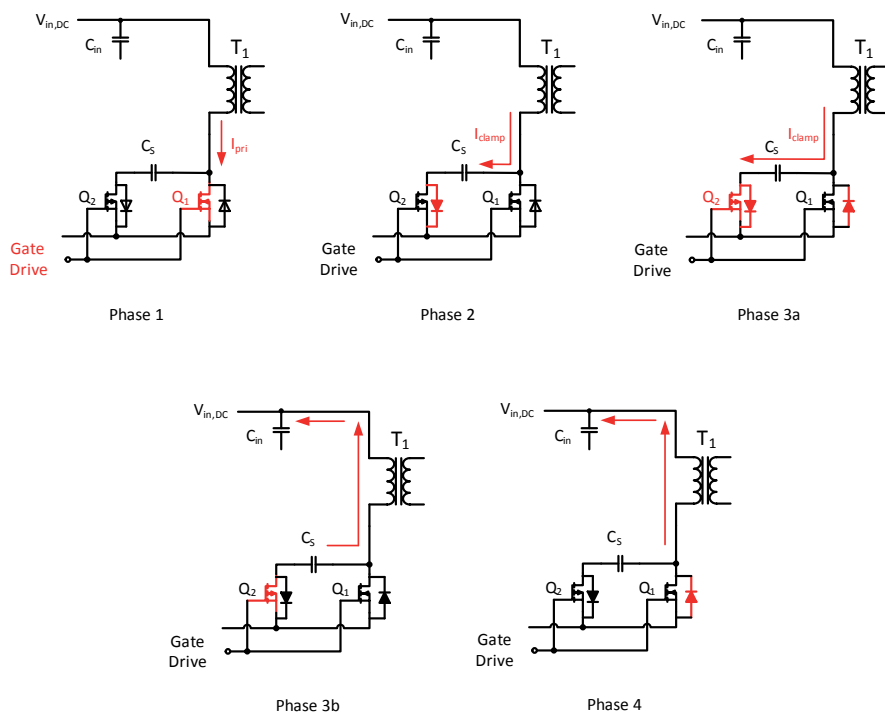


Fig. 8.11: Single-ended flyback low side active clamp current flow.

Phase 1. Q1 on. Q2 off. Q1 switches on in near-ZVS. Energy is stored in the magnetising and leakage inductances. The voltage across the clamp capacitor is zero.

Phase 2. Q1 off. Q2 off (transition time) . The energy stored in the leakage inductance is diverted into low side clamp capacitor by the body diode of Q2 (the body diode is forward biased). The voltage across Q2 stays at 1 diode drop.

Phase 3a. Q1 off. Q2 on. Q2 switches on in near-ZVS. The clamping capacitor rapidly absorbs the energy stored in the leakage inductance via the low R_{DSon} impedance of Q2.

Phase 3b. Q1 off. Q2 on. Once the energy in the leakage inductance has been fully dissipated, the current reverses and energy is transferred from the clamp capacitor back into the input capacitor.

Phase 4: Q1 off, Q2 off. The body diode of Q1 holds the voltage across Q1 to one diode drop. Any remaining energy is returned to the input capacitor via this body diode. The voltage across the clamp capacitor is proportional to the duty cycle and V_{in} :

$$\text{Eq. 8.15} \quad V_{C,clamp} = V_{in} \frac{1}{1-D}$$

Practical Tip: Equation 8.15 shows that at the highest V_{in} , where the duty cycle D will be smallest, that the factor $(1/1-D)$ will approach 1. The voltage across the clamp capacitor will be equal to $V_{in,max}$. At $V_{in,min}$. the duty cycle will be large and the factor $(1/1-D)$ will be much higher than 1. Therefore, the clamp capacitor needs to be a high voltage type.

8.2.1.3 Regenerative Clamp

A regenerative snubber can be made using an additional winding on the transformer which has one end tied to ground. The free end injects current into the clamp capacitor to help cancel out the voltage spike created when the switching transistor turns off. (Fig 8.12).

The advantage of this circuit is that no active switching is required; the current injection is through steering diodes only.

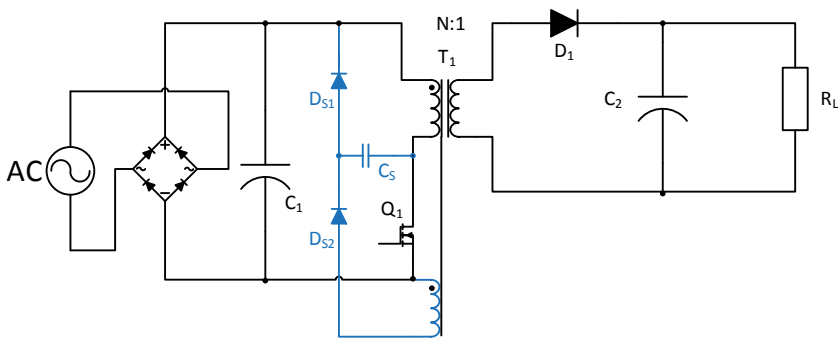


Fig. 8.12: Single-ended flyback with regenerative snubber using an auxiliary winding tied to ground.

8.3 Quasi-Resonant Flyback Converter

A Quasi-Resonant (QR) converter can be made to work with most AC/DC topologies, but it is most commonly used as a single ended flyback. The main difference is that the QR converter PWM timing is dependent on the switch current minima rather than on the output voltage alone. A standard flyback controller has a fixed PWM frequency which defines when the next cycle starts, but the QR uses a free-running oscillator with variable off time.

As in the standard flyback topology, the QR topology PWM controller turns on the switch ON to store energy in the transformer core and then turns the switch OFF to allow the energy to be transferred to the secondary. Once the current in the output rectifier diode has fallen to zero, then both input and output windings currents will fall to zero. Any remaining energy in the core will be reflected back into the primary which will start to resonate at a frequency dependent on the primary inductance, L_p , and the lumped drain capacitance, C_D , consisting of the sum of the switch capacitance, the coupling capacitance between the windings and any other stray capacitances.

Eq. 8.16:
$$f_{RESONANCE} = \frac{1}{2\pi\sqrt{L_p C_D}}$$

Resonant Frequency of a Transformer in QR Mode

With a primary inductance of 500µH and a C_D value of 1nF, the resonant frequency will be around 225 kHz. The voltage across the (open) switch will be the supply voltage superimposed with this resonant oscillation. By choosing to reset the PWM cycle when this voltage is at minimum (valley switching) means that the effective voltage across the switch will be below the supply voltage. This means that the switch now has a much lower turn-on voltage stress and lower turn-on current, both of which will give a measureable increase in efficiency.

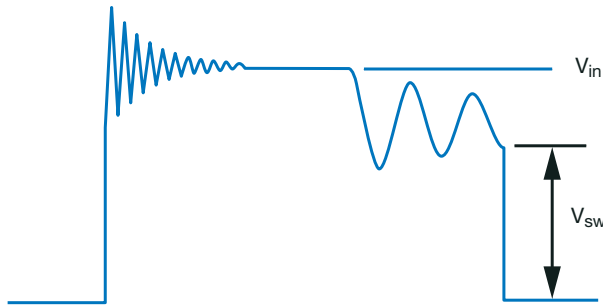


Fig. 8.13: QR valley switching

Another advantage of QR operation is that the PWM period timing changes slightly with each cycle depending on the accuracy of the valley detection circuit. This timing jitter flattens out the EMI spectrum and reduces the peak EMI levels. A reduction of 10dB in the conducted interference levels can readily be achieved compared to a conventional flyback circuit. A disadvantage of QR operation is that the PWM frequency is load-dependent and frequency limiting or valley-lockout circuits are needed to cope with no-load conditions.

8.4 Half-Bridge Resonant Mode Converter

A further development of the QR converter is the fully resonant mode converter design. A Resonant Mode (RM) converter can be made with series resonance, parallel resonance or series parallel resonance (also known as LCC) topologies, but the half-bridge LCC circuit offers particular advantages in resonant mode, so for the sake of simplicity, only this topology will be considered.

The objective of a resonant mode converter is to add sufficient additional capacitance and inductance so that the resonant tank allows Zero Voltage Switching (ZVS). The advantage of ZVS is extremely low losses.

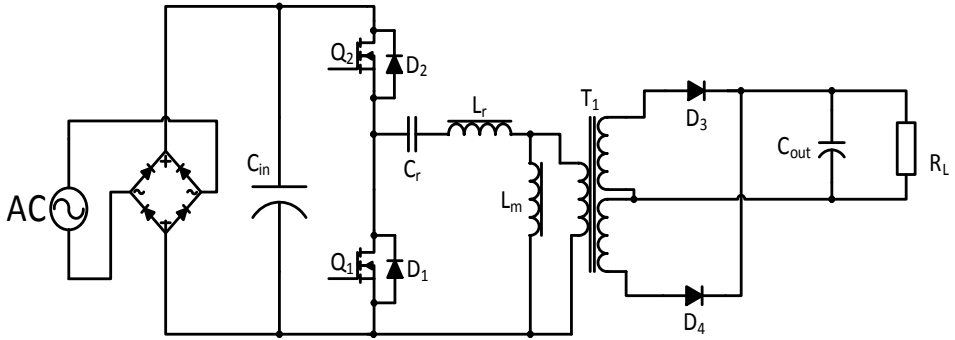


Fig. 8.14: Half-Bridge LLC Resonant Mode topology

This topology has two resonant frequencies. The first being the series resonance tank formed from C_r and L_r and the second the parallel resonance tank formed by C_r and $L_m + L_r$. Typically, both L_m and L_r are wound side-by-side on the transformer to reduce leakage inductance effects.

The double resonant frequencies of a LCC converter can be calculated from Equation 8.17:

$$\text{Eq. 8.17: } f_{Resonance,1} = \frac{1}{2\pi\sqrt{L_r C_r}}$$

$$f_{Resonance,2} = \frac{1}{2\pi\sqrt{(L_r + L_m)C_r}}$$

The advantage of the double resonances is that one or the other takes precedence according to load. So while a series resonant circuit has a frequency that increases with reduced load and a parallel resonant circuit has a frequency that increases with increasing load, a well-designed series parallel resonant circuit has a stable frequency over the whole load range. The switching frequency and values of L_r and C_r are chosen so that the primary winding in continuous resonance and sees an almost perfect sinusoidal waveform. The two half-bridge switches Q1 and Q2 are operated in antiphase. When the FETs are activated, the voltage across them is actually negative. The Gate-Drain voltage is only the internal diode drop and the gate drive current is thus extremely low. As the voltage transitions to positive, the FETs are already ON and start to conduct as the sinusoidal voltage passes through zero.

Combined with the low switching losses and the low transformer losses due to the sinusoidal drive waveform, conversion efficiencies exceeding 95% are readily achievable. Another advantage is that the EMI emissions are extremely low as the entire power train is sinusoidal.

The disadvantages of the LCC converter topology is that the required inductances can be high in order to get a stable resonant frequency with a good Q factor (i.e. low C_r). The converter must also be tuned to operate below the maximum possible gain to allow it start up without problems. Typically a working gain of 80-90% of the maximum is a safe margin.

Additional pulse-mode circuitry may be needed for no-load operation. Although the LLC load range theoretically includes zero load, in practice component tolerances can make the converter unstable with no load.

Finally, the side-by-side transformer construction requires careful design if the creepage and clearance separations required for safety are to be met.

8.5 Full-Bridge Resonant Mode Converters

8.5.1 Phase-Shifted Resonant Full Bridge

A phase-shifted full bridge resonant converter uses a conventional full bridge topology with the addition of a series inductor on the input. The two pairs of switching transistors are driven with two fixed 50% duty cycle PWM signals which are then phase shifted to control the power delivery. (fig.8.15). If the overlap between the two 50% duty PWM signals is low, then only a small amount of energy is transferred across the transformer. If it is high, then full power is transferred. Regulation is thus achieved by shifting the phase of the two PWM signals alone.

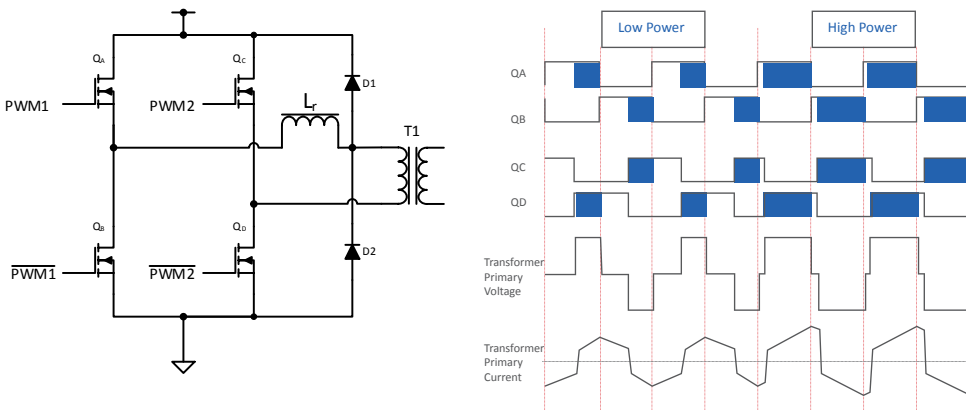


Fig. 8.15: Simplified Phase shifted resonant full bridge schematic and the wave form. The PWM signals are fixed frequency and fixed 50% duty cycle. The blue shaded areas represent the amount of overlap between the two PWM drive signals which controls the amount of power transmission.

The advantages of the phase-shifted full bridge topology is that due to the fixed-frequency resonant operation, all of the transistors switch at zero voltage (ZVS) or near zero voltage, so switching losses are very low. The transistor drive circuit is simplified because only two fixed frequency PWM signals which can be very easily generated from flip-flop circuits (50% duty cycle) are needed to drive all four switches. The resonance inductor, L_{res} , can be omitted if the inherent resonance between the transistor's Coss capacitance and transformer leakage inductance is sufficient to ensure ZVS operation. In this case, both D1 and D2 could also be omitted.

Output Regulation can be done be either voltage mode, average current or peak current control (by adding a current transformer in series with the high voltage supply), all without changing the basic topology. Peak efficiencies of over 95% are readily achievable with this topology, which makes it especially suitable for higher power AC/DC designs.

The disadvantages of the phase-shifted full bridge topology is that the PWM signals must be very precise or have either fixed dead-bands which reduces efficiency or have variable dead-band delays to avoid shoot-through at low loads, making the PWM drive not so simple in practice. Freewheeling (turning on QA + QC or QB + QD simultaneously to circulate the current) is often necessary to clamp the reflected load current and to ensure ZVS conditions which further complicates the drive control and reduces efficiency. Such operating condition-based switching control is often only realizable in practice by microcontrollers running parallel state machines or expensive mixed-signal controllers with internal logic elements.

The supply voltage range is restricted because the efficiency is dependent on resonant ZVS or near-ZVS which is dependent on the square of the supply voltage (eq. 8.18), so a PFC front end is necessary for a universal mains supply. For higher AC supply voltages (for, example 480VAC), it may be necessary to use cascode switching FETs to meet the Vds requirements. The resonant inductance needed for ZVS turn-on can be calculated from equation 8.18:

$$\text{Eq. 8.18: } L_{res,min} = (2C_{oss} + C_{pri}) \left(\frac{V_{supply}}{I_{pri,peak}} \right)^2$$

The junction capacitance of the two switches in each leg of the full bridge are effectively in parallel during switching, so the individual transistor C_{oss} value needs to be doubled and added to the measured primary winding capacitance to calculate the resonance capacitance. If the combination of the transformer leakage and magnetizing inductances exceed $L_{res,min}$ under worst case conditions, then no external inductor is needed.

Practical Tip: In the equation above, note that doubling the AC supply voltage not only increases the numerator, but also reduces the peak current in the denominator by a squared factor, meaning that a 16 times smaller resonance inductance is needed!

Although the basic concept of the phase-shifted full bridge resonant converter is to use a fixed-frequency PWM frequency, there are some designs that combine phase-shift control at full load with variable frequency PWM control at low loads to realise a high efficiency across the complete load range.

8.5.2 Resonant Full Bridge

If a series capacitor is added to the circuit shown in fig. 8.11, then a resonant converter with zero voltage switching (ZVS) or Zero Current Switching (ZCS) can be created:

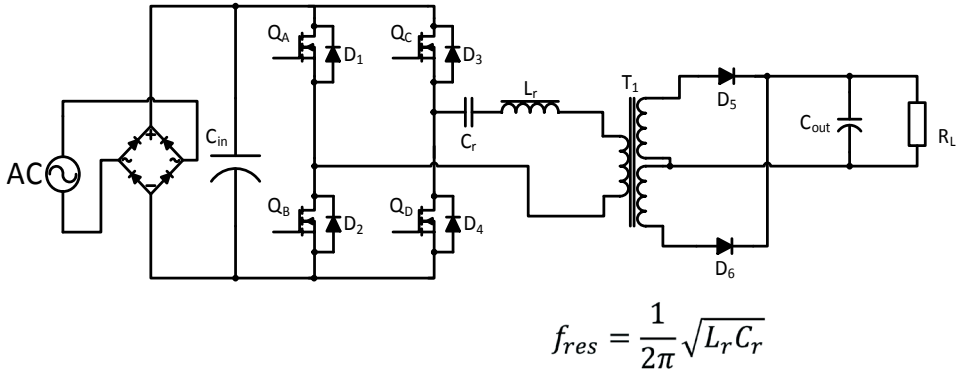


Fig. 8.16: Series Resonant full bridge with resonant frequency f_{res}

Unlike the phase-shifted resonant converter, there is no overlap between the PWM signals with a defined dead time to avoid any chance of an overlap.

Power transfer is controlled by changing the PWM frequency above, equal to or below the resonant frequency of the C_{res} and L_{res} tank circuit. This gives three possible modes of operation:

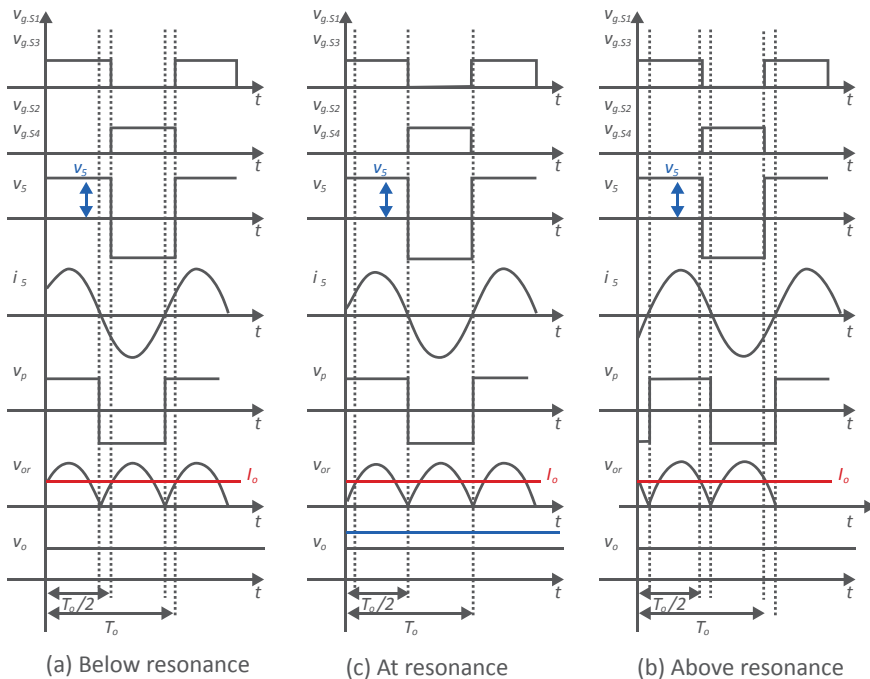


Fig. 8.17: Below resonance, the resonant input current, I_s , leads the PWM switched voltage, V_s . At resonance, I_s is in phase with V_s and above resonance, I_s lags V_s .

Mode 1: below resonance. The input current leads the switched supply voltage, i.e. the impedance is capacitive. The transistors switch in ZCS mode.

Mode 2: at resonance. The input current is in phase with the switched supply voltage, i.e. the impedance is purely resistive. The transistors switch in ZCS mode and the output voltage is at its maximum.

Mode 3: above resonance. The input current lags the switched supply voltage, i.e. the impedance is inductive. The transistors switch in ZVS mode.

The output voltage is at a maximum when the switching frequency is equal to the resonant frequency:

$$\text{Eq. 8.19: } |V_{out}| = \frac{0.9V_{in}}{\sqrt{1 + Q^2\left(\omega + \frac{1}{\omega}\right)^2}}$$

Where ω is the relative operating angular frequency, $\frac{\omega_{sw}}{\omega_{res}}$, and Q is the quality factor:

$$\text{Eq. 8.20: } Q = \frac{1}{2\pi f_{res} C_r R_{AC}}$$

Where R_{AC} represents the transformer load.

The 0.9 factor in the numerator of Eq. 8.19 comes from a relationship of $\frac{2\sqrt{2}}{\pi}$ which means that at resonance, the output voltage is $0.9V_{in}$ (refer to figure 8.18)

Output power can be reduced by changing the PWM frequency either above or below the resonant frequency, but as ZVS control is optimal for both turn-on and turn-off losses whereas ZCS only helps with turn-off losses, typically an increase in frequency is used to reduce the output power.

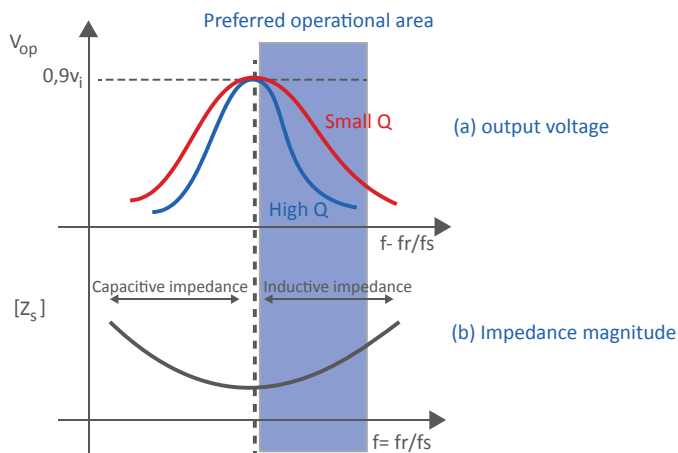


Fig. 8.18: Output voltage control by increasing the PWM frequency above resonance

The advantages the variable frequency full bridge resonant controller is high efficiency over a wide load range as the topology remains in resonance from full load down to light load.

The disadvantage is that no-load operation is not possible without losing resonant operation and therefore the control over the output voltage, so a minimum load is always required.

This drawback can be eliminated by adding an additional resonance capacitor in parallel with the transformer primary winding to make a series-parallel resonant full bridge (fig. 8.19). This topology will stay in resonance from full load down to no-load conditions with good light load-ing efficiency, but requires a PFC front end to provide a stable bus voltage.

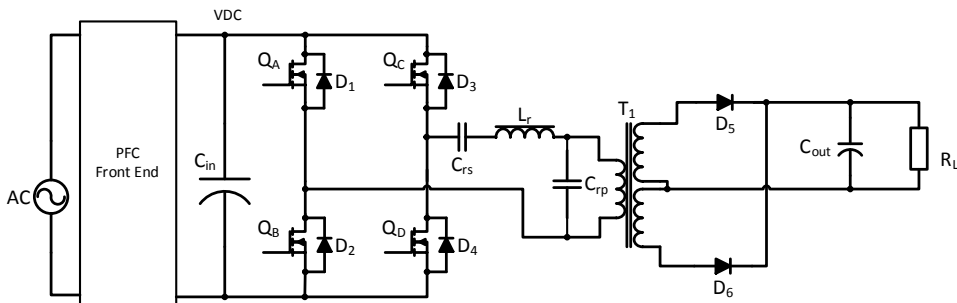


Fig. 8.19: Series-Parallel Resonant full bridge converter.

8.6 Single-Ended Forward Converter

Although the forward converter seems similar to the flyback topology, it functions in a completely different way, relying on continuous transformer action to transfer power from input to output rather than intermittently storing the energy in the magnetic field of the core gap. The input voltage is converted into a regulated output voltage as a function of the turns ratio of the transformer and no gap is needed nor desirable. Figure 8.20 shows the simplified circuit (refer to the DC/DC Book of Knowledge for the voltage and current waveforms and explanation of the transfer function).

As the power transfer is continuous over time, we speak of volt-seconds. The volt-seconds during the ON time must not exceed the volt-seconds during the OFF time; otherwise the core will eventually saturate due to a process called flux walking (refer to the DC/DC Book of Knowledge, Chapter 10). This is guaranteed by adding a reset winding that ensures that the core is fully demagnetized at the end of each switching cycle.

As the reset winding ensures that the core fully desaturates at the end of each cycle, the duty cycle can be higher than 50%, but it is more typically kept below 50% to give a margin of error. This limits the input voltage range of the converter to typically 2:1, making a universal input AC/DC forward converter more difficult to design than a flyback. Thus AC/DC forward converters are usually used with a PFC front end to give a stable DC bus voltage to work from.

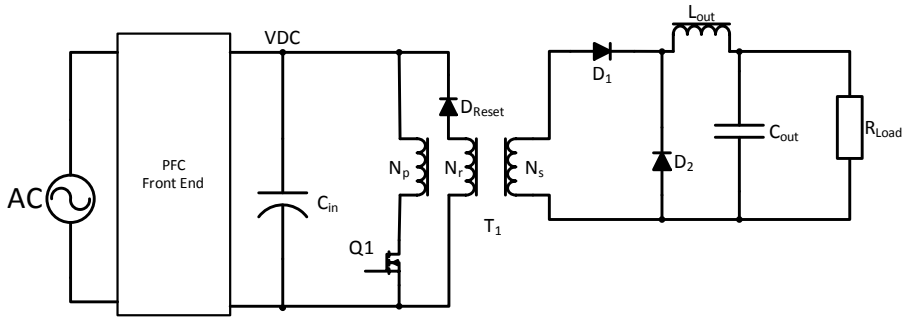


Fig. 8.20: Forward Topology (simplified)

As a forward converter transfers has a continuous magnetic core, the magnetic field is more evenly distributed and the associated hysteresis losses and radiated EMI from the concentrated fields across a gap in the flyback topology are avoided.

Other advantages are that the lower peak current reduces winding and diode losses and lead to a lower input and output ripple current (Fig. 8.21). The reset winding transfers excess stored energy back into the PFC capacitor rather than simply having to dissipate the energy in a snubber network. For the same output power, a forward converter will therefore be more efficient than a flyback.

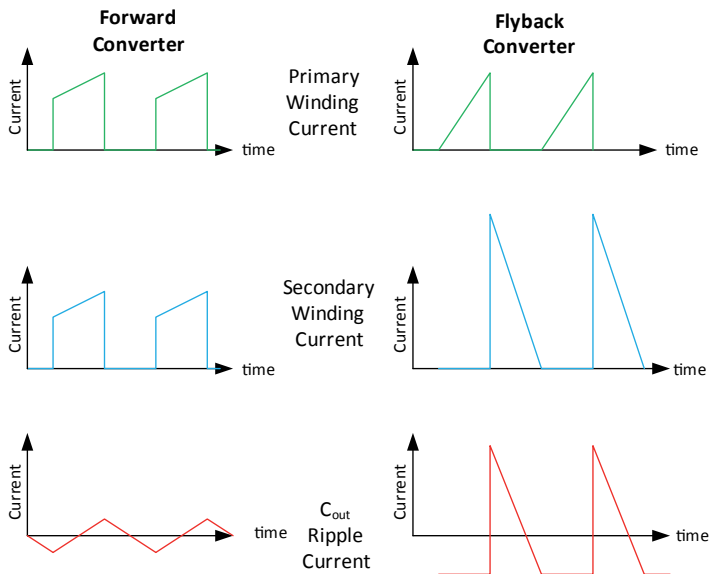


Fig. 8.21: Comparison of forward and flyback waveforms. The peak currents in the forward topology are lower and in particular, the output capacitor has a much lower ripple current.

The disadvantage of the forward topology is a more complicated transformer construction which makes meeting the required creepage and clearance separations more troublesome and an increased component cost as an output inductor, L_{out} , is needed for each output. If a bipolar (\pm) output is required where the positive and negative output voltages are complementary, then a transformer style (two inductors sharing the same core) output inductor can be used to save costs. This is not a true transformer but two mutually coupled inductors, so it is important that the windings are bifilar wound to get good coupling. This will improve the cross regulation and reduce the output ripple considerably compared to two independent chokes.

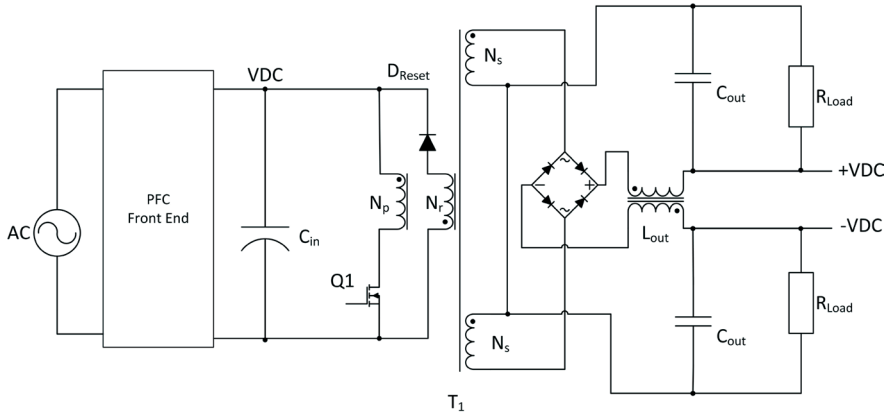


Fig. 8.22: Forward converter with bipolar output using a mutually coupled output inductor.

If multiple independent outputs are required, then each forward converter output needs an output inductor and capacitor, so in this case, the flyback topology would often be a better choice (but refer also to the current-fed forward converter Section 8.6.2).

As with the flyback topology, snubbers are needed to suppress transients to protect the active components. Unlike the flyback, additional voltage transients caused by leakage inductance between the primary and reset windings need to be controlled. In the conventional forward clamp topology with the same number of turns on the primary and reset windings, if the voltage across the switching transistor when it turns off exceeds double the supply voltage, then current will begin to flow in the reset winding. However, this transfer of energy is not instantaneous. The time taken for the current to transfer from the primary to the reset winding is slowed down by the leakage inductance between the primary winding and the reset winding. During this delay, the voltage on the switching transistor will exceed double the supply voltage and can overstress the transistor. The capacitor C_{clamp} mitigates this overvoltage by providing a low impedance path through the reset winding diode (fig 8.23).

As the current flows back into the input capacitor, energy is returned into the circuit rather than being simply dissipated through a clamping resistor, so this is an example of a lossless clamp.

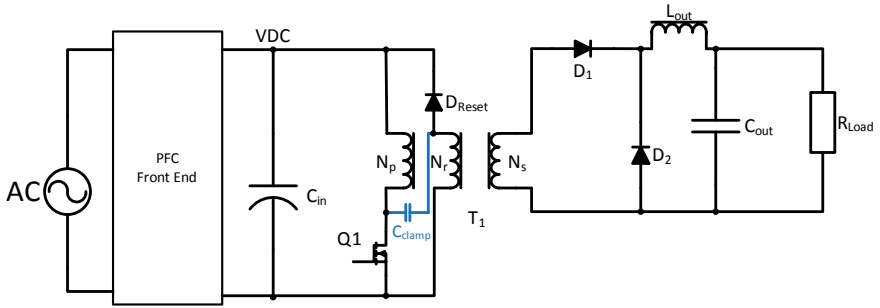


Fig. 8.23: lossless clamp forward converter (simplified)

The required clamping capacitance can be calculated from the following equation (assuming that the primary and reset windings have the same number of turns):

$$\text{Eq. 8.21: } C_{clamp} = \frac{L_p (I_{load}/N_{ps})^2}{2V_s V_{os}}$$

Where L_p is the primary inductance, N_{ps} is the primary/secondary turns ratio, V_s is the supply voltage and V_{os} is the desired maximum overshoot voltage.

As the reset diode has to carry the excess energy transferred via the clamping capacitor, it must be peak current rated $> I_{load}/N_{ps}$. The voltage rating must, of course, be higher than $2V_s$.

In addition to the primary side clamp, there is often a need to add snubbers across the switching transistor and secondary diode D_2 to control any high frequency ringing that can cause EMI problems.

This is because when Q_1 switches on, current starts to flow in the rectifier diode, D_1 , until it has fully charged the output capacitor and now only has to supply the load current. At this point, the voltage across the diode will increase further due to the reflected input voltage transferred by the transformer leakage inductance. As no more current can flow in the load, the current starts to oscillate across the diode D_2 junction capacitance. Adding a snubber $C_{ssn} + R_{ssn}$ across D_2 will absorb this excess energy and damp the ringing (fig. 8.24).

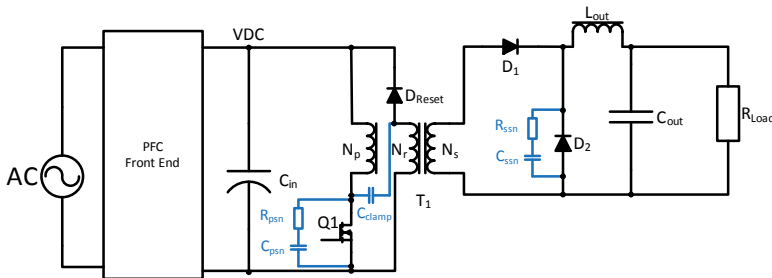


Fig. 8.24: forward converter with both over-voltage clamp and primary side and secondary side snubbers.

Practical Tip: Finding the optimum values for C_{ssn} and R_{ssn} can be done by experiment:

1. measure the ringing frequency without a snubber.
2. add sufficient capacitance in parallel with D2 until the frequency is halved
3. the parasitic capacitance, C_{para} , is 1/3 of the added capacitance.
4. the parasitic inductance can be calculated from Equation 8.22:

$$\text{Eq. 8.22: } L_{para} = \left(\frac{1}{2\pi f_{ring}} \right)^2$$

5. The snubber resistor should be ideally the same as the characteristic impedance:

$$\text{Eq. 8.23: } R_{ssn} = Z_0 = \sqrt{L_{para} / C_{para}}$$

6. The power dissipated in the snubber resistor can be calculated from:

$$\text{Eq. 8.24: } P_{diss} = f_{sw} C_{ssn} V_{pk}^2$$

Where f_{sw} is the operating switching frequency, C_{ssn} is the secondary snubber capacitor and V_{pk} is the peak voltage across D2.

If the power dissipation in the snubber resistor is too high, then a compromise may be required to increase the stress on the diode in exchange for reducing the stress on the snubber.

8.6.1 Interleaved Single-Ended Forward

Forward converters are typically used up output currents of around 25A. Above this current, the high discontinuous primary current cannot be easily handled by increasing the size of the input capacitor bank and by paralleling up the primary switching transistors. Furthermore, the output inductor and capacitor become very bulky.

Synchronous rectification (SR) on the output helps reduce the losses, but using SR makes it difficult to parallel the outputs of two forward converters if more power is required (the SR switching can interfere with the load share current balancing circuit).

One solution to high current, low voltage forward converters is to interleave the power stage using two transformers switched 180° out of phase (Fig 8.25). The additional complexity adds some cost, but this is often balanced out by the reduced size of the input and output capacitors as the ripple currents are significantly reduced (each forward converter stage exhibits a dis-

continuous RMS ripple current but when added together the overall current is more continuous and approaches DC – See Fig.8.26). Only one input and one output capacitor is needed which also reduces the cost.

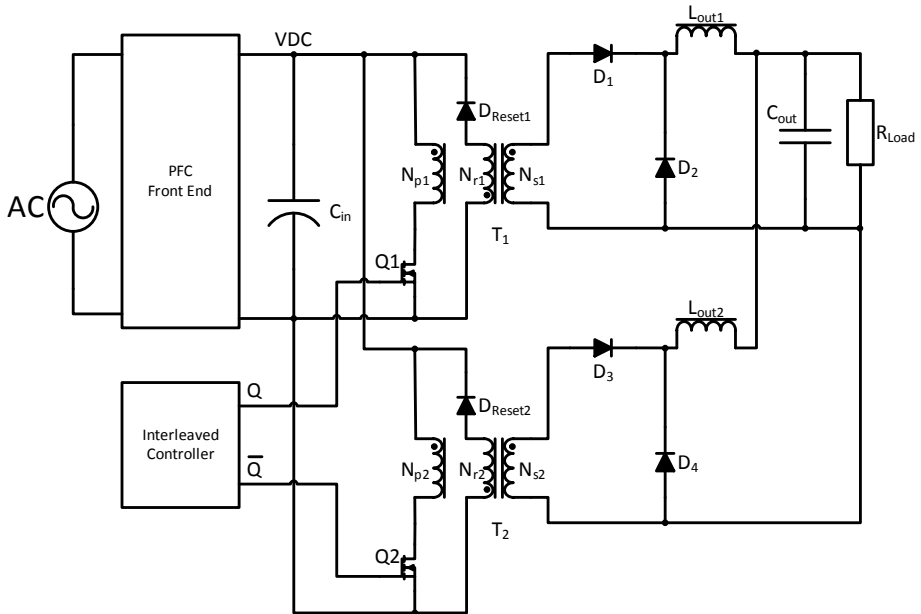


Fig. 8.25: Interleaved single-ended dual forward converter topology

The idealized waveform shown below is only valid for a 50% duty cycle. If the duty cycle is changed, then the output currents of the two stages are not perfectly complementary and the ripple currents will increase.

The input capacitor, C_{in} , will have a ripple current of approximately:

$$\text{Eq. 8.25: } I_{\text{ripple}, C_{in}} \approx \frac{I_{OUT}}{2N} \sqrt{2\delta(1-2\delta)}, \text{ for } \delta \leq 0.5$$

$$I_{\text{ripple}, C_{in}} \approx \frac{I_{OUT}}{2N} \sqrt{4\delta(1-0.5\delta)(1-\delta)}, \text{ for } \delta > 0.5$$

Where N is the transformer turns ratio and δ is the duty cycle.

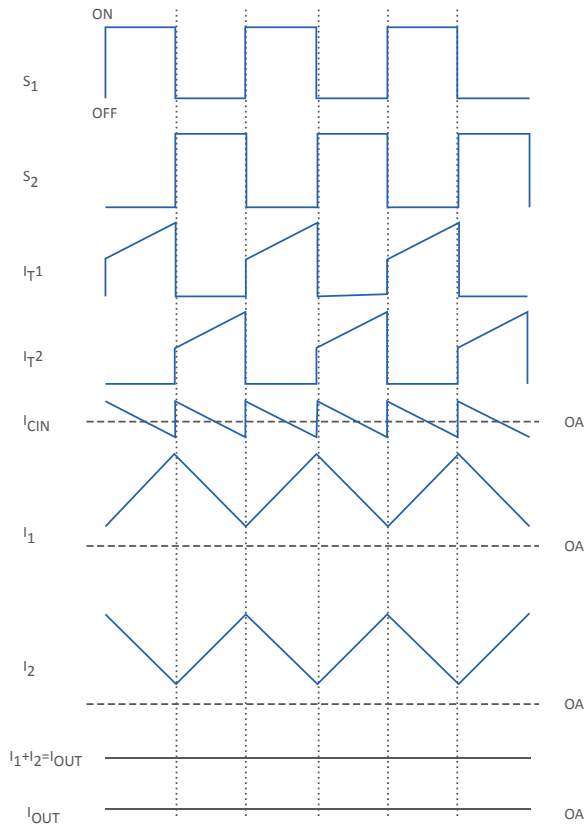


Fig. 8.26: interleaved forward converter waveforms. Note the reduced input and output RMS ripple currents (the output current is almost DC).

Plotted on a graph, fig. 8.27 shows the relationship of normalized input capacitor ripple current to duty cycle. The worst case input ripple occurs at 0.25 and 0.75 duty cycle.

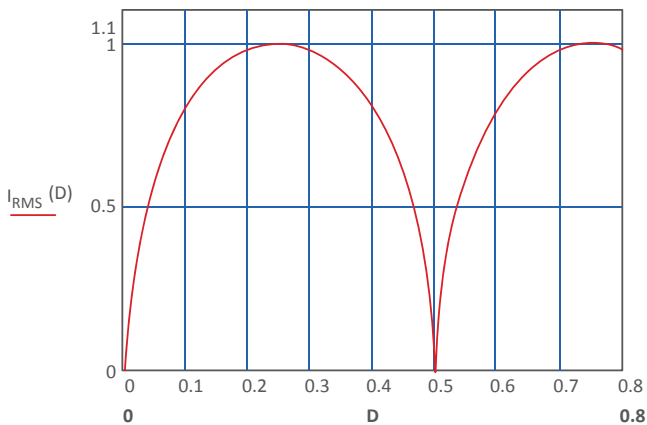


Fig. 8.27 Input ripple (normalized) vs duty cycle for an interleaved forward converter

The output ripple current follows a different relationship as in Equation 8.25:

$$\text{Eq. 8.26: } \frac{I_{\text{ripple,COUT}}}{I_{\text{ripple,LOUT}}} \approx \frac{1-2\delta}{1-\delta}, \text{ for } \delta \leq 0.5$$

$$\frac{I_{\text{ripple,COUT}}}{I_{\text{ripple,LOUT}}} \approx \frac{1-2(1-\delta)}{1-(1-\delta)}, \text{ for } \delta > 0.5$$

Plotted on a graph, fig. 8.28 shows the relationship of the ripple cancellation factor, $K(\delta)$, (capacitor ripple current divided by inductor ripple current) to the duty cycle.

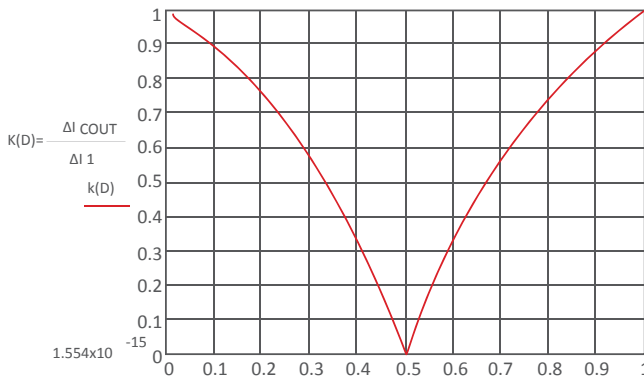


Fig. 8.28: Ripple cancellation factor (normalized) vs duty cycle.

As can be seen from figures 8.27 and 8.28, the interleaved forward converter is most efficient if the duty cycle is very close to 0.5. Therefore, a PFC front end is essential to compensate for input voltage variations while keeping the duty cycle constant.

If more output current than 50A is needed, then three input power stages and transformers can be wired in parallel with 120° phase shift. With 0.33 duty cycle, the input and output ripple currents will all superimpose to give a very low combined overall ripple current. And if even more current is needed, then two 180° interleaved forward converters can be paralleled to deliver 100A. The current balance between these paralleled stages must be very carefully controlled; even a small deviation in the phase current sharing between the stages will increase the ripple currents dramatically.

In practice, some kind of active duty cycle control is needed to compensate for component tolerances, temperature variations and dynamic loads. In addition, each of these paralleled power stages will need their own snubber networks on the primary switch and secondary diodes which will reduce the overall efficiency, especially at low loads. Interleaving the power stages reduces conduction losses (the current paths have lower impedances) but increases the switching losses. At high output currents, conduction losses dominate, but at low output currents, switching losses dominate.

Practical Tip: One technique to improve the efficiency over the whole load range is to shut down one or more parallel phases at low loads. This can add as much as 15% to the low load efficiency by operating the converter as a single phase forward converter with all of the current flowing through one power stage only. Another saving can be made by switching off the synchronous rectification on the secondary side under low-load conditions and relying on paralleled diodes across the FETs to rectify any residual output current.

Without digital control, such complex feedback mechanisms are impractical, but with a programmable controller it is possible to ensure efficiencies of close to 95% across a very wide load range.

In order to get the best of both worlds and have good efficiency at both very heavy load and light load, a forward converter topology is often preferred for high power, high efficiency designs.

8.6.2 Current-fed Single-Ended Forward

As previously mentioned, a forward converter relies on a storage inductor on the output as ideally no energy is stored or lost in the transformer itself. This means that a multiple output voltage-fed forward converter rapidly becomes very expensive as every output requires its own inductor.

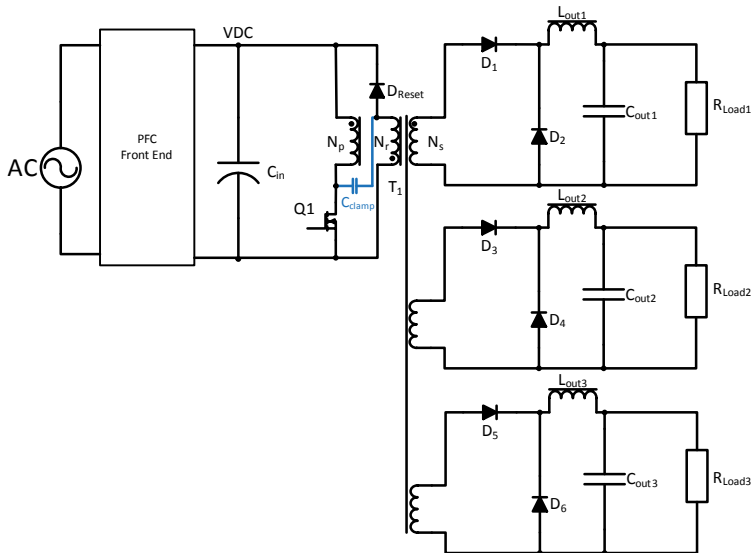


Fig. 8.29: Triple output voltage-fed forward converter with inductors on each output.

The current fed forward topology adds the inductive storage element on the primary side, making the topology a current converter rather than a voltage converter. This eliminates the necessity of an output inductor and makes multiple outputs more commercially attractive. The disadvantage is that a current source rather than a voltage source is required, typically realized by adding a chopper or buck converter input stage. Output regulation can be achieved

by controlling the PWM signal of the input stage only, leaving the forward converter running with a fixed 50% duty cycle (alternately, the buck converter can be operated with a fixed duty cycle and the forward converter duty cycle modified for regulation). In either case, the topology is insensitive to the rise and fall times so high frequency PWM frequencies can be used to reduce the inductor and transformer sizes.

Current fed forward converters typically use two-transistor, push-pull or full-bridge topologies (see following sections). This is because the two switches must overlap, so that the current flow through the transformer is continuous and uninterrupted (any break in the current flow would cause destructively high voltages to develop). The primary side inductor limits the current when both switches are on, which also gives the advantage that the topology is inherently short-circuit protected. This is very important for high power applications, as designing a reliable over-current trip with high dynamic current loads is tricky; as the current fed forward topology can tolerate brief short circuit conditions without damage, the over-current trip time can be extended to avoid nuisance tripping in noisy electrical environments.

As an active PFC boost stage is impractical (boost followed by a buck followed by a forward converter), current-fed forward converters are typically used where power factor correction is not an issue, such as in three phase supplies or where the power is higher than 3kW and the regulations do not apply.

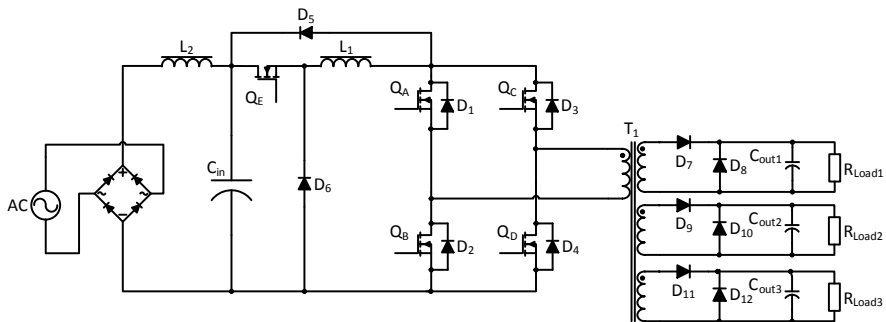


Fig. 8.30: Triple output current-fed full bridge forward converter.

L_2 , C_{in} , Q_E and D_6 form the current source. L_1 is the forward primary side storage inductor replacing the inductors on each output. The full bridge configuration avoids the need for a reset winding as long as the duty cycle $\leq 50\%$. D_5 clamps and recycles any excess energy back into the input capacitor.

8.7 Two-Transistor Topologies

8.7.1 Two-transistor Forward Converter

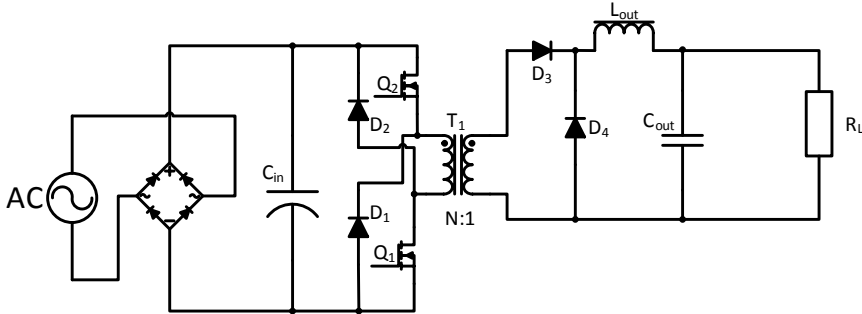


Fig. 8.31: Two-transistor forward topology

Two-transistor (TT) converters are considered one of the most reliable topologies for higher power AC/DC converters. There are several reasons for this:

1. The switching transistors have to handle the only the maximum input voltage (which is a fixed voltage if a PFC front end is used). Any turn-off switching transients caused by parasitic elements are gated by the fast recovery diodes. This means that the transistors need only be rated for the input voltage plus some headroom, rather than for double the input voltage as in a single-ended switched topology.
2. Timing is not critical – as both transistors turn on and off together, there is no requirement for any dead times to avoid shoot-through.
3. No snubber networks are needed. Both the residual magnetizing energy and any energy stored in the leakage inductance are transferred back into the PFC capacitor at the end of each cycle by the two diodes. This enhances the efficiency and reduces EMI as excess energy is not dissipated but recycled.
4. There is no need for a reset winding, simplifying the construction of the transformer and lowering the cost.
5. As the topology is hard switching, no reverse voltages appear across the MOSFETs under any operating condition, so the transistor body diodes are not stressed.

The disadvantages are that ZVS-operation is not possible which limits the operating frequency and that the duty cycle must be kept below 0.5 to allow the transformer time to reset on each cycle. Also the freewheeling diodes must be the more expensive high voltage fast-acting type.

Although both transistors are driven by the same PWM signal, the high side FET will need a floating gate driver which also adds cost. However, as the FETs need only be rated for V_{in} , the additional costs are often balanced out by cheaper power-FET prices.

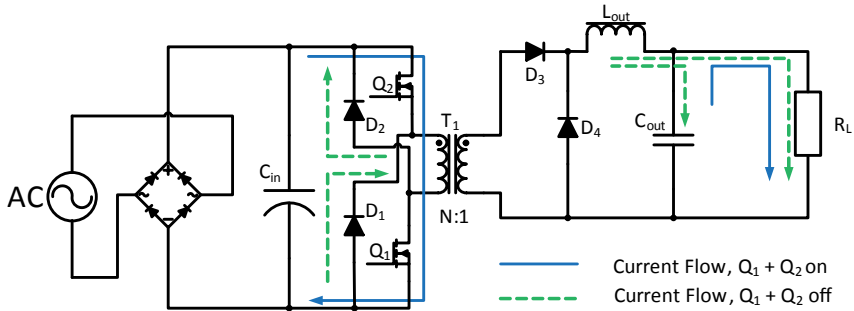


Fig. 8.32: TT-Forward topology CCM current paths with the transistors on (blue) and off (green). Excess energy is returned to the input capacitor at the end of each cycle, so no snubber is required.

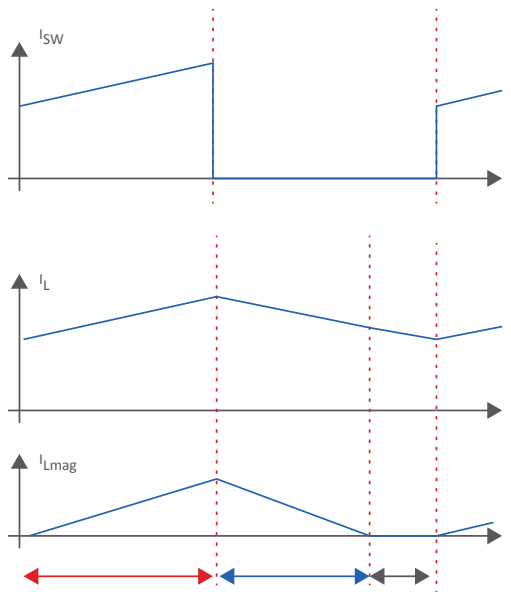


Fig. 8.33: Current flowing in the switch (I_{sw}), secondary winding (I_L) and in the primary winding, $I_{L, mag}$. As a rule-of-thumb, the peak $I_{L, mag}$ is chosen to be 1/10th of $I_{sw, peak}$.

During the first part of the cycle (red), both transistors are on and the freewheeling diodes are biased off. The current through the transistors (I_{sw}) and in the primary winding (I_{pri}) ramps up. During the second half of the cycle, the transistors are turned off ($I_{sw} = 0$) and the primary current and magnetizing current ramp down again through the freewheeling diodes back into the input capacitor, until the core has been completely demagnetized (green section). The

freewheeling diodes then turn off. The time until the next cycle starts (blue section) is the margin needed to ensure that the core is completely reset each cycle. During this time, the primary winding current still continues to ramp down as current is still circulating through the output diode (CCM operation).

8.7.2 Push-Pull Forward Converter

The Push-Pull topology uses a centre-tapped primary and secondary transformer windings and alternately switching transistors. This adds to the complexity of the transformer construction and increases the switching voltage stress on the transistors to $2V_{in}$, but allows four quadrant use of the magnetic core. In other words, double the power for the same sized transformer core compared to a single ended forward design, this makes the push-pull topology suitable for AC/DC converters up to 1kW.

However, as the full input current flows through each primary half-winding, they each need to cope with double the current compared to a single-ended design, so they need to be suitably dimensioned to cope.

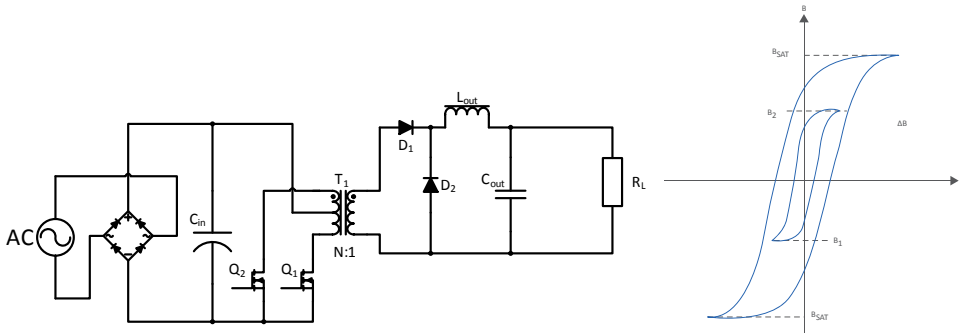


Fig. 8.34: Push-Pull Topology and the B-H curve operating area

To avoid core saturation, both transistors need to be switched on for the same time so that the core magnetic flux density swings reliably from B_1 to B_2 with each cycle and does not “flux-walk” into saturation. Any imbalance caused by timing errors, winding differences or unequal voltage drop across the output diodes can cause a gradual drift into core saturation as there is no separate core reset mechanism. There are a number of techniques that can be used to avoid or detect impending core saturation; the simplest is to use peak current mode feedback to adjust the T_{on} times to keep the peak current under control. If voltage mode regulation is required for the application, then an alternative is to add a small air gap to the core so that the core flux density is reduced to manageable levels.

The switching transistors need to cope with at least double V_{in} (add 20% margin for safety, i.e. 900V rated transistors are needed for a 230VAC input) and be switched with a dead time to avoid shoot-through which creates severe problems for the output diodes during the dead-times unless diode snubbers are added.

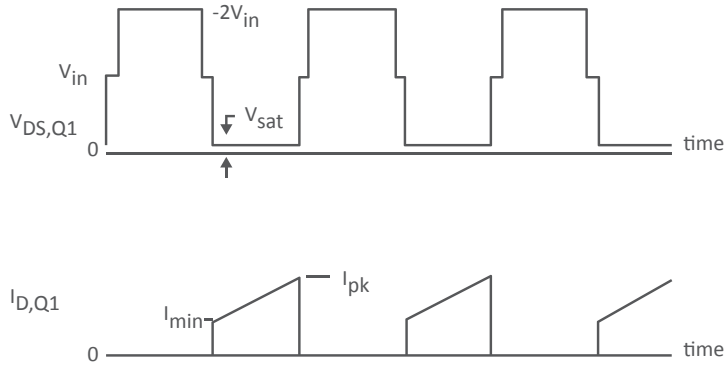


Fig. 8.35: Primary side switching waveform (only Q1 shown for simplicity. Q2 is identical but 180° out of phase)

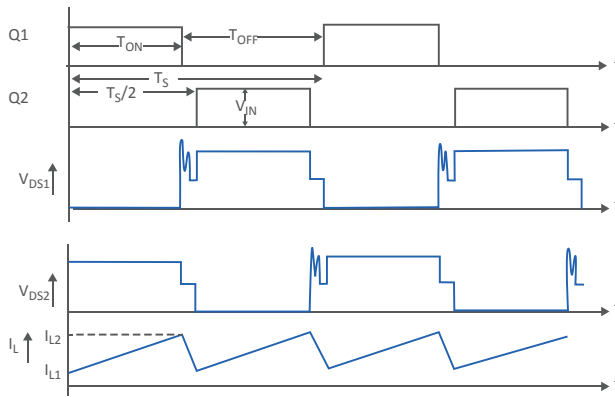


Fig. 8.36: Secondary side switching waveforms showing the need to add output diode snubbers.

8.7.3 Current-Fed Push-Pull Forward Converter

An alternate solution that avoids the need for output diode snubbers is to add an inductor on the primary side to make the push-pull current fed. Then the primary side switching waveforms must overlap to keep the current flow continuous:

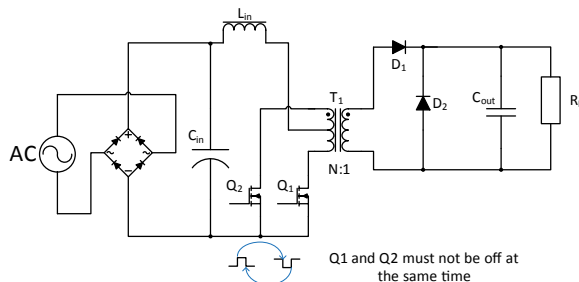


Fig. 8.37. Current-Fed Push Pull

Making the Push-Pull current fed changes the V_{in}/V_{out} relationship:

$$\text{Eq. 8.37. Voltage Fed: } V_{out} = V_{in} \left(\frac{n_{sec}}{n_{pri}} \right) 2 \left(\frac{t_{on}}{t_{on} + t_{off}} \right)$$

$$\text{Eq. 8.38. Current Fed: } V_{out} = V_{in} \left(\frac{n_{sec}}{n_{pri}} \right) \frac{1}{2 \left(1 - \left(\frac{t_{on}}{t_{on} + t_{off}} \right) \right)}$$

8.7.4 Two-transistor Flyback

The advantages of the two-transistor topology can also be extended to a flyback topology.

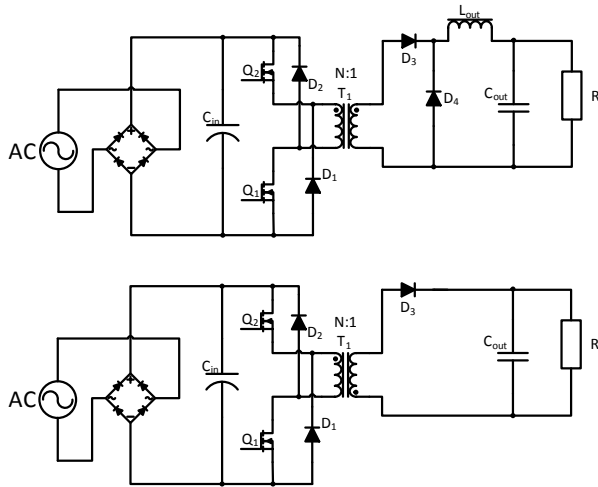


Fig. 8.38: Comparison of Two-Transistor Forward (top) and Two-Transistor Flyback (bottom) topologies.

As with the TT-forward topology, both transistors in the TT-flyback topology are turned on and off simultaneously. Note that the output winding is reversed with respect to the forward topology. All of the advantages of the two-transistor forward converter also apply to the two-transistor flyback converter:

1. The switching transistors have to handle the only the maximum input voltage (which is a fixed voltage if a PFC front end is used) as the overall voltage stress is divided equally over the two transistors.
2. Timing is not critical – as both transistors turn on and off together, there is no requirement for any dead times to avoid shoot-through.
3. No snubber networks are needed. The leakage inductance energy is gated by the fast recovery diodes and recycled into the input capacitor.

- As the topology is hard switching, no reverse voltages appear across the MOSFETs under any operating condition, so the transistor body diodes are not stressed.

As flyback converters are typically very low-cost applications, the two-transistor flyback is seldom seen despite its inherent advantages, mainly due to the added cost of the additional high-side transistor with its floating gate drive and the need for two expensive fast-acting freewheeling diodes.

The two-transistor flyback can be used in CCM, DCM or CrCM modes, just like the single-ended topology.

In continuous conduction mode, the voltage across each transistor will show a clamped ringing caused by the resonance of the switching transistor's C_{oss} Capacitance and the primary inductance before stabilizing at half of the combined input and output voltage (figure 8.39). As this ringing is clamped by the recovery diode and quickly damped by the primary winding resistance, there is no need for a snubber.

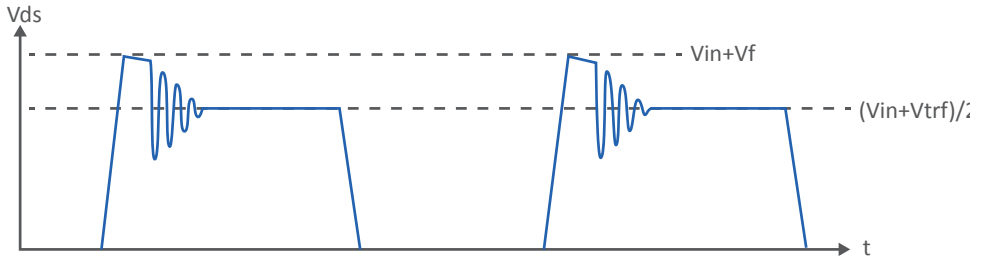


Fig. 8.39: Two-Transistor Flyback in CCM. Vf is the forward voltage drop of the recovery diode, so the maximum voltage stress on each transistor is $V_{in} + V_f$. Vref is the reflected output voltage.

In discontinuous conduction mode, there will be an additional ringing seen on the waveform as the output current falls to zero, again caused by the interaction of the transistor's output capacitance and the primary winding inductance (figure. 8.40). Again the recovery diodes clamp the oscillation to limit the voltage stress on the switching transistors.

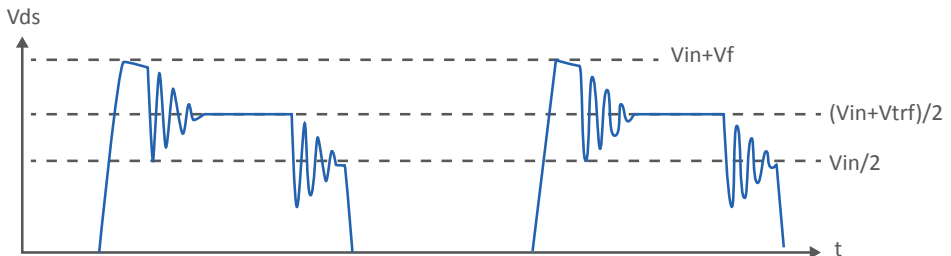


Fig. 8.40: Two-Transistor Flyback in DCM.

8.8 Using paralleled transformers to increase the power.

An often used technique to increase the power of an AC/DC converter is to operate multiple transformers in parallel. This can be done with the forward topology very simply by directly connecting the two transformers to the same power stage and output rectifiers. Note: the switching is not interleaved but simply paralleled.

The transformers need to be fairly well matched to ensure good power sharing:

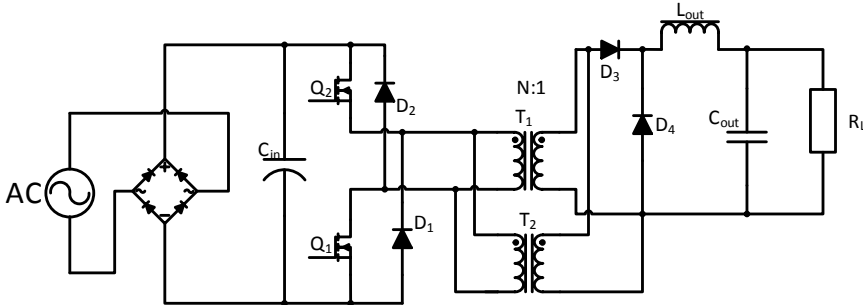


Fig. 8.41: Directly paralleled forward transformers

To allow for production tolerances, it is often better to use separate forward diodes. The current sharing ratio then becomes simply the ratio of the diode forward resistances which are more tightly controlled than the transformer parasitics:

$$\text{Eq. 8.39: } \frac{I_{sec,T1}}{I_{sec,T2}} = \frac{D1_{Ron}}{D2_{Ron}}$$

Practical Tip: As the diode on-resistance is temperature dependent, mount both D_1 and D_2 close together or on the same heatsink so that they remain thermally matched or, better still, use a double diode with a common cathode:

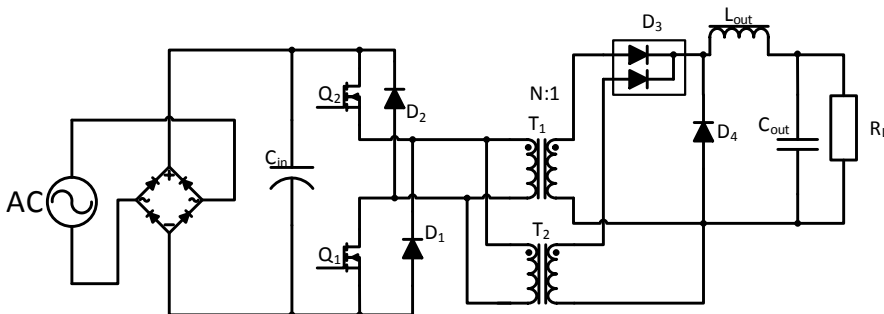


Fig. 8.42: Paralleled transformers with separate forward diodes.

It is also possible to operate transformers in series to share the dissipated power and reduce the core temperatures. This is more commonly called a stacked topology. An elegant solution is to use a capacitive divider to set the centre voltage at half the rectified DC bus voltage. The voltage stress on the switching transistors is then halved. The stacking can be repeated if higher voltages need to be accommodated:

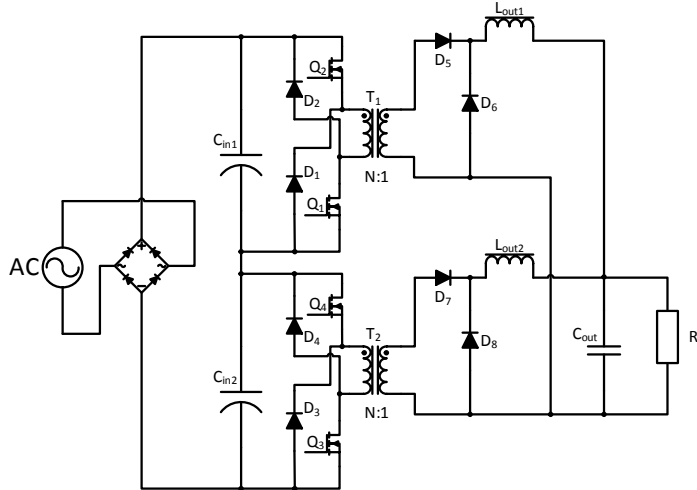


Fig. 8.43: Stacked full bridge forward converter. Each switching transistor has half the voltage stress of a single stage. If three transformers and capacitors were to be used, then each transistor has a third of the voltage stress.

In this interesting example of a stacked interleaved transformer flyback*, only a single active clamp is required. This variation of a stacked converter uses auxiliary windings on each transformer to improve the power factor by injecting current back into the DC bus voltage (a technique called input current shaping):

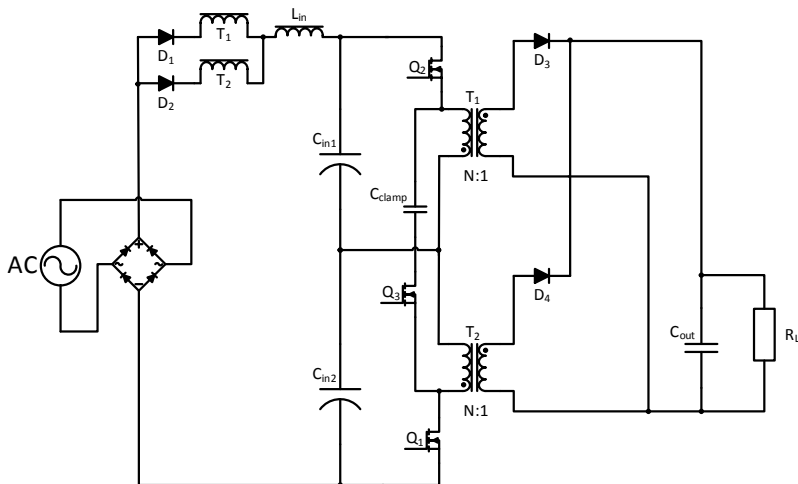


Fig. 8.44: Stacked flyback topology with capacitor divider

Q1 and Q2 are operated alternately with a suitable dead time between them. During the dead time, Q3 is operated to actively clamp the combined transformer voltage by circulating the current back into clamp capacitor Cclamp. As the clamp current flows in both directions, Cclamp must be non-polarized and Q3 switched with a floating driver supply:

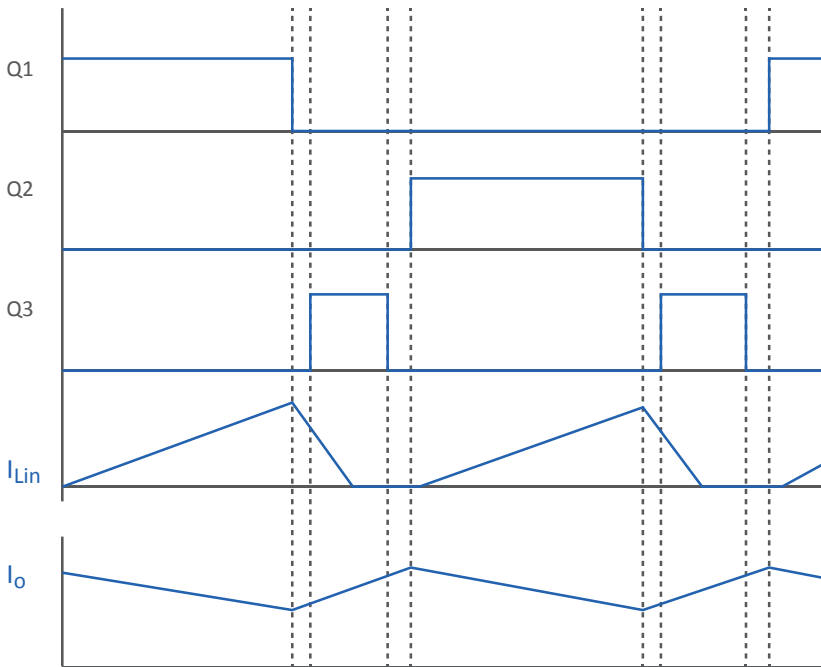


Fig. 8.45: Stacked converter switching sequence. S3 is the active clamp switching waveform.

***Reference:** Example is based on “A Single-Phase Single-Stage AC-DC Stacked Flyback Converter with Active Clamp ZVS”, Yuntong Li and Gerry Moschopoulos, Western University, London, Canada.

Published in: 2018 IEEE Applied Power Electronics Conference and Exposition (APEC)

DOI: 10.1109/APEC.2018.8341297

Stacking or paralleling transformers can increase the power handling if space (especially height) is limited and offers many opportunities for innovative switching topologies, such as the examples given above. The main disadvantages are increased costs and the difficulty of matching the transformers precisely enough so that parasitic effects (especially leakage inductance differences) do not affect the performance. Nevertheless, it is a useful technique in certain situations.

8.9 Poly-Phase supplies

For higher power AC/DC converters, two or more phases can be used. To full-wave rectify a three phase input, six diodes are needed:

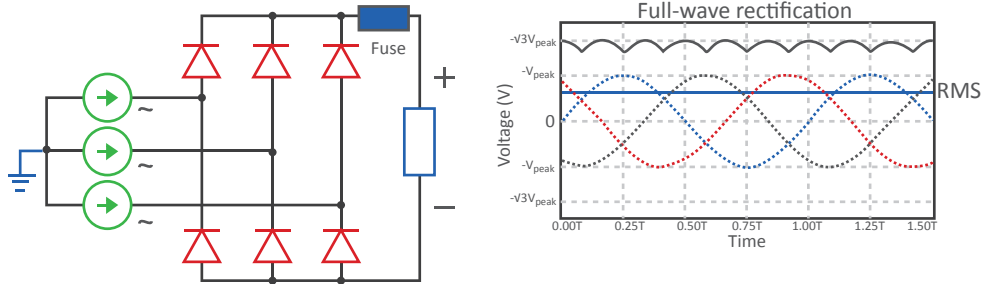


Fig. 8.46: 3-phase input rectifier

A full-wave 3-phase rectifier will generate a peak DC rectified output voltage of:

$$\text{Eq. 8.39: } V_{pk} = \sqrt{3} V_{in,peak} \text{ or}$$

$$\text{Eq. 8.40: } V_{pk} = \frac{3\sqrt{6} V_{in,rms}}{\pi} \cong 2.34 V_{in,rms}$$

The forward voltage drop across the diode bridge can be assumed to be around 1.2V and can be usually ignored.

Nominal 3-Phase RMS supply voltage	Peak rectified DC Voltage (approx.)	Mean rectified DC Voltage (approx.)
208VAC/60Hz	486VDC	464VDC
230VAC/50Hz	538VDC	514VDC
277VAC/60Hz	648VDC	619VDC
380VAC/50Hz	889VDC	849VDC
400VAC/50Hz	934VDC	892VDC
415VAC/50Hz	970VDC	926VDC
480VAC/60Hz	1123VDC	1072VDC

Table 8.1: Three phase full wave rectified DC voltages

The common point of the three phase supply can be tied to neutral or to ground, but in many industrial installations earth is preferred. This means that standard single phase input AC/DC converters cannot be used with phase-to-phase AC power supplies because without a neutral reference point, the voltage between and two phases is much higher ($\sqrt{3}$ of the phase-to-neutral voltage), for example, a three phase supply with 230VRMS on each phase has a phase-to-phase voltage of nearly 400VAC.

Even if the standard single phase input AC/DC converter had an input voltage range that was wide enough to handle the higher input voltage of phase-to-phase operation, there is a separate issue with surge handling capability. A standard single phase converter needs to withstand at least 1kVAC surges (IEC 61000-4-5, Class 2) in order to meet typical indoor industrial and commercial performance requirements, but three phase supplies are more often classed as Over Voltage Category III installations with a minimum of 4kVAC surge withstand capability (IEC 61000-4-5, Class 4). These are minimum levels. More typically, 2kVAC surge capability for single phase and 6kVAC surge capability for poly phase installations are specified, meaning multiple filter stages are required for compliance.

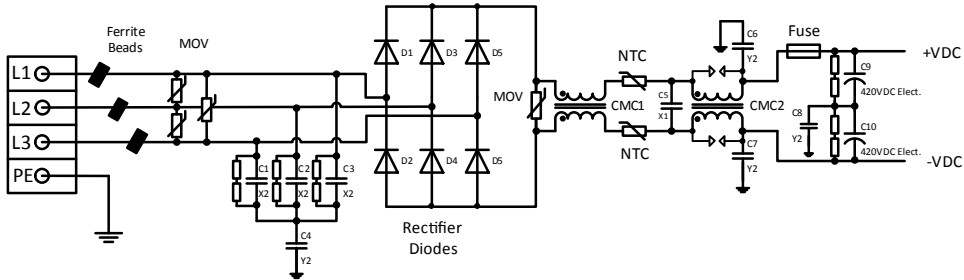


Fig. 8.47: Example of a three phase input filter

Practical Tip: the junction of three phases should be zero volts, so the three phases can be filtered before the rectifier using three X-class capacitors wired to a common point which is then grounded via a Y-class capacitor. As the three phase supply is assumed to be current limited, only a single fuse after rectification is required for safety compliance.

8.9.1 Three phase PFC

The PFC circuit shown in section 7.2.1 cannot be operated from a three phase supply by simply using a 6-diode input bridge rectifier instead of a 4-diode bridge rectifier because the boost regulation is DCM and the highly discontinuous input current would give a very high THD of $\approx 30\%$.

Only if individual inductors on each input are used with CCM control can a three-phase PFC controller with a single switch be implemented:

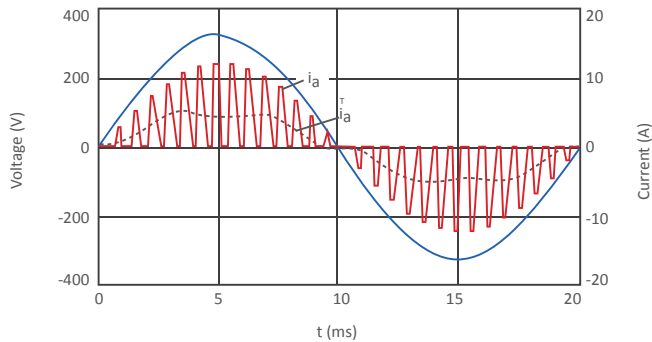
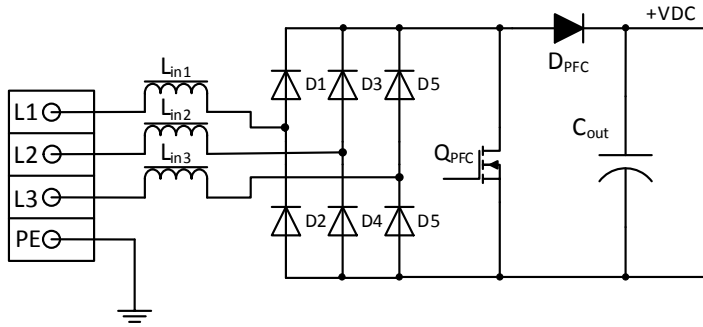


Fig. 8.48: Three phase input PFC with CCM control (only one of the phases shown)

The circuit shown above has the advantage of simplicity, but the disadvantage that the voltage stress on the switching transistor is now very high (realistically, at least a 900V FET would be required).

One solution to the problem of high switching voltage stress is to use an active three level rectifier such as the Vienna rectifier shown below (there are many variants of this basic topology, but essentially the goal of all of them is to reduce the switching stress on the transistors by using a capacitive divider to halve the supply voltage). The input diodes can be either partly or fully replaced with synchronized switching transistors to increase the efficiency further:

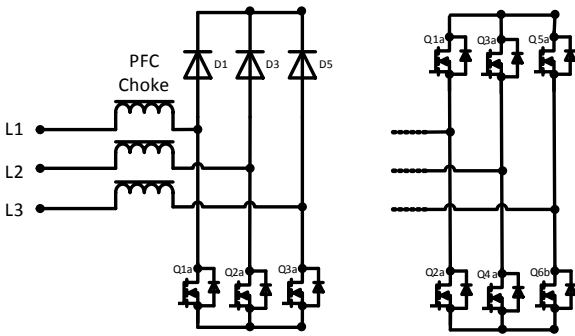
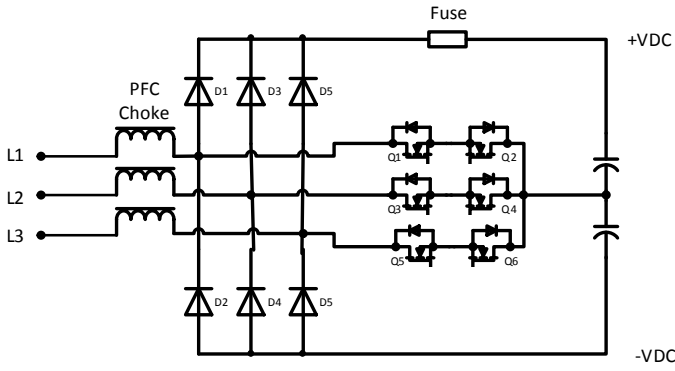


Fig. 8.49: 3 phase Vienna Rectifier topology PFC with alternative half or full active input switching.

Despite the reduced input current ripple, a multiple stage EMC filter is typically still required:

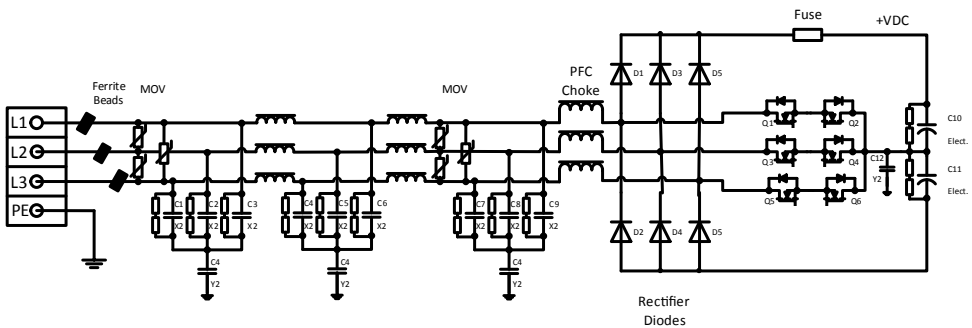


Fig. 8.50: Example of an EMC filtered Vienna topology PFC input stage.

Chapter 9

Transformerless AC Power supplies

If isolation is not required, then a very low cost AC/DC power supply can be made without using a safety isolation transformer. There are several techniques available to handle the large voltage difference between the AC supply and the DC output.

9.1 Capacitively-coupled AC/DC

This is one of the simplest AC power supply designs. A dropper resistor would dissipate too much power and get very hot, but the AC reactance of a series capacitor can be used to drop the input voltage without dissipating too much energy.

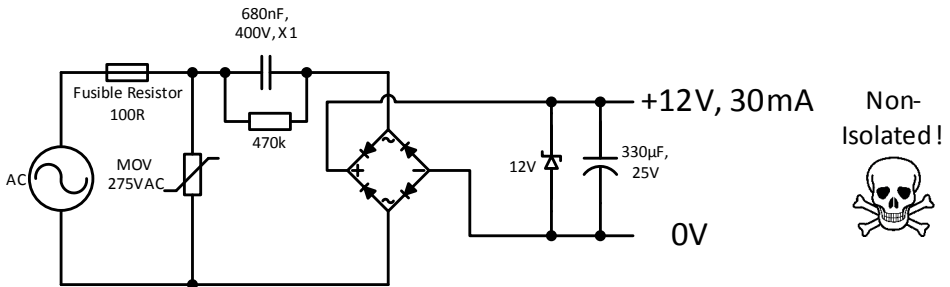


Fig. 9.1: Capacitively coupled AC/DC converter

The reactance of the dropper capacitor is:

$$\text{Eq. 9.1: } X_c = \frac{1}{2\pi C f}$$

So for a 115VAC input and the 680nF capacitor shown above, X_c works out to be about 3.9 kOhms for 60Hz mains and 4.6 kOhms for 50Hz mains. This is much less than 470k so the parallel resistor can be ignored for the remaining calculations (it is required to discharge the capacitor when the power is switched off and to act as a primitive EMI filter to reduce the conducted harmonics).

The dropper capacitor current can be derived from:

$$\text{Eq. 9.2: } I_{rms,max} = 2\pi C f V_{AC,rms}$$

So for an 115VAC/60Hz input, $I_{rms} = 43354 \text{ C} \approx 40\text{mA}/\mu\text{F}$ and for a 230V/50Hz input, $I_{rms} = 72257 \text{ C} \approx 70\text{mA}/\mu\text{F}$.

The above circuit will have a maximum output current of 47mA for 230VAC supply or 27mA for a 115VAC supply, so the Zener diode needs to have a 1W rating to survive a no-load condition ($12V \times 0.047A = 564mW$)

The MOV is required to avoid AC surge voltages from exceeding the rating of the dropper capacitor. The fusible resistor has two functions: to act as a fuse if the circuit malfunctions or the output is short-circuited and to act as a resistor to limit both the inrush current and MOV current.

Practical tip: The output voltage rise is not instantaneous. With each peak half-cycle of the mains input, current flows into the output capacitor, but during the cross-over period, very little charging current flows. Thus the output rises in small steps until the Zener diode voltage limit is reached. Increasing the load slows down the rise time so any rise-time sensitive circuitry operated from such power supplies should have either an under voltage lockout or a long start-up time delay.

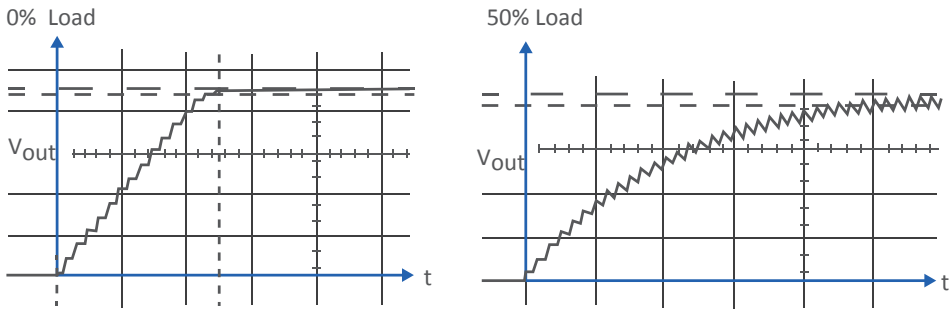


Fig. 9.2: DC output voltage rise with and without an output load.

Typical transformerless applications include passive IR movement detectors or relay time delay circuits (the relay output contacts provide the necessary output isolation to the mains supply and a 555 timer is not too fussy about the input voltage regulation).

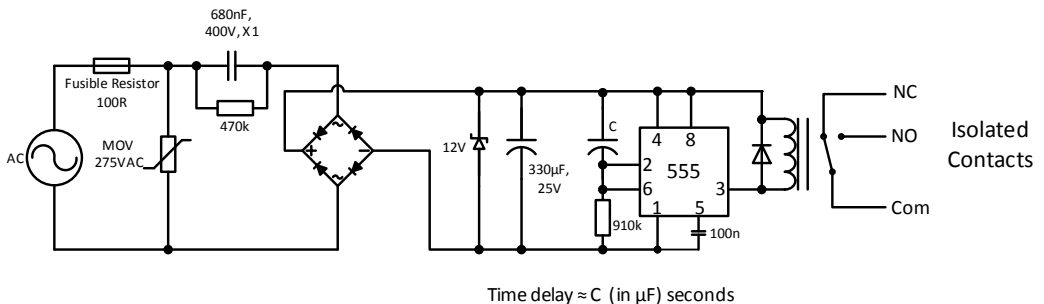


Fig. 9.3: Example of a turn-on-delay circuit.

9.2 Non-Isolated Buck Regulator

The disadvantages of a limited output current and the slow stabilization time for the capacitively coupled transformerless power supply can be overcome using a high voltage non-isolated buck converter. The AC input is rectified and smoothed to provide a high voltage DC bus which can then be efficiently down-converted to a low voltage output.

The output current restriction is lifted so that higher power designs can be achieved and the very wide input voltage range of the buck converter means that a much smaller bulk capacitors can be used compared with equivalent isolated designs (see input stage below, where a 2.2µF bulk capacitor is all that is needed for a 2.5W design)

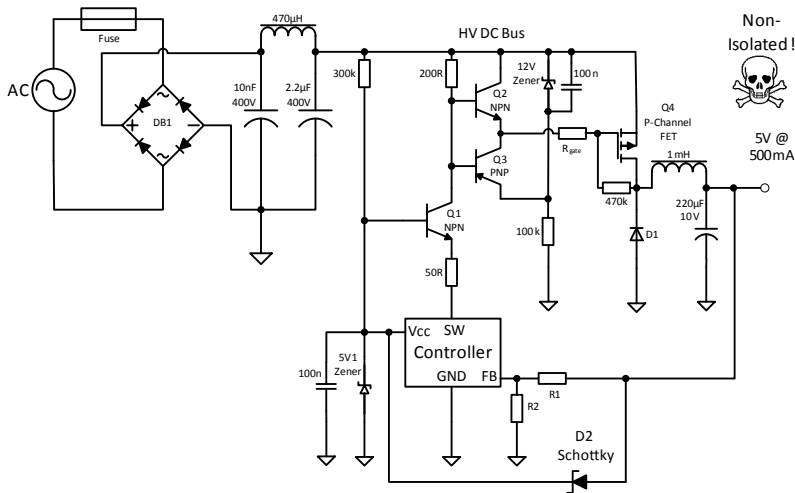


Fig. 9.4: Example of a non-isolated high input voltage buck converter

The controller IC is a standard buck converter controller that operates from a 5V supply (it is not necessary to have a high voltage part, even though this design is non-isolated).

The rectified 115V or 230VAC mains input (160VDC or 325VDC) is used to supply the start-up supply voltage via the 300k dropper resistor and the 5.1V Zener. Once the power supply is operational, the 5V output is fed back via the Schottky diode (D2) to bootstrap the supply voltage from the output.

Transistor Q1 acts as a constant current sink. The base is tied to 5V, forcing the emitter to be one junction drop lower at $5V - 0.7V = 4.3V$. When the controller output, SW, is high, then no current flows through Q1 as it is reverse biased. When the controller output is low, then the current flowing out of the emitter is $4.3V/50R = 86mA$. The current flowing in to the collector must be the same as the current flowing out of the emitter, so the current through the 200R resistor is also 86mA, irrespective of the voltage of the DC bus. The volt drop across the 200R resistor will be equal to $200R \times 0.086A = 17.2V$. The duty cycle of the controller will be very

short when regulating, so this relatively high current will only flow for 1.5% of the time and a ¼ W resistor will suffice.

The push-pull transistor pair Q2 and Q3 level shift the controller's PWM control signal to a high-side gate drive for the P-channel FET, Q4, which switches between the high voltage DC supply and a voltage that is 12V lower than that, as set by the 12V Zener diode in series with the 100k resistor to ground. The output is then smoothed by the output inductor and capacitor to provide a regulated 5VDC supply.

Q2 and Q3 are general purpose bipolar transistors, only Q1 and Q4 have to withstand the full DC bus voltage. A Spice simulation (simulated without any feedback) shows that the output soon settles to 5.0VDC. In Fig. 9.5 below, the blue trace is the output voltage referenced to ground, the red trace is the gate drive signal and the green trace is the 12V Zener diode voltage (both referenced to the HV bus supply).

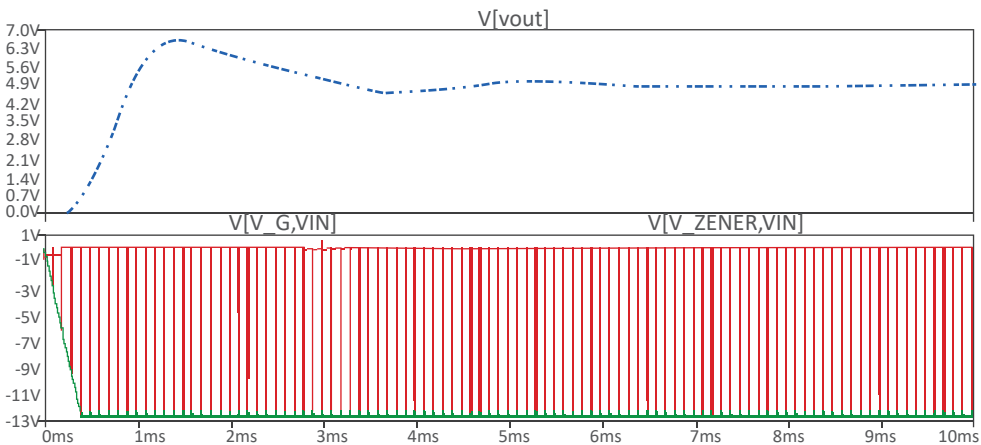


Fig. 9.5: SPICE simulation of the circuit shown above without feedback. With feedback, the initial over-voltage peak would be regulated out.

There are a number of design limitations to this high voltage buck converter design due to the extremely short on-time. The operating frequency is limited to around 30kHz by the slow response time of the power transistors. This means that a controller IC has to be selected with an adjustable frequency setting as most standard buck converter ICs operate at much higher frequencies. Secondly, the output has a strong saw-tooth ripple even with heavy filtering. The biggest advantage is that the output current is restricted only by the P-channel FET's power rating and the output inductor power dissipation limits.

9.3 High Voltage Linear Regulators

An alternative to the capacitive dropper or discrete buck converter AC/DC is to use a high input voltage linear or switching regulators. With a linear regulator, the output current is limited

to 10mA or less, but this is sufficient for many microcontrollers and Internet-of-Things (IoT) applications. One of the characteristics of IoT is that the data links are wireless, so the individual nodes need have only a power supply input without any output connectors³ and can be permanently sealed. An isolated internal power supply is therefore not necessary.

Although very inefficient (<3%!), high voltage linear regulators offer tight regulation, low quiescent current and wide AC input range supply from 85VAC to 250VAC or DC supply voltage from around 60V to up to 450V. The output voltage can also be adjusted over a wider range than most other solutions. High voltage linear regulators are also available as SMD components making very compact low cost solutions possible.

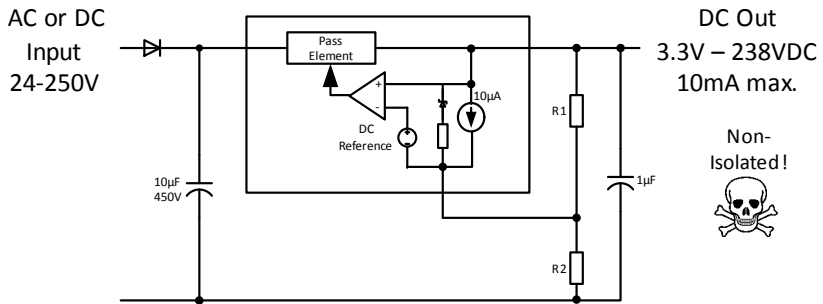


Fig. 9.6: functional block diagram of a high voltage linear regulator

9.4 Off-Line Regulator IC

For slightly higher output currents (up to 175mA), a very compact and cost efficient non-isolated off-line AC/DC converter can be constructed using an integrated switcher IC that contains a built-in high voltage switching transistor, a high voltage current source for the internal power supply and a minimum off-time PWM controller with over-current, short-circuit and over-temperature protection, all in one integrated monolithic package. More advanced ICs also include frequency jittering to reduce the EMC signature and cycle skipping to reduce the no-load consumption.

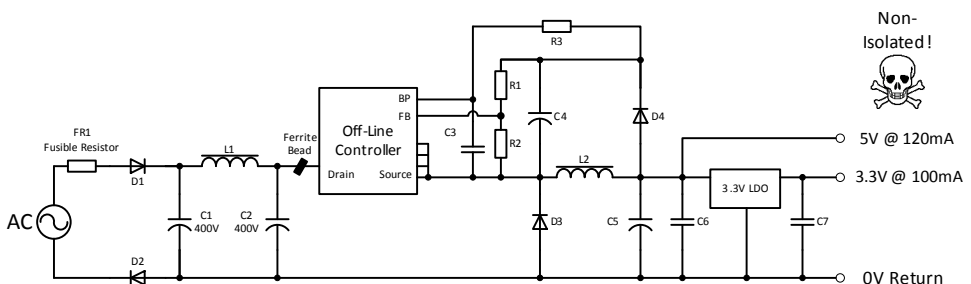


Fig. 9.7: Off-line AC/DC converter with dual outputs

³ The only problem is the antenna connection. If an external stick antenna is used, then the metal SMA connector represents a touchable live conductor. The stick antenna must be either fully enclosed within the plastic enclosure or, more often, an on board ceramic or PCB trace antenna is used instead.

The input is half-wave rectified by diodes D1 and D2 and followed by a simple EMC filter formed by C1, L1, C2 and the ferrite bead. The fusible resistor limits the inrush and input ripple currents and acts as a fuse in the event of a failure. As the controller IC is floating with a direct connection to the high voltage input only, a “trick” is needed to make the circuit work.

The trick is the combination of D3, D4 and C4. If the D3 and D4 are the same part with the same characteristics, then the resulting voltage across C4 is the same as that across C5. In other words, the output voltage is reflected onto C4. The output voltage can thus be regulated and set by the ratio of R1 and R2 connected across C4, even though the common of C4 is not connected to the output. The source-pin referenced voltage across C4 also allows the internal high input voltage shunt regulator to be bypassed and the IC to be powered via R3 once it has started up.

For many IoT applications, it is useful to have a main 5V supply for the 2.4GHz radio or a 12V supply for a relay coil plus a 3.3V supply for the microcontroller and sensors. Adding a low cost LDO regulator to the 5V or 12V main output adds an additional 3.3V output with very little increase in the BoM cost or overall size of the solution.

The overall efficiencies are high because there are no transformer losses:

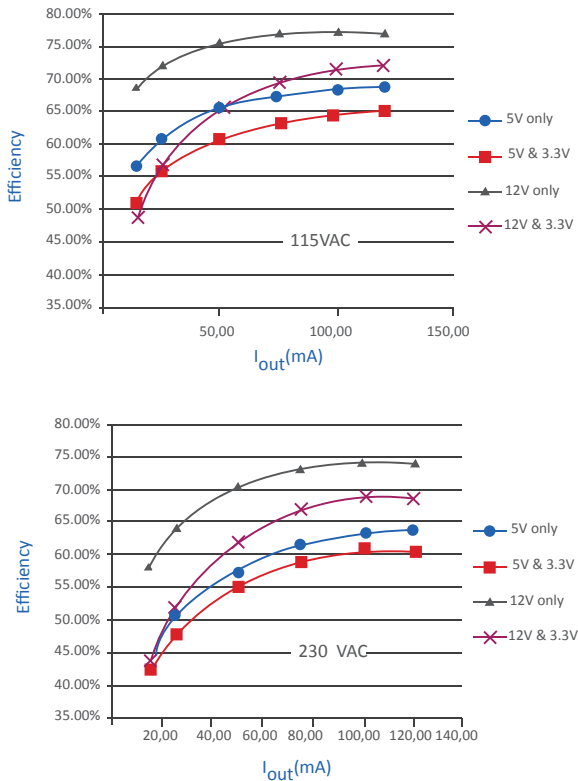


Fig. 9.8: Efficiency/load graphs for 115VAC input and 230VAC input for an off-line converter
 For controller ICs with pulse-skipping mode, the no-load power consumption is also very low over the entire input voltage range.

V rms [V]	5V ONLY	5V & 3.3V	12V ONLY	12V & 3.3V
85	19	23	25	47
115	21	24	24	48
230	26	29	31	54
265	29	32	34	57

Table 9.1: Measured no-load power consumption (mW). Dark green fields show compliance with 5I no load power consumption limits ($\leq 0.03W$). Light green fields show 4★ compliance ($\leq 0.15W$)

Finally, the PCB can be made very small, making it ideal for building in to IoT applications:

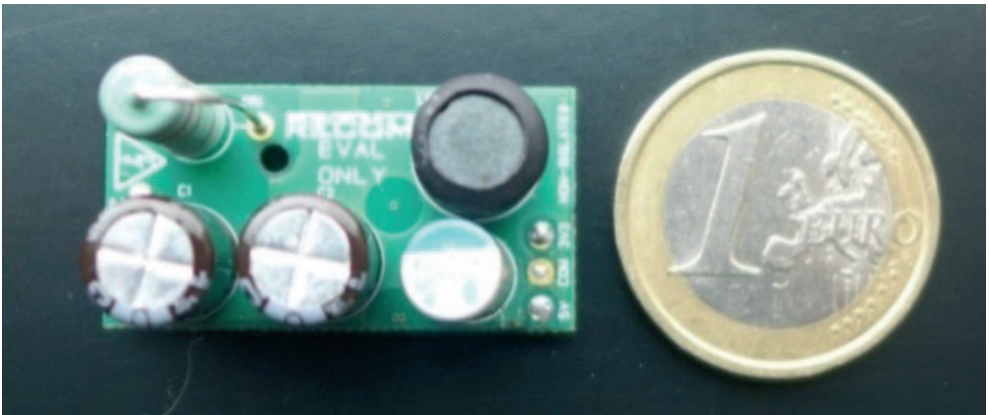


Fig. 9.9: Example of a non-isolated off-line switcher design.

Despite its small size (33 x 17 mm) this off-line switcher demonstrator has a universal input voltage range, dual regulated outputs which are short circuit protected and meets EMC regulations without any external components.

Chapter 10

Wireless power

Most of us are familiar with an electric toothbrush charger. The toothbrush simply slots on to a spigot and the battery charging indicator starts to blink without there being any electrical connection. At its most basic, the charging circuit consists of a relaxation oscillator that generates a varying magnetic field which is intercepted by a matched coil in the toothbrush to transfer power wirelessly to the rechargeable battery.

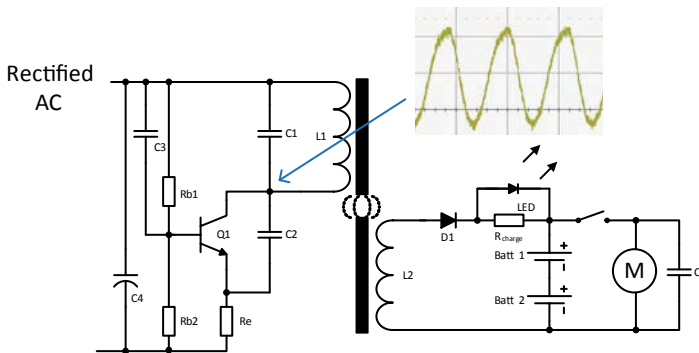


Fig. 10.1: Simplified electric toothbrush charging circuit using a Colpitts oscillator

This self-oscillating design uses a Colpitts oscillator to generate an AC sine wave output from the rectified and stabilized DC input. On switch-on, the transistor Q1 is turned on by the bias resistors on its base connection and the capacitor C1 starts to charge up. The increasing voltage across C1 generates an increasing magnetic field in the inductor L. Once the capacitor C1 is fully charged, the voltage across the inductor L is constant and the magnetic field starts to collapse. This induces a voltage across it that is higher than the supply voltage, turning off Q1 via C2 and holding it off until the magnetic field in the inductor has dissipated. The cycle then begins again. The resulting waveform through the inductor is approximately a sine wave. The resonant frequency of a Colpitts oscillator is given by:

$$\text{Eq. 10.1: } f_{res} = \frac{1}{2\pi\sqrt{LC}} \text{ , where } C = \frac{C_1 C_2}{C_1 + C_2}$$

The matching receiver coil must be accurately positioned to intercept the resulting magnetic field generated by the transmitter coil. The induced AC voltage is rectified and used to trickle-charge the rechargeable batteries. As the battery voltage rises, the voltage drop across the resistor R_{charge} reduces and the charging LED extinguishes.

The maximum power transmission (minimum losses) can be calculated from:

$$\text{Eq. 10.2: } \eta_{max} = \frac{2}{(kQ)^2} \left(1 + \sqrt{1 + (kQ)^2} \right)$$

Where Q is the system quality factor:

$$\text{Eq. 10.3: } Q = \frac{2\pi fL}{R}$$

And k the coupling coefficient between the transmitting inductance L_T and the receiving inductance L_R , which is derived from:

$$\text{Eq. 10.4: } k = \frac{M}{\sqrt{L_T L_R}} = \frac{n_T n_R P_{RT}}{\sqrt{L_T L_R}}$$

Where n_T and n_R are the number of turns of each coil respectively and P_{RT} is the permeance between them (equivalent to the magnetic conductivity), which in turn is derived from:

$$\text{Eq. 10.5: } P_{RT} = \frac{\mu_0 A}{l}$$

Where μ_0 is the permeability of air, A is the cross-sectional area and l is the magnetic path length.

The oscillator frequency, f, can be chosen to be high (100s of kHz) to keep Q high and therefore the efficiency high, but it should not be too high to avoid EMC issues, relaxation losses and other ohmic losses due to the skin effect.

It follows that if the two coils are placed in close proximity then the magnetic path length will be small and the permeance high, giving a higher mutual inductance and a higher coupling coefficient, k. In the case of the rechargeable toothbrush, the spigot design accurately positions the transmitting coil around the ferrite core of the receiving coil to maximise the power transmission, as can be seen from the original patent application drawing from 1964 below:

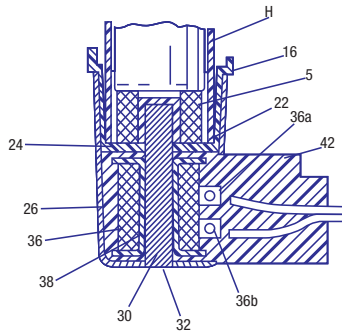


Fig. 10.2: Original patent drawing for an inductive charger for an electric toothbrush

The electric toothbrush charger is a special case of near-field wireless power transfer system. The mechanical design means that coil alignment is not an issue, safety is not critical as the power transferred is very low and the simple oscillator circuit keeps the cost down, which is essential for a mass-produced consumer product.

Inductive chargers for mobile phones or other rechargeable devices are much more complex. Some of the most commonly used wireless power transfer open standards are Qi (pro-

nounced “chee”) and the Power Matters Alliance (PMA) standards for inductive charging or the Airfuel Alliance for magnetic resonance power transfer.

10.1. Resonant wireless power transfer

Resonant inductive coupling uses three or more often four coils. The intermediary coils are resonant tank circuits with a capacitor in series with the winding. The resonance windings act as “magnetic lenses”, boosting the magnetic field from the transmitting coil and concentrating the received field for the receiving coil. If even only a small part of the transmitted alternating magnetic field is intercepted by the receiver resonator, it will pick up some of the energy, so separation distance and alignment is not so critical. Resonant power transmission applications include battery-less smartcards, RFID tags and near-field communication systems. Data communication and adaptive feedback is typically via Bluetooth:

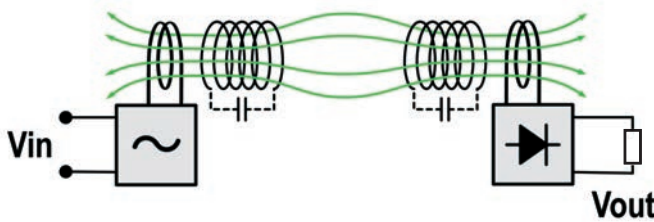


Fig.10.3: Resonant wireless power transfer schematic

10.2. Inductive wireless power transfer

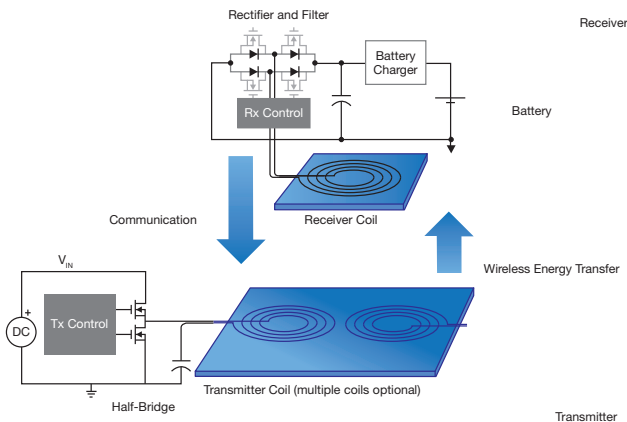


Fig. 10.4: Wireless power transfer schematic

Inductive charging is more efficient than resonant charging but more sensitive to coil alignment, so the choice between them is mostly application specific. The transmission range is limited to around 50mm, reducing to 5-10mm if the transmitter or receiver coils are not perfectly aligned,

although multiple coils and/or adaptive controllers can be used to make the alignment less critical.

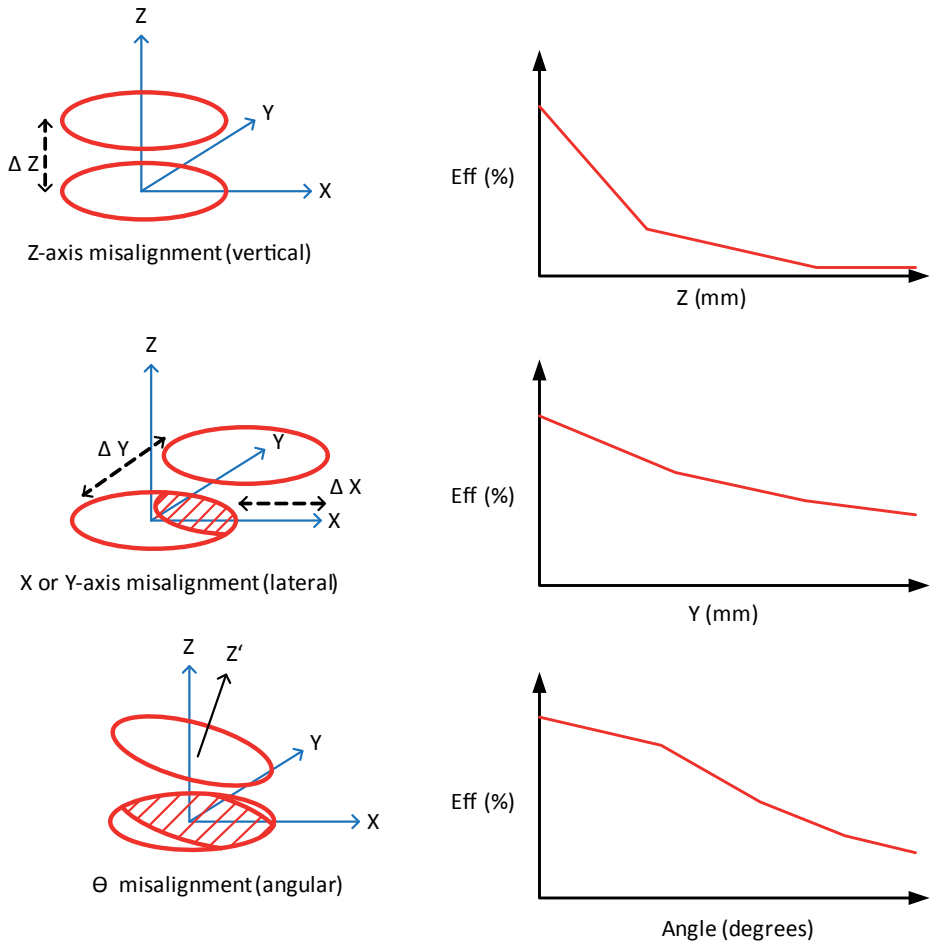


Fig. 10.5: Effect of various misalignments on transfer efficiency (typical transfer curves).

The energy transfer follows a square law in the Z direction (coil separation), a roughly linear relationship for lateral misalignment (coils not perfectly overlapping) and a non-linear relationship for angular misalignment (receiver tilted with respect to the transmitter coil).

Unlike the simple electric toothbrush charger, inductive charging systems such as Qi use flat coils with no magnetic cores and runs at higher frequencies (typically between 0.1MHz and 1MHz). This allows higher power transfer rates from 3W up to 70W or more, but then creates the problem of unwanted or hazardous induced voltages in any conductive metallic objects placed into the magnetic field. This hazard is eliminated by bidirectional data communication between the transmitter and receiver so that the full output power is only activated after the receiver has been properly identified as a Qi-compatible device and that there are no metallic obstacles in the way.

Communication is achieved by the receiver generating coded load pulses which the transmitter can detect and decode (Fig. 10.6).

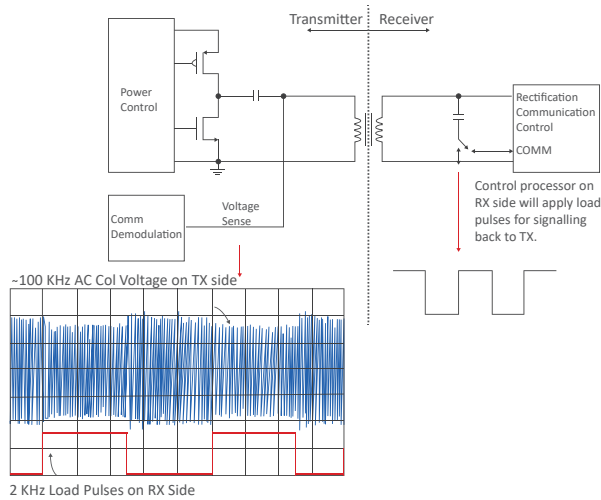


Fig. 10.6: Bi-directional data communication via pulse modulation (used, for example, in the Qi system)

A further advantage of data communication is that the receiver can send a received signal strength value back to the transmitter to form a closed loop control system to handle load transients, misalignments and fault conditions. Other systems use a separate radio link to transmit data back to the transmitter.

Wireless charging is nowadays most commonly used to recharge mobile phones, but it also has a place in industry for IoT applications. For example, consider a remote sensor module that is hermetically sealed against liquids, contaminants and vapours with no external connectors. It could be placed next to a piece of heavy industrial equipment and transmit local environment sensor readings such as ambient temperature, magnetic field strength, acoustic noise levels or shock/vibration via a data link that uses an on-board chip antenna. The system could be powered from an internal supercapacitor or rechargeable battery whose voltage is monitored and transmitted along with the other data. Once the internal power source becomes drained, the whole sensor module is removed to a safe environment and placed on a recharging pad to recharge the internal energy store. Thus wireless charging is not just a “gimmick” for industrial applications; it could become an accepted element in many harsh environment applications.

10.3 PCB Inductive power transfer

A small amount of power (1-2W) can be transferred across the isolation barrier using a core-less transformer formed from adjacent PCB spiral tracks. The dielectric strength of FR4 PCB material is 800V-1500V/mil, so a standard 4 layer PCB with 40 mils between layer 2 and layer

3 will have an isolation voltage of at least 30kVDC (care must be taken with vias to maintain a minimum separation).

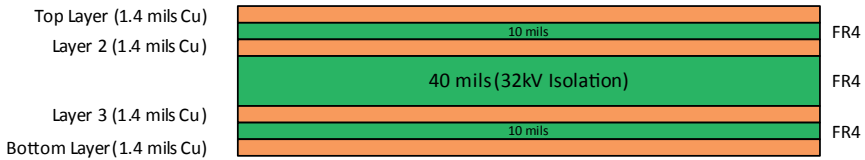
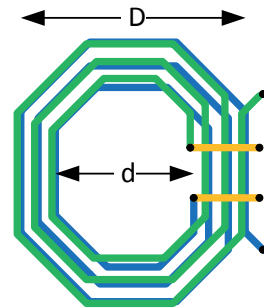


Fig. 10.7: FR4 PCB transformer

The inductance of two overlying PCB spirals was worked out by Wheeler in 1928:

Fig. 10.8: Spiral track coupled coils



Eq. 10.6:
$$L = 9.35 \mu_0 \frac{n^2 \left(\frac{D+d}{2}\right)}{1+2.8\left(\frac{D-d}{D+d}\right)}$$

Where μ_0 is the permeability of FR4 which is typically around 1, d is the inner diameter of the spiral, D is the outer diameter and n the number of turns.

The mutual inductance between the overlaid spirals is given by:

Eq. 10.7:
$$L_M = 2 K \sqrt{L_1 L_2}$$

Where the coupling coefficient, K, is typically 0.5 to 0.6 for two layers separated by 40 mils of FR4.

The efficiency is not high (around 25%), but the advantage of fully automated production and high isolation makes PCB coreless transformers a useful technique.

Practical Tip: Inductive coupling for wireless data rather than power transfer can also be useful to replace the optocoupler in the feedback circuit in a conventional AC/DC converter or to communicate fault conditions from the secondary to the primary across the isolation barrier.

With the rise of digital power supplies, the output regulation as well as the synchronous rectification timing can be digitally controlled from the primary side microcontroller using such simple inductive coupling across the isolation barrier. As the system is symmetrical, bi-directional data can be sent by duplicating the transmitter and receiver circuitry on both sides.

The implementation is relatively straightforward using a four-layer PCB : two opposing loops are formed from the PCB tracks on the top and bottom layers to create the transmitting and receiving coils and the data is transmitted by modulating the high frequency drive signal.

The electrical insulation is guaranteed by the PCB material and as both loops is embedded and shielded with ground planes above and below, the transfer characteristic is largely independent of moisture, dirt, interference or other environmental conditions. Even so, some signal conditioning is usually required to ensure data integrity.

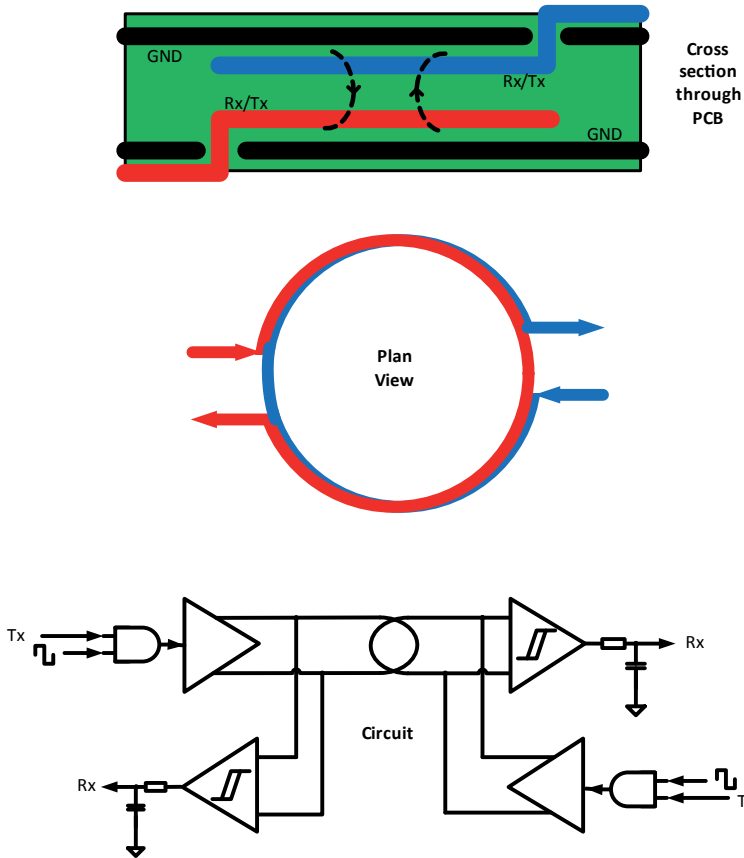


Fig. 10.9 : PCB inductive communication arrangement.

The PCB track connections are transmission lines that have to be impedance matched with the transmitter and receiver amplifiers to avoid unwanted reflections. The PCB material (FR4) acts as a dielectric between the trace carrying the RF signal and the ground plane with characteristic impedance (in ohms)

$$\text{Eq. 10.8: } Z_0 = \frac{87}{\sqrt{\epsilon_r + 1.41}} \ln \left(\frac{5.98H}{0.8W + T} \right)$$

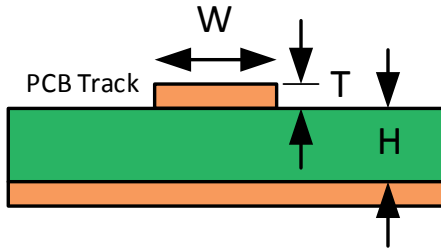


Fig. 10.10: PCB stripline geometry and characteristic impedance (Z_0) relationship.

For a standard PCB, the dielectric constant, ϵ_r , is equal to 4, so if the 1 ounce copper track is 20 mil wide and the PCB thickness is 10 mil, the resulting impedance will be 50 Ohms. For a 75 Ohm impedance, reduce the track thickness to 8.3 mils.

The PCB transmission lines will also have a characteristic capacitance [pF/in] of:

$$\text{Eq. 10.9: } C_0 = \frac{0.67(\epsilon_r + 1.41)}{\ln\left[\frac{5.98 H}{0.8 W + T}\right]}$$

And a propagation delay [in ps/in] of :

$$\text{Eq. 10.10: } t_{prop} = 85\sqrt{0.475\epsilon_r + 0.67}$$

For multilayer PCBs where the tracks are embedded between two ground or power planes, the above relationships need to be modified slightly:

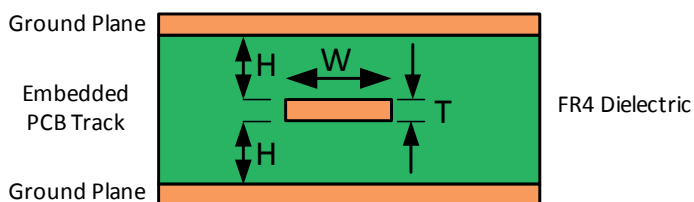


Fig. 10.11: Embedded transmission line in a multilayer PCB

Multilayer PCB characteristic impedance [ohms]:

$$\text{Eq. 10.11: } Z_0 = \frac{60}{\sqrt{\epsilon_r}} \ln\left(\frac{1.9 B}{0.8 W + T}\right)$$

Multilayer PCB characteristic capacitance [pF/in]:

$$\text{Eq. 10.12: } C_0 = \frac{1.41(\epsilon_r)}{\ln\left[\frac{3.81H}{0.8W+T}\right]}$$

Multilayer PCB propagation delay [ps/in]:

$$\text{Eq. 10.13: } t_{prop} = 85\sqrt{\epsilon_r}$$

NOTE: PCB dimensions are still commonly defined in imperial measurements (inch, mils), so these have been used here instead of the metric system.

Chapter 11

Feedback

The general arrangement for any closed loop system is shown below:

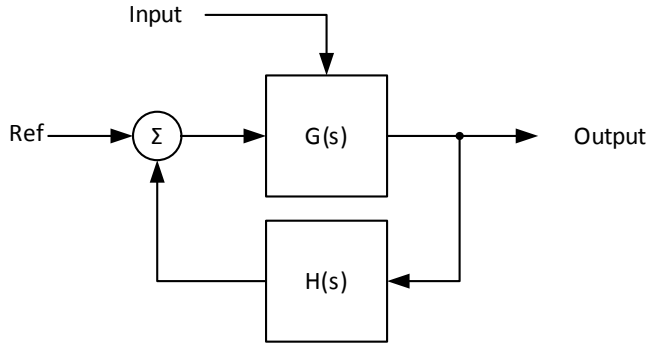


Fig. 11.1: Generalized block diagram of a feedback system

There are two gain blocks: G which represents the power gain and H which represents the feedback gain (which is normally less than one, i.e. attenuation). The summing point has a non-inverting reference voltage input and an inverting input for the feedback signal (Negative feedback). The (S) suffix indicates that these two gain blocks are in the S-domain, i.e., they have both DC and AC components. The AC component means that both the gains will change with frequency and that the differences in the frequency dependency will cause a phase shift in the feedback.

In the case of a power supply, the system input is the supply voltage and the system output is the output voltage, but the feedback can be either current or voltage based.

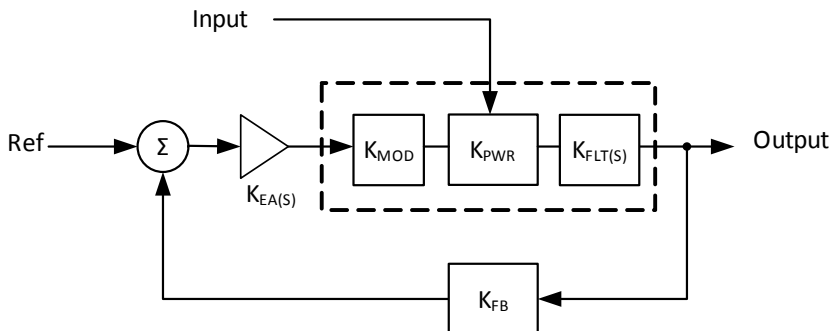


Fig. 11.2: Generalized feedback block diagram for a power supply

Where the open loop gain, $G_{OL(S)}$ is:

$$\text{Eq. 11.1: } G_{OL(S)} = K_{PWR} + K_{FILT(S)} + K_{FB} + K_{EA(S)} + K_{MOD}$$

The simplest implementation of such a closed loop power supply system is a type 1 feedback using operational amplifiers (Op-Amps).

11.1 Measuring Loop Stability

The degree of immunity to instability can be found by carrying out a bode plot test where small perturbations are injected into the feedback system and the response measured. This can be done using specialist equipment or tested by using standard laboratory equipment and an audio transformer:

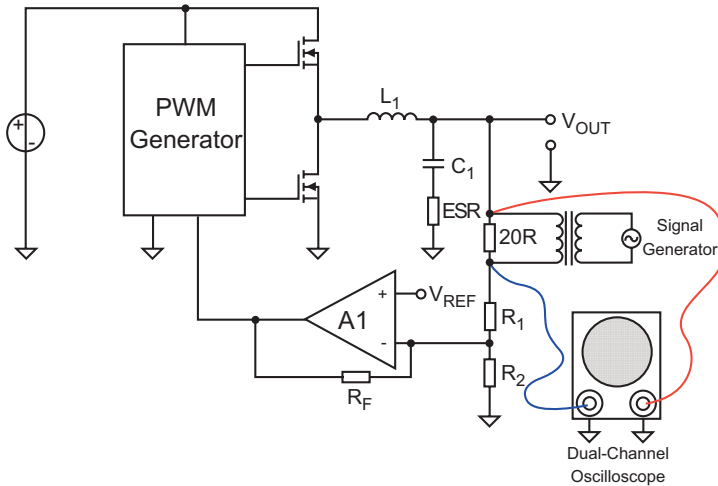


Fig. 11.3: Set up for deriving loop stability experimentally (reproduced from DC/DC BoK)

Practical Tip: In practice, the choice of audio transformer, shunt resistor and way the test leads are connected influence the measurements considerably. You will get more accurate results using a commercially available frequency analyser with matched injection isolation transformers than if you attempt to make your own.

The phase margin is the number of degrees of phase when the gain is zero. The gain margin is the number of decibels of gain when the phase is zero. The combination of the two determines the loop stability.

The compensation is sufficient if the phase margin is 45° or higher and the gain margin is at least -6dB (preferably closer to -10dB). The margins need to be checked under all operating condition extremes (max V_{in} , min V_{in} , min. load*, max. load, min. temperature, max. temperature) to guarantee stable operation.

***NOTE:** loop stability measurements can only be done on a constantly running system. If the AC/DC controller goes into pulse-skipping mode at low loads, then no proper measurements can be made.

The injection point in the loop is optimum if the impedance on one side of the injection point is much higher than on the other, for example between the low impedance output stage and the high impedance resistor divider to the feedback comparator (as shown below in Figure 11.5) It would also be possible in theory to inject the signal between the comparator output and PWM controller input, but in many controller ICs, this point is internal inside the IC and not accessible.

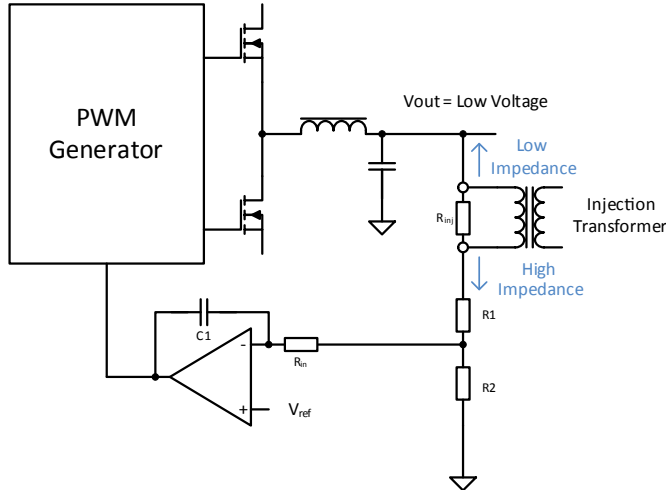


Fig. 11.4: Suitable injection point for low output voltages

However, for high voltage outputs such as a PFC stage, the injection point shown in figure 11.5 is not ideal. This is because the perturbation signal is so attenuated by the high resistance voltage divider that the measurements become unreliable. In this situation, an additional buffer op-amp can be used to allow the signal to be successfully injected. The op-amp is unity gain, so will not affect the readings as long as it has a high enough bandwidth.

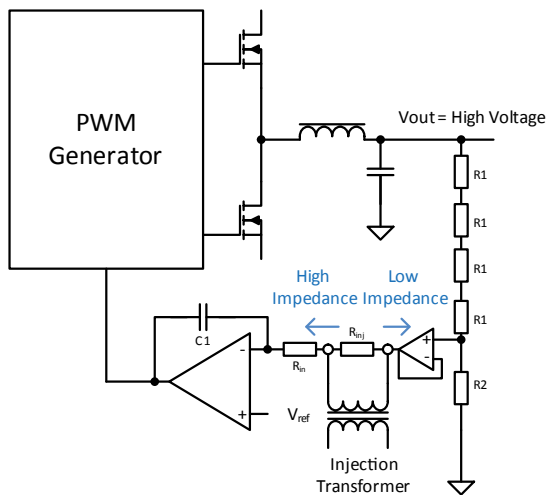


Fig. 11.5: Alternate injection point using a unity gain op-amp for high output voltages

If the injected perturbation signal is too weak, then the measurements will become increasingly inaccurate at low frequencies because the signal-to-noise ratio will be too low. If the injected signal is too strong, then the measurements will become erratic at higher frequencies as the perturbations will over-ride the internal feedback voltage levels.

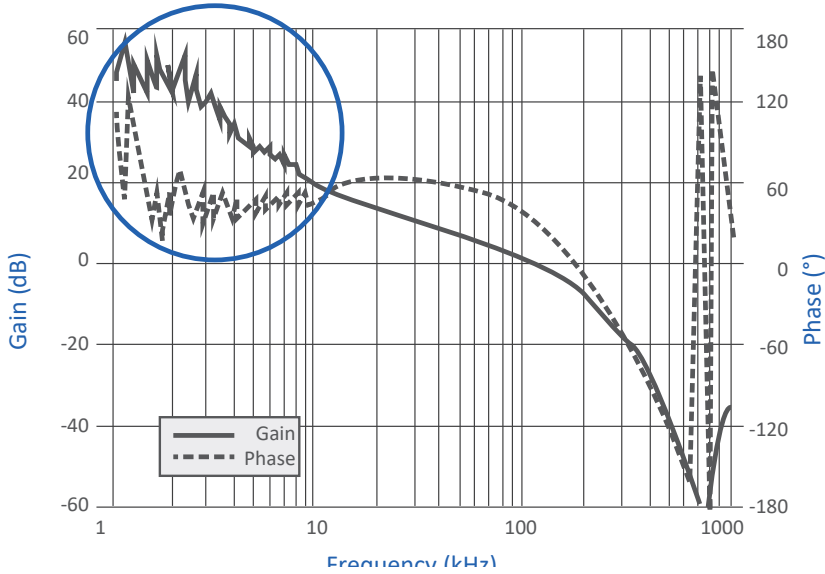


Fig. 11.6: Bode Plot showing instability at low frequencies (blue circle) caused by poor signal-to-noise margin. The plot becomes noisy.

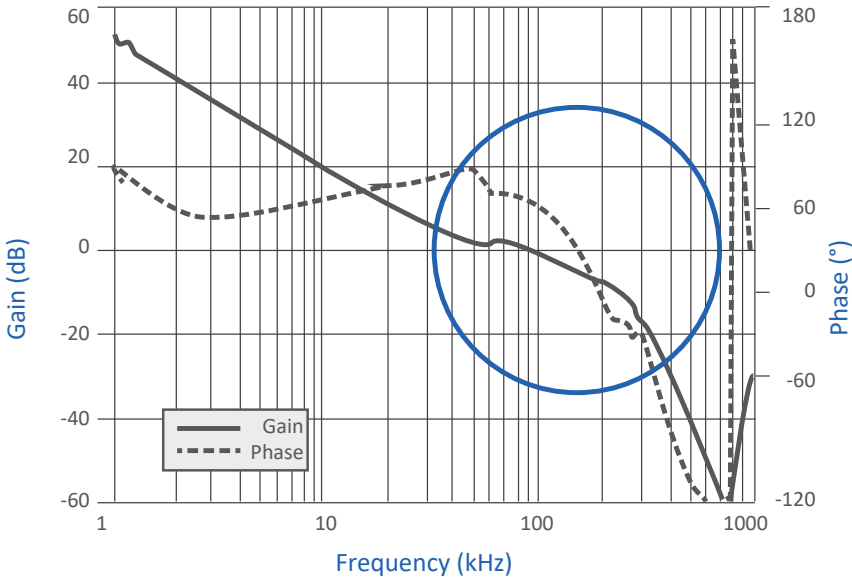


Fig. 11.7: Bode Plot showing erratic readings at higher frequencies (blue circle) caused by excessive perturbation signal strength. The plot is no longer smooth.

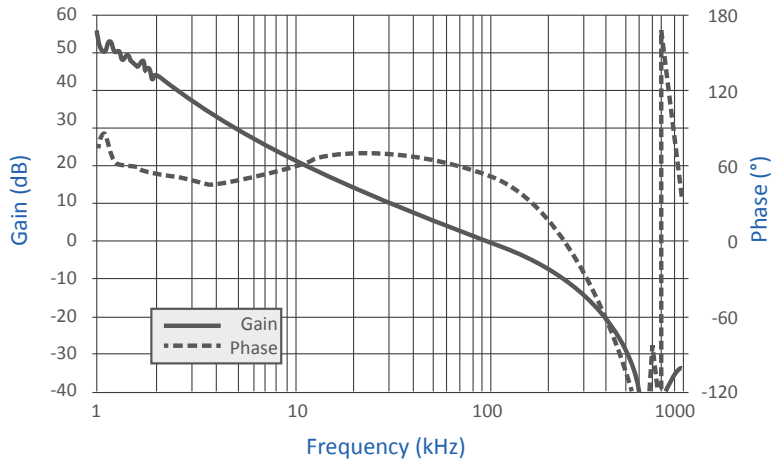


Fig. 11.8: Bode Plot with optimal signal injection.

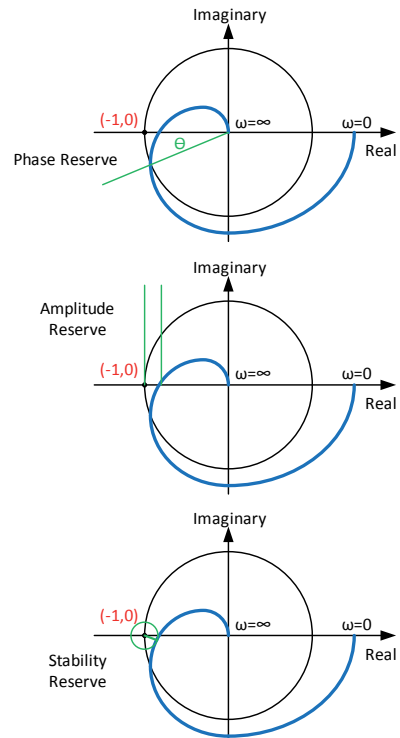
Another way of visualizing the same gain and phase information is to use a Nyquist diagram. Most professional-grade frequency analysers can output the measurements as either a bode plot or a Nyquist diagram. The advantage of a Nyquist diagram is that not only the gain and phase margins can be determined, but also the stability margin, which occurs at the frequency where the curve is closest to the $(-1,0)$ point (refer to Fig. 11.9).

The factor -1 takes into account the -180° phase change implicit in negative feedback. The Nyquist diagram can also be reflected along the imaginary axis to show the instability point at $(1,0)$ for the entire feedback loop.

Fig. 11.9: Nyquist Diagrams for negative feedback loop stability. From the plotted results, the angles and separations from the instability point $(-1,0)$ can be measured to derive the phase margin, gain margin and stability margin.

The phase reserve is the angle between the plot and the real axis where it crosses the $-1,0$ circle. The amplitude reserve is the separation between the plot and the $-1,0$ point measured along the real axis.

The stability reserve is the separation between the plot and the $-1,0$ point measured at its closest approach.



11.2 Type 1 Feedback Loop Compensation Calculation

It is also possible to determine stability by calculation, depending on the type of compensation circuit used in the feedback loop.

A Type 1 feedback is shown below in both voltage (output voltage controlled by input voltage) and transconductance (output current controlled by input voltage) variants:

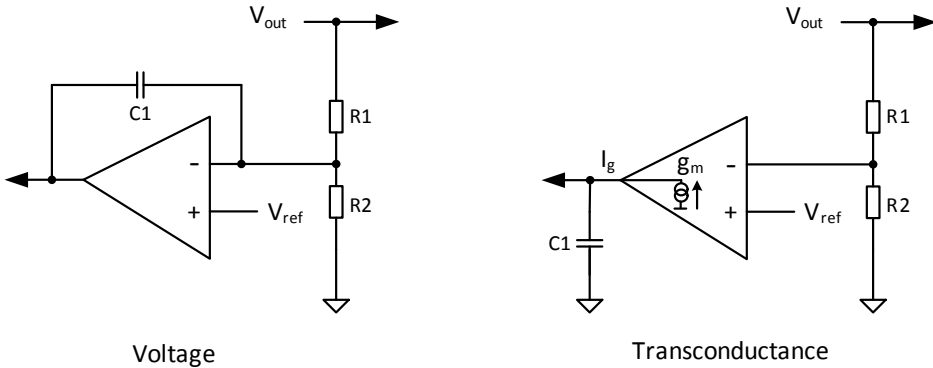


Fig. 11.10: Type 1 feedback circuits (voltage and transconductance versions)

For example, if the desired output voltage is 5.0 volts and the reference voltage is 2.5 volts, then resistor R1 will be made equal to R2 so that the output voltage is divided by two.

These circuits are integrators: sudden changes in the input signal are turned into a more slowly ramping output signal which gives the power supply some immunity from breaking into oscillation by over correcting for changes in load or input voltage. The output ramp rate is dependent on R1 and C1 only, R2 plays no role in integration coefficient.

The gain/phase response for a type 1 feedback system is shown below:

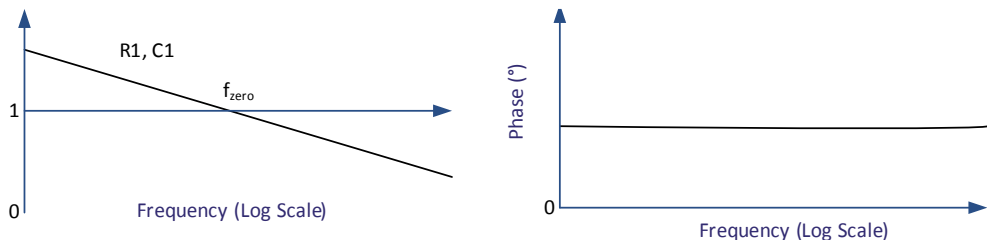


Fig. 11.11: Type 1 Feedback gain and phase relationship with frequency

The point at which the gain = 1 is the system zero.

For voltage Feedback:

$$\text{Eq. 11.2: } f_{zero} = \frac{1}{2\pi R_1 C_1}$$

For transconductance feedback, the transfer function is: (written in the s-format)

$$\text{Eq. 11.3: } H(s) = -g_m \frac{R_2}{R_1 + R_2} \frac{1}{sC_1}$$

Practical Tip: The choice of the resistor values used in the divider network is unimportant for the transconductance circuit as only the ratio affects the gain. The circuit would have the same frequency response if either two 10k resistors or two 100k resistors were used for R1 and R2, for example. However, in the voltage feedback version, R1 appears in the frequency equation but R2 does not. Changing R1 from 10k to 100k would alter the gain plot. Therefore, if the output voltage needs to be trimmed when using voltage feedback, only R2 should be made variable and R1 kept fixed.

The slope of the gain is -20dB per decade, defined by the classic integration function of R1 and C1. If the op-amp has an ideal linear response time to small signal changes, then both the gain slope and the phase shift are constant over frequency. This can become a problem with repetitive or sudden step changes in the load or supply voltage. At higher frequencies than the system zero, the power supply struggles to maintain regulation as the phase and gain margins are too low.

11.3 Type 2 Feedback Loop Compensation

A solution to the problem of low gain and phase margins is to selectively boost them at higher frequencies. The Type 2 feedback circuit and gain and phase frequency responses are shown below:

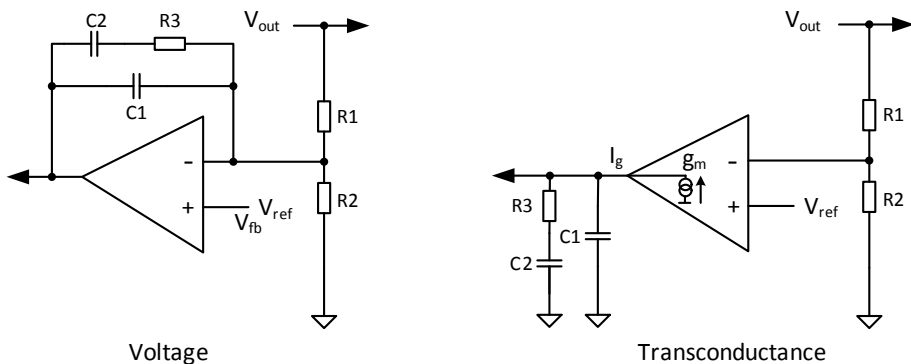


Fig. 11.12: Type 2 feedback circuits (voltage and transconductance versions)

As is evident from the frequency graphs in Fig 11.13, the additional C2 and R3 components have added both a gain boost and a phase boost at higher frequencies. The phase boost is

limited to 90° , meaning that the maximum overall phase shift is 180° . The peak of the phase boost response lies at the half way point between the zero and pole frequencies.

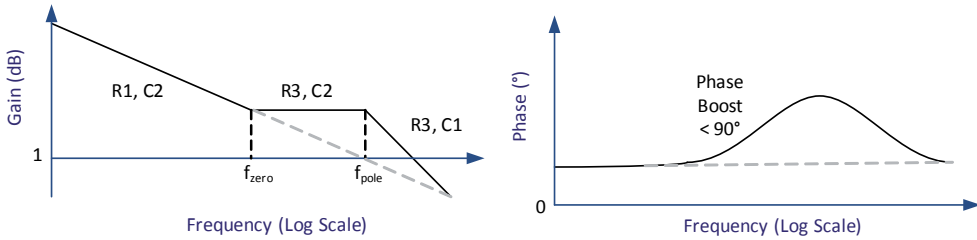


Fig. 11.13: Type 2 gain and phase relationship with frequency

The new relationships are (assuming that C_2 is much larger than C_1):

Type 2 voltage feedback:

$$\text{Eq. 11.4: } f_{zero} = \frac{1}{2\pi R_1 C_2}, \quad f_{pole} = \frac{1}{2\pi R_3 C_2}$$

Type 2 transconductance feedback transfer function (written in s-format)

$$\text{Eq. 11.5: } H(s) = -g_m \frac{R_2}{R_1 + R_2} \frac{1 + R_3 C_2}{s(C_1 + C_2) + s^2 R_3 C_1 C_2}$$

This equation combines the three main factors of the DC gain and the zero and the pole terms, which individually can be derived from the following relationships:

$$\text{Eq. 11.6: } G_0 = \frac{R_2}{R_1 + R_2} \frac{g_m R_3 C_2}{(C_1 + C_2)}$$

$$\text{Eq. 11.7: } f_{zero} = \frac{1}{2\pi R_3 C_2}, \quad f_{pole} = \frac{C_1 + C_2}{2\pi R_3 C_1 C_2}$$

The gain at the crossover frequency is:

$$\text{Eq. 11.8: } |G_{f_c}| = G_0 \frac{\sqrt{1 - \left(\frac{f_{zero}}{f_{pole}}\right)^2}}{\sqrt{1 - \left(\frac{f_c}{f_{pole}}\right)^2}}$$

11.4 Type 3 Feedback Loop Compensation

In some fast transient response power supply circuits, even the additional gain and phase boost created by the Type 2 compensation may not be sufficient. This is especially true for CCM power stages that suffer from a large phase swing when the resonant frequency is exceeded.

Type 3 compensators place an additional “speed up” circuit across the input voltage potential divider:

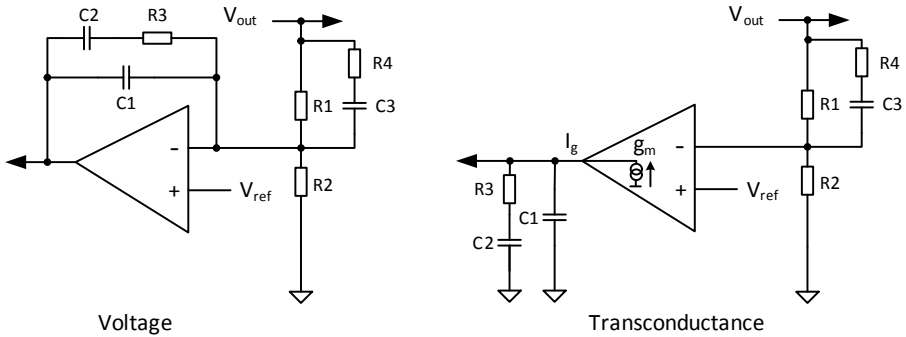


Fig. 11.14: Type 3 feedback circuits (voltage and transconductance versions)

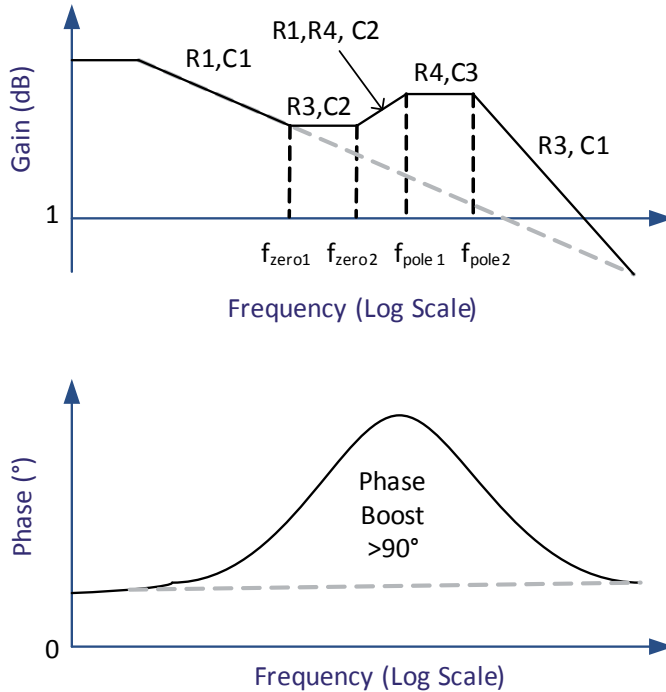


Fig. 11.15: Type 3 gain and phase relationship with frequency

As is evident from the frequency graphs, the additional C4 and R4 components have added more gain and a phase boost at higher frequencies. The phase boost is now more than 90°, meaning that the maximum overall phase shift is 225°. The new relationships for Type 3 voltage feedback are (assuming that C2 is much larger than C1 and R1 is much larger than R4):

$$\text{Eq. 11.9: } f_{zero1} = \frac{1}{2\pi R_1 C_2}, f_{zero2} = \frac{1}{2\pi R_1 C_3}, f_{pole1} = \frac{1}{2\pi R_4 C_3}, f_{pole2} = \frac{1}{2\pi R_3 C_1}$$

Type 3 transconductance feedback transfer function (written in s-format)

$$\text{Eq. 11.10: } H(s) = -g_m \frac{R_2 + s(R_1 + R_4)R_2 C_3}{R_1 + R_2 + s(R_1 R_2 + R_1 R_4 + R_2 R_4)C_3} \frac{1 + sR_3 C_2}{s(C_1 + C_2) + s^2 R_3 C_1 C_2}$$

This equation combines the five main factors of the DC gain and the four zero and the pole terms, which individually can be derived from the following relationships:

$$\text{Eq. 11.11: } G_0 = \frac{g_m R_2 R_3 C_2}{(R_1 + R_2)(C_1 + C_2)}$$

Eq. 11.12:

$$f_{zero1} = \frac{1}{2\pi R_3 C_2}, f_{zero2} = \frac{1}{2\pi(R_1 + R_4)C_3}$$

$$f_{pole1} = \frac{C_1 + C_2}{2\pi R_3 C_1 C_2}, f_{pole2} = \frac{1}{2\pi\left(R_4 + \frac{R_1 R_2}{R_1 + R_2}\right)C_3}$$

The gain at the crossover frequency is then:

$$\text{Eq. 11.13: } |G_{f_c}| = G_0 \frac{\sqrt{1 + \left(\frac{f_{zero1}}{f_c}\right)^2} \cdot \sqrt{1 + \left(\frac{f_c}{f_{zero2}}\right)^2}}{\sqrt{1 + \left(\frac{f_c}{f_{pole1}}\right)^2} \cdot \sqrt{1 + \left(\frac{f_c}{f_{pole2}}\right)^2}}$$

11.5 Optocoupler Feedback Loop Compensation

In practice, most AC/DC power supplies require input/output isolation. The feedback path is no longer direct but via an opto-isolator which also has a frequency dependent response. The most common opto-coupler circuit uses the 431 shunt regulator to control the optocoupler LED current. The 431 is a very versatile IC that acts like a tuneable Zener diode. A typical circuit is shown below:

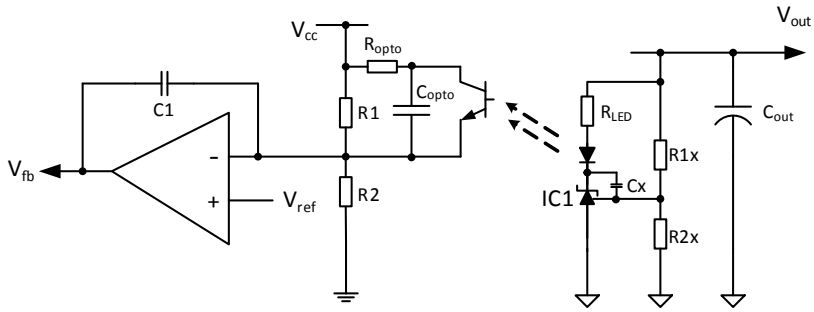


Fig. 11.16: Opto-coupler isolated feedback circuit (with a Type 1 comparator).

In this circuit, R1x and R2x define the shunt regulator (IC1) threshold voltage (and therefore the output voltage regulation point), R_{LED} is the current limiting resistor for the optocoupler LED and Cx is used to define the AC response of the 431 IC. On the primary side, the phototransistor bypasses R1, filtered by the R_{opto} , C_{opto} components.

If the output voltage rises too high, IC1 starts to conduct more current and the LED shines more brightly, causing the phototransistor to bypass more current and pull the junction of R1 and R2 closer to V_{cc} , regulating the output voltage down. If the output voltage falls, the optocoupler LED current is decreased and the R1 bypass current also decrease causing the junction voltage of R1 and R2 to drop, forcing the op-amp to increase its output drive to compensate. The feedback is thus a closed loop, even though the output is galvanically isolated from the input.

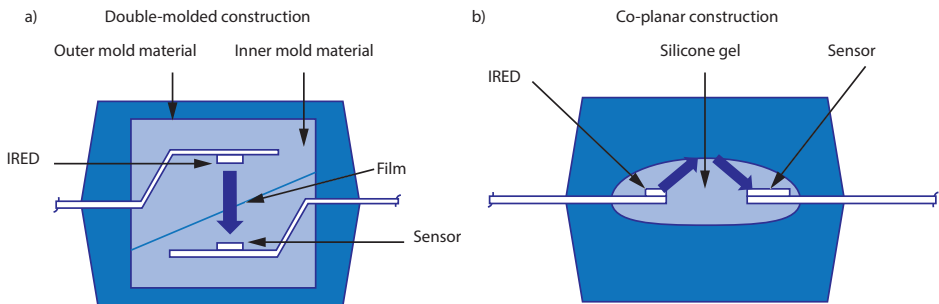


Fig. 11.17: Types of optocoupler. a) is the over-and under type, b) the side-by-side type.

The over-and-under type (fig. 11.17a) typically has a transparent high dielectric strength film between emitter and receiver to improve the isolation withstand voltage.

The total internal reflection type (fig. 11.17b) is a more complicated construction method, but does not need a separating film and has a lower coupling capacitance as the input and output planes are sideways on.

Adding these extra active components obviously affects the gain and phase frequency response of the feedback loop. If we take the simplest Type 1 comparator, the opto-coupler adds an additional pole and changes the flat phase response plot so that it behaves more like a type 2 feedback loop:

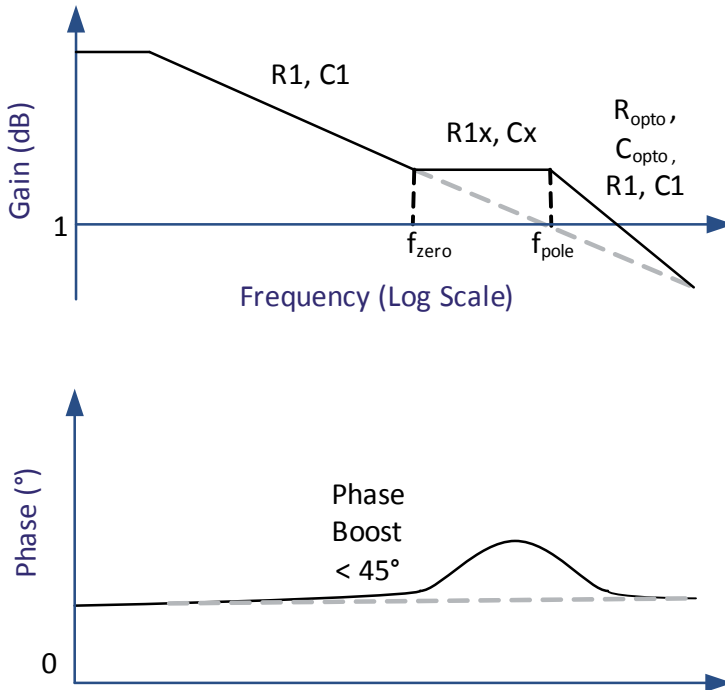


Fig. 11.18: Type 1 comparator gain and phase relationship when modified with opto-coupled feedback

Practical Tip: The gain of the optocoupler (the current transfer ration, CTR) is both age and temperature dependent, which makes calculating the tolerances tricky. The datasheet CTR figure is usually given at 25°C, but it will increase if the temperature drops to the freezing point and decrease if the temperature rises. At 100°C ambient, the CTR will be around 70% of the datasheet value.

The main problem is that the optocoupler is typically positioned very close to the power transformer as they are both placed across the isolation gap. The transformer can run very hot under full load conditions and the heat radiating out can easily cause the CTR to become too low for proper regulation. The optocoupler output current can be increased by increasing the LED current, but then the no-load power consumption can become significant. Also the aging of the optocoupler is very dependent on the LED drive current, so increasing the LED current from, say, 5mA to 15mA will reduce the effective lifetime (the point where the CTR drops to 50% of its nominal value) from around 400k hours to 150k hours. Thus the position of the optocoupler on the PCB and its ambient temperature affects the optimal resistor values that need to be chosen!

11.6 Secondary side feedback compensation

It is also possible to add additional components to compensate on the secondary side for deficiencies in gain or boost. One common amendment is to add R_{comp} and C_{comp} components to cancel out the unwanted pole caused by the output capacitor's own ESR:

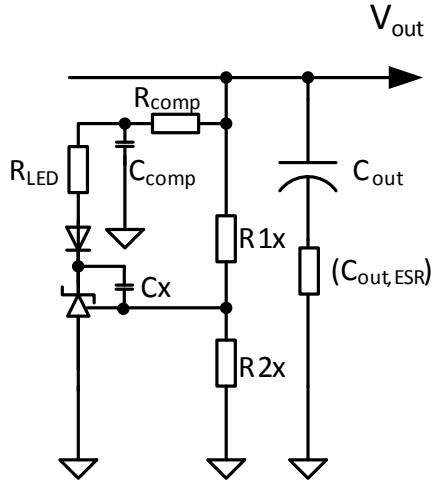


Fig. 11.19: Output Capacitor ESR zero cancellation (R_{comp} , C_{comp})

Another useful secondary side compensation technique is to add HF bypass components across the LED current limiting resistor to increase the useful bandwidth of the opto-coupler (the response time is dependent on the LED current)

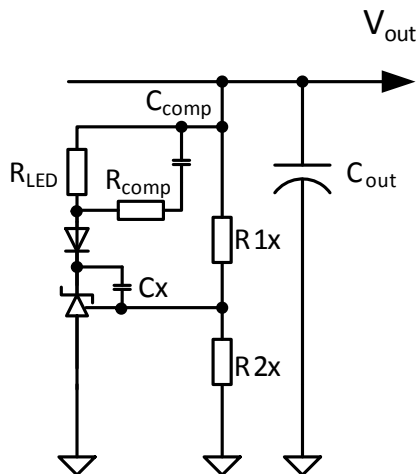


Fig. 11.20: High frequency boost (R_{comp} , C_{comp})

The gain/phase characteristic of a power supply will have multiple overlying components caused by the contributions from the power stage, compensation network and control loop elements. It is possible to calculate all of the terms involved and guarantee stability under all operating conditions by design, but confirmation by real-life measurement is needed to check that component tolerances and temperature effects do not cause the power supply to drift into a region where instability can occur.

11.7 Magnetic feedback

As mentioned previously, the CTR of an optocoupler varies with temperature and degrades with age. It also deteriorates when subjected to radiation in the form of neutron bombardment or gammas rays. The radiation permanently damages the sensitive photo junction in the receiving transistor as well as reducing the efficacy of the LED, eventually reducing the CTR to near zero. This makes optocoupler feedback undesirable for military, space or high altitude applications.

An alternative to opto-coupled isolators is to use magnetic feedback. A separate transformer can be used to close the feedback loop while keeping the isolation intact. There are several ways of doing this:

11.7.1 Output side powered PWM feedback transformer.

A secondary side powered PWM oscillator drives a small signal transformer with a PWM signal that is proportional to the output voltage. The output winding on the primary side is rectified and smoothed to deliver a control voltage for the main switching oscillator:

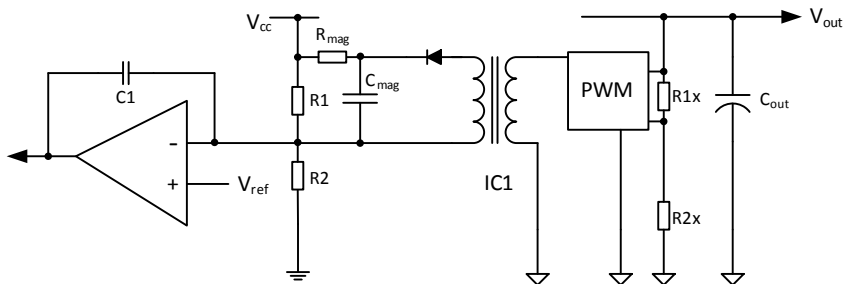


Fig. 11.21: Magnetic feedback using separate PWM transformer

Care needs to be taken to ensure that the circuit starts up correctly as the feedback regulation transformer is powered by the output voltage. Therefore the same circuit is shown here as used with the previous opto-coupler feedback design, R1 and R2 set the maximum permissible output voltage which can then only be regulated down by the feedback from the PWM oscillator. The PWM oscillator needs to run at a high enough frequency to ensure a fast response to load changes and to keep the ripple acceptable without making C_{mag} too big.

A good starting point would be $\times 10$ to $\times 20$ the main oscillator frequency.

The advantage of this design is that it will work with any single-output topology; forward, flyback or resonant. The disadvantage is that the response time is relatively slow, so it is not suitable for dynamic loads and that the output voltage always peaks to the maximum on power-up unless a soft-start circuit is used.

10.7.2 Direct magnetic feedback.

Forward converters rely on an output inductor to store energy and maintain the output voltage during the power transformer reset. The current in the output inductor ramps up and down continuously, so the inductor can be used as the primary winding of a feedback transformer without any additional circuitry on the secondary side. This solves one of the major problems of all secondary feedback circuits: namely how to reliably power the necessary feedback components on the secondary side? If the power supply is started up with a short or an overload on the output, then output regulation can be very difficult to control as the output voltage cannot stabilize.

With direct magnetic feedback, the voltage induced on the primary side winding of the feedback transformer is sampled just after the main power switch is turned off by a sample-and-hold circuit and then buffered to be used to control the main oscillator:

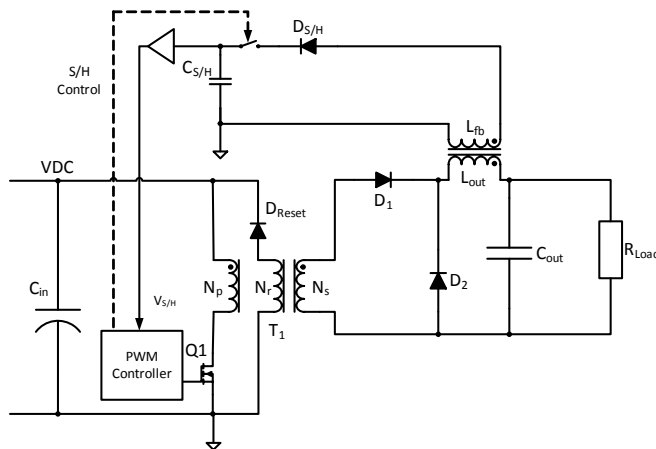


Fig. 11.22: Direct sampling magnetic feedback

The advantage of this circuit is the simplicity of implementation on the secondary side and its accuracy, as the sample-and-hold window can be adjusted to ignore any switching transients and to sample the induced output voltage only when it is stable. It also works well with multiple outputs that share a common output magnetic core (Fig 11.23). The induced feedback signal is then the summation of the output voltages.

The disadvantage of direct sampling is the difficulty of maintaining proper regulation under no load conditions. With no output load, the power switch on-time becomes very short and the

sampling window even shorter. It can be nearly impossible to get an accurate feedback voltage to ensure proper regulation. Therefore, direct magnetic feedback should only be used with power supplies with a minimum load specification.

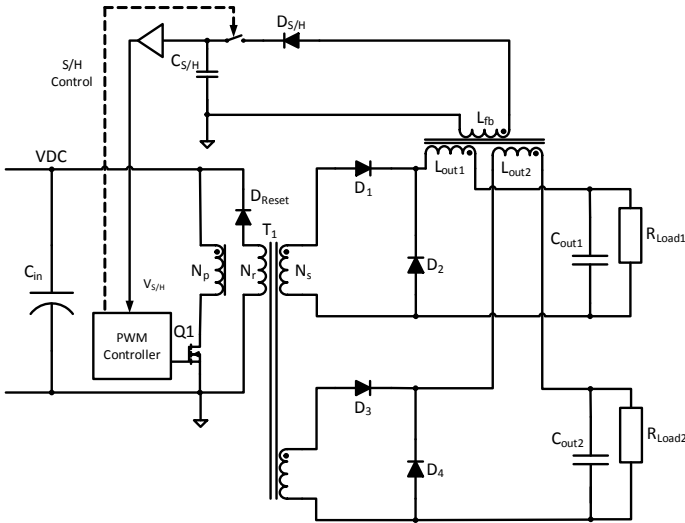


Fig. 11.23: Direct sampling magnetic feedback with multiple outputs

11.7.3 Primary side driven magnetic feedback.

One further method of implementing magnetic feedback deserves a mention, and that is a primary side driven signal transformer. This technique combines the previous two examples: a PWM-driven 1:1 transformer with fixed operating frequency and a simple sample-and-hold circuit to detect the appropriate measurement point in the cycle. Its main advantage that the secondary side feedback circuit is separately powered from the main power stage so will function correctly even if the output is turned off. The schematic is shown below in Figure 11.24:

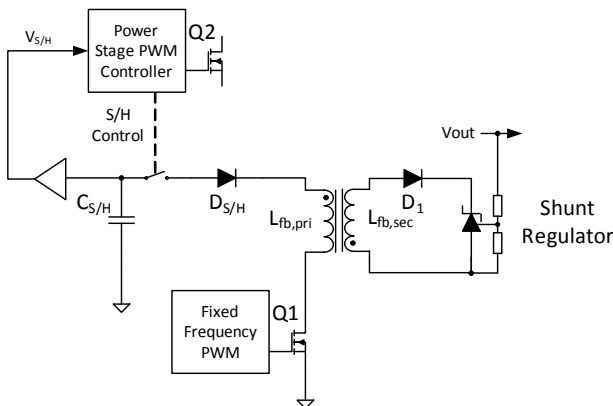


Fig. 11.24: Magnetically coupled shunt regulator schematic

The topology is essentially flyback. When the PWM signal is high, current flows through the primary winding and the transformer core becomes magnetized. Due to the reversed output winding, no current flows through the shunt regulator as the negative output voltage is blocked by the diode D1. When the PWM signal is low, the output voltage becomes positive as the magnetic field inside the core collapses, but is now clamped by the shunt regulator at a voltage determined by the output voltage V_{out} .

The reflected voltage on the primary side is the same as on the secondary side minus the diode drop, but with reversed polarity. The negative primary voltage can be sampled using the simple peak detector formed from $D_{S/H}$ and $C_{S/H}$ and then inverted or used as a negative reference voltage to modulate the feedback of the main power stage.

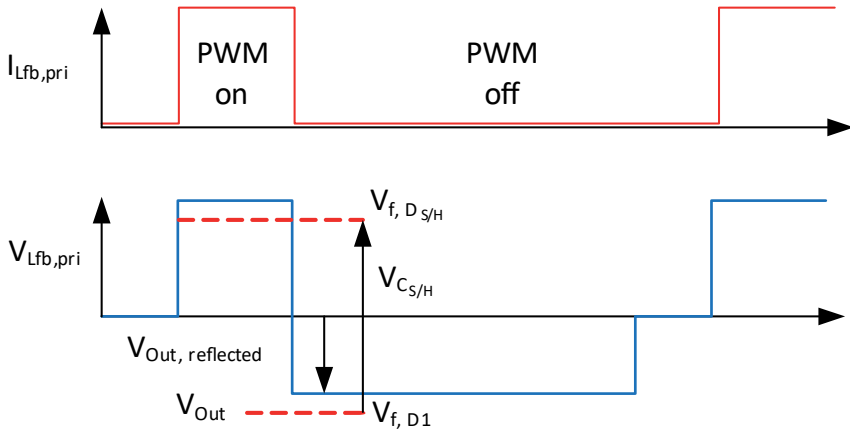


Fig. 11.25: Waveforms of the magnetically coupled shunt regulator.

A practical circuit is shown below in figure 11.26 using a constant on-time PWM modulation signal.

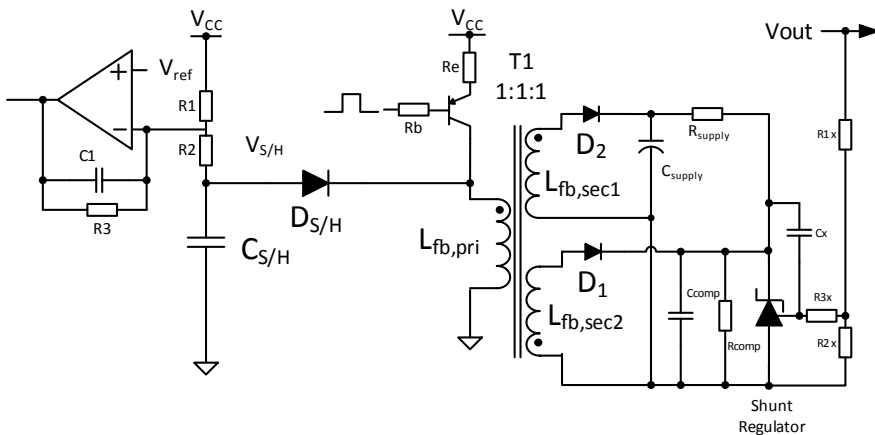


Fig. 11.26: Practical circuit for a magnetically coupled shunt regulator

A 1:1:1 transformer is used so that one output winding can be half wave rectified by D2 to create an isolated supply voltage for the shunt regulator. As this winding is not reversed with respect to the primary, the current that flows into C_{cv} is not measured by the hold capacitor C_H due to the blocking diode D_H (the voltage on the primary side is positive and equal to the voltage on the output capacitor C_{cv} minus one diode drop).

The voltage across C_H slowly charges up through R1B and R1A, “resetting- “ the negative hold capacitor voltage. When Q1 is switched off, the output voltages are reversed. Now D2 is reverse biased and D1 is forward biased.

The reflected primary winding voltage is negative and equal to the shunt regulator voltage plus the forward drop of D1. The voltage across C_H is pulled down via D_H to this negative voltage. If all of the diodes are the same with the same forward voltage drops, then the voltage across C_H is exactly equal to the shunt regulator voltage. Thus, the voltage on the hold capacitor is renewed every cycle and tracks changes in the output voltage accurately. Once the core has become completely demagnetized, then all of the diodes become reverse biased and no more current flows. At this point, the PWM signal should be triggered to start the next cycle so that the hold capacitor voltage does not droop.

The disadvantage of this technique is that the peak detector output is negative, so in some designs, it would need to be inverted with another op-amp stage to be useful. Secondly, the transformer must not go be allowed to go into saturation, so the core cannot be made too small even though the transmitted power is low. Finally, the value for C_H is a compromise between being high enough for low ripple and low enough for a fast response.

The advantages are the cycle-by-cycle tracking of the output voltage and the ability to operate at high ambient temperatures of 100°C or more as no opto-couplers are used.

11.8 Capacitively coupled feedback

As more and more power supplies now use digital controllers, the use of digital isolators is also becoming more prevalent. The feedback path is no longer purely analogue, but the output voltage is sampled and converted into a digital control signal using general purpose microprocessors or custom DSPs (Digital Signal Processors). The DSP can be either on the primary side for a full digital control topology or on the secondary side sending back data to modulate an analogue primary side controller or two microprocessors can be used to send data back and forth. The advantage of a microprocessor on the primary side is a guaranteed start up but at the cost of needing to generate a clean low voltage supply from the high voltage mains supply. The advantage of a microprocessor on the output side is that the microprocessor power supply is much simpler, and the ability to have multiple outputs or switchable constant voltage or constant current modes. The disadvantage is that start up into a short circuit may be compromised.

Microprocessors are nowadays so cheap that it is often easier to use them on both the primary

and secondary sides and use a digital isolator to communicate between them. Capacitively coupled digital isolators offer very high isolation (typically 5kVAC/1 minute) in a very compact package with cleaned-up outputs with well controlled slew rates.

Capacitively coupled digital isolators come in two main flavours: modulated or edge triggered. A modulated digital isolator consists of a capacitively coupled modulator and demodulator than run at a much higher frequency than the signal bandwidth being transmitted. Data is transmitted by On-Off Keying (OOK) meaning that the digital input is simply used to gate a high frequency oscillator typically running at 10s of Megahertz, so data rates from DC up to 100Mbps are possible.

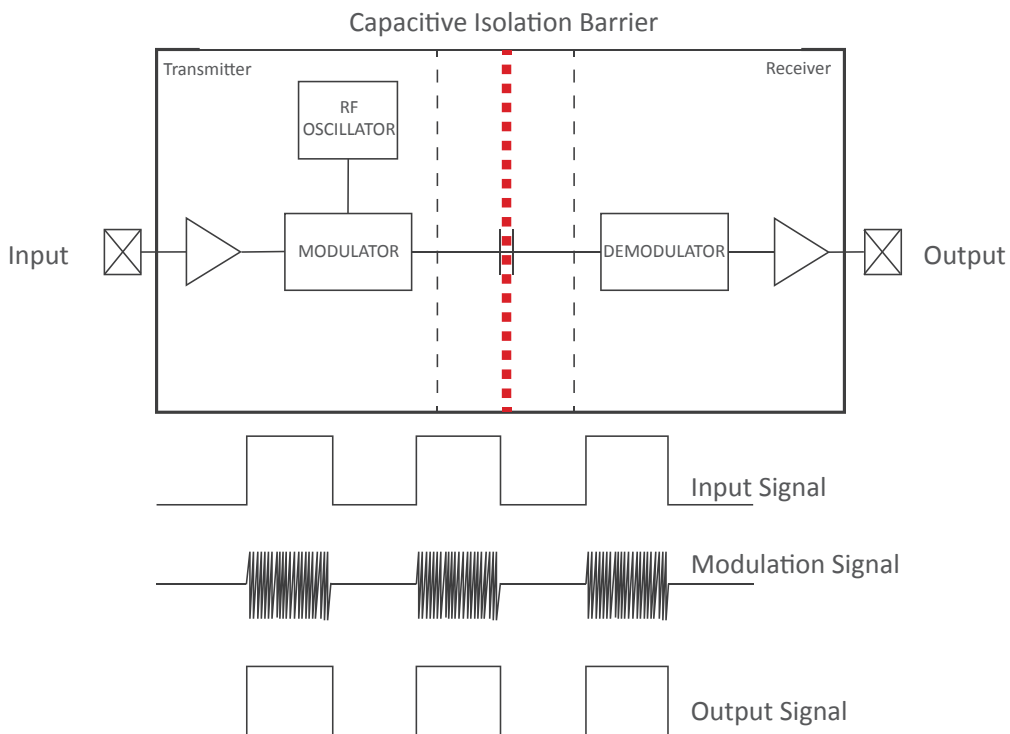


Fig. 11.27 Schematic of a capacitively coupled modulated digital isolator

The disadvantage of using modulated couplers is the very high internal operating frequency which can cause EMI problems if a spread spectrum oscillator is not used or if the PCB layout is not carefully designed with lots of decoupling capacitors and separated ground/power planes.

The relatively slow reaction time of the demodulator creates a propagation delay of 10-100ns, which for fast control loops may be significant delay. The alternative is to use edge triggered communication:

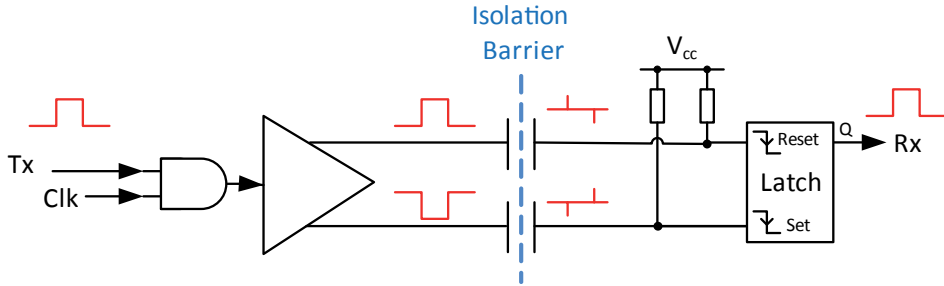


Fig. 11.28: Schematic of a capacitively coupled edge-triggered digital isolator

Edge triggered digital isolators have lower propagation delays and higher data throughput than modulated digital isolators, but are more expensive and despite the differential inputs can be more susceptible to interference from stray electric fields.

11.9 Primary side regulation

Although digital isolators find many uses in high end, space and military applications, they are too expensive for many cost sensitive industrial and commercial power supplies. Primary side regulation (PSR) is the most commonly used method as even the cost of the optocoupler can be significant in a design with a BoM budget of only a few dollars. PSR also has the advantage that the auxiliary winding is needed in any case to bootstrap power the controller IC and to reduce the power lost in the start-up resistor chain. A typical IC-based PSR topology is shown below, along with the waveforms.

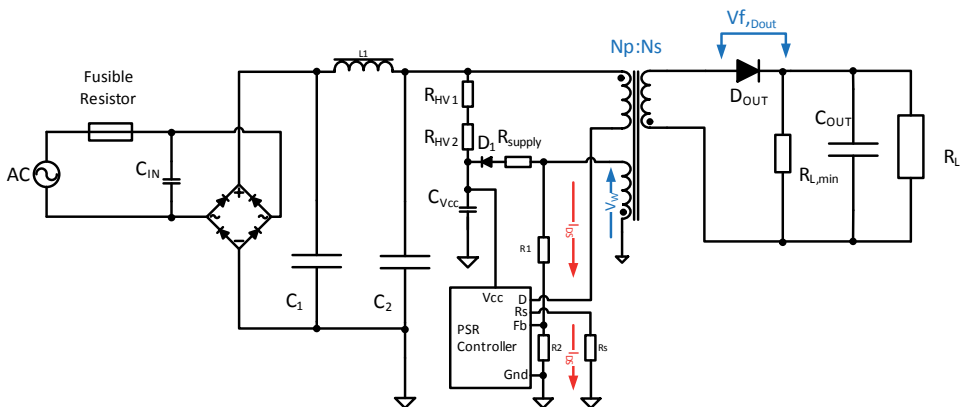


Fig. 11.29: Primary side regulated controller with integrated power switch.

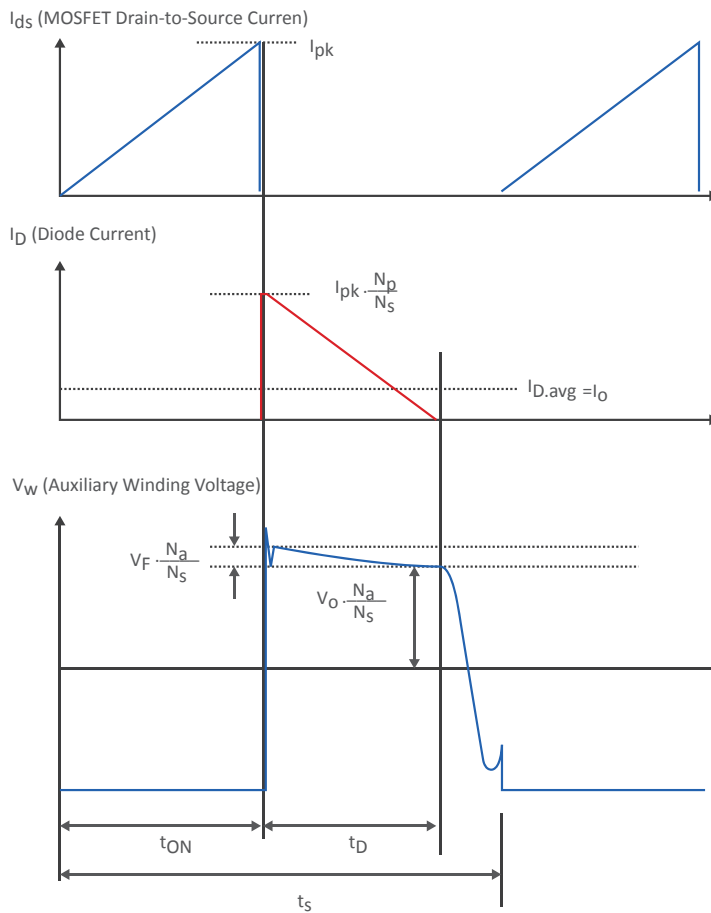


Fig. 11.30: Typical PSR waveforms

There are four distinct phases of operation:

Phase 1: the MOSFET is gated on and current through the primary winding increases linearly until it reaches the peak current limit, I_{pk} , which is detected by measuring the voltage across the sense resistor, R_s .

Phase 2: The MOSFET is turned off and the energy stored in the core is released through the output diode as the magnetic field collapses. The current through the diode decreases from a peak current of I_{pk} times the primary to secondary turns ratio, $N_p : N_s$ linearly down to zero.

Phase 3: The voltage on the auxiliary winding, V_{AW} , meanwhile decreases from a peak voltage of the auxiliary to secondary turns ratio multiplied by $(V_{out} + \text{diode drop}, V_F)$ to just $N_a : N_s$ multiplied by V_{out} as the diode current decreases to zero. At this point the auxiliary winding voltage is sampled via the resistor divider $R1$ and $R2$. The resistor divider ratio is the opposite of the auxiliary turns ratio, so the voltage on V_{FB} is simply the output voltage. This is used to regulate the PWM controller.

Phase 4: The transformer goes into quasi-resonant mode. The auxiliary voltage is monitored for the next valley before restarting the cycle. This allows the main power MOSFET to switch on at the minimum primary voltage to reduce the switching stress.

The big advantage of PSR is the low component count as the necessary PWM control, sample-and-hold and protection circuitry is all integrated inside the control IC. The auxiliary winding does not just eliminate the need for an opto-coupler, it also provides enough bootstrap power to run the IC. A high value resistor chain $R_{HV1} + R_{HV2}$ from the rectified input voltage is used to start up the IC, but as soon as it is running, the IC switches to the rectified low voltage supply from the auxiliary output via R_{supply} and D1. This reduces the power consumption considerably and increases the efficiency.

The disadvantages are the need for an auxiliary winding. This does not add much cost, but can make the transformer construction more complex, especially if split primary windings are used. The windings need to be carefully arranged so that the insulation withstand voltage and the clearances are not affected by the extra winding. Also the topology require discontinuous operation to sample the reflected output voltage on the auxiliary winding correctly, and this makes constant current converters more difficult to design to ensure DCM under all operating conditions.

Also a dummy load resistor, R_{Lmin} , is needed to keep the switching frequency above a minimum limit and to stop the output voltage rising out of specification under no-load conditions (refer to the next chapter for low power consumption techniques)

In general, the advantages outweigh the disadvantages to such an extent that quasi-resonant PSR is the most commonly used AC/DC topology for almost all low power converters.

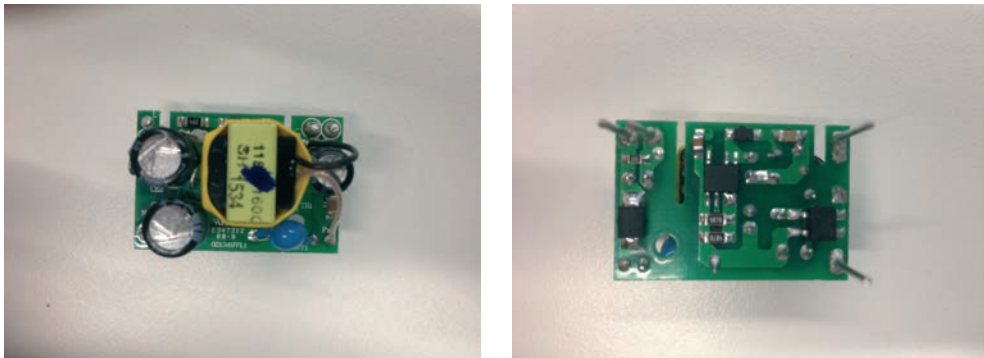


Fig. 11.31: Photos of the top and bottom sides of the RECOM RAC02 series showing the compact assembly and low component count possible with PSR topology

Chapter 12

Low Standby Power Consumption Techniques

Until relatively recently, one of the main selling points of any AC/DC design was the full load efficiency. This is mainly because the figures are often very impressive (if a 100W AC/DC power supply needs 1W to power its internal 'housekeeping' power consumption, then it can be advertised as being 99% efficient). However, the same power supply with a 1W load would only be 50% efficient and all power supplies have zero efficiency under no-load conditions.

The regulatory authorities have recognized that most power supplies operate most of the time under no-load standby conditions, so have introduced standards for standby as well as full load efficiencies. This is because consumer electronics are so widespread that the average home has now upwards of 40 mains-powered devices in it which even in standby consume between 5%-10% of the total electricity demand.

The main energy efficiency regulations for external power supplies standby (no load) power consumption are:

US Department of Energy (DoE) Energy Star	$\leq 0.30 \text{ W up to } 10\text{W}, \leq 0.5 \text{ W up to } 250\text{W}$
CECP (China Energy Conservation Program)	$\leq 0.30 \text{ W up to } 10\text{W}, \leq 0.5 \text{ W up to } 250\text{W}$
EU EcoDesign (Energy using Products-EuP)	$\leq 0.30 \text{ W for non-PFC}, \leq 0.5 \text{ W for PFC}$
Australia High Efficiency	$\leq 0.5 \text{ W up to } 180\text{W}$

Table 12.1: Comparison of standby power consumption limits.

External battery charger power supplies have stricter limits (0.075W up to 50W, 0.15W up to 250W) as it is assumed that they will be left plugged in yet spend most of their time in standby. Internal built-in power supplies have a more relaxed specification (500mW in standby, 1W if there is an active display) as it is assumed that the device will be switched-off or disconnected if not needed.

The losses in an AC/DC converter which are not load dependent are can be split into passive and active losses:

Eq. 12.1:

$$P_{loss} = LOSS_{passive} (LOSS_{HV \text{ dropper}} + LOSS_{HV \text{ Bleeder}} + LOSS_{feedback}) + f (LOSS_{clamp} + LOSS_{switch})$$

There are several techniques that can be used to reduce the no-load or light-load power consumption.

12.1 Passive Losses

12.1.1 HV start up disconnect

All AC/DC controllers need a start-up circuit. The rectified high voltage DC bus is fed via high resistance dropper resistors (usually two or more are used in series to spread the voltage stress across each resistor) and a Zener diode limiter to the V_{cc} input of the controller IC. Usually, as soon as the controller starts up, the operating V_{cc} current is then supplied by an auxiliary winding (which can also act as the feedback for primary side feedback applications). Thus the HV start-up circuit must only provide enough current to start the controller IC oscillating; thereafter the “bootstrap” auxiliary winding takes over to provide the operating current (so called because of the image of pulling oneself up into the air by tugging on one’s own bootstraps or shoe-laces).

Fig.12.1 shows such an arrangement. R_{HV1} and R_{HV2} are the two high voltage dropper resistors wired in series to reduce the voltage stress across each resistor and ZD1 is the voltage limiting Zener diode (typically around 15V). After start-up, the operating current will be supplied by the auxiliary winding rectified by D1 and smoothed by C_{Vcc} . To avoid overloading the Zener diode, a series resistor R_{supply} limits the running current to a safe level.

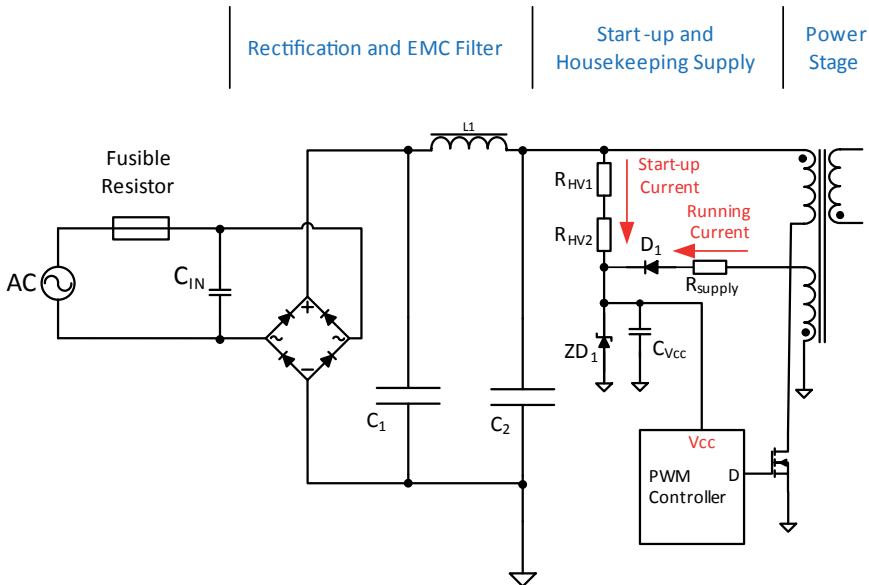


Fig. 12.1 HV start-up circuit with bootstrap.

Even if the majority of the operating current is provided by the auxiliary winding, significant current still flows through the HV start-up resistors after start-up (equal to the rectified DC mains voltage – ZD1 divided by $R_{HV1} + R_{HV2}$). This represents a loss that becomes significant under no-load conditions. R_{HV1} and R_{HV2} cannot be reduced, otherwise the controller IC will either not have enough current to start up or the start-up time (time to fully charge up C_{Vcc}) would become unacceptably long.

One solution is to disconnect the HC start-up resistors immediately after a successful start-up by adding the components shown in blue in Fig 12.2:

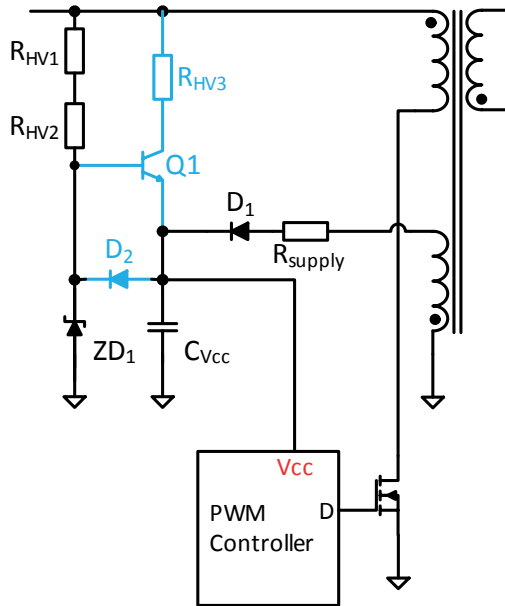


Fig. 12.2: Detail of the HV start-up with disconnect circuit.

During start-up, the base of Q1 is clamped at the Zener voltage, V_{ZD1} . The controller supply voltage, V_{cc} , is one base-emitter drop lower than this. Once the controller has started, the auxiliary winding increases the V_{cc} voltage until it is clamped to $V_{ZD1} + V_{fD1}$, or one diode drop above the V_{ZD1} Zener voltage. This reverse bias turns off Q1, which was supplying the start-up current via R_{HV3} . The supply current for the controller is now supplied only from the auxiliary winding. The no-load residual current is now just the bias current flowing through $R_{HV1} + R_{HV2}$, but as this needs to be only just enough to turn on Q1 during start-up, it is much lower than the start-up current needed by the controller IC. A big advantage is that R_{HV3} can now be made relatively low to give a high start-up current to give a fast turn-on time without affecting the HV dropper resistor loss after start up.

The beauty of this circuit is that it works with any topology or controller, analogue or digital. It also has the advantage that if the mains input voltage suffers a brown-out or black-out sufficiently long to stop the converter from running, that it auto-resets. There are controller ICs that incorporate such auto-disconnect circuits internally, but an external circuit allows more fine

adjustment between stand-by power consumption and start-up time. The main disadvantages are that Q1 must be an expensive high voltage type and the residual losses due to the Zener bias current through R_{HV1} and R_{HV2} .

12.1.2 Half-wave HV start up

A variation on the above circuit is to supply the HV start-up dropper resistor through separate diodes rather than the output of the bridge rectifier. This adds the cost of the additional diodes, but halves the voltage drop across the dropper resistor as the AC input is only half-wave rectified instead of being full-wave rectified. The big advantage is that the rectified HV voltage range between high-line voltage and the low-line is reduced, so in many cases, only one dropper resistor is needed instead of two, even for a wide range 100-240VAC input. The biggest disadvantage is that C_{VCC} must be made large enough to adequately smooth the half-wave rectified input at the low-line input voltage which can lead to a longer start-up time.

12.1.3 Bleeder Resistor Losses

External power supplies that are not permanently wired-in⁴ require a input discharge circuit to protect the user from a residual energy shock from the exposed connectors when the power supply is unplugged. The requirement is that the voltage stored in the input filter (mainly in the X-capacitor placed across the supply) should be reduced to a safe level (less than 60V) within 1 second of disconnection (IEC decision: CTL DSH 1080). Simply adding a bleed resistor, R_{dis} , across the input would meet this requirement (Fig. 12.3), but at the cost of a significant no-load power consumption.

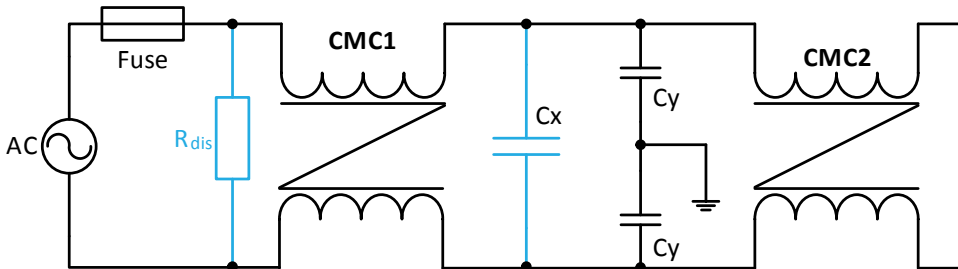


Fig. 12.3: Placement of an X-capacitor bleeder resistor, R_{dis} .

For a 230VAC/50Hz mains supply, a suitable fixed bleeder resistor would consume between 12mW and 20mW under no-load conditions, depending on the size of the X-capacitor required (the dropper resistor consumes VAC^2/R).

⁴ Note: built-in power supplies or power supplies that are permanently connected to the mains supply do not need this protection circuit.

Alternatively, there are several low power automatic X-capacitor discharge ICs that are available that monitor the zero-crossing of the input and then discharge the X-capacitor if the mains is disconnected:

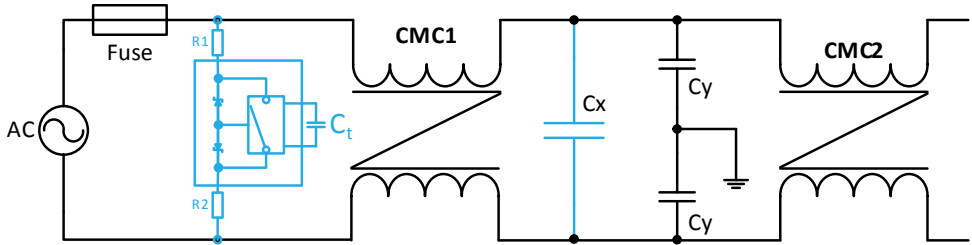
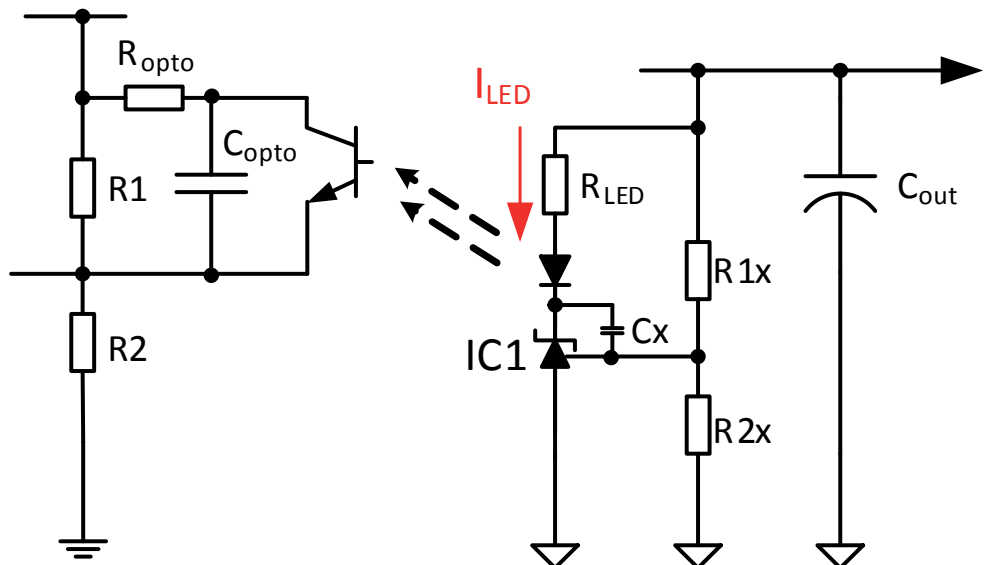


Fig. 12.4: Block diagram of an automatic X-capacitor discharge circuit.

C_t determines the delay time before the discharge is triggered, R_1 and R_2 limit the discharge current and provide additional surge protection for the IC. Such ICs typically consume only 1mW in standby.

12.2 Feedback Losses

The secondary side shunt regulator circuit is powered from the output capacitor. If an optocoupler is used, then the series regulator current limiting resistor, R_{LED} , must be set high enough to drive the LED inside the optocoupler with enough current that the opto-transistor functions over the entire output voltage (including ripple) and operating temperature range. As the current transfer ratio decreases to as low as 50% at extremes of temperature, an adequate optocoupler current at lower or higher operating temperatures means at 20°C, the LED current must be double.



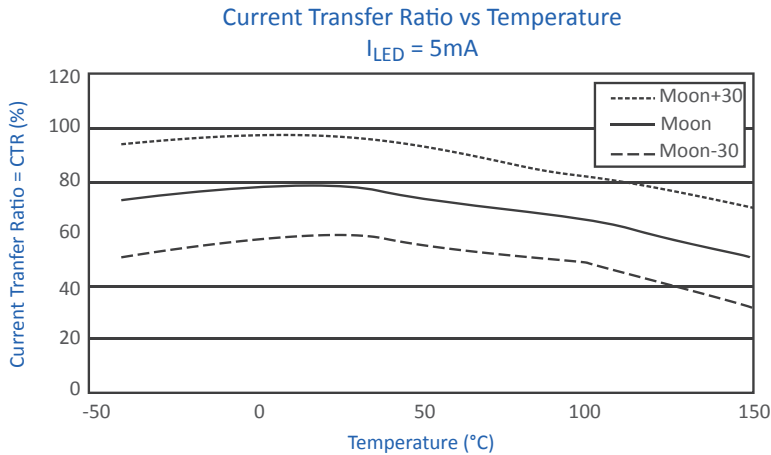


Fig. 12.5: Optocoupler LED current and CTR vs temperature graph.

Practical Tip: Under no-load, room temperature conditions, the largest power loss is usually the feedback circuit which can contribute 10-30mW to the overall power consumption! This is because a minimum current of 1mA is required for a 431 shunt regulator to maintain regulation and to supply its internal circuitry. However, to compensate for the opto-coupler performance deterioration over time and operating temperature, a minimum of 2mA must be set. For a 12V output, this current alone contributes 24mW on the output side or close to 30mW on the input side with efficiency losses.

On the primary side, the photo-transistor needs a pull-up resistor, R_{opto} , to ensure correct start up. This resistor cannot be made too large otherwise the feedback will become unstable or the optocoupler output will fall below the minimum compensation voltage that the controller can accept ($V_{comp,min}$). Many controller ICs include an internal constant current source for the opto-coupler input which eliminates the need for an external R_{opto} pull-up resistor and reduces the stand-by power consumption. Equation 12.2 shows the calculation to determine the largest acceptable R_{LED} value:

$$\text{Eq. 12.2: } R_{LED} = \frac{V_{out} - V_{shunt}}{V_C - V_{comp,min}} R_{opto} CTR_{min}$$

CTR_{min} is the worst case current transfer ratio of the optocoupler over the entire operating temperature range and taking aging into account. A higher CTR will allow a higher value of R_{LED} and a lower no-load power consumption.

An alternative solution is to use an active feedback regulator which avoids the minimum cathode current requirement of the 431 shunt regulator. The following example shows a current controlled feedback loop .

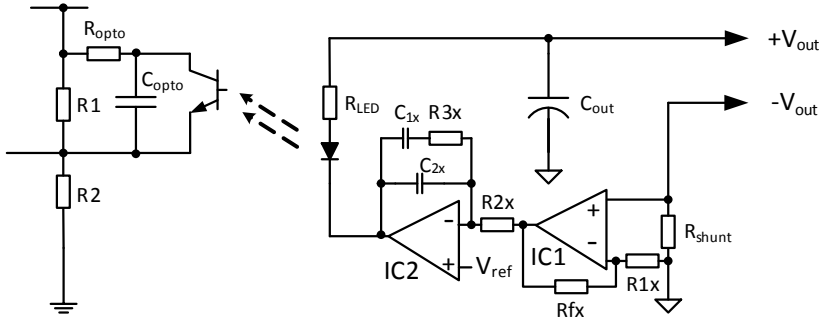


Fig. 12.6: Active feedback loop control (current controlled)

The output current is measured directly using the current shunt resistor R_{shunt} and then amplified by IC1. IC2 adds frequency compensation and supplies the drive current for the optocoupler LED. The advantage of this circuit is that either current or voltage can be used for the feedback control making a constant voltage or constant current power supply easy to implement. Also the gain ($R1x/Rfx$) can be optimized for the best optocoupler performance.

There is a further variation on this circuit where the optocoupler op-amp is replaced with a PWM generator. The PWM output can drive the optocoupler LED harder because as long as the mark/space ratio is below 50%, the average current is still low. The output is then integrated by C_{comp} to recover the original control signal.

The disadvantages of active feedback controllers are that they need a regulated supply and reference voltages which also adds to the overall losses and the additional cost. For very low standby power consumption, primary-side regulation is usually needed to eliminate the losses in the shunt regulator and optocoupler.

12.2 Active losses

Active losses are characterised by a dependence on the switching frequency. Each time the transformer is energized or de-energized, losses occur in the switching or clamping circuits. To make the analysis easier, the commonly-used QR flyback topology is assumed.

12.2.1 Clamp Losses

A passive snubber is designed to dissipate the excess energy stored in the leakage inductance of the transformer each time the main power switch is turned off. The power lost in the clamping circuit shown in Fig. 8.4 is given in Equation 8.5, but it can also be rewritten as equation 12.3:

$$\text{Eq. 12.3 } P_{diss,snubber} = V_{CL} f \frac{I_{peak} t_{on,D}}{2}$$

Where V_{CL} is the voltage across the clamp capacitor, f is the switching frequency and t_{on} , D is the turn-on time for the diode. The clamp losses can be decreased by reducing the voltage across the clamp capacitor (not very helpful as this increases the voltage stress on the switching transistor), by using a faster switching diode to reduce the t_{on} time or by reducing the switching frequency or load.

12.2.2 Variable switching frequency

Under full load a the converter will run at the minimum switching frequency determined by the input voltage and minimum off-time of the controller. As the load is reduced, the switching frequency will increase as I_{peak} reduces and the off time increases. The free-running QR switching frequency is given by equation 12.4 which is plotted in Fig 12.7:

Eq. 12.4:
$$f = \frac{1}{I_{peak} L_{pri} \left(\frac{1}{V_{DC}} + \frac{1}{V_{reflected}} \right) + \pi \sqrt{L_{pri} C_{oss}}}$$

Where V_{DC} is the rectified supply voltage, $V_{reflected}$ is equal to V_{out} x turns ratio and C_{oss} is the switching transistor drain-source capacitance. For a fixed input and output voltage, the switching frequency is inversely proportional to the primary peak current which is load dependent.

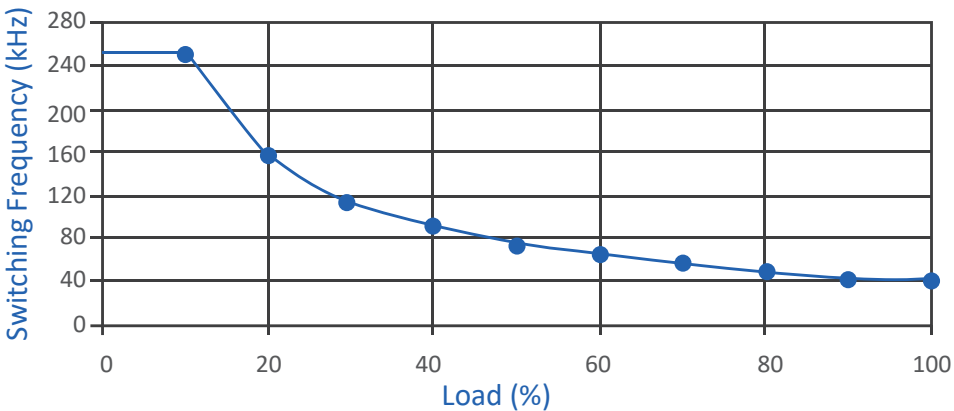


Fig. 12.7: Typical relationship between QR switching frequency and load.

The inverse relationship between switching frequency and load means that the power dissipation in the snubber remains constant from full load down to light load. This means that proportionally, the losses in the snubber become more significant as the load decreases. The switching losses are also frequency dependent; although the conduction losses decrease with load, the switching losses increase as the load decreases. The clamp and switching losses together mean that a power supply that operates very efficiently at full load will become

increasingly inefficient at loads below 50%.

One solution to this problem is to introduce variable valley switching and pulse skipping under light load conditions.

12.2.3 Variable valley switching

Under light load conditions, the switching frequency will have reached its maximum. Any further reduction in load can only be accommodated by changing from CCM or CrCM mode to DCM mode. In effect, the controller does not switch on again after the first minimum (valley), but waits for the second, third, fourth, etc. valley before initiating the next switching cycle (fig 12.8). The switching voltage increases slightly with each successive valley, but the stretched cycle time reduces the power consumption to give a net reduction in the losses.

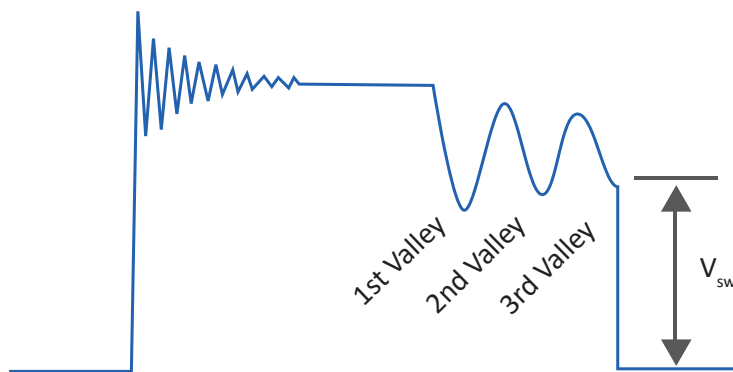


Fig. 12.8: example of a third valley switching.

As the transformer is fully de-energized at the start of the first valley, the output voltage must be maintained by the output capacitor until the next cycle. As the number of valleys increases, it becomes less important (and much more difficult to detect) the minima of the next valley, so the next cycle can be triggered even if the voltage is not a minimum. It becomes more important to maintain the output voltage regulation than to minimise the switching losses by only switching at precisely the next valley.

Under no-load conditions, even this slowed-down, multiple valley switching cycle becomes wasteful of energy. There is a minimum on-time defined by the slew rate of the FET driver and the gate capacitance, so under no-load conditions the output capacitor may be over-charged. The output voltage rises and cannot be regulated back down.

12.2.4 Pulse skipping

No-load power consumption can be reduced using a technique called pulse skipping. Instead of a regular switching cycle, the converter generates a short burst of pulses and then idles to minimize the power dissipation and to keep the output voltage below the maximum limit. The short burst charges up the output capacitor to V_H and then the output voltage slowly decays

until a lower threshold, V_L , is reached, whereupon the controller generates the next burst. The idle time is either fixed (the designer must choose the size of output capacitor to maintain the output between V_H and V_L) or can be made variable by changing a timer capacitor or by programming an internal register.

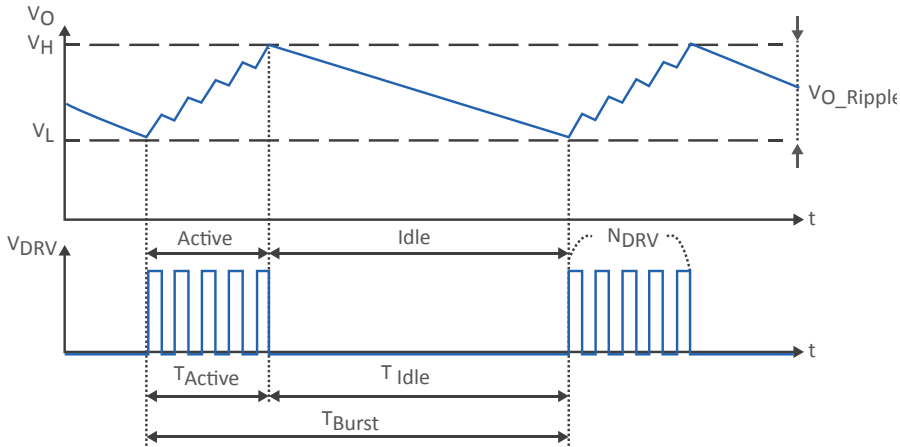


Fig. 12.9: Pulse skipping

Using pulse skipping, the no-load power consumption can be reduced to below 100mW. The disadvantage of the pulse-skipping technique is a high output ripple and the difficulty of filtering out the bursts of high frequency operation on both the main input and on the auxiliary winding controller supply circuit.

Practical Tip: Use only a TVS snubber with pulse skipping controllers. A clamping capacitor would become completely discharged between bursts, so the magnetising energy in the transformer would be first diverted into the clamp capacitor before being transferred to the output. For the first few switching cycles in the bursts, the clamp dissipation would be disproportionately high compared to a low capacitance TVS snubber clamp. Additionally, the ESR of the output capacitor will affect the losses in burst mode. The increased ripple voltage is best accommodated by either a low ESR electrolytic or two electrolytics wired in parallel to reduce the overall ESR.

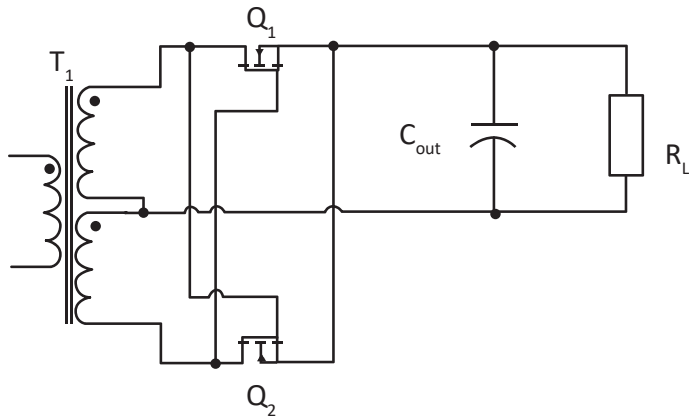
12.2.5 Synchronous rectification

The forward voltage drop across the secondary side rectification diodes generates a significant power loss, especially at lower output voltages. If a typical silicon rectification diode has a V_f of 600mV, then for a 3.3V output, then the rectifier diode dissipates 18% of the available output power. Replacing the output rectifier with a synchronous rectifier (SR) using MOSFETs reduces the power dissipation to approximately $I_{out}^2 \times R_{DS,ON}$. (There are some additional MOSFET losses associated with the body diode conduction losses, gate drive dissipation and output capacitance losses, but these losses are small compared with the output current dissipation.)

For a typical power MOSFET with $2\text{ m}\Omega$ $R_{DS,ON}$ resistance, the power loss is only $20\mu\text{W}$ for a 100mA load current, compared to 60mW for the diode equivalent. So even for low output currents, SR can be a useful technique to reduce the low-load power consumption.

If the secondary winding output voltage is high enough and CCM or CrCM modes are used, then the MOSFETs can be self-driven. For low output voltages or DCM, the MOSFETs are not turned on fully for a large part of the switching waveform and the body diodes start to dissipate too much power. Figure 12.10 shows a typical cross-connected self-driven SR circuit.

Fig. 12.10: self driven SR circuit for higher secondary voltages.



The problem of low gate-source voltages can be overcome by adding an auxiliary secondary winding to drive the MOSFETs as in Figure 12.11.

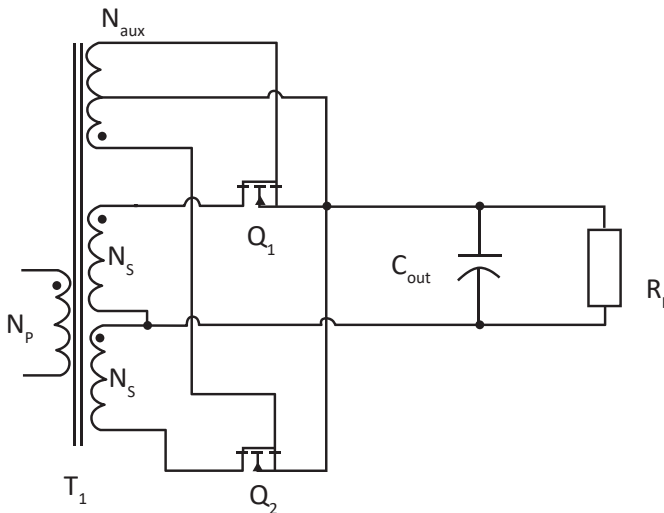


Fig. 12.11: self driven SR circuit for low secondary voltages.

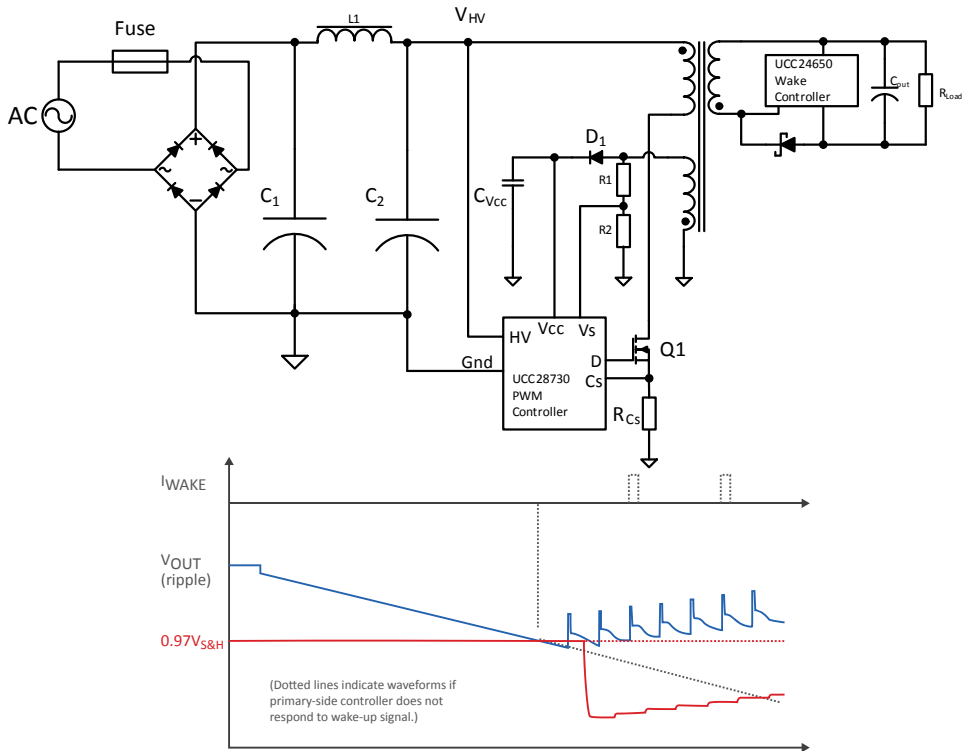


Fig. 12.13: An example of a zero-standby solution.

Under no-load conditions, the controller goes into deep sleep mode and turns off the main power stage completely. The power consumption of the controller IC is now minimal and the output voltage is supplied only by the output capacitor, C_{out} .

If the output voltage drops below a certain limit, then the secondary side wake controller issues a short burst of short circuit pulses across the secondary winding which is detected on the primary side to wake up the PWM controller and initiate normal operation. The average power consumption of these short periods of activity interspersed with long sleep periods is below 5mW.

12.3 Measuring standby power consumption

It is not easy to measure the power consumption of an AC/DC converter in standby without the use of a power analyser. Especially for very low standby consumption designs (<100mW), an expensive high-end power analyser is required. The reasons for this are four-fold:

1 High sample rate: A high sample rate is needed to capture the short high frequency burst signals. It is not sufficient to just detect the peak input current; the waveform must also be measured and analyzed. A sample rate of 20MHz is required to accurately measure a short current peak lasting only a few milliseconds.

2 High sensitivity: The peak input current of a low standby converter may be only 100-200µA. To get an acceptable measurement accuracy, a 1-2 µA current resolution is needed. Voltage resolution is not so critical (around 1V volt resolution is acceptable), but care must be taken when converting to true RMS values (see next section).

3 No auto-ranging: As most of the time, the power supply consumes very little power, any auto-ranging function will automatically select the highest possible resolution range. When a sudden burst signal occurs, the autoranging circuit may not react quickly enough. Therefore the autoranging function must be disabled.

4 Large memory: Due to the high sample rate and very long averaging time (minimum 500 mains cycles) , an analyser with a very deep memory is needed. Even with a high-end power analyser costing upwards of 30k€ , the no load power consumption can only be measured with a reliable accuracy of only around $\pm 2\%$.

Chapter 13:

Measuring AC

13.1 AC voltage measurements

The simplest way of measuring an AC voltage is to use a multimeter. The meter will respond to the AC component of the input and ignore any DC offsets. This gives a more-or-less accurate AC value but can lead to false power calculations if the DC component also contributes to the load current.

Since the average of a purely sinusoidal waveform is zero, the meter needs to measure either the peak-to-peak voltage, the average rectified voltage or the true RMS voltage. For the same AC signal, the displayed values will be different! For example, if we set up a waveform generator to give a 10V sinusoidal waveform output it will have a peak-to-peak voltage of 10.00V, a rectified average voltage of 6.37V and an RMS voltage of 7.07V. Electronic multimeters use RMS because this is the equivalent DC voltage that would give the same heating effect with a resistive load.

However, if the AC signal is not a pure sine wave, the readings will be very different depending on the waveform:





Response to sine wave	Response to square wave	Response to single phase diode rectifier	Response to 3 phase rectifier with one phase missing
			
Correct	10 % high	40 % low	5 % to 30 % low

Fig. 13.1: Effect of the waveform on the average RMS readings

The solution to all of these problems is a “True RMS” multimeter which can accommodate both the AC and DC components of continuous waveforms and display the correct result:

Eq. 13.1:
$$V_{RMS,true} = \sqrt{\frac{V_{AC,peak}^2}{2} + V_{DC}^2}$$

However, the situation is made more complex if the AC signal is discontinuous. Then, even a true RMS voltmeter will not give the correct reading. Unfortunately, such discontinuous signals are very common in AC/DC circuits, such as the trapezoidal signal from a switching transistor, the saw tooth voltage across a diode or the triangular voltage across an inductor.

The equivalent RMS voltage is an integral over time:

Eq. 13.2:
$$V_{RMS} = \sqrt{\frac{1}{T} \int_0^T V^2(t) dt}$$

So the only way to measure the RMS value of a discontinuous signal accurately is with an oscilloscope.

With any digital meter or digital storage oscilloscope (DSO), another important source of error is the crest factor. This is simply the ratio of the peak to RMS voltages. If a digital meter is to measure the signal accurately, it must have sufficient dynamic input voltage range to cope with the crest factor which can vary from 1 for a square wave, $\sqrt{2}$ for a sine wave up to 10 or more for an asymmetrically pulsed input.

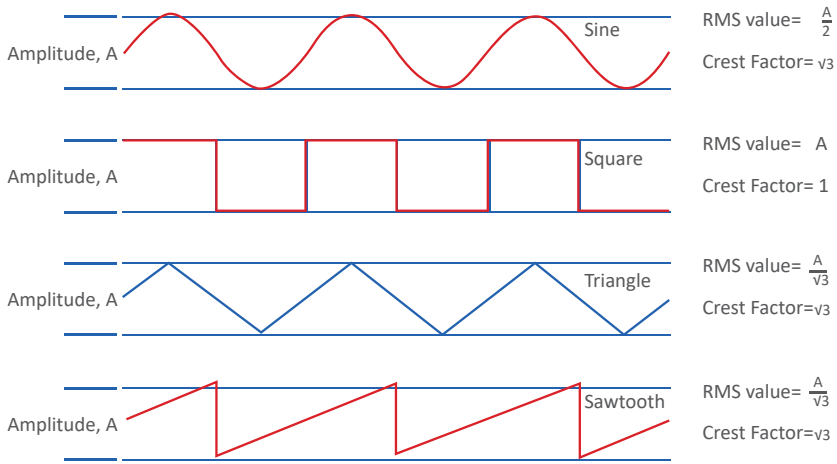
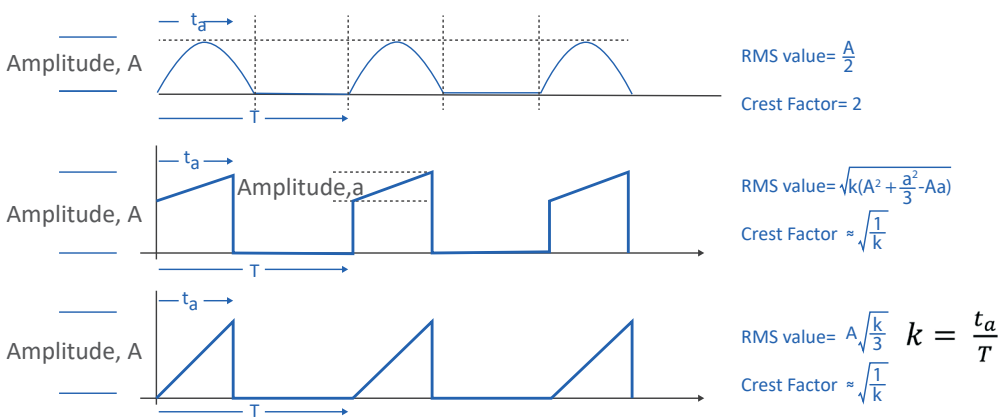


Fig. 13.2: Continuous Waveforms



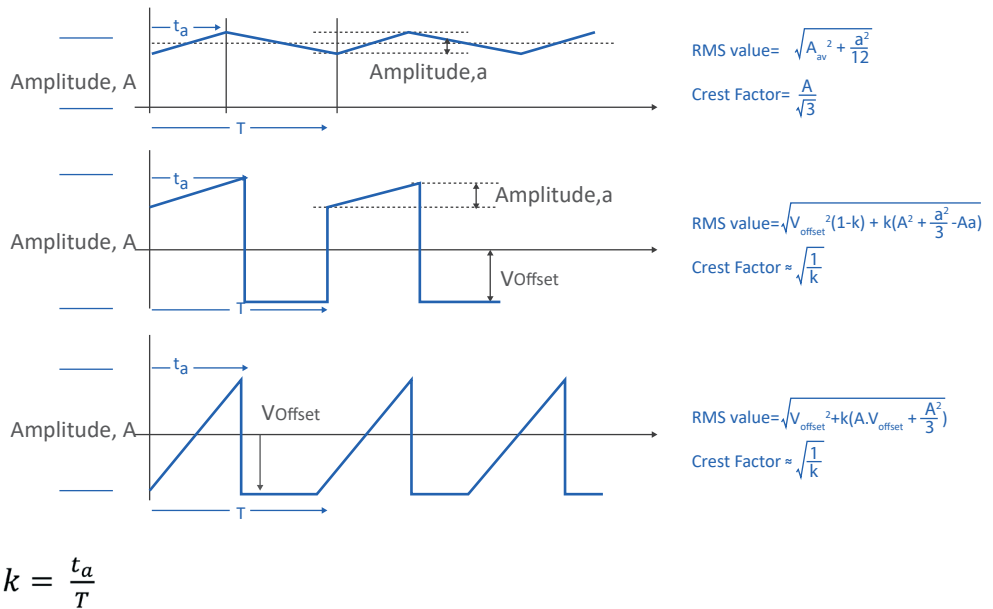


Fig. 13.3: Discontinuous Waveforms

Practical Tip: passive oscilloscope probes must always be calibrated before any AC measurements are done. All oscilloscopes have a square wave reference output on the front panel. The oscilloscope probe should be hooked on to this output and the small variable capacitor in the plug adjusted until the display shows a flat-topped square wave. Figure 13.4 below shows two identical probes connected to the same internal square wave source. Channel 2 is correctly adjusted. Channel 1 is not:

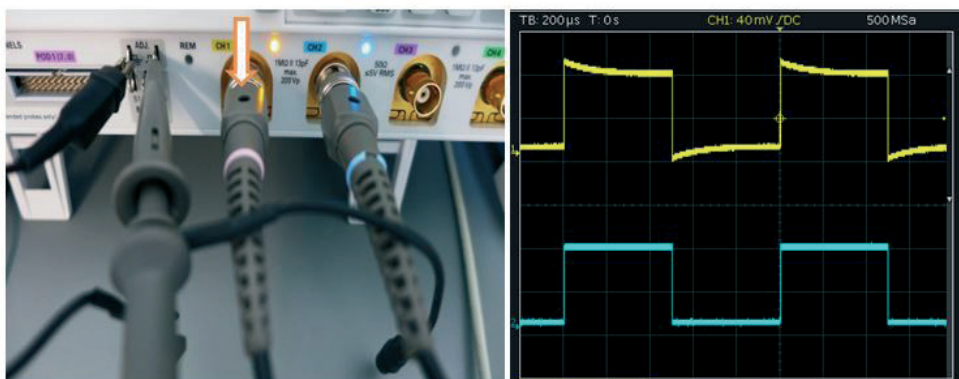


Fig. 13.4: Passive oscilloscope probe calibration. Both channels are measuring the same signal. Channel 1 needs to be calibrated using the trimmer access hole in the plug (arrowed).

For most measurements, the 10:1 attenuator setting should be used on the probe. This will increase the probe's DC impedance from 1 MOhm to 10 MOhm and reduce the loading of the probe on the measured signal at the cost of a less accurate measurement of very small signals.

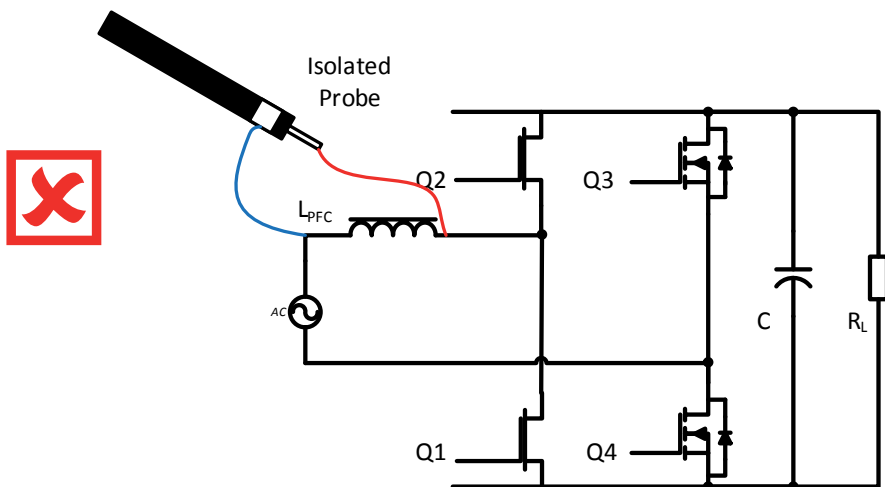
Great care must be taken when measuring high voltages such as AC mains or rectified AC using oscilloscope probes. The ground connection of the probe is connected to earth via the power lead, so simply connecting the probe to the high voltage circuit will blow the fuse or trip the earth leakage detector in the mains supply.

There are several solutions to this problem:

1. use an isolated active probe.
2. use an active differential voltage probe (also isolated, but with a higher input voltage range)
3. run the oscilloscope from a mains isolation transformer and disconnect the ground wire. Also make sure that there are no connectors used for remote control (GPIB or USB) that could ground the oscilloscope through the data lines.

Note that option 3 means that any exposed metalwork (for example the BNC connectors) may no longer be a ground potential, so be especially careful when using an isolated oscilloscope. To measure hazardous voltages, use only option 1 or 2.

Practical Tip: when using an isolated probe or isolated oscilloscope, the probe tip and probe ring can be connected between any two arbitrary points on the circuit being tested. However, the ring should be connected to a stable voltage and not a switching node to avoid false readings. In the following example, the correct way to measure the voltage across a totem pole PFC choke is to use two probes and then use the mathematical function of the oscilloscope to display the difference:



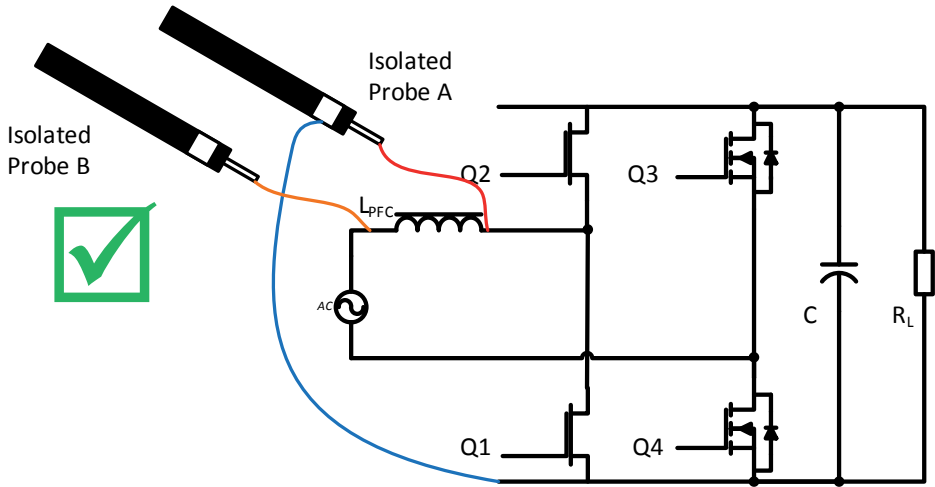


Fig. 13.5: Incorrect and correct method of measuring the voltage across a PFC choke. Both ends of the PFC choke see a varying voltage, so an independent stable reference point is needed.

13.1.1 High frequency AC voltage measurements

The 10%-90% rise time of a probe is related to its bandwidth with the formula:

$$\text{Eq. 13.3: } t_{\text{rise}} \approx \frac{0.35}{\text{Bandwidth}}$$

This means that the commonly used 20MHz BW limit setting will stop the oscilloscope from reacting to any edges that are faster than around 17.5 nS. This is great for removing unwanted switching artefacts from low frequency AC/DC converters but not so good for the next generation of fast switching SiC or GaN-based power supplies where such rise times are part of the signal.

The AC impedance of an oscilloscope probe is the summation of the various impedances in series and parallel of its component parts, so the voltage seen by the DSO will be equal to:

$$\text{Eq. 13.4: } V_{\text{apparent}} = V_{\text{actual}} \frac{Z_{\text{probe}}}{Z_{\text{probe}} + Z_{\text{tip}} + Z_{\text{clip}} + Z_{\text{circuit}}}$$

These additional impedances will cause an overshoot (ringing) for a step change which can be usually be successfully dampened out by measuring the high frequency signal via a high ohmic series resistor and/or by avoiding the use of the probe ground clip (the clip has the highest impedance of all of the impedance factors).

The following diagrams are reproduced from the DC/DC book of knowledge to show the adverse effect of using the ground clip when measuring ripple and noise:

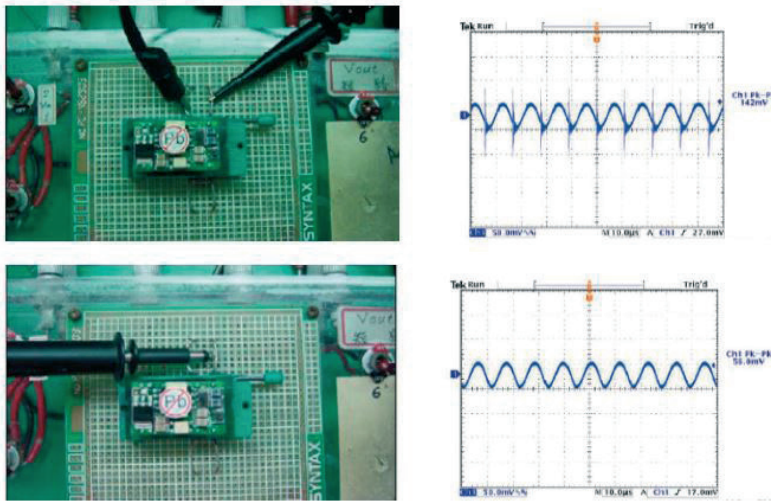


Fig. 13.6: incorrect and correct way to measure ripple and noise. The measurement with the earth clip gives an apparent peak-to-peak reading of 142mV. The correct measurement without the clip gives a correct peak-to-peak reading of 56mV.

13.2 AC Current Measurement Techniques

13.2.1 Precision Shunt Resistor

If a precision resistor is placed in series in a circuit, the voltage developed across it is directly proportional to the current flowing through it. This is the principle by which most multimeters with a current input measure current. If the meter has a full scale reading of $\pm 200\text{mV}$, a $100\text{ m}\Omega$ shunt resistor will allow up to $\pm 2\text{A}$ to be measured. A very simplified multimeter schematic with selectable full scale voltage and current ranges is shown below:

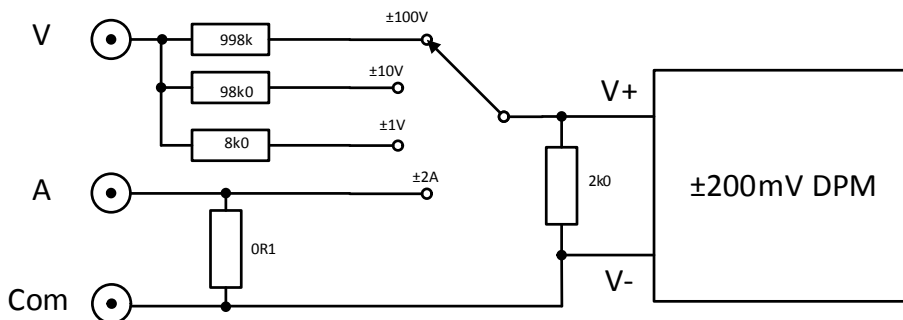


Fig. 13.7: Multimeter input range selector (simplified)

The 100mOhm shunt resistor must be kept low-ohmic so that the in-circuit voltage drop is insignificant (in the example above only 200mV) and to reduce the errors caused by self-heating. All resistive materials have a temperature coefficient of resistance (TCR) which will cause a change in the resistance with temperature, so it is important that the shunt resistor is made of a material with a very low TCR, ideally less than ± 100 ppm/ $^{\circ}\text{C}$.

For a fixed shunt resistor on a PCB that is used to measure direct or alternating currents, the additional errors caused by the copper tracks can become very significant (copper has a typical TCR of around $+0.004\%/^{\circ}\text{C}$ or $+4000$ ppm/ $^{\circ}\text{C}$). To avoid measurement errors, four terminal (kelvin contact) shunt resistors should be used, so that the voltage measurement tracks are not carrying any significant current themselves:

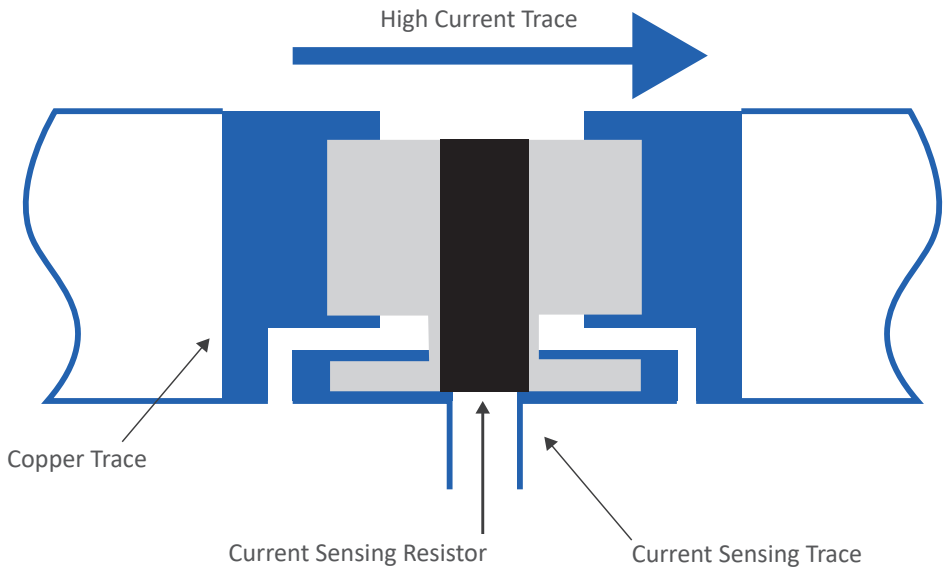


Fig. 13.8: Four-terminal current sensing shunt resistor

The advantage of shunt resistors is that they can be used to measure both DC and AC currents and that they can be suitably dimensioned to measure both very small and very large currents. With careful track layout, shunt resistors can also be used to accurately measure high frequency alternating currents.

Often a simple low pass filter formed by a capacitor in series with the shunt and high ohmic resistors placed in the measurement legs will allow clean current measurements to be made even on noisy installations. Finally, the performance does not deteriorate with short-circuit or high surge currents: there is no avalanche or thermal runaway failure mode.

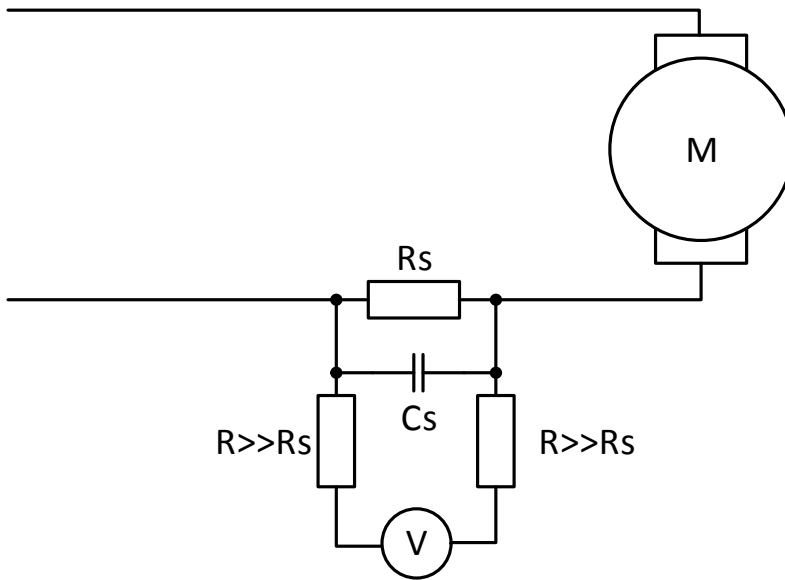


Fig. 13.9: Shunt resistor with low pass filtering (used to measure the supply current for a noisy motor in this example)

Practical Tip: current shunts can run hot enough to affect adjacent components, so always leave a good clearance gap and use thick copper traces to help dissipate the heat. High current capability shunts are often raised off from the PCB. This avoids overheating the FR4 material beneath the central high-resistance hot-spot of the shunt and helps with air cooling. Check also that the expansion coefficients of the shunt and PCB are not too mismatched to avoid thermally-induced cracking and solder-joint stress.

The disadvantages of using a shunt resistor are that the measurement contact is direct without any isolation, that the power dissipation in the shunt resistor can affect the readings and that very low ohmic shunts need high voltage magnification to generate a useful signal which introduces noise, drift and offset errors. Furthermore, high precision power shunt resistors (0.1% or better) with low TCR and low drift are expensive components.

13.2.2 Shunt + Current Mirror

As a current sensing shunt resistor is not isolated nor necessarily referenced to ground, this can create problems when attempting to measure the current in a higher voltage circuit. The following example shows how to use a current mirror to voltage shift the current output to a level, say, suitable for the input pin of a microcontroller. DC and DC offset AC (for example output ripple current) can be measured with this circuit.

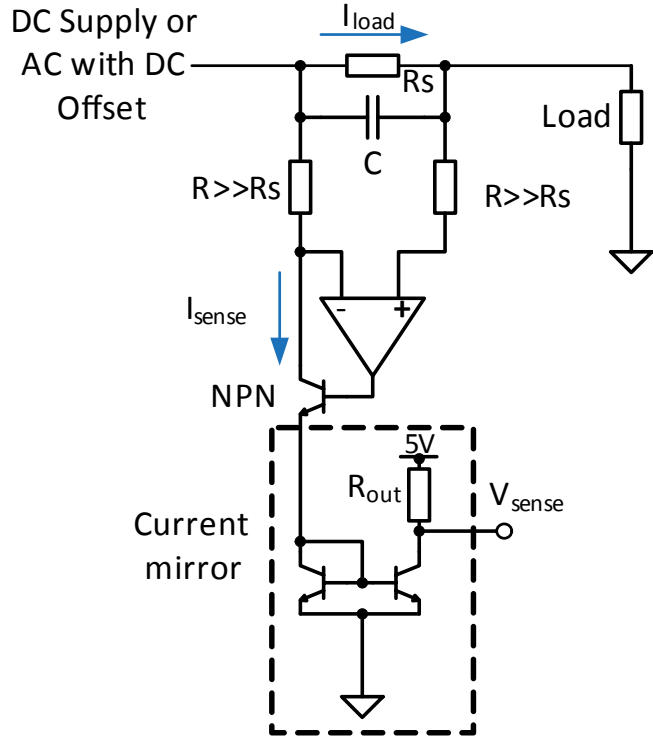


Fig. 13.10: Current sense shunt resistor and current mirror level shifter.

The voltage developed across the current sense resistor, R_s , is amplified by the Op-amp to generate an output current, $I_{sense} = R_s / R$. As this current is referenced to the high voltage supply, it needs to be current mirrored to generate an output voltage, V_{sense} , which is referenced to the 5V supply.

The V_{sense} output voltage is:

$$\text{Eq. 13.5: } V_{sense} = I_{load} R_{out} \frac{R_s}{R}$$

13.2.3 Shunt + isolation amplifier

The use of a current mirror in combination with a high-side shunt resistor is useful for medium supply voltages, but not safe for higher supply voltages. To measure the current in a PFC stage or AC conductor, safety isolation is required. One technique to accurately measure AC or DC currents on a high voltage supply is to use an isolation op-amp with an isolated DC/DC supply:

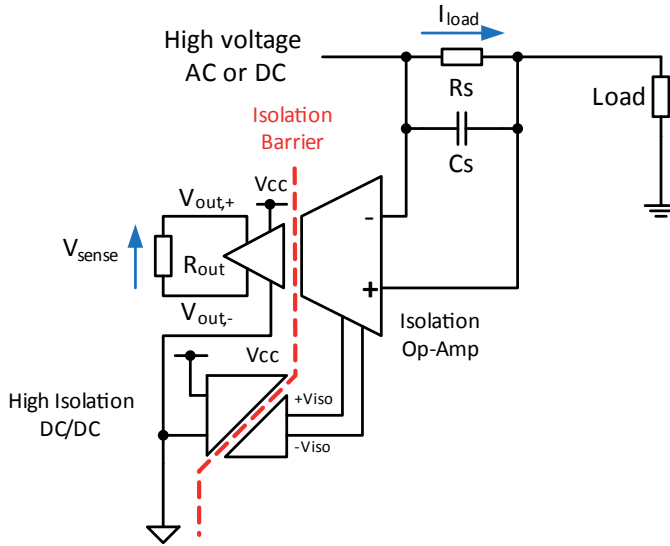


Fig. 13.11: Isolated current sense shunt resistor.

13.3 Current transformer

A transformer can be used to measure the AC current flowing in a conductor if the conductor passes through it to effectively make a single turn:

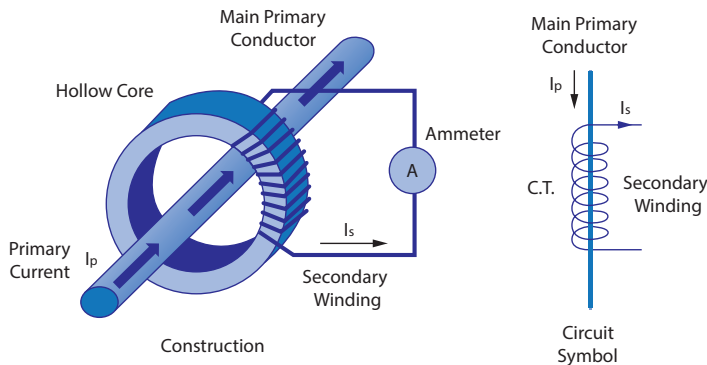


Fig. 13.12: Current transformer construction.

The secondary current, I_s , is proportional to the primary current, I_p divided by the secondary turns:

$$\text{Eq. 13.6 (for a single turn primary)} \quad I_s = \frac{I_p}{N_s}$$

Current transformers (CTs) are useful for measuring high AC currents as the output current can be made a ratio of 20:1 to the conductor current by simply winding 20 turns on the secondary. If more sensitivity is required, then the primary conductor can be wound twice around the core to increase the full scale reading to 10:1. Split-core versions are also available that can be clamped around a conductor or opened to allow more primary turns to be added without needing to cut the wires.

Practical Tip: Never operate a current transformer without a load. If the output current has a 20:1 attenuation, then the open-circuit output voltage has an x20 multiplication, so a current transformer measuring mains current can easily generate thousands of volts across the terminals if the load is disconnected. Always short circuit the outputs if the load is not attached! Current transformers cannot measure DC currents, so only the AC component (for example, the ripple current) will generate an output signal. As the measurements rely on the performance of the high permeability magnetic core, a current transformer will have a bandwidth limit, a rated minimum and maximum primary current, a maximum primary voltage rating and an accuracy rating (typically between 0.2% and 3%, valid over a primary current in the range of 5% to 120%). Finally, CTs have a maximum output burden rating due to the secondary impedance interacting with the ammeter load. If the output load is too high, the output reading will be too low and the CT will also load the supply.

The main advantages of a current transformer are an output which is also a current source, high isolation withstand voltage, near-lossless measurement and a bidirectional output. Fig. 12.7 shows a CT used in a high power phase-shifted full bridge application to provide an isolated current feedback signal:

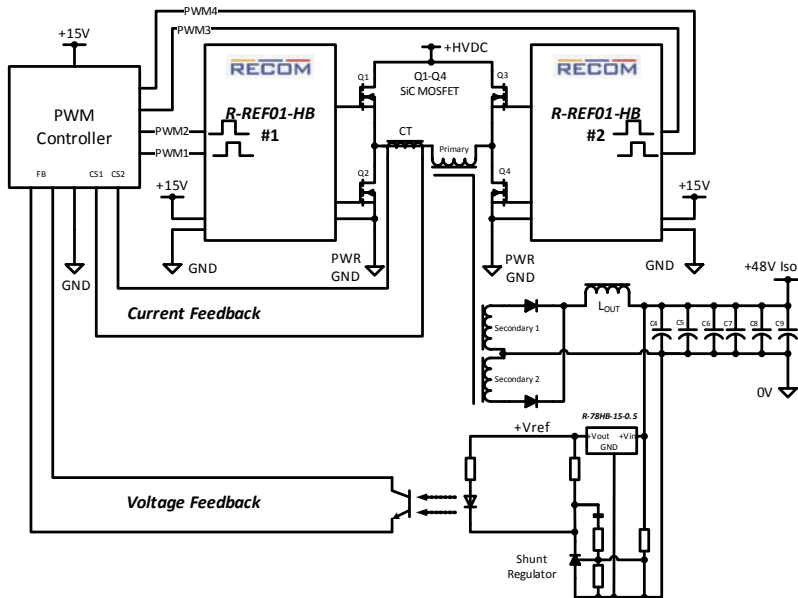


Fig. 13.13: Current Transformer (CT) used in a 1kW full bridge demonstrator.

13.3.1 Compensated CT (AC Zero-flux)

To increase a current transformers low-frequency response, a feedback circuit can be added to cancel out the load caused by the secondary winding. A separate winding is used to cancel out the magnetic flux in the core:

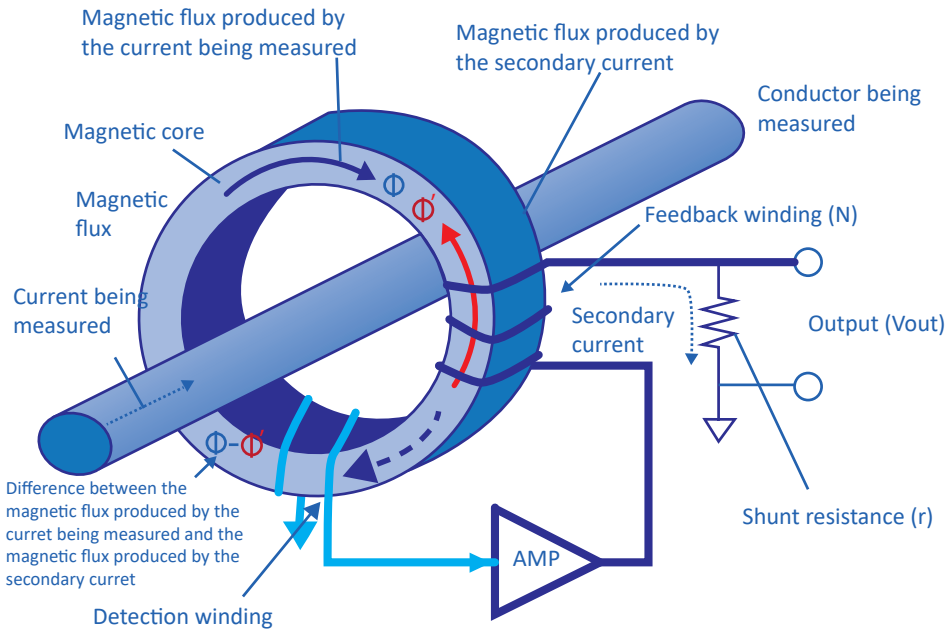


Fig. 13.14: AC zero flux current transformer.

AC zero-flux CTs eliminate the B-H characteristics of the magnetic core, so offer high linearity, low insertion impedance and a wide bandwidth. However, the detection winding and AC amplifier add cost.

13.4 Rogowski Coil

Although similar in appearance to a split-core current transformer, a Rogowski Coil (RC) does not operate in the same way, generating an output voltage proportional to the measured current instead of an output current. An RC needs no magnetic core which reduces the cost and the loading on the primary conductor and the quick response is useful for measuring small, fast changing currents.

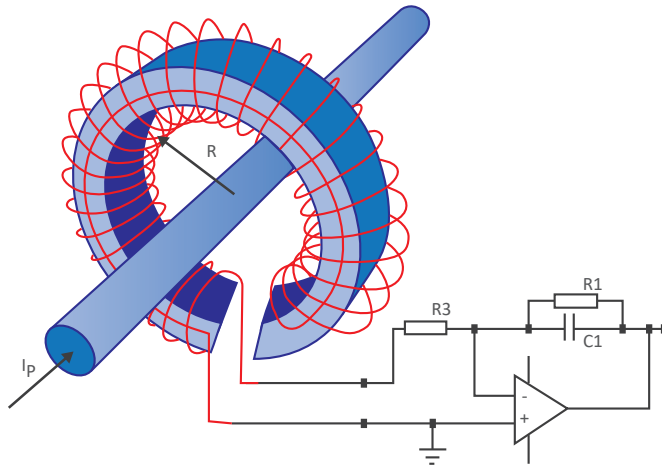


Fig. 13.15: Rogowski Coil

The output voltage $v(t)$ is dependent on the rate of change of the primary current, I_p :

$$\text{Eq. 13.7: } v(t) = \frac{-AN\mu_0}{l} \frac{dI_p(t)}{dt} = -M \frac{dI_p(t)}{dt}$$

Where A is the cross-sectional area of the core, N the number of secondary turns with length l and μ_0 is the magnetic constant, $4\pi \times 10^{-7}$. As these are all fixed units, the resulting output voltage is simply equal to the rate of change of the primary current dI_p/dt multiplied by $-M$, a constant dependent on the mechanical dimensions only.

The secondary wiring is wired in a helical arrangement with the return wire passing back under the secondary so that both wire ends are at the same end of the open core. This makes it very useful for clamp-style current meters as no wires bridge the gap. Flexible RC designs exist where the secondary is wound over a plastic tube that can simply be wrapped around the primary conductor or conductors.

As the output is proportional to the rate of change of the primary current rather than its absolute value, the signal is usually integrated with an operational amplifier to generate a voltage that is directly proportional to the current. This introduces some errors in the measurements due to amplifier offsets and integration times and creates a frequency response that drops off at both low and high frequencies. Nevertheless, over a wide range of frequencies the response is linear and flat.

13.5 Hall Effect Current Sensor

The Hall Effect current sensor relies on monitoring the voltage induced by a magnetic field created by the primary current rather than measuring the current directly.

When current flows through a thin flat conductor, no potential difference appears across the

transverse (longer) sides unless the charge carriers are influenced by an external magnetic field. The magnetic field exerts a transverse force which causes a charge imbalance to occur, resulting in a voltage developing between the transverse sides which is proportional to the magnetic field strength.



Fig. 13.16: Principle of the Hall Effect sensor.

The hall voltage, V_H , is directly proportional to the bias current, I , and the magnetic field strength, B , and inversely proportional to the number of charge carriers per unit volume, n , the charge on each carrier, e , and the thickness of the flat conductor, d :

$$\text{Eq. 13.8: } V_H = \frac{I B}{n e d}$$

The hall effect will occur in any flat conductor, but as $n = 10^{29} \text{ m}^{-3}$ for copper and $n = 10^{25} \text{ m}^{-3}$ for silicon, the resulting hall effect voltage for a silicon conductor will be 1000 times greater. Therefore semiconductors are more often used rather than metallic conductors for Hall Effect sensors.

The bias current, I , can be supplied from a constant current source to create an output that is only dependent on the external magnetic field strength, B or the sensor can be placed between the poles of a permanent magnet in order to measure an external bias current. In this way, the hall sensor can measure DC current.

To use a Hall Effect sensor to measure AC current in an external conductor, it can be placed in the air gap of a transformer core through which the primary conductor passes:

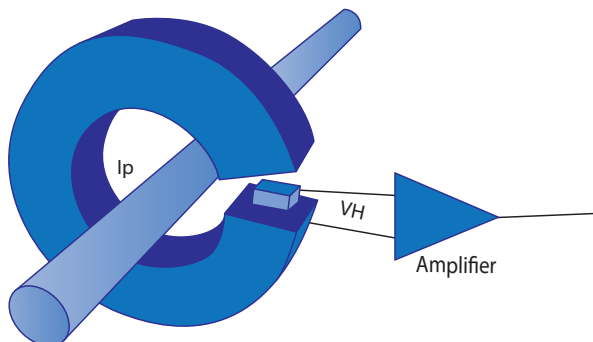


Fig. 13.17: Hall effect current sensor

Hall Effect current sensors can measure large currents or low currents, depending on how they are set up. Unlike the Rogowski coil and current transformer, a Hall Effect current sensor can be used to measure both AC and DC currents.

However, the performance of the magnetic core, external magnetic fields and amplifier errors such as offsets or gain drift can reduce the measurement accuracy.

13.6 Flux Gate current sensor

A flux gate current sensor combines elements of both the Hall Effect and AC zero-flux sensors. The current flow through the primary conductor creates a magnetic field which is detected by a probe coil inside the gap normally occupied by the Hall Effect sensor.

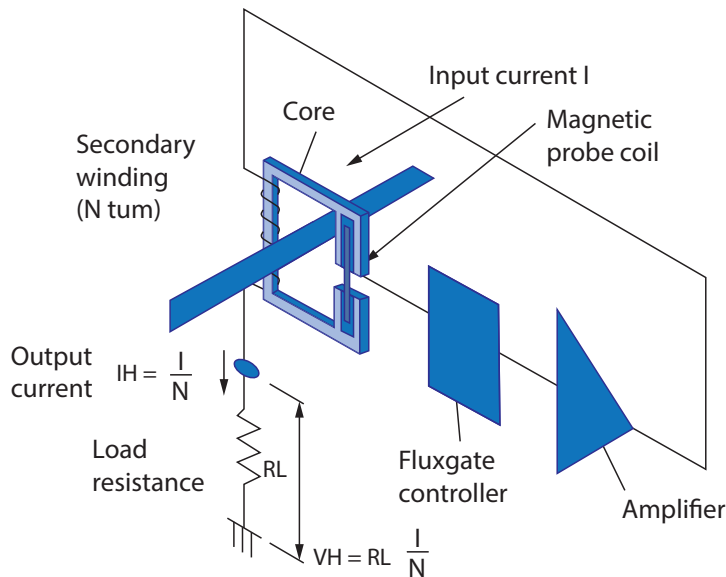


Fig. 13.18: Fluxgate Current Sensor

The output is amplified and fed back into a secondary winding to nullify the magnetic field as in the zero-flux sensor. The compensation current can be returned to ground via a resistor to give an output voltage proportional to the current flowing in the primary conductor. This closed loop system creates a more accurate measurement than other equivalent current sensors as temperature and aging effects can be compensated out, it also means that DC currents can be measured.

The magnetic material used has a non-linear B-H characteristic, so it saturates very easily. The Fluxgate controller uses this non linearity to make a very sensitive measurement system, relying on the feedback to bring the magnetic flux back to zero for any small changes in primary current and on core saturation to protect the system from heavy over current situations such as a primary short circuit.

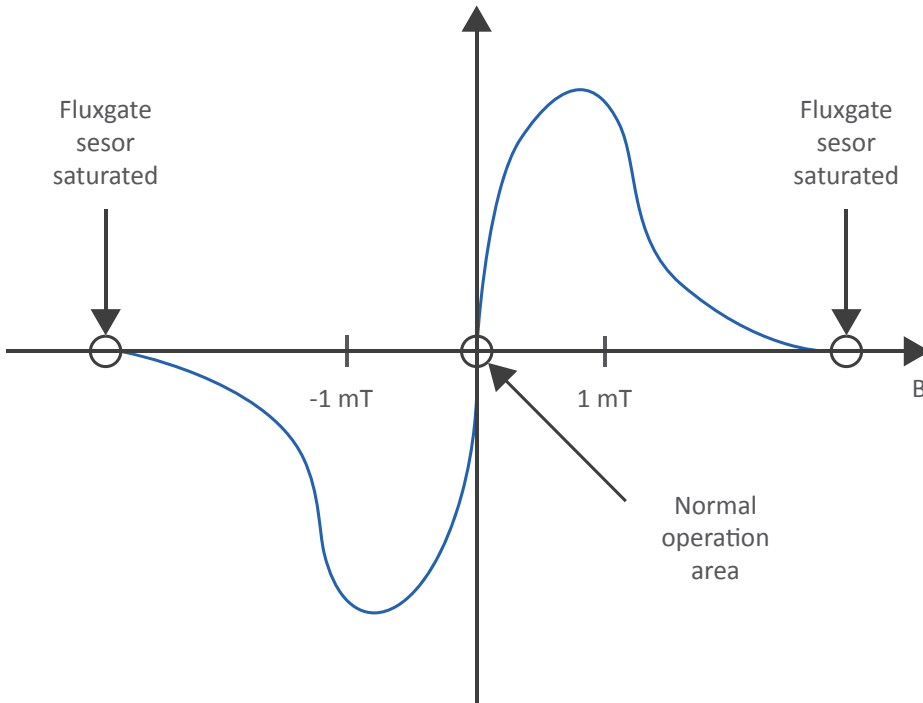


Fig. 13.19: Fluxgate core B-H curve

Fluxgate transducers make very good residual current measurement (RCM) sensors. An AC cable carrying both live and neutral wires is placed inside the sensor. The magnetic field from the supply and return conductors cancel out, leaving only any difference to be accurately sensed and amplified.

The disadvantages of the fluxgate current sensor is that any residual core magnetism caused by exposure to external magnetic fields will distort the measurements. Smart fluxgate controllers have a demagnetisation function to reset the core with a controlled AC drive signal before making a new measurement.

13.7 GMR current sensor

Giant Magnetoresistance (GMR) is a quantum spin effect that causes certain layered ferromagnetic materials to change their resistance under the influence of an external magnetic field. The sensor is placed in the gap of a magnetic core in the same way as the Hall Effect current sensor to measure AC current or placed in a coil to measure DC current.

A GMR sensor consists of a Wheatstone bridge with two active GMR elements and two passive shielded legs. This doubles the output sensitivity to the ΔR change to the intrinsic resistance, R , caused by the GMR effect.

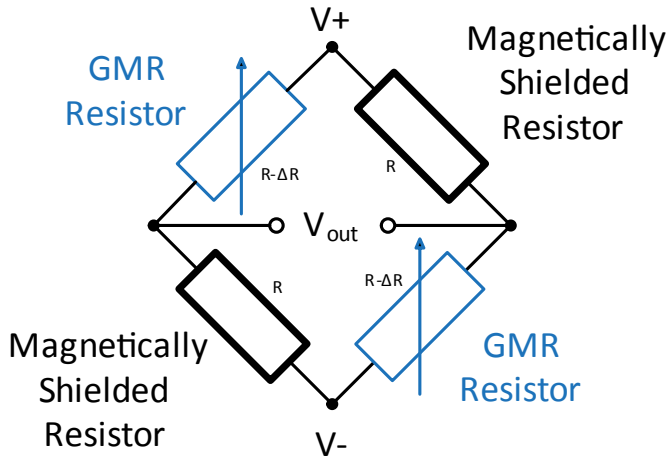


Fig. 13.20: GMR Wheatstone Bridge

The GMR sensor has a very fast reaction time and is very sensitive, so it is a useful sensor for measuring small signal AC currents up to 5MHz. Despite the Wheatstone bridge arrangement, it still needs careful thermal compensation for accurate readings as the GMR effect is relatively weak.

Sensor Technology	Shunt	CT	Zero AC Flux	Rogowski	Hall Effect	Fluxgate	GMR
Current	AC or DC	AC	AC	AC	AC or DC	AC or DC	AC or DC
Frequency	DC to MHz	50Hz-10kHz	50Hz-100kHz	100kHz-100MHz	DC to 1MHz	DC to 100kHz	DC to 5MHz
Isolation	None	Yes	Yes	Yes	Yes (AC) or none (DC)	Yes	Yes
Non Linearity	0.01%	0.05%	0.05%	0.05%	0.1%	0.001%	0.01%
Relative Cost	Low	Low	Medium	Low	Medium	High	High

Table 13.1: Comparison of the main current measuring techniques

References and Further Reading

Ceraolo, M and Poli, D (2014) “Fundamentals of Electric Power Engineering: From Electromagnetics to Power Systems”, First Edition, Copyright IEEE, Published by John Wiley and Sons, Inc.

NA, Z (2018) “A Study of Electrolytic Capacitor Thermal Conductivity, Behaviour & Measurement”, Mentor Graphics, Engineering Edge , Volume 5, Issue 1

Lee, B-H and Kim, C-E (2012) “No-Load Power Reduction Technique for AC/DC Adapters”, IEEE Transactions on Power Electronics, Vol. 27, No. 8

Siebt, A, (2014) “DC and AC Signals/Parameters and their correct Representation by Measuring Instruments”, Bodo’s Power, Oct.

Kolar, J.W and Friedli, T (2011) „The Essence of Three Phase PFC Rectifier Systems“, PES Laboratory, ETH Zurich, published in the Proceedings of the 33rd IEEE International Telecommunications Energy Conference, Amsterdam.

HBD853/D (2014) “Power Factor Correction (PFC) Handbook”, ON Semiconductor

Yarborough B (2015) “Components and Methods for Current Measurement”, Vishay

Knight, D.W. (2015) “AC Electrical Theory- An introduction to phasors, impedance and admittance, with emphasis on radio frequencies “, http://www.g3ynh.info/zdocs/AC_theory/AC_theory.pdf

Mammano, R.A. (2017) “Fundamentals of Power Supply Design”, Published by Texas Instruments Inc.

Sandler, S.M. (2014) “Power Integrity”, Published by McGraw-Hill Education

Some Recommended Application Notes

SLUA535 (2010) “Understanding and Designing an Active Clamp Current Mode Controlled Converter using the UCC2887A”, Texas Instruments Inc.

AN-8033 (2009) “Design Guideline for Primary Side Regulated (PSR) Flyback Converter Using FAN103 and FSEZ13X7”, Fairchild (now ON Semiconductor)

AN-4147 (2006) “Design Guidelines for RCD Snubber of Flyback Converters”, Fairchild (now ON Semiconductor)

SLUP340 (2016) “Switch Mode power converter compensation made easy”, Texas Instruments Inc.

SLUP325 (2014) “Control challenges for Low Power AC/DC Converters”, Texas Instruments Inc.

About the Author

Steve Roberts was born in England. He obtained a B.Sc. in Physics and Electronics at Brunel University, London (now University of West London) before working at University College Hospital. He later spent 12 years at the Science Museum as Head of Interactives, where he completed his M.Sc. at University College, London. He moved to Austria, joining RECOM's Tech Support team developing custom converters and answering customer's questions before becoming Technical Director for the RECOM group at their new headquarters in Gmunden, Austria.



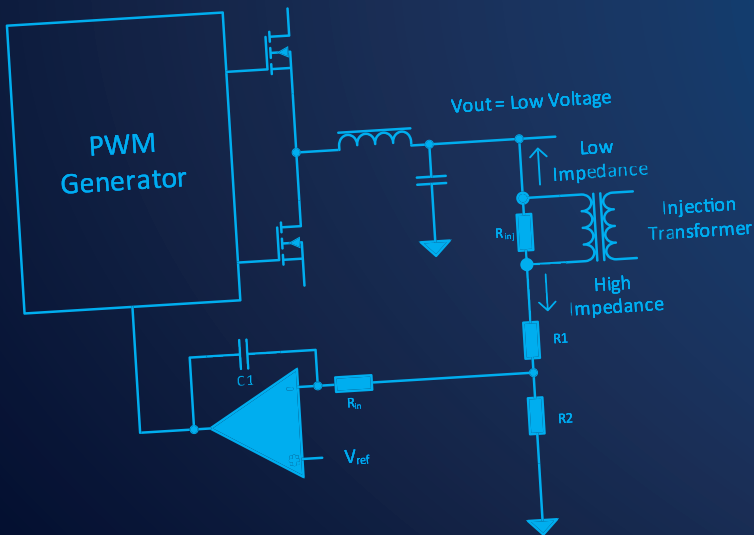
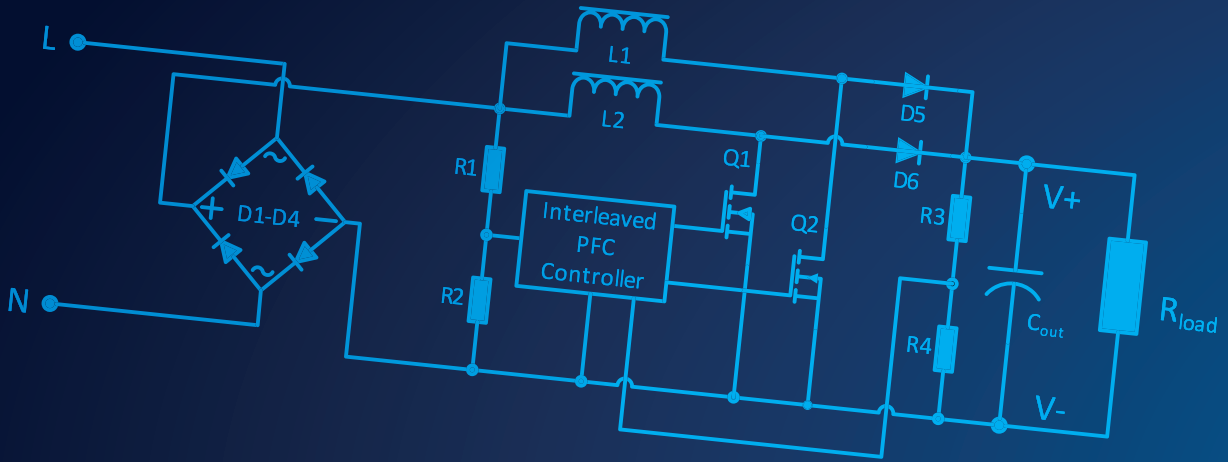
About Recom

It was about 30 years ago when we showed our first hand made DC/DC converter to a leading German manufacturer of cellular phones. The product successfully passed all tests and a few weeks later we received our first order for 8000 pieces. A new product category was born „DC/DC converters in the form of a module.

At that time the shift from analogue to digital electronics accelerated the demand for DC/DC modules due to the need for standardized on-board switching power supplies. In addition, I/O ports or amplifier channels required isolation to increase safety or to eliminate earth loops - another important requirement that DC/DC converters could fulfil. RECOM was there from the very early days to supply reliable, efficient and modular solutions for customers that did not want to invest the time and effort designing their own discrete converters.

From 2006, RECOM extended its portfolio to include AC/DC converters – primarily for existing customers that again did not want to invest the time and effort in certifying their own discrete converters. In the meantime, RECOM offers AC/DC converters from 1W up to 1kW in a variety of different form factors such as PCB mount, wired, low profile and DIN-rail mounting for use in both single-phase and three-phase supplies. RECOM plans to expand the AC/DC range beyond the existing low and mid-range products to break through the 10kW barrier – in effect offering a “one stop shop” for all DC/DC and AC/DC products for industrial, medical, transport and household applications.

Today, RECOM's ultra-modern campus-style headquarters in Gmunden and a separate R&D Centre in Vienna provides room for expansion to meet these ambitious goals. A team of international engineers works in well-equipped, state-of-the-art labs to create a constant flow of new products and customer solutions. We have also invested heavily in our own EMC test chambers in Gmunden and Vienna to be independent from external facilities.



WE POWER YOUR PRODUCTS
www.recom-power.com

**RECOM Power GmbH and
 RECOM Engineering GmbH & Co KG**
 Münzfeld 35, 4810 Gmunden, Austria